

Université de la Méditerranée

Faculté de Médecine de Marseille

Ecole Doctorale des Sciences de la Vie et de la Santé

THESE

Présentée et publiquement soutenue par

Amarender R. Bogadhi

pour obtenir le titre de

Docteur en Sciences

de l'Université de la Méditerranée

Spécialité : Neurosciences

**An experimental and theoretical study of Visual
motion integration for Smooth pursuit**

- A hierarchical recurrent bayesian framework

Composition du jury :

Président	Pr Franck Vidal	LNC, Marseille, France
Rapporteurs	Dr Philippe Lefevre	UCLouvain, Belgium
	Dr Jacques Droulez	LPPA, CNRS, Paris, France
Examinateur	Dr Laurent Madelain	Univ - Lille3, Lille, France
Directeurs	Dr Guillaume Masson	INT, CNRS, Marseille, France
	Dr Anna Montagnini	INT, CNRS, Marseille, France

Le Avril 2012

Université de la Méditerranée

Faculté de Médecine de Marseille

Ecole Doctorale des Sciences de la Vie et de la Santé

THESE

Présentée et publiquement soutenue par

Amarender R. Bogadhi

pour obtenir le titre de

Docteur en Sciences

de l'Université de la Méditerranée

Spécialité : Neurosciences

**An experimental and theoretical study of Visual
motion integration for Smooth pursuit**

- A hierarchical recurrent bayesian framework

Composition du jury :

Président	Pr Franck Vidal	LNC, Marseille, France
Rapporteurs	Dr Philippe Lefevre	UCLouvain, Belgium
	Dr Jacques Droulez	LPPA, CNRS, Paris, France
Examinateur	Dr Laurent Madelain	Univ - Lille3, Lille, France
Directeurs	Dr Guillaume Masson	INT, CNRS, Marseille, France
	Dr Anna Montagnini	INT, CNRS, Marseille, France

Le Avril 2012

Abstract

This thesis addresses two studies by studying smooth pursuit eye movements for a translating tilted bar stimulus. First, the dynamic integration of local visual motion signals originating from retina and second, the influence of extra-retinal signals on motion integration. It also proposes a more generalized, hierarchical recurrent bayesian framework for smooth pursuit. The first study involved investigating dynamic motion integration for varying contrasts and speeds using a tilted bar stimuli. Results show that higher speeds and lower contrasts result in higher initial direction bias and subsequent dynamics of motion integration is slower for lower contrasts. It proposes an open-loop version of a recurrent bayesian model where a recurrent bayesian network is cascaded with an oculomotor plant to generate smooth pursuit responses. The model responses qualitatively account for the different dynamics observed in smooth pursuit responses to tilted bar stimulus at different speeds and contrasts. The second study investigated the dynamic interactions between retinal and extra-retinal signals in dynamic motion integration for smooth pursuit by transiently blanking the target at different moments during open-loop and steady-state phases of pursuit. The results suggest that weights to retinal and extra-retinal signals are dynamic in nature and extra-retinal signals dominate retinal signals on target reappearance after a blank introduced during open-loop of pursuit when compared to a blank introduced during steady-state of pursuit. The previous version of the model is updated to a closed-loop version and extended to a hierarchical recurrent bayesian model. The hierarchical model qualitatively explains the experimental findings and can be considered a more generalized framework to study not only integration of local visual motion signals, extra-retinal mechanisms for smooth pursuit but also dynamic interactions between the two.

Keywords : Motion Integration, Smooth Pursuit, Prediction, Hierarchical recurrent bayesian model

Acknowledgements

I would like to thank Guillaume and Anna for giving me this opportunity and their valuable guidance through out. If it wasn't for Anna's mentoring, the transition to research in neuroscience wouldn't have been smooth. I would like to thank Lolo for the informative discussions we had on Bayesian Modelling and Kalman filter. Discussions with Jerome have been helpful in understanding saccades and in general different eye movements. I would also like to thank CODDE network for the workshops which were enjoyable in every sense and Marie Curie – ITN for the financial support.

I would like to thank Fred in setting up REX system used for the direction anisotropy experiments. I would like to extend my thanks to Anna and Claudio for setting up the EYELINK lab where blanking experiments were carried out.

I would like to extend my thanks to Taraabte and Joelle for helping me with the administrative work.

Thanks to Freddo and Seb for pushing something of scientific interest to come to the table during Journal Clubs. Thanks to all the colleagues for sharing their excellent ideas during Journal Clubs. Claudio has been immensely kind and kept me in a wonderful company especially during the initial years. Joach, Alex, Jerome, Paola and Fred require special mention for their patience and help in every second thing I had to do in french. Mina and Giacomo have always been generous. Andrew helped with some of the recommended reading.

I am grateful to the some of the excellent teachers I have had who inspired me to pursue research. I will be indebted to my parents, family and friends for all the support they have provided all along.

Preface

Brain and Sensory – Motor Transformation

Every organism is a part of an environment that is dynamic in nature. Survival in a dynamic environment requires interaction. An organism has to be capable for movement to interact with its environment. The ability to make a movement underlines the necessity for a brain. The most often cited example to underline the necessity for a brain by the researchers in Motor Control is that of the sea squirt. It digests its own brain when it doesn't need to make a movement in its future and finds a suitable rock to affix to and cements itself in place. If motor action (movement) is the reason for an organism to have a brain, there is a need to understand how the information in the environment collected through senses is transformed for an appropriate motor action inside the brain. This transformation is called sensory-motor transformation as shown in figure 1.

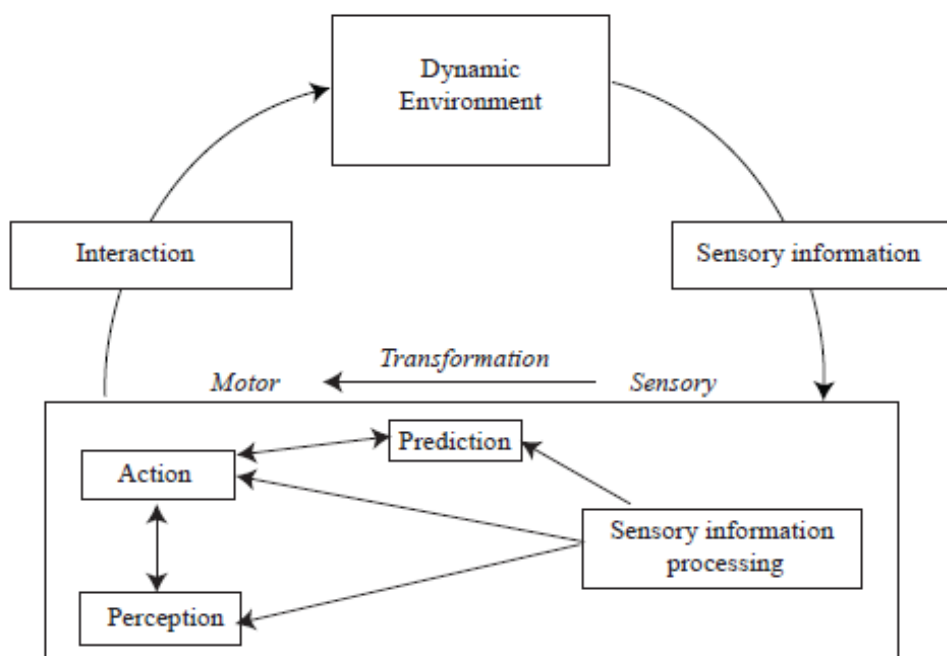


Figure 1. Sensory to motor transformation

To interact with a dynamic environment, an organism's brain collects information about the outside world through its senses, process this sensory information to have a perceptual account of it and act on the environment either voluntarily or involuntarily. Broadly speaking, the subject of this thesis is the sensory-motor transformation in the primate brain.

Tracking and Visual Motion

The primary sensory information in a dynamic environment that has to be processed for our very survival is Visual motion. Processing of Visual motion limits our perception and the subsequent actions on the environment. This makes visual motion information processing a foremost model to be studied as an example sensory processing system.

Given the non-uniform distribution of the photoreceptors on the retina, tracking a moving object to stabilize its image on the fovea is necessary to extract the details of the moving object. Tracking a moving target with our eyes requires a sensory estimation of the velocity of the target and a subsequent motor transformation of the velocity estimate (see (Lisberger et al 1987) for a review). This allows for an accurate temporal account of the dynamics involved in visual motion information processing to be reflected in tracking responses (See Chapter 3 for details). Also, because of the simplicity in terms of the kinematics and the dynamics involved with eye movements (Robinson 1964; 1965) compared to limb movements (Atkeson & Hollerbach 1985), visually guided eye movements provide a better platform as a model for motor system to study the brain mechanisms involving sensory-motor transformation.

Tracking as a probe to visual motion processing

Tracking a moving target with our eyes requires a sensory estimation of the velocity of the target and a subsequent motor transformation of the velocity estimate. Neurons in the early visual areas can only detect motion locally (Hubel & Wiesel 1968). Because of the ambiguity involved with each local motion measurement (aperture problem (Wallach 1935)), responses of the local motion detectors in the early visual system need to be integrated to arrive at a global velocity estimate of the moving target. Middle temporal (MT) region in the superior temporal sulcus (STS) is a more likely candidate for the integration of local motion signals because of its position in the hierarchy of the visual motion pathway (Felleman & Van Essen 1991) and also, neurons in MT are highly direction selective (Albright 1984). Inactivation of MT leads to deficits in motion perception (Newsome & Pare 1988) as well as pursuit initiation (Newsome et al 1985). Middle temporal (MT) and medial superior temporal (MST) of STS has been tightly linked to pursuit and chemical lesion studies in monkeys show that they provide visual motion information necessary to guide smooth eye movements (Dursteler & Wurtz 1988; Komatsu & Wurtz 1988; Newsome et al 1985; Newsome et al 1988). This common ground for motion processing and smooth pursuit at the level of MT suggest that tracking responses ought to carry the signature of the dynamics involved in motion integration. Unlike the perceptual account which is a snap shot readout, visuo-motor

transformation for tracking provides a better metric to study visual motion processing in precise temporal detail.

Dynamics of Motion Integration for Smooth Pursuit

The local motion signals in visual motion scene are integrated to obtain the object's global velocity. Psychophysical studies suggested that the motion integration is dynamic and two different motion sensitive units be involved in dynamic motion integration (Castet et al 1993; Lorenceau et al 1993; Wilson et al 1992; See Chapter 4 for details). The early part of the dynamics is driven by the ambiguous motion signals (1D component), later by unambiguous motion signals (2D component) for both perception and in MT neurons. Physiological studies of MT neurons using bar field (Pack & Born 2001) and plaid stimuli (Smith et al 2005) also show that MT neurons initially respond to 1D motion signals and later to 2D motion signals (See Chapter 4 for details).

Several studies (Born et al 2006; Masson & Castet 2002; Masson et al 2000; Masson & Stone 2002; Wallace et al 2005) show that smooth eye movements, short latency ocular following and smooth pursuit provide an accurate account of the dynamics in motion integration unlike a snap shot readout in the perceptual studies (See Chapter 5 for details). This dynamics is similar to the dynamics observed in MT (Pack & Born 2001). Pursuit studies investigating various properties of pursuit use a simple stimulus like a dot which is unambiguous. Tilted bar stimulus and various complex figures (e.g. diamonds) are easy to track like a dot but also has ambiguous motion signals (1D) along its edges and unambiguous motion signals (2D) at the terminator endings. Tracking such a stimulus (e.g. Tilted bar and complex figures like diamond) results in an initial directional bias driven by the 1D signals and later tuned to object's global velocity by 2D motion signals. Thus, tilted bar stimulus proves ideal to investigate dynamic motion integration for smooth pursuit. In this thesis, we use a tilted bar stimulus to investigate the dynamic motion integration and the effects of prediction on dynamic motion integration.

Modelling the Dynamics of Motion Integration for Smooth Pursuit

The perceived direction for type-I plaids is best predicted by Intersection of Constraints (IOC) or Feature Tracking (FT) principles (Movshon et al 1986). Intersection of Constraints utilizes the geometric relation between local velocity samples and the object velocity to extract the object velocity from the local samples (Fennema & Thompson, 1979; Marr & Ullman, 1981). Features from a moving object provide unambiguous motion information about the velocity of the object. Feature tracking involves selecting features in the moving

object and tracking them. The perceived direction of type-II plaids is explained by Vector Average (VA) of the local velocity samples (Wilson et al 1992).

The perceived direction, explained by different rules for different stimuli, for e.g. IOC/FT for type-I plaid and VA for type-II plaid suggested that a more general rule might be at work. Bayesian inference assuming slow prior provides a more general framework to model perception for different stimuli under different conditions (Weiss et al 2002). The output of the model is a perceptual response which is essentially static. Other models for motion perception using explicit features or luminance smoothness could explain the dynamics associated with motion perception (Berzhanskaya et al 2007; Tlapale et al 2010; Bayerl & Neumann 2007).

A model (Montagnini et al 2007) processing 1D and 2D motion information parallelly in a recurrent bayesian framework has been proposed to understand the dynamic nature of motion integration at the level of MT. Since tracking responses carry dynamics of motion integration in a greater detail than perceptual accounts, modelling motion integration for eye movements can provide a better understanding of the dynamic nature of motion processing and the subsequent motor transformation for smooth eye movements (See Chapter 5 for details). The models for smooth pursuit (Bennett & Barnes 2003; Churchland et al 2003; Krauzlis & Lisberger 1994; Robinson et al 1986) have largely focused on the oculomotor dynamics investigated using a simple stimulus like a dot. In this thesis, we extend the previous model (Montagnini et al 2007) with a cascade of an oculomotor plant (Goldreich et al 1992) to an open-loop version of the model to explain the dynamic motion integration for smooth pursuit (Bogadhi et al 2011; See chapter 6). With the observations from the experiments investigating role of prediction on motion integration, the open-loop version of the model is extended to a closed-loop hierarchical recurrent bayesian framework to understand the role and interactions between retinal and extra-retinal signals.

Probabilistic inference for Smooth Pursuit

Probabilistic inference has been successful in explaining motion perception to a variety of stimuli (Weiss et al 2002). Such a framework accommodates uncertainty in the motion information in the measurement likelihoods (Weiss et al 2002) and also expectation can be represented through the prior which can alter motion perception (Sotiropoulos et al 2011). Representing uncertainty in the measurements and prior expectation gives a simple, yet powerful framework to investigate predictive behaviour of the system under investigation possibly to optimally adapt to changes in the measurements.

One of the major limitations to the approach taken by previous oculomotor models

investigating sensory-motor transformation for smooth pursuit is, they are not equipped to represent uncertainty. Sensory noise is the major source of variance in the motor action as motor action is planned so as to minimize motor noise, and hence sensory noise could play a crucial role in the motor transformation of the sensory estimate (Harris & Wolpert 1998; Osborne et al 2007; Osborne et al 2005). Motor transformation has to minimize the detrimental effects of noise by using information from multiple modalities, for example sensory estimate as well as internal estimate indicative of prediction (See, van Beers et al 2002a for a review). Probabilistic inference could be employed to deal with uncertainties in multiple modalities (e.g. Sensory and Prediction) for human sensory-motor processing (Kording & Wolpert 2004). Moreover, growing body of evidence suggests for a probabilistic computation in human sensory-motor control (See, Wolpert 2007, for a review).

An engineering answer for such an adaptive system is a kalman filter (Kalman 1960). It involves projecting the current estimate of the system based on the prior knowledge and correcting the predictions based on the measurement. A mix of measurement and prediction are used to estimate the current state based on their reliability reflected from their variances. Studies investigating sensory-motor transformation already suggest for a mix of measurement based signal and an internal signal based on reliability extracted from their respective uncertainties for an optimal performance in a motor task (Van Beers et al 2002b).

Following the idea of kalman filter, this thesis proposes a hierarchical recurrent bayesian framework to understand both motion integration as observed in smooth pursuit and also predictive nature of pursuit. Such an approach allows for a mix of prediction and measurement based on their reliability measured from their respective variances. The combined estimate is used to drive the pursuit response. The hierarchical framework would allow to investigate the adaptive behavior of pursuit as well as the role of prediction on motion integration as observed in pursuit responses (See chapter 8).

Outline of the thesis:

In short, this thesis investigates the dynamic motion integration and the role of prediction on dynamic motion integration, for smooth pursuit and proposes a hierarchical recurrent bayesian framework to understand both, dynamic motion integration and the effect of prediction on dynamic motion integration. The outline of the thesis is described below.

The thesis consists of four parts. The first part is a general introduction to tracking and visual motion. It describes why tracking provides an ideal platform to study dynamics in visual motion processing. The second part describes the aperture problem and perceptual account of it. The third part describes the action account of aperture problem with the help of

smooth pursuit eye movements and proposes an open-loop recurrent bayesian model cascaded with an oculomotor plant to explain the dynamic motion integration for smooth pursuit. Fourth part describes the literature on extra-retinal signals driving pursuit in the absence of retinal signals. It also describes the study investigating the interaction between retinal and extra-retinal signals, and proposes a hierarchical recurrent bayesian model to understand these interactions. The outline of the thesis is as follows.

Part 1 : General Introduction : Tracking Objects and Visual Motion

Chapter 1 : Tracking Objects

An introduction to tracking eye movements and its physiology. A brief description about the control systems approach to model smooth pursuit and studies investigating predictive behavior for smooth pursuit.

Chapter 2 : Visual Motion

Introduction to visual motion and pathway for the flow of motion information starting from retina and describes magnocellular and parvocellular pathways leading to Dorsal and Ventral streams. Provides a brief introduction to speed and directional selectivities in V1 and MT.

Part 2 : Aperture Problem and Motion perception

Chapter 3 : Local motion detection and aperture problem

Description of the problem (aperture problem) encountered by the neurons in the early visual cortex because of the ambiguity in their local velocity measurements of a moving object. It also provides a brief overview of the models for local velocity detection namely reichardt detector, gradient model and the spatio-temporal energy models.

Chapter 4 : Psychophysics of motion perception

An overview of different schemes (e.g. Vector Averaging, Intersection of constraints, feature tracking) for combining local motion information to explain the psychophysical account of aperture problem using plaid stimuli is provided. The physiology of the plaids is briefly discussed. It also describes psychophysics, physiology and computational studies investigating the role of 2D motion information in motion integration. At the end, a more general framework using bayes principle is presented.

Part 3 : Motion Integration for behaviour

Chapter 5 : Smooth eye movements and dynamic motion integration

Description of the dynamics with which the ambiguous and the unambiguous local velocity measurements are combined (motion integration) to solve the aperture problem and obtain the true velocity of the moving object. Since the sensory estimate of the velocity of the moving object is transformed into motor action (eye movements), the smooth eye movements provide a window into the dynamics of motion integration. Behavioural account of the dynamics in motion integration is described in this section.

Chapter 6 : A Recurrent bayesian model of dynamic motion integration for smooth pursuit

Proposes an open-loop version of a recurrent bayesian model to reflect the dynamic solution to the aperture problem as observed in smooth pursuit. The recurrent bayesian network is cascaded with oculomotor plant to produce the output of the model which is compared with the smooth pursuit data. This work is published in Vision Research (Bogadhi et al 2011).

Part 4 : Prediction for Smooth Pursuit

Chapter 7 : Role of prediction for smooth pursuit during transient disappearance of a target

Reviews the literature describing the role of extra-retinal signals and models for smooth pursuit using different paradigms namely, repetitive patterns, expected target motion and transient blanking.

Chapter 8 : Dynamic Interactions between retinal and extra-retinal signals in motion integration for smooth pursuit

Describes the two experiments conducted to study the interactions between retinal and extra-retinal signals in open-loop and steady-state stages of smooth pursuit. It proposes a hierarchical model to understand these interactions between retinal and extra-retinal signals at different stages of pursuit. This work is submitted for publication.

Chapter 9 : Role of prediction on motion integration for smooth pursuit

This chapter describes the study using expected target motion paradigm to investigate the role of prediction on motion integration at initiation for smooth pursuit. It also describes the simulated responses of the hierarchical model described in the previous chapter.

Discussion :

A short summary of the thesis followed by different perspectives and possible future work.

Table of Contents

Part 1 : General Introduction : Tracking Objects and Visual Motion	2
1. Tracking Objects	4
1.1. Introduction	4
1.2. Initiation and Steady-state of pursuit	4
1.3. Control systems approach to Pursuit	9
1.4. Prediction for tracking	13
1.5. Physiology of Smooth Pursuit	14
1.6. Summary	16
2. Visual Motion	18
2.1. Introduction	18
2.2. Physiology of Visual motion	19
2.2.1. Basic Visual Pathway	19
2.2.2. Magnocellular and Parvocellular pathways	20
2.2.3. Dorsal and Ventral Streams	21
2.2.4. Dorsal Stream : Flow of motion information	21
2.3. Representation of Motion in Visual Cortex	22
2.3.1. Speed Selectivity	23
2.3.2. Direction Selectivity	25
2.4. Motion estimation	25
2.5. Summary	26
Part 2 : Aperture Problem and Motion perception	28
3. Local motion detection and aperture problem	30
3.1. Aperture problem	30
3.2 Reichardt detector	31
3.3. Spatio-Temporal Motion Energy Model	32
3.4. Gradient Model	34
3.5. Summary	35
4. Psychophysics of motion perception	36
4.1. Solving Aperture problem	36

4.1.1. Vector Averaging (VA)	36
4.1.2. Intersection of Constraints (IOC)	37
4.1.3. Feature tracking	38
4.2. Stimuli for Motion integration	39
4.3. Psychophysics of plaids	40
4.3.1. Conditions for Coherence	40
4.3.2 Models for the perception of coherence	41
4.3.3. Noise Masking experiment	41
4.3.4. Adaptation experiment	42
4.4. Physiology of plaids	43
4.5. Alternate computations to IOC	44
4.6. Perceptual account of the dynamic motion integration	45
4.6.1. Role of terminators in motion integration	45
4.6.2. 1D to 2D	45
4.7. Physiological account of the dynamics of 1D and 2D motion integration	46
4.7.1. Bar field stimuli	47
4.7.2. Plaid stimuli	48
4.8. End-stopped V1 cells	49
4.9. Models for motion integration	50
4.9.1. Two stage model : Extended S and H Model	50
4.9.2. Parallel Pathway models	51
4.9.3. Form-Motion Models	53
4.10. General framework : Bayesian approach	54
4.11. Summary	56
Part 3 : Motion Integration for behavior	58
5. Smooth eye movements and dynamic motion integration	60
5.1. Smooth eye movements	60
5.2. 1D to 2D	61
5.2.1. Barberpole stimulus	61
5.2.2. Uni-kinetic Plaids	62
5.2.3. Type-I and Type-II Diamonds	63
5.2.4. Tilted bar stimuli	64
5.3. 1D and 2D	66

5.4. Summary	66
6. Pursuing motion illusions: a realistic oculomotor framework for Bayesian inference		
	68
6.1. Introduction	69
6.2. Methods	73
6.2.1. Experimental methods	73
6.2.2. Experiment 1: Pursuing pure 1D and pure 2D stimuli	74
6.2.3. Experiment 2: Effect of line length on smooth pursuit	74
6.2.4. Experiment 3: Directional anisotropies in initial and steady state velocities	75
6.2.5. Experiment 4: Pursuing a tilted line	75
6.2.6. Mathematical methods: tuning the Bayesian recurrent model	75
6.3. Results	77
6.3.1. Experiment 1: Tuning the recurrent Bayesian model with variances of pursuit responses to a blob or a line of varying contrast	77
6.3.2. Experiment 2: Using effects of line length to tune the 2D oculomotor plant	79
6.3.3. Experiment 3: Using directional anisotropies to tune a 2D oculomotor model	81
6.3.4. A recurrent Bayesian model for dynamic motion integration	84
6.3.5. Model description	85
6.3.6. Tuning the model parameters	86
6.3.7. Experiment 4: Model and Smooth pursuit responses to translating tilted lines	88
6.4. Discussion	92
Part 4 : Prediction for Smooth Pursuit 96		
7. Role of prediction for smooth pursuit during transient disappearance of a target	98
7.1. Role of extra-retinal signals for smooth pursuit - different paradigms	98
7.1.1. Repetitive Patterns	98
7.1.2. Expected target motion	99
7.1.3. Transient blanking	100

7.1.3.1. Blanking in steady-state	100
7.1.3.2. Blanking at initiation	102
7.2. Models	103
7.2.1. Positive feed-back gain model	103
7.2.2. Short term memory model	104
7.3. Summary	105
8. Dynamic Interaction between retinal and extra-retinal signals in motion integration for smooth pursuit	108
8.1. Introduction	109
8.2. Methods	111
8.3. Results	116
8.3.1. Experiment 1: Target blanking during the steady-state phase of pursuit	116
8.3.2. Experiment 2: Target blanking during the initiation of pursuit	122
8.4. Discussion	128
8.4.1. Dynamic weighting of retinal and extra-retinal signals	129
8.4.2. A hierarchical inference model for smooth pursuit	131
8.4.3. Model Results	137
8.4.4. Comparison with previous models (Bennett & Barnes 2004; Barnes and Collins, 2008b)	138
8.5. Conclusion	139
9. Role of prediction on motion integration for smooth pursuit	142
9.1. Experimental Evidence (Montagnini et al 2006)	142
9.2. Model Simulation	143
9.3. Summary	144
Discussion	146
Summary	146
Perspectives	149
<i>Abbreviations</i>	156
<i>List of Figures</i>	158
<i>References</i>	162

Part - 1

General Introduction : Tracking Objects and Visual Motion

Chapter 1

Tracking objects

This chapter gives an introduction to smooth pursuit eye movements and its properties. It also describes the control systems approach to model smooth pursuit and its limitations. Studies investigating predictive behavior for smooth pursuit are briefly discussed. An overview of the physiology underlying pursuit is presented.

1.1. Introduction

Eye movements can either be reflexive or voluntary. Reflexive eye movements are Vestibular Ocular Reflex (VOR), Optokinetic Nystagmus (OKN) and Vergence eye movements. They serve the purpose of stabilizing the moving image onto the retina (see (Ilg 1997; Kawano 1999) for a review). During self motion, image of the object on the retina is displaced (referred to as retinal slip) and Vestibular Ocular Reflex (VOR) compensates for the retinal slip resulted from self motion. Reflexive eye movements evoked by residual motion of visual image on the retina are called Optokinetic Nystagmus (OKN). The early component of OKN is called Ocular following response (OFR). Humans perform two types of voluntary eye movements namely saccadic movements and smooth pursuit eye movements (see (Krauzlis 2005) for a review). Saccadic eye movements are ballistic in nature and serve to scan parts of the visual scene. Smooth pursuit eye movements are voluntary smooth eye movements used to track a moving object and stabilize its image on the retina (Krauzlis 2005; Lisberger 2010). Some of the early studies differentiated saccadic eye movements from smooth pursuit eye movements (Dodge 1903; Westheimer 1954). This thesis deals with smooth pursuit eye movements and hence this chapter focuses on literature discussing various aspects of smooth pursuit.

1.2. Initiation and Steady-state of pursuit

Stimulus for Pursuit Initiation

Although smooth pursuit is a voluntary response, a moving target (Rashbass 1961) or an expectation of a moving target (Kowler & Steinman 1979a; b) is needed to initiate pursuit

response. Studies in open-loop conditions (retinally stabilized target) suggest that retinal position error of a stationary target can evoke smooth eye movements (Pola & Wyatt 1980; Segraves & Goldberg 1994; Wyatt & Pola 1981). A stationary cue depending on the context can evoke smooth eye movements in preparation of upcoming pursuit (Tanaka & Fukushima 1997; Tanaka & Lisberger 2000).

Subjects asked to generate smooth pursuit in the absence of a moving visual target can only produce a stair-case of saccadic eye movements. Rashbass (1961) showed that a moving target is required to initiate pursuit and once its initiated it responds to change in target position through pursuit or a saccade depending on the amount of retinal slip resulted by the step in target position. Follow up studies indicated that retinal positional errors of the target were effective once the pursuit is initiated and were ineffective for pursuit initiation (Morris & Lisberger, 1987; Carl & Gellman, 1987). Study by Carl and Gellman (1985) using step-ramp paradigm shows a weak pursuit response in the direction of step which later responds in the direction of the ramp. A more recent study using a flashed target showed that position information is effective as an input to smooth pursuit during tracking but not during fixation (Blohm et al 2006).

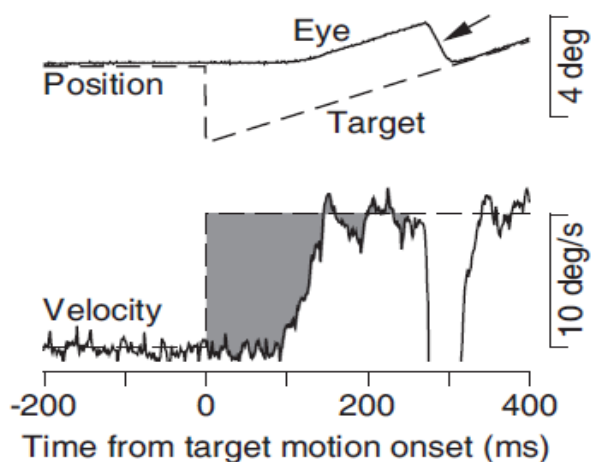


Figure 1.1. Smooth pursuit responses (eye position and eye velocity) to a target moving with a constant velocity preceded by a step displacement in the target position (Lisberger, 2010).

Smooth Pursuit Response

Figure 1.1 shows an example pursuit response to a moving target. Eye starts to move in the direction of the target after a latency of ~100ms. The response shown in the figure 1.1 is free of catch-up saccades. A typical pursuit response is a mix of initial smooth acceleration and a

saccade to catchup with the moving target followed by smooth velocity. A saccade is executed when the retinal slip of the target exceeds a threshold target displacement (Rashbass 1961). The threshold target displacement is about $0.25^\circ - 0.5^\circ$. If the target step is displaced in the opposite direction before the ramp execution so that after pursuit initiation the retinal position error is less than the threshold target displacement, catch-up saccade is eliminated as seen in figure 1.1. This is called step ramp paradigm and is widely used to eliminate saccadic displacements in the early pursuit responses.

Components of Open-loop Pursuit

Once the pursuit is initiated, after ~ 250 ms eye reaches the velocity of the target and the retinal slip is effectively zero. This is also referred to as steady-state of pursuit and the initial raising phase until which the feed-back (typically first 100ms after pursuit onset) is not processed is referred to as open-loop phase of pursuit. Pursuit response in the open-loop has two components, an early component measured in the first 20ms of initiation and a late component in the next 60-80ms. This is shown in the figure 1.2.

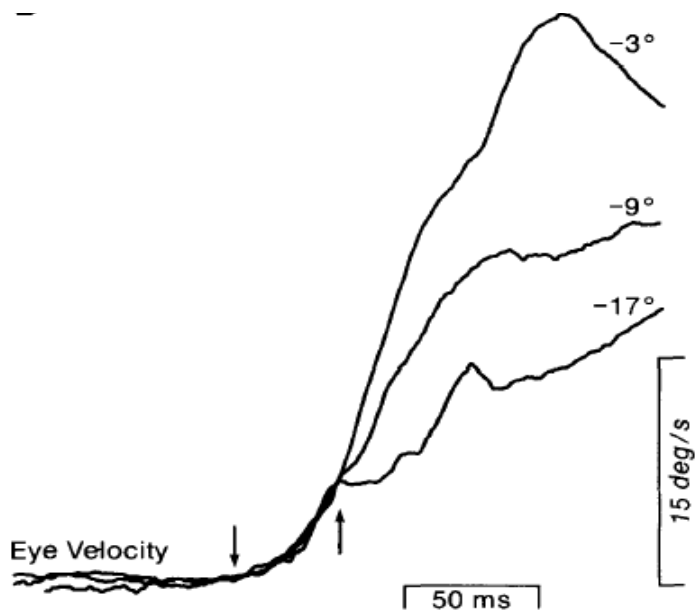


Figure 1.2. Eye velocity traces for a target moving at $30^\circ/\text{s}$ starting at different positions (numbers shown on top of each trace). Downward arrow shows pursuit initiation and upward arrow shows transition from early to late component (Lisberger & Westbrook 1985).

Late component depends on different properties of visual inputs namely initial position of the target, background illumination, velocity of the stimulus where as the early component is independent of the above parameters but exhibits direction selectivity

(Lisberger & Westbrook, 1985 Tychsen & Lisberger, 1986). Degrading effects on pursuit initiation because of the lesions in striate cortex and MT indicate to the role of these cortical areas involved in velocity computation required for pursuit (Newsome et al 1985; Segraves et al 1987). The agreement between velocity selectivity in pursuit responses (Lisberger & Westbrook 1985) and in the population responses of MT (Maunsell & Van Essen 1983) in 60-80ms interval suggests MT as a physiological neural substrate driving the late component of initial pursuit. Cells in cortico-pontine projection system have comparable responses to early component in the first 20ms. These cells are direction selective, have large receptive fields and respond over wide range of speeds (Baker et al 1976). In addition, the cortical projection onto pontine nuclei doesn't emphasize central retina similar to early component (Cohen 1981).

Steady-state Pursuit and Oscillations

During the steady-state of pursuit, the retinal slip is zero and studies stabilizing image on the fovea equivalent to steady-state, suggest that eye velocity memory drives pursuit in the absence of retinal slip (Morris & Lisberger 1987). Steady-state pursuit often show oscillations around the steady-state eye velocity. The period of the oscillations varies between 220-400ms. These oscillations were reduced during the open-loop conditions (target stabilized). This suggests that oscillations are primarily driven by visual motion related signals. If the visual inputs signal only retinal velocity error, the period of the oscillations should be approximately four times the latency of the visual input (Robinson 1965). However, the predicted period of oscillation shortens as the sensitivity to retinal acceleration error increases (Morris & Lisberger 1985). The natural delay (typically ~90ms) because of the computation in the visual inputs to drive the pursuit system leads to oscillations (Goldreich et al 1992) and is shown in figure 1.3. Changing the target viewing conditions (e.g. contrast and size of the stimulus) changes the natural delay. This is evident in the figures 1.3A and 1.3B where the latency of responses is 86ms and 132ms respectively. On top of that, electronically controlled feed-back delay is imposed and the responses are shown for different delays in panels A and B of figure 1.3.

Gain Control for Pursuit

During the steady-state tracking, gain of the pursuit response is equal to 1 as eye velocity matches the target velocity. Studies investigating online gain control perturb the velocity of the target. When the velocity of the target is perturbed during fixation and steady-state of

pursuit, the responses were higher during steady-state of pursuit compared to during fixation (Schwartz & Lisberger 1994). Even expectation can alter the gain of the responses to perturbations (Kodaka & Kawano 2003; Tabata et al 2005). Micro-stimulation in Frontal Pursuit Area (FPA) during initiation enhances the pre-saccadic pursuit and the same during a perturbation in the eye velocity facilitates the response to perturbation (Tanaka & Lisberger 2001). This suggests that FPA is involved in the online gain control for pursuit.

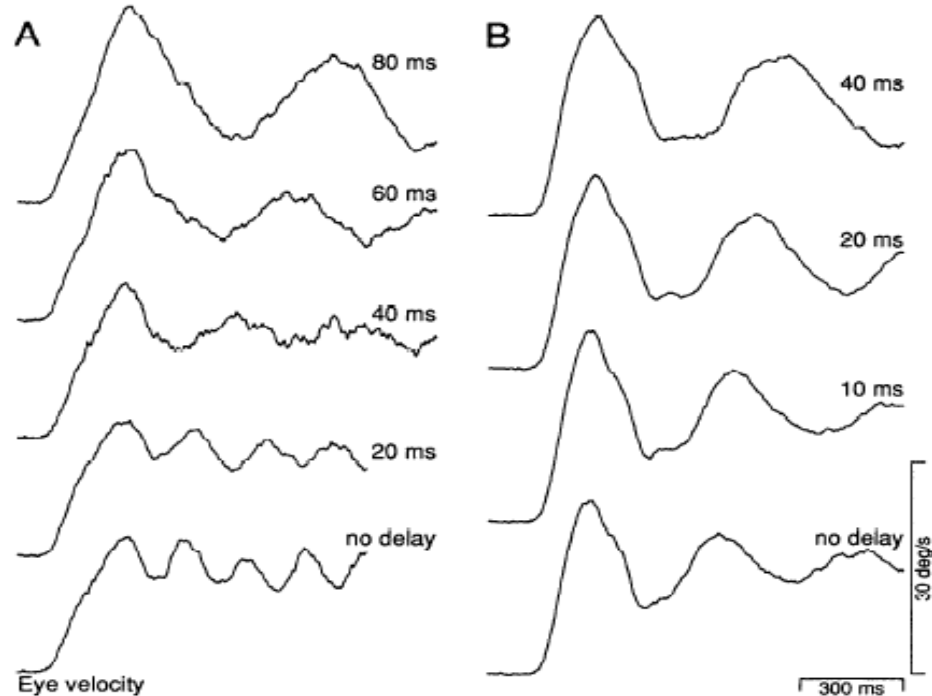


Figure 1.3. Effect of feed-back delay on oscillations. Numbers on top of each trace show the feed-back delay. (A) when the target is 0.5° in size and bright viewing conditions resulting in a latency of 86ms (B) when the target is 0.1° in size and dim viewing conditions resulting in a latency of 132ms (Goldreich et al 1992).

Fixation and Pursuit systems

If the moving object stops after translation, pursuit velocity exponentially drops to zero and is free of oscillations compared to onset of pursuit. This is taken as evidence that onset of pursuit is controlled by pursuit system and offset of pursuit is controlled by fixation system (Luebke & Robinson 1988). Oscillations can still be observed when the target stopping is made uncertain (Krauzlis & Miles 1996). These results suggest that rather one system might be involved in transition from fixation to pursuit and pursuit to fixation.

Multiple inputs to Pursuit system

Eye acceleration increases with retinal position error, retinal velocity error and retinal acceleration error (Lisberger et al 1981; Lisberger & Westbrook 1985; Tychsen & Lisberger 1985). Relation between sensitivity to retinal acceleration error and the period of oscillation argues for multiple inputs to pursuit system related to both image velocity and acceleration (Lisberger et al 1987). Other behavioral studies also suggested multiple visual motion signals might be involved in driving pursuit and signals related to image acceleration might contribute to pursuit responses along with velocity (Krauzlis & Lisberger 1987; 1994b; Lisberger & Westbrook 1985). However, physiological studies in MT didn't find any signature of image acceleration in individual cells but suggested image acceleration information could be reconstructed from population responses of MT (Lisberger & Movshon 1999). This could explain the limitations in processing acceleration information for both perception and pursuit because image acceleration is not explicitly represented, but derived and hence unreliable unlike speed (Watamaniuk & Heinen 2003). Models with multiple visual inputs were developed to understand the dynamics of smooth pursuit which will be discussed in next section (Krauzlis & Lisberger 1989; 1994a).

1.3. Control systems approach to Pursuit

Pursuit as a negative feed-back system

The purpose of pursuit is to stabilize the image of the moving object on the retina. The visual image motion drives the eyes, resulting in reduction of the retinal slip of the image. This is considered as a negative feed-back system as shown in figure 1.4A. The model response (dotted line) although looks similar to eye velocity (solid line), the time period of oscillation is much smaller. The major drawbacks of such a simple linear arrangement of delay and a first order transfer function are, (a) the gain can never be more than 1 which is not the case with some subjects (b) the acceleration and the time period of oscillation cannot match simultaneously with the observations because matching the acceleration decreases the time period of oscillation and vice-versa.

The oscillations could be avoided by negating the role of physical negative feed-back for pursuit with an internal positive feed-back (Robinson 1971; Robinson et al 1986; Young et al 1968) or using non-linearity in multiple motion related signals such as velocity and acceleration (Krauzlis & Lisberger 1989; 1994). For their respective dependence on positive feed-back and multiple signals related to image motion, they are referred as Internal feed-

back models and Image motion Models.

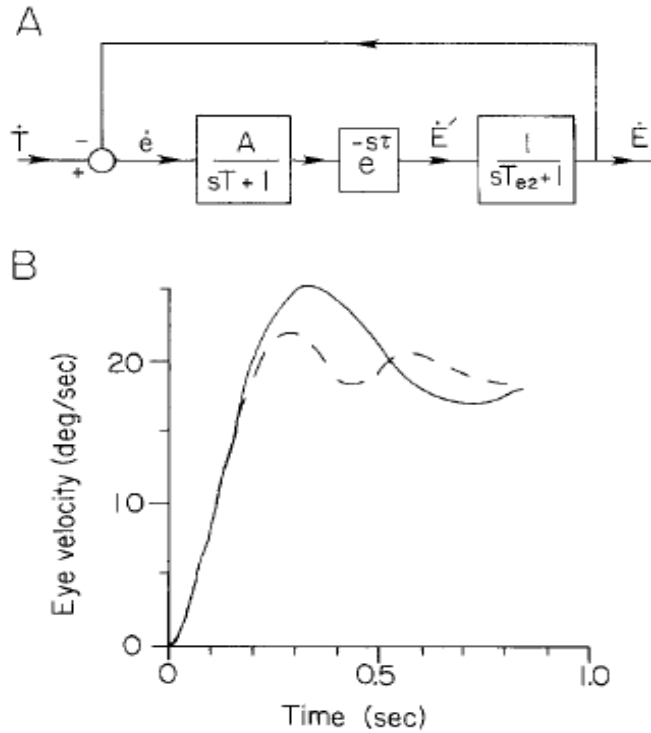


Figure 1.4. (A) Negative feed-back model for pursuit (B) the model response (dotted line) compared with pursuit response for a target moving at 20°/s (Robinson et al 1986).

Internal Positive feed-back Models

The basic model discussed in the above section cannot maintain tracking with a gain of 1 which would drive the retinal slip to zero and with it a transient drop in the eye velocity to zero. Also, the typical latency of ~ 100 ms would make system unstable. It was suggested that a central neural signal encoded in world co-ordinates could drive pursuit (Young et al 1968). Robinson (1971) recognized that the brain did not receive a signal related to target velocity from any individual sensory input and proposed that an internal copy of the target velocity was reconstructed by adding an efferent copy of the eye velocity with the processed retinal slip. This is referred to as internal feed-back model, shown in figure 1.5.

An internal copy of target velocity is computed by adding the retinal slip with an efferent copy of the eye velocity. By appropriately delaying the positive feed-back, ringing effects of the negative feed-back are eliminated. Feed-forward part of the model accounts for the initial acceleration and the internal feed-back part is used to explain the frequency of oscillations. Introducing plasticity into the model is compatible with plasticity in the pursuit system (Optican et al 1985).

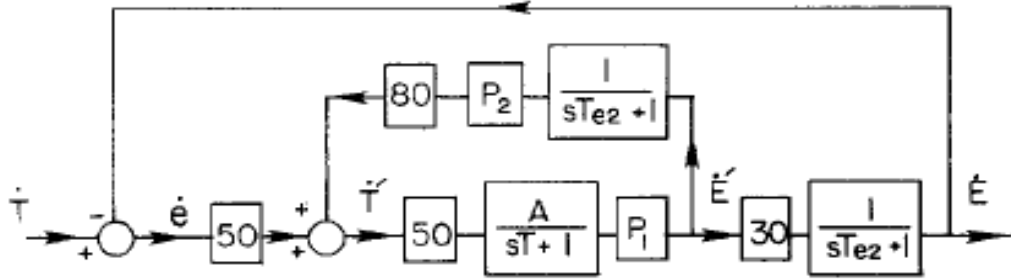


Figure 1.5. Internal positive feed-back model for pursuit. Numbers in boxes denote delays. P_1 and P_2 are associated with plasticity (Robinson et al 1986).

Psychophysical evidence of efference copy was first demonstrated by Steinbach (1969) and since then many studies investigating prediction in pursuit (discussed in next section) support the idea of an efference copy. However, dependence of frequency of oscillations on feed-back delay doesn't support the idea that frequency of oscillations could be accounted by internal feed-back (Goldreich et al 1992).

Image motion Models

Target velocity is passed through a low-pass filter before subtracting it from the eye velocity to produce image velocity. The input to the model is the image velocity which feeds the three parallel pathways namely, motion transient pathway, image velocity pathway and image acceleration pathway (Krauzlis & Lisberger 1989; 1994). Motion transient pathway responds to a threshold in velocity for 20ms and the response is equivalent to the initial 20ms early component of pursuit. The late component is driven by the image motion and image acceleration pathways. The integrator at the end is considered an equivalent implementation of eye-velocity memory.

The changes in the frequency of ringing with the changes in feed-back delay is accounted by the non-linear functions in image velocity and image acceleration pathways. An extended version of the model with a internal positive feed-back and extra-retinal signal accounts for the different dynamics observed during onset and offset of pursuit (Krauzlis & Lisberger 1994).

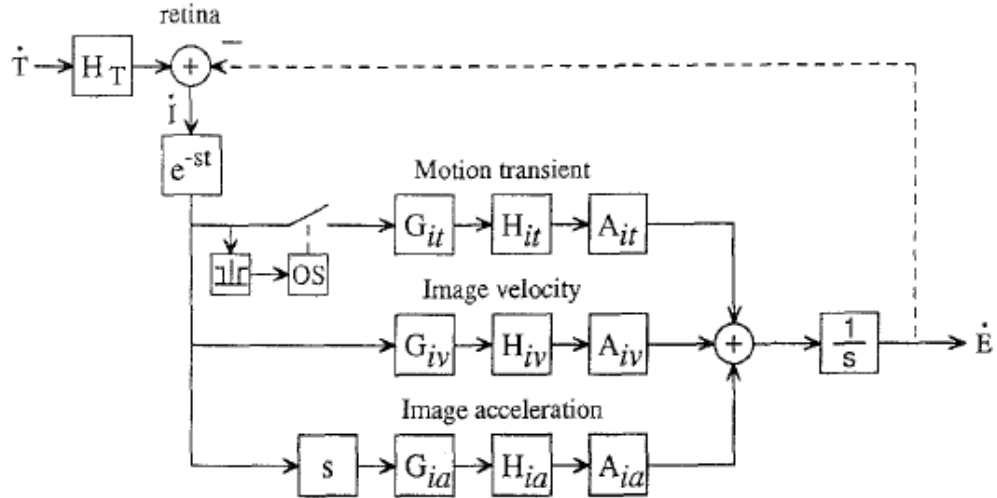


Figure 1.6. Image motion model with multiple pathways. In each pathway, G is the corresponding non-linear function, H is the second-order transformations and A is the gain (Krauzlis & Lisberger 1994).

Apart from the two dominant models briefed above, there were other models proposed to understand the stability and dynamics of smooth pursuit. A linear version of the image motion model couldn't explain the dependence between damping ratio in the oscillations and the feed-back delay (Goldreich et al 1992). A later model implementing a positive internal feed-back of image acceleration was proposed to explain the dependence between damping ratio in the oscillations and the feed-back delay (Ringach 1995). A more recent study studied the dynamics of smooth pursuit maintenance by extracting optimal linear filters that link the fluctuations in eye velocity to target velocity. The extracted filters have a high contrast sensitivity and fast dynamics suggesting the pathway for pursuit dynamics have similar characteristics. Furthermore, the filters extracted during fixation resemble the filters during pursuit suggesting a common underlying mechanism (Tavassoli & Ringach 2009).

Limitations to the approach

Although control systems approach has been used to model dynamics and stability of pursuit (Goldreich et al 1992; Krauzlis & Lisberger 1989; 1994; Robinson et al 1986; Tavassoli & Ringach 2009), there are limitations to the approach (Steinman 1986). This approach has yielded fruitful insight into the dynamics and stability of smooth pursuit which is more related to mechanics of pursuit. However, it has limited our understanding on two other

important mechanisms underlying pursuit, namely sensory processing and cognition. Sensory processing is responsible to extract speed and direction of the moving object which cannot be understood in this approach alone. Numerous studies which will be discussed in the next section have shown the effects of cognition on pursuit and certainly the models described above haven't looked into. Some of the recent models have incorporated cognition into smooth pursuit models but that has only yielded parameters to be fit manually (Barnes & Collins 2008; Bennett & Barnes 2004).

1.4. Prediction for tracking

A motor action solely based on sensory-motor transformation would not be sufficient to optimally respond to changes in the sensory information that can be predictable. To adapt to a dynamically changing environment, prediction plays an important role. Here we introduce briefly, studies that show predictive tracking in humans using different paradigms. A more detailed account of this is given in chapter 7.

The first studies demonstrating prediction for tracking used repetitive patterns of motion, usually a sinusoid (Dodge et al 1930; Westheimer 1954). For the first two to three cycles of the sinusoid, the smooth pursuit responses are delayed by the typical latency. In the later cycles, the responses lead the stimulus indicating the predictive nature of pursuit (Barnes & Asselman 1991). Even when the pattern of motion is made unpredictable using aperiodic patterns, subjects employ an average of past stimulus timing reversal in the pattern for predictive pursuit (Collins & Barnes 2009). Furthermore, when the target changes its velocity sequentially subjects generate anticipatory pursuit prior to the change in velocity for about four sequences (Barnes & Schmid 2002).

Expected target motion where target repeatedly moves in one direction also elicits slow eye movements in the direction of expected motion (Kowler & Steinman 1979a; b). Furthermore, static or verbal cues can also elicit anticipatory responses (Kowler 1989). Even causal knowledge of physical world can elicit anticipatory eye movements (Badler et al 2010). The anticipatory response is scaled to the expected target velocity (Freyberg & Ilg 2008). These studies suggest that different sources of knowledge about the future target motion can be used to evoke anticipatory smooth pursuit movements.

Transiently blanking a target during pursuit results in an exponential decay in the eye velocity if there is no expectation that the target would reappear (Pola & Wyatt 1997). However, if the subjects expects the target to reappear they could maintain eye velocity for about 4s albeit with a reduced velocity (Becker & Fuchs 1985). Several studies using

transient blanking of the translating target at different times during pursuit suggest the predictive nature of pursuit (Barnes & Collins 2008a; b; Bennett & Barnes 2003; 2004; Churchland et al 2003; Madelain & Krauzlis 2003; Bennett & Barnes 2006; Bennett et al 2007; Bennett et al 2010; Orban de Xivry et al 2008). Some of these studies would be discussed in detail in chapter 7.

The observations pointed above is better understood with the hypothesis suggesting for a short term storage of premotor drive which could be used as an anticipatory drive in the presence of expectation for target motion (Barnes & Schmid 2002). A model following this idea has been proposed to explain the predictive properties observed for smooth pursuit (Barnes & Collins 2008; Bennett & Barnes 2004).

1.5. Physiology of Smooth Pursuit

The middle temporal (MT) and medial superior temporal (MST) areas in the superior temporal sulcus (STS) process visual motion and oculomotor signals driving pursuit (see (Ilg 1997) for a review). The oculomotor signals are sent to the flocculus and ventral paraflocculus (VPF) in the cerebellum through the visuo-motor nuclei in the pontine nuclei (PON). These cerebellar regions through its projections to the vestibular nucleus (VN) drive the eyes. A second cortico-ponto-cerebellar pathway originates in the frontal eye field (FEF) provides outputs exclusively to vermis (VERM) in the cerebellum via pontine nuclei (PON). This is shown in figure 4 (Krauzlis 2004). Here, a brief overview of studies in cortical areas MT, MST, FEF and SEF involved in motion processing, gain control and anticipatory pursuit is provided (Krauzlis 2004).

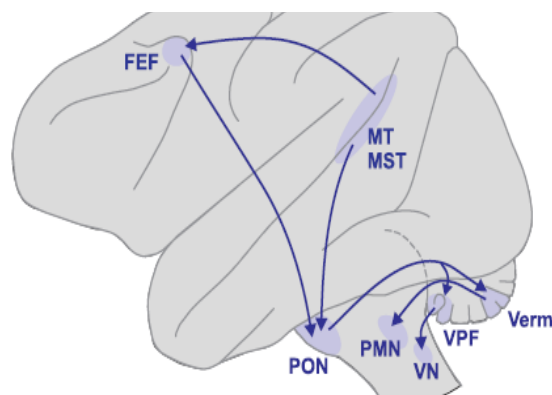


Figure 1.7. Physiology of Pursuit (Krauzlis 2004)

Deficiency in the pursuit initiation because of the lesions in striate cortex show that it

is intimately involved in the velocity computation required for pursuit (Segraves et al 1987). MT and MST of STS has also been linked to pursuit and chemical lesion studies in monkeys show that they provide visual motion information necessary to guide smooth eye movements (Dursteler & Wurtz 1988; Komatsu & Wurtz 1988; Newsome et al 1985). Chemical lesions in MT result in retinotopic deficits effecting the initiation of pursuit (Newsome et al 1985) and the same in MST result in directional deficits effecting the steady state of pursuit (Dursteler & Wurtz 1988). Since in both areas cells respond to pursuit also, apart from retinal image motion, blanking a target or using an imaginary target was used to separate the motion related activity from pursuit related activity. Area MT neurons respond only when retinal image motion is present whereas MST neurons respond when there is no retinal image motion (Newsome et al 1988) or during tracking imaginary target (Ilg & Thier 2003). Lateral part of MST (MSTl) respond to retinal input and is sensitive to retinal motion whereas dorsal part (MSTd) show an extra-retinal influence. Stimulating MSTl modifies ongoing pursuit but not initiate pursuit whereas stimulation in MSTd is ineffective (Komatsu & Wurtz 1989). These studies suggest that MT and MSTl are linked to processing of retinal signals whereas MSTd might be involved in mixing retinal and extra-retinal signals.

Smooth eye movement region of the frontal eye fields (FEFsem) contains neurons that exhibit direction-selective pursuit responses which lead pursuit (MacAvoy et al 1991; Tanaka & Lisberger 2002b). FEFsem lesions degrade visually guided pursuit (Keating 1991a; b; Lynch 1987). Inactivation of FEFsem diminishes initial smooth pursuit acceleration (Shi et al 1998). FEFsem neurons show decreased firing at initiation that correlates well with the decreasing eye acceleration (Tanaka & Lisberger 2002b). FEFsem lesions impair predictive pursuit and these neurons exhibit prediction related activity to visual target motion (Keating 1991a; MacAvoy et al 1991; Fukushima et al 2003). Stimulation of FEFsem evokes smooth eye movements (Gottlieb et al 1993). Evoked smooth eye movements has two components, a direction selective component and a gain related component (Tanaka & Lisberger 2001; 2002a). Individual Neurons in FEFsem are highly correlated with the behavior at specific times during a trial suggesting that FEFsem might regulate pursuit in a temporally selective fashion (Schoppik et al 2008). FEFsem is tightly linked to online gain control and might play a role in predictive pursuit.

Neurons in supplementary eye fields (SEF) show some selectivity for tracking direction and the discharge is maintained even in the absence of target motion suggesting the extra-retinal role of SEF in pursuit (Heinen 1995). Single neuron activity peaks when the changes in target motion is predictable (Heinen & Liu 1997). Stimulation of SEF increases

pursuit eye velocity, more so when applied during pursuit compared to during fixation (Missal & Heinen 2001; Tian & Lynch 1995). Stimulation of SEF when the target motion is predictable enhances anticipatory pursuit (Missal & Heinen 2004). SEF might also be involved in encoding decision rule and interpreting sensory signals in the context of the decision rule for smooth pursuit initiation (Kim et al 2005; Yang et al 2010).

1.6. Summary

Tracking a moving target with our eyes requires sensory estimation of the velocity of the target and a subsequent motor transformation of the velocity estimate. Since visual motion processing and tracking share a common physiological ground at the level of MT and MST of STS (Dursteler & Wurtz 1988; Dursteler et al 1987; Newsome et al 1985; Newsome et al 1988), visuo-motor transformation for tracking provides a better account of temporal dynamics involved in visual motion processing. Next chapter gives an introduction to visual motion and the physiology underlying its processing.

Control systems approach to smooth pursuit has been widely used to study stability and dynamics of pursuit (Robinson et al 1986; Krauzlis & Lisberger 1994). This approach has limitations (Steinman 1986). These models are not equipped to explain visual motion processing for smooth pursuit and also the predictive nature of pursuit. However, recent models utilizing a short term store of target velocity to explain prediction for pursuit has been proposed (Barnes & Collins 2008; Bennett & Barnes 2004). These models employ a gain parameter along with a switch that selects either sensory based drive for pursuit or predictive drive for pursuit. The gain parameter is influenced by expectation and other cognitive factors.

One of the major limitations to the approach taken by previous oculomotor models for smooth pursuit is, they are not equipped to represent uncertainty. Noise in the sensory estimation is critical to the subsequent motor transformation as it is major source of variance in the final motor outcome with motor noise being minimized with motor planning (Harris & Wolpert 1998; Osborne et al 2007; Osborne et al 2005). Motor action has to take into account the noise in the estimate so as to minimize resulting inaccuracy (See, van Beers et al 2002a for a review). Studies investigating sensory-motor transformation already suggest for a mix of measurement based signal and an internal signal based on reliability extracted from their respective uncertainties for an optimal performance in a motor task (Van Beers et al 2002b).

An engineering approach for such an adaptive behavior is a kalman filter (Kalman 1960). It involves projecting current states of the system based on the past states and

correcting the predictions based on the measurement. A mix of measurement and prediction are used to estimate the current state based on their reliability reflected from their variances. Evidence suggests such an internal model could be in place for sensory-motor transformation (Wolpert et al 1995).

This thesis proposes a hierarchical recurrent Bayesian framework to explain both, motion integration and prediction for smooth pursuit, inspired by the idea of kalman filter for predictive tracking.

Chapter 2

Visual Motion

This chapter introduces to visual motion, more precisely first order motion. It provides brief introduction to visual pathway from retina to early visual cortex and describes magnocellular and parvocellular pathways leading to Dorsal and Ventral streams. Speed and Directional selectivities arising in V1 and MT for motion perception are discussed.

2.1. Introduction

Intuitively, Motion occurs as a dimension like space or color where it creates an immediate experience (Nakayama 1985). Physically it is a reconstruction from two basic dimensions, space and time. The space-time representation of motion is used in motion detection models which will be discussed in chapter 3. Simply put, Motion is the change in position of an object with time. On the retina, visual motion occurs when ever something moves in the environment or during the self motion of the observer. However, we can perceive motion with a variety of stimuli that doesn't necessarily have an object changing its position with time. Motion perception can be of different orders depending on the physical attribute (e.g. Luminance, contrast) that leads to motion perception. This is briefly described below.

2.1.1. Different orders of motion perception

First order motion

First order motion perception involves perception of an object that differs in luminance from its back ground. First order motion is detected by the change in luminance at one point and correlating with the change in luminance at another point after a fixed delay. This thesis deals with first order motion and chapter 3 provides a brief overview on several motion detectors proposed in the literature (See (Burr & Thompson 2011; Nishidha 2011) for reviews).

Second order motion

In second order motion, motion is perceived due to moving contour resulted from changing

contrast or texture without changing the mean luminance of the stimulus (See (Ilg & Churan 2010) for a review).

2.1.2. Motion detection and the Correspondence problem

To detect first order motion, one has to measure change in luminance of the object on two successive instants of time and match the corresponding points. In a cluttered environment with multiple moving objects which is the case very often, establishing correspondence between respective luminance points on two successive frames poses a problem and this is referred to as correspondence problem. When the motion detection is local, very often visual scene doesn't contain features that help establish correspondence between two successive snapshots. The lack of correspondence exhibits itself as aperture problem which will be discussed in chapter 3. In this thesis we are interested in how outputs of each of the motion detectors operating at a local spatial scale, are integrated for global motion detection.

2.2. Physiology of Visual motion

2.2.1. Basic Visual Pathway

Seeing is a process. It starts with photons stimulating the photo receptors in the retina situated at the back of the eye. The output of the retina is coded in electrical signals. The majority of these visual signals are made available by the basic visual pathway (see figure 5) to the whole of the brain. These signals travel down the optic nerves leaving the retina. At optic chiasm, the optic nerves divide. Fibers from the nasal half of the retina cross to the opposite side of the brain and fibers from the temporal half of the retina go to the same side of the brain (Hubel).

Past the chiasm, crossed fibers from the contralateral eye join the uncrossed fibers from the ipsilateral eye to form the optic tract. Fibers of the optic tract end on the cells of the lateral geniculate nucleus (LGN) of the thalamus. The fibers of the LGN project to the neurons in the occipital cortex.

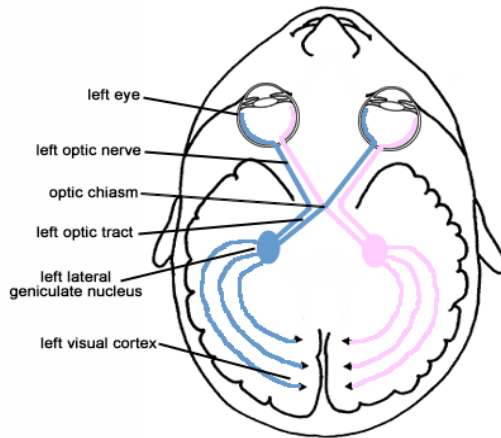
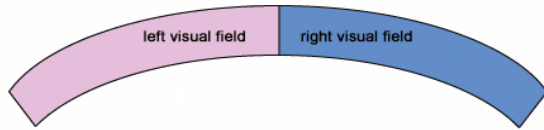


Figure 2.1. Basic Visual Pathway from retina to cortex

2.2.2. Magnocellular and Parvocellular pathways

Ganglion cells are of two types. Midget ganglion cells receive inputs from the midget bipolar cells. Parasol ganglion cells receive input from the diffuse bipolar cells. Both the types have center-surround receptive fields (Kuffler 1953). Midget cells respond with sustained firing when light shines in their excitatory regions whereas Parasol cells respond transiently. Midget cells provide information mainly about the contrast whereas the Parasols convey information about the image changes over time. Midget ganglion cells form the parvocellular pathway and Parasol ganglion cells form the magnocellular pathway and project to LGN. A third type of ganglion cells called bistratified cells form the koniocellular pathway to LGN (Wolfe 2006).

Neurons in the magnocellular layers are physically larger than the ones in the parvocellular layers. Functional studies in which magnocellular and parvocellular layers are chemically lesioned indicate that the magnocellular layers respond to large, fast moving objects, whereas the parvocellular pathway carries information for processing details of stationary objects (see (Merigan & Maunsell 1993) for a review). LGN neurons have concentric center-surround receptive fields like retinal ganglion cells. The projections onto the LGN from the retinal ganglion cells are such that the retinotopy is preserved (Hubel).

The magnocellular (M) and parvocellular (P) pathways feed into two extrastriate cortical pathways: the dorsal pathway and the ventral pathway.

2.2.3. Dorsal and Ventral Streams

Early research indicated that the P pathway continues in the ventral cortical pathway that extends to the inferior temporal cortex, and that the M pathway becomes the dorsal pathway that extends to the posterior parietal cortex (See (Maunsell & Newsome 1987; Merigan & Maunsell 1993) for a review). Results of experiments that selectively inactivate the P and M pathways as they pass through the lateral geniculate nucleus suggest that there is no explicit segregation between the pathways in V1 (Nealey & Maunsell 1994). However, inactivating the magnocellular layers of the lateral geniculate nucleus eliminates the responses of many cells in MT and always reduces the responses of the remaining cells and blocking the parvocellular layers produces a much weaker effect on cells in MT (Maunsell et al 1990). In contrast, blocking the activity of either the parvocellular or magnocellular layers in the lateral geniculate nucleus reduces the activity of neurons in V4 (Ferrera et al 1994). This suggests that the dorsal pathway to MT seems primarily to include input from the M pathway, whereas the ventral pathway to the inferior temporal cortex appears to include input from both the M and P pathways. Here, we focus on the dorsal stream which predominantly involves motion processing at least at the level of MT which is higher up in the visual hierarchy.

2.2.4. Dorsal Stream : Flow of motion information

Flow of visual information for the processing of visual motion starting from retina to various structures is shown in figure 6. The M pathway projects from the magnocellular layers of the lateral geniculate nucleus to the striate cortex, first to layers 4C α and 6 of primary visual cortex (V1) and then to layer 4B. MT receives information directly from the layers 4B and 6 and indirectly from the thick stripes of V2 and V3 (Felleman & Van Essen 1991).

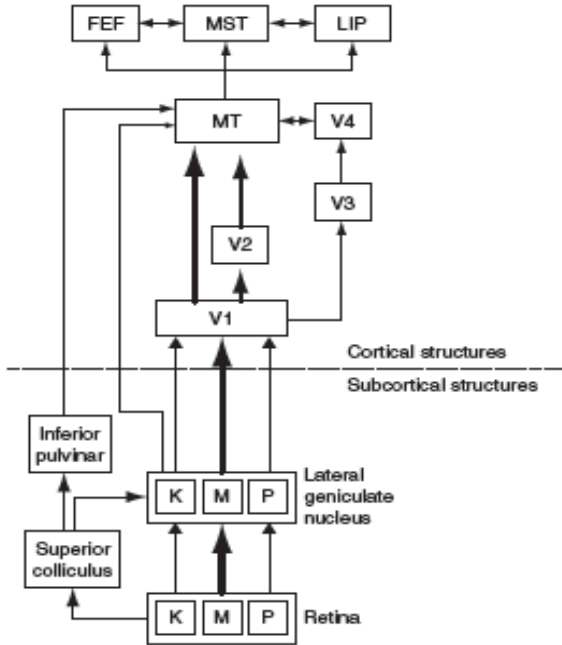


Figure 2.2. Motion processing pathways from the retina to different cortical areas. Thickness of the lines indicate the strength of the pathway (Price & Born 2009)

MT passes information to areas including dorsal part of middle superior temporal area (MSTd) and lateral part of middle superior temporal area (MSTl) which are higher up in the hierarchy. MSTd also receives extra-retinal input (Ilg & Thier 2003; Newsome et al 1988). Both MT and MST connect to higher cortical areas such as area 7a, the lateral intraparietal area (LIP), and frontal eye fields (FEFs) which are involved in guiding decision making and eye movements and also to subcortical structures such as the accessory optic system, pontine nuclei, superior colliculus, and pulvinar to guide eye movements such as pursuit and optokinetic nystagmus (Ilg 1997).

The next section describes the visual motion processing in the early dorsal stream predominantly in V1 and MT, which involves extracting speed and direction of the moving object.

2.3. Representation of Motion in Visual Cortex

Early physiological studies identified Middle temporal area of visual cortex (MT/V5) as a specialized area for processing visual motion (Allman et al 1973; Dubner & Zeki 1971). Processing visual motion involves extracting speed and direction of the moving object. Middle temporal area of visual cortex (MT/V5) has neurons that respond selectively to visual motion and tuned for speed and direction of an object moving in their receptive fields

(Maunsell & Van Essen 1983). Speed tuning and direction tuning are largely independent and doesn't effect each other (Lagae et al 1993; Rodman & Albright 1987). However, speed and direction estimation might share a common neural source for noise (Osborne & Lisberger 2009). Microstimulation in MT alters direction and speed of pursuit responses, as well as speed perception and direction discrimination (Carey et al 2005; Groh et al 1997; Liu & Newsome 2006; Salzman et al 1992). Chemical lesions in MT leads to deficits in visual motion processing which selectively impairs motion perception as well as pursuit responses (Newsome & Pare 1988; Newsome et al 1985). Lesions in MT also impairs speed discrimination (Rudolph & Pasternek, 1999). These studies suggest that MT is intimately involved in visual motion processing for perception and action. The following sections present a brief overview of studies investigating how speed and direction is selectively represented, especially in V1 and MT of visual cortex.

2.3.1. Speed Selectivity

Motion could be characterized in the Fourier domain and speed is defined as the ratio between temporal frequency and the spatial frequency. Speed could be visualized as a tilt in the spatio-temporal domain. One way to test the speed-tuning of neurons in motion sensitive areas is using a moving sinusoidal grating at different spatial frequencies and see if the response field is tilted in spatio-temporal space. This is shown in figure 2.3. For an example MT neuron which is not speed-tuned (figure 2.3.A,B) varying the spatial frequency shifts the preferred speed and this is also reflected in the spatio-temporal frequency plot where there is no tilt in the response field. Similarly, for an example MT neuron which is speed-tuned (figure 2.3.C,D) varying the spatial frequency doesn't change the preferred speed and this is also reflected in the spatio-temporal frequency plot where there is a tilt in the response field. When two sinusoidal gratings are used, neurons dependence on spatial frequency declines and becomes more speed tuned. This could be because of speed-tuning non-linearities which then explains why square gratings elicit more speed-tuned responses (Priebe et al 2003).

Motion sensitive neurons in primary visual cortex of cat could be tuned for speed independent of form, i.e. changing the spatial frequency alters the temporal frequency tuning such that preferred speed is maintained (Movshon 1975). This is often referred to as spatio-temporal inseparability. Alternatively, neurons could have separate spatial frequency tuning and temporal frequency tuning. Early studies in primary visual cortex of cat demonstrated spatio-temporal separability (Friend & Baker 1993; Holub & Morton-Gibson 1981; Tolhurst & Movshon 1975).

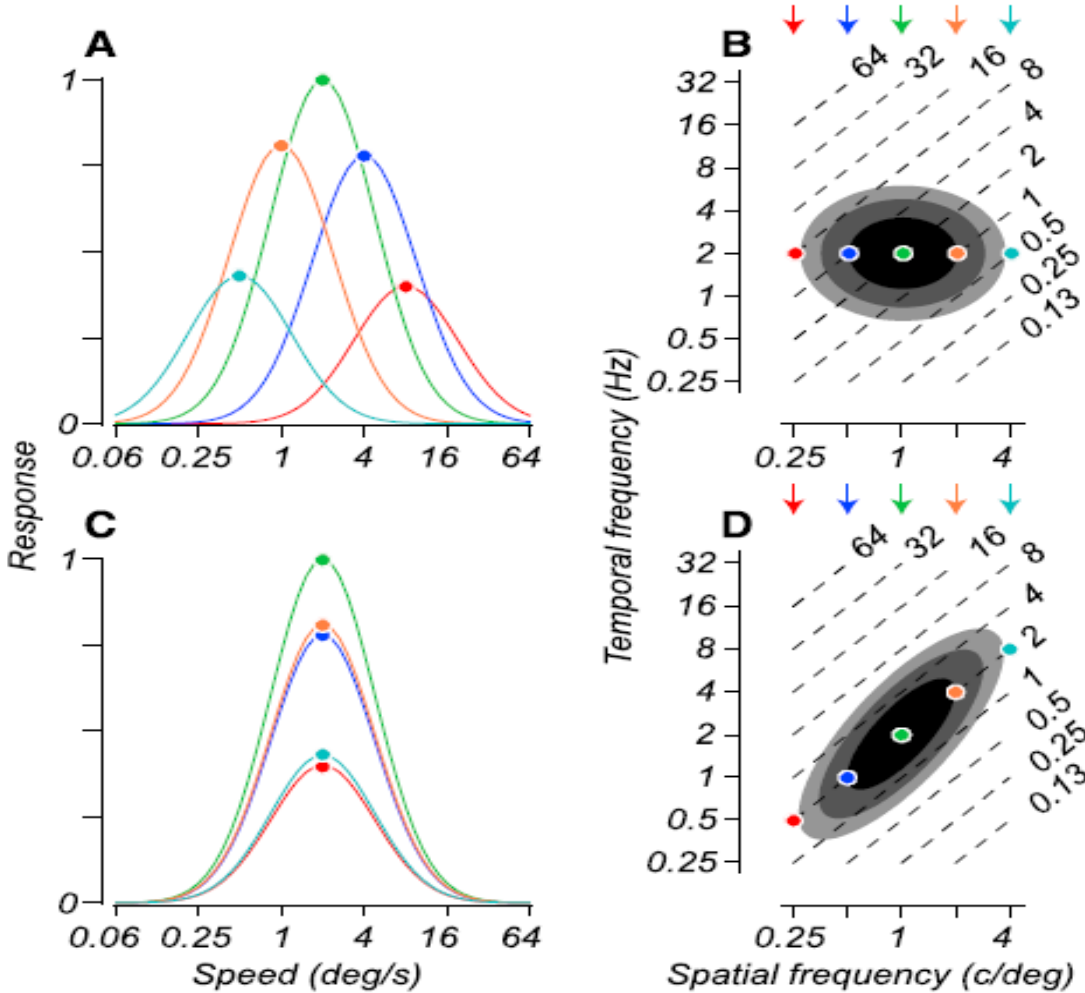


Figure 2.3. Speed tuning in MT neurons. (A,C) Responses of an MT neuron as a function of speed at different spatial frequencies (shown in different colors). (B,D) Response field of the same neuron in spatio-temporal frequency domain (Priebe et al 2003).

Initial study on speed-tuning in MT using different spatial and temporal frequencies concluded that MT neurons are speed-tuned (Perrone & Thiele 2001). However, a later study analyzing the spatio-temporal response profiles for different speeds suggest that only 25% of MT neurons are speed tuned (Priebe et al 2003). Furthermore, MT doesn't have a columnar organization of speed tuned neurons (Liu & Newsome 2002). A similar study in V1 showed that speed-tuning in V1 neurons is no different than it is in MT suggesting that speed-tuning in MT could be inherited from V1 (Priebe et al 2006). Effects of contrast on speed tuning was also investigated. Neurons in V1 that were not speed tuned for low contrast conditions became more speed tuned for high contrast conditions and neurons in MT shifted their preferred speeds to lower speeds for lower contrasts (Krekelberg et al 2006; Priebe et al 2006). Presumably, this could be because of the contrast gain modulation in their receptive

fields. A model implementing a weighted intersection mechanism could explain the 25% speed tuning observed in V1 and MT neurons along with contrast modulation of speed tuning and suggested that the percentage of speed-tuned neurons could be higher (Perrone 2006).

2.3.2. *Direction Selectivity*

Motion sensitive units contributing to primate motion perception are first encountered in primate visual cortex (V1) in the visual pathway. Nearly 20-30% of neurons in V1 respond to a narrow range of directions and are direction selective (Hubel & Wiesel 1968). Neurons are classified as simple, complex and hyper-complex. Simple cells respond to stimuli moving in the preferred direction. Complex cells are similar to simple cells except that they are phase insensitive. They respond to motion of the stimulus in the preferred direction starting anywhere in the receptive field. Hyper-Complex cells also known as end-stopping cells respond to terminator endings of the stimuli moving in the preferred direction. Most of the neurons in layer 4B which provides bulk of the connections to MT are end-stopped (Sceniak et al 2001). Evidence suggests that direction selective neurons in V1 project to MT (Movshon & Newsome 1996).

All neurons in MT exhibit high direction selectivity (Albright 1984). Many neurons also show inhibition by motion in the null direction, a property which gives rise to the motion after effect (MAE). All the direction-selective neurons in MT are organized into a map, with neurons that are tuned to the same direction of motion grouped together in columns, and adjacent columns representing different directions of motion (Albright et al 1984). MT neurons reflect ~80% of information about motion direction in the first 100ms of stimulus presentation (Osborne et al 2004).

In short, V1 motion sensitive cells detect motion locally from visual motion scene and this local motion information from different cells is integrated at the level of MT. Since motion integration is the primary focus of the thesis, it would be discussed in detail with the data from psycho-physics, physiology and smooth eye movements, in Parts 2 and 3.

2.4. Motion estimation

Target motion activates MT neurons. Because of the tuned responses, neither the activity of a single MT neuron nor an average activity of the population gives an unambiguous estimate (See, lisberger 2010, for a review). The population responses in MT has to be estimated for both perception and action. This is indeed a more generic question how population activity is

estimated for perception and action. Several possible computations could lead to an estimate. They include winner take-all, vector summation or vector averaging (Groh 2001; Pouget et al 1999; Robinson 1972; Salinas & Abbott 1994).

Vector averaging is insensitive to the amplitude of the population since its is normalized with the total population activity. Vector averaging determines center of mass of the population activity which can explain the strong dependence of initial 100ms of pursuit on speed (Lisberger & Westbrook 1985) and the effects of degraded motion (Churchland & Lisberger 2001). However, vector averaging cannot explain the relationship between MT responses and pursuit for different forms and contrasts (Krekelberg et al 2006; Priebe & Lisberger 2004).

The neural estimate changes from trial to trial which is particularly evident in pursuit responses. Majority of the variance in pursuit could be accounted by the error in sensory estimation (Osborne et al 2005). The error in sensory estimation for pursuit is only slightly higher than for perception in both speed and direction discrimination (Osborne et al 2007). This might suggest that perception and pursuit might be effected by the same source of noise. Averaging over population should eliminate noise but that is not the case. Since the activity of neurons with similar stimulus preferences (e.g. speed or direction) fluctuate together from trial to trial, averaging cannot eliminate correlated noise (Haung & Lisberger 2009; Zohary et al 1994). However, role of sensory noise in motor transformation is not well investigated as opposed to motor noise which plays a critical role in motor planning (Harris & Wolpert 1998).

2.5. Summary

Neurons in the Early visual cortex (V1) are the first to detect motion along the visual pathway that leads to perception (Hubel & Wiesel 1968). They respond to motion in a preferred direction and they are characterized as direction selective cells. However, they can only detect motion locally because of their limited receptive field sizes and these local measurements are ambiguous (aperture problem). Chapter 3 describes aperture problem and local motion detection. Because of the ambiguity involved with each local motion measurement (aperture problem), responses of the local motion detectors in the early visual system need to be integrated to arrive at a global velocity estimate of the moving target. On the outset, MT is a more likely candidate for the integration of local motion signals because of its position in the hierarchy (Felleman & Van Essen 1991) of the visual motion pathway and also, neurons in MT are highly direction selective (Albright 1984) and inactivation of

MT leads to deficits in motion perception (Newsome & Pare 1988) as well as pursuit initiation (Newsome et al 1985). Chapter 4 describes perceptual account of the motion integration and chapter 5 describes the action account of motion integration through smooth eye movements.

Part - 2

Aperture Problem and Motion perception

Chapter 3

Local motion detection and aperture problem

The previous chapter described direction selective neurons in V1, that detect motion locally. This chapter describes the aperture problem for the early visual motion selective neurons. It also describes three different motion detection mechanisms namely reichhardt detector, Motion energy detector and gradient detector that are widely discussed in the literature. Aperture problem is also described in the context of each motion detection mechanism.

3.1. Aperture problem

Motion sensitive cells in V1 have limited receptive field sizes that detect motion locally in visual motion scene (Hubel & Wiesel 1968). The motion information viewed through this aperture is ambiguous. This is illustrated in the figure below. Consider two successive frames of a tilted bar translating upwards as shown in the figure below. Consider the receptive field of a motion sensitive neuron extracting information along the bar as shown by a circle in the figure below.

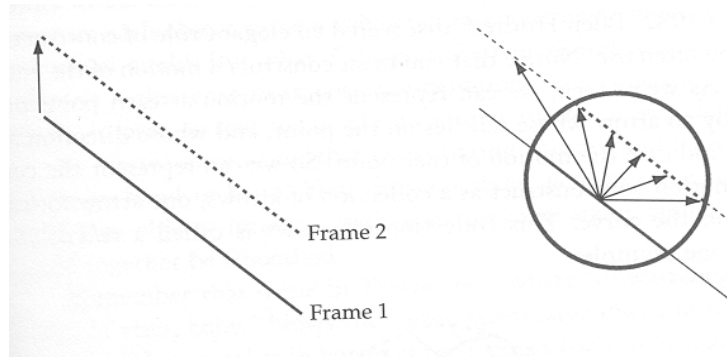


Figure 3.1. Aperture problem

The change in the luminous information between frames, when viewed through this aperture would indicate a family of motion vectors. The motion information along the bar is essentially ambiguous and this results in the aperture problem (Wallach 1935; Wuerger et al

1996). All motion sensitive cells extracting local motion information which is ambiguous encounter aperture problem (see, Hildreth & Koch 1987; Krekelberg 2008, for reviews).

3.2 Reichardt detector

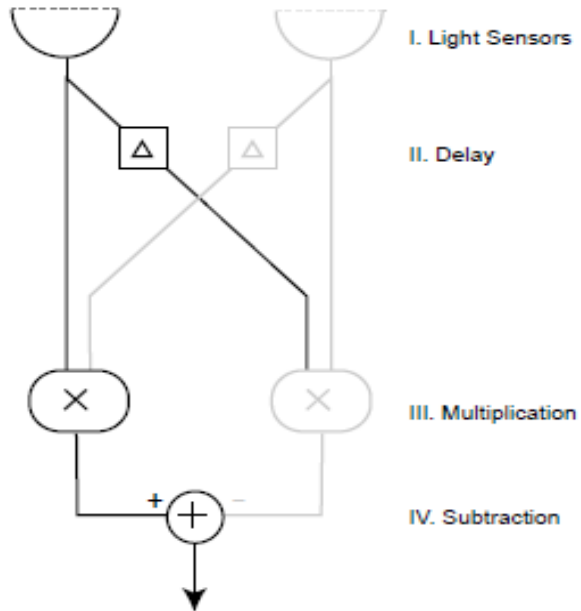


Figure 3.2. Reichardt detector (Krekelberg 2008)

Reichardt detector is the simplest motion detector designed based on the observations made in beetle (Hassenstein & Reichardt 1956). A schema of it is shown in figure 3.2. It has two light sensors. The output of one sensor is delayed and multiplied with the output of the other sensor. This is essentially a space-time correlation (Reichardt 1961) between signal from sensor at one location and a delayed signal from sensor at next location. This stage determines the direction selectivity of the detector. The output of the rightward motion detector is substracted from the leftward motion detector to improve the selectivity of the detector.

Although the reichardt detectors can select motion in a direction, they can signal motion for objects moving in a different direction with a shape that can trigger both the light sensors with the given delay. This is illustrated in the figure below. This is aperture problem manifestation for the reichardt detectors (Bradley & Goyal 2008).

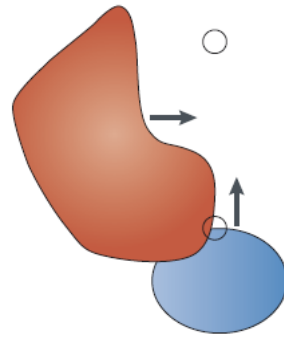


Figure 3.3. Aperture problem with Reichardt detector (Bradley & Goyal 2008)

3.3. Spatio-Temporal Motion Energy Model

Adelson and Bergen (1985) proposed spatio-temporal filtering model to extract motion energy. They reasoned if motion is represented in space-time, the tilt of the path traced by the object in space-time shows the velocity of the object. The figure 3.4 below shows the space time representation of a bar moving right (Adelson & Bergen 1985).

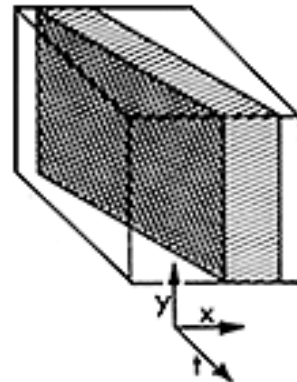


Figure 3.4. Space-time representation of motion (Adelson & Bergen 1985)

If the tilt in the space-time representation gives the velocity of the object, filters that are oriented in space-time would signal motion in a selective direction. The figure below shows an example of the tilts in space-time plots representing different velocities and filters oriented in space-time to extract selective motion.

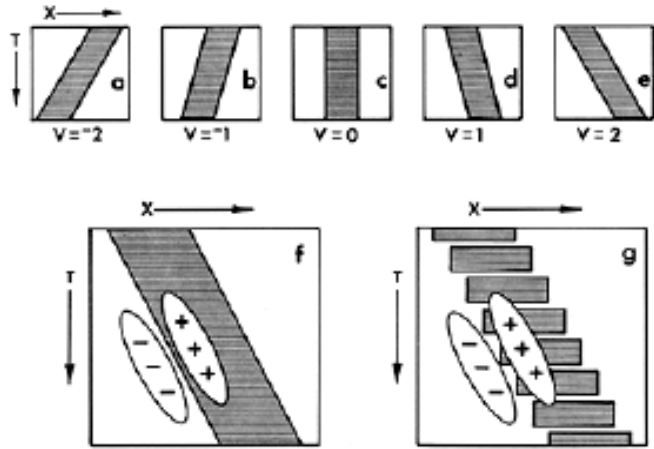


Figure 3.5. Extracting motion with space-time oriented filters. (a-e) space-time representation of different velocities. (f,g) Filters oriented in space-time to extract motion (Adelson & Bergen 1985)

To build a motion selective unit that responds to motion, the input to the unit is passed to the Spatial impulse response function and then the temporal impulse response function. The resultant spatio-temporal response is separable and doesn't have an orientation in the space-time representation as shown in the figure 3.6 below. This means the unit would detect motion but is not direction selective. To build a motion selective unit that is direction selective the spatio-temporal filter should have an orientation in space-time, and the spatio-temporal response is inseparable. However, spatio-temporal oriented filter can be created by summing the output of four separable filters that are identical except for a shift at receptive field center and a temporal delay (Watson & Ahumada 1985).

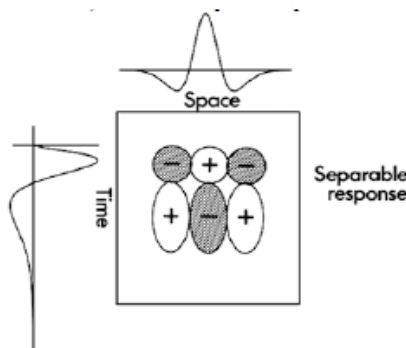


Figure 3.6. Spatio-temporal filter (Adelson & Bergen 1985)

The spatio-temporal filters oriented in space-time are direction selective and are equivalent to simple direction selective cells (shown in figure below). However, they are

phase sensitive. A quadrature pair is used to build phase insensitive direction selective unit. The output of the two filters of the quadrature pair is squared to extract the energy in the response. This is the motion energy step which is equated to complex cell. The schema of the motion energy model is shown below.

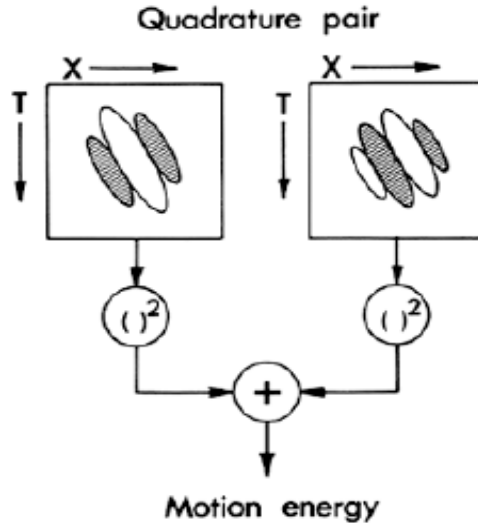


Figure 3.7. Motion energy model (Adelson & Bergen 1985)

The transformation of spatio-temporal frequency filters in the space-time domain to frequency domain yields a small spherical spectrum (band pass) where as the moving object represents a plane in frequency space (Watson & Ahumada 1985). Since many planes can pass through this small spherical spectrum, a simple direction selective unit cannot determine the object velocity. This is the manifestation of aperture problem in motion energy model.

3.4. Gradient Model

The principle of the gradient models is that the spatial and temporal change must coincide in an image to give rise to motion. This is expressed mathematically as,

$$I_x V_x + I_y V_y = -I_t$$

where,

I_x , I_y , I_t is the partial derivative of Image intensity at position (x,y) and time t, denoted as $I(x, y, t)$ w.r.t. x, y, t respectively.

V_x , V_y denote the x and y components of object velocity.

The gradient equation has two unknowns in V_x , V_y . Clearly with one equation, which stands for one local measurement we cannot determine an object velocity. This is the manifestation of the aperture problem in the gradient models (Bradley & Goyal 2008).

3.5. Summary

An extended version of the Reichardt detector (van Santen & Sperling 1985) along with motion energy model and the model proposed by Watson and Ahumada (1985) have essentially the same computations except the order of the computations is different between models. They share a common theme to define motion in frequency space and analyse motion using spatio-temporal filters (Krekelberg 2008). As described in the previous sections, none of the local motion detection mechanisms are free of aperture problem. The output from several local motion detectors is integrated to solve the problem. This integration is a dynamic process which will be discussed in the coming chapters.

Chapter 4

Psychophysics of motion perception

This chapter describes different schemes for combining local motion information to construct object's global velocity. Psychophysical and physiological studies investigating these schemes are presented. Psychophysical, physiological and computational studies looking at the role of 1D and 2D motion information for motion perception is described along with dynamics of motion integration. A unifying model using bayesian inference which explains much of the psychophysical data is described.

4.1. Solving Aperture problem

Local measurements on the visual motion scene are ambiguous (aperture problem) irrespective of which motion detection mechanism used, as described in the previous chapter (Wallach 1935; Wuerger et al 1996). Aperture problem is solved by combining the local motion estimates to obtain the object's global velocity (see (Bradley & Goyal 2008; Hildreth & Koch 1987) for a review). Several schemes are proposed how the visual system could combine these local motion estimates. They are as follows.

4.1.1. Vector Averaging (VA)

The simplest way to combine the local motion vectors is to take the vector sum (vector average) of the two. Although it does not provide an accurate estimate of object's speed and direction, it is correlated. The output of VA scales with the input and is dependent on the shape of the object. This is shown in the figure below. As the object size increases, even when the local velocity estimate is the same, the object's speed given by VA decreases.

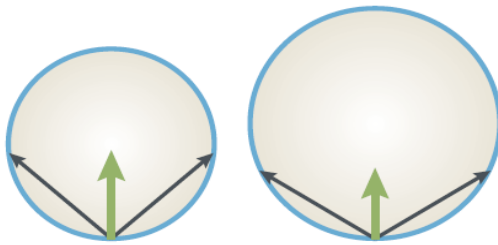


Figure 4.1. Vector Average for objects of different shapes (Bradley & Goyal 2008)

4.1.2. Intersection of Constraints (IOC)

Intersection of Constraints utilizes the geometric relation between local velocity samples and the object velocity to extract the object velocity from the local samples (Fennema & Thompson, 1979; Marr & Ullman, 1981). Any local velocity sample could be expressed as

$$S_l = S_o \cos(\theta_l - \theta_o)$$

where, S is the speed and θ is the direction. The subscripts indicate local or object's speed and direction. Since there are two knowns in the above equation, we need two samples. Solving the equations one would arrive at the object's velocity estimates, i.e. Speed and direction. Shown below is the geometric equivalent of solving two equations.

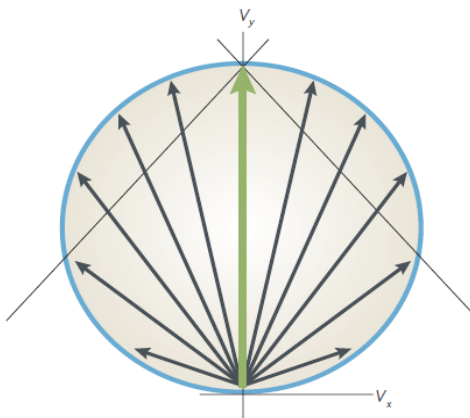


Figure 4.2. Constructing IOC solution from local velocity samples (Bradley & Goyal 2008)

Shown in the figure above is the representation of local velocity vectors in the velocity space. Note that the length of the vector is dependent on the cosine of the angle between object's velocity vector and local velocity sample. To obtain the object velocity from the local velocity samples, draw perpendicular to any two local velocity samples and the intersection between the two is the tip of the object's global velocity starting from the origin. This is illustrated in figure 4.2. One of the widely known model implementing IOC principle to compute object's velocity from local velocity samples is 'S and H' model.

S and H Model

S and H model (Simoncelli & Heeger 1998) is an extension of the motion energy model (Adelson & Bergen 1985), which models the local velocity computation equivalent to the output of component direction selective (CDS) cells. The output of the CDS cells are combined in a linear way and passed through non-linear stages of half wave rectification and divisive normalization. This stage is equivalent to MT which provides the output of the pattern direction selective (PDS) neurons tuned to speed and orientation. This is better understood in the frequency domain. As noted in the previous chapter, the spatio-temporal filters of the local velocity estimation stage (CDS) are blobs of band-pass filters in the frequency domain(Watson & Ahumada 1985). This is shown in the figure below. A plane in the frequency space denotes the object's velocity. To compute the object's velocity the local samples lying on the object's velocity plane has to be pooled. This is the second stage of the S and H model shown in the figure below. In effect, Cells (PDS) in the second stage of the model are velocity tuned independent of the spatio-temporal composition of the stimulus.

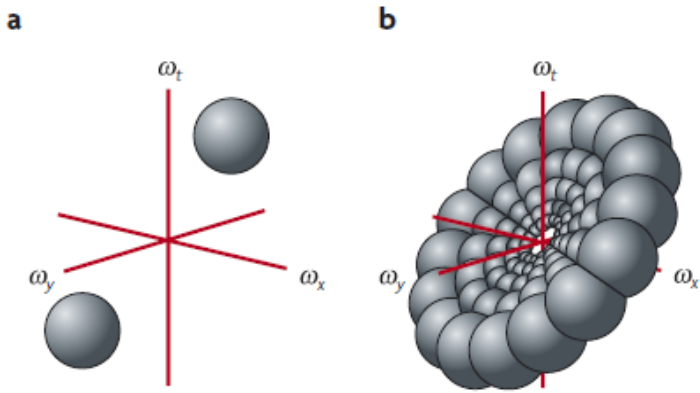


Figure 4.3. CDS and PDS cells in frequency space. (a) band pass blobs of CDS cell in frequency domain (b) pooling of PDS cell in frequency domain

This is not the case with physiology. Velocity tuning is found to be rare in MT (Priebe et al 2003) and is no different than it is in V1 (Priebe et al 2006).

4.1.3. Feature Tracking (FT)

Features from a moving object provide unambiguous motion information about the velocity

of the object. Feature tracking involves selecting features in the moving object and tracking them. In contrast, Motion sensitive units in the early visual cortex doesn't signal a moving dot. This makes explicit feature tracking less viable. However, models using selected features along with simple motion energy pathway were proposed(Nowlan & Sejnowski 1995; Wilson et al 1992) . These models will be discussed in section 4.9.

4.2. Stimuli for Motion integration

A variety of simple stimuli are used to study motion integration. Different stimuli reflect different proportion of ambiguous (1D) and unambiguous motion signals (2D) .

Bar field stimulus : A single translating bar has 1D motion signals along the bar and 2D motion signals from the terminator endings. This is shown in the inset of figure 4.4a. The 1D motion vector is perpendicular to the orientation of the bar and has an upward component where as the 2D motion vector has a downward component. A field of such bars in a circular window is used to study the dynamics of 1D and 2D motion integration (Lorencean et al 1993).

Barber pole stimulus : A series of bars translating behind a rectangular aperture forms the barber pole stimulus (figure 4.4b). The motion information along the bar is 1D in nature and motion information at the intersection along the borders is 2D in nature (Castet et al 1999).

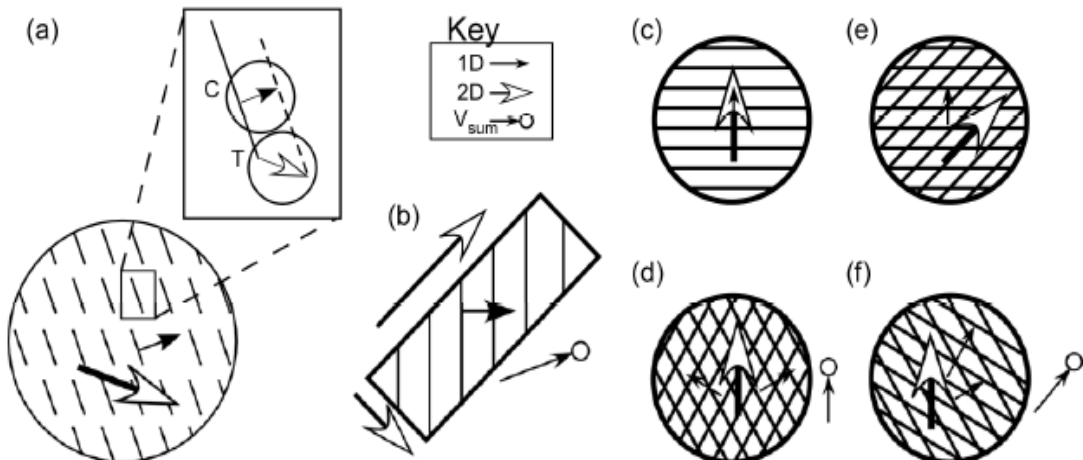


Figure 4.4. Different stimuli for motion integration (a) Field of bars, shown in the inset are the 1D and 2D motion vectors for each bar (b) Barber pole stimulus (c) Grating (d) Type-I plaid (e) Uni-kinetic plaid (f) Type-II plaid. (Born et al 2010)

Grating : Circular windowed moving sinusoidal gratings are the source of 1D motion signals

(figure 4.4c).

Type-I Plaid : Type-I plaids are constructed by combining two circular windowed sinusoidal gratings that are rotated with respect to each other (figure 4.4d). The gratings are the source of 1D motion signals. The intersection between gratings are blobs whose velocity is the VA of the two gratings (Adelson & Movshon 1982; Movshon et al 1986).

Unikinetic Plaid : It is a superposition of a moving horizontal grating on top of a static oblique grating (figure 4.4e). 1D motion signals are upward where as the 2D motion signals from the intersections have a horizontal component (Masson & Castet 2002).

Type-II Plaid : Similar to Type-I plaids except that the perceived direction is different from two components and the VA (figure 4.4f)(Wilson et al 1992).

4.3. Psychophysics of plaids

Perception of visual plaid stimuli depends on different properties of the component gratings, namely spatial frequency, contrast, speed, angle between the gratings. Plaids with similar spatial frequency and contrast result in the percept of a single motion direction referred to as coherence. Coherent percept is used as a measure of integration of 1D motion signals in the component gratings. The conditions for coherence is investigated by Adelson and Movshon (1982), which is summarized below.

4.3.1. Conditions for Coherence

Coherent percept for plaids is tested by using a component grating as a standard and the other as the test. Effect of contrast on the probability to detect the test grating (open circles) and for a coherent percept (closed circles) is shown in the figure 4.5a below. With contrast, the probability to detect the test grating increased monotonically and for the coherence, although the test grating is visible for a considerable range of contrasts (0.01-0.07) it didn't result in a coherent percept (figure 4.5b).

The threshold for a coherent percept is shown in figure 4.5b as the spatial frequency of the test grating varied for two different spatial frequencies of standard grating. The dip in the two plots indicates the threshold for coherence is lowered when spatial frequency of the test grating is similar to that of the standard. The speed and orientation of the gratings also effects coherence. Coherence decreases as the speed of the gratings increases, as the angle between them increases.

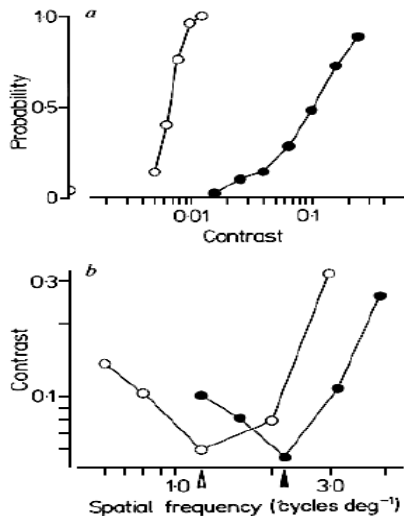


Figure 4.5. Conditions for Coherence (a) Effect of contrast on the probability to detect a test grating (open symbols) and probability for a coherent percept (solid symbols). (b) Effect of spatial frequency for a coherent percept for two different spatial frequencies of standard grating(Adelson & Movshon 1982).

4.3.2 Models for the perception of coherence

Two models could explain the perception of coherent pattern motion. The first is a model which passes the image through non-oriented band pass filters for different spatial frequencies parallelly. The output of these filters select the blob like features at the intersections of the gratings and assigns this velocity to the whole pattern. If the gratings are of same spatial frequency, they are passed through the same filter and the blobs at the intersection are detected and the unambiguous velocity is assigned to the whole pattern. Whereas if the gratings are of different frequencies, they are not passed through the same filter hence there would be no peaks or troughs to be tracked(Movshon et al 1986).

The second model is a two stage model with oriented band pass filters in the first stage. The output of these filters is sent to local motion analyzers which signal the 1D motion components of the individual gratings. These 1D signals are combined at a later stage using an IOC principle to obtain a pattern velocity. These two hypotheses are further tested using Noise masking and adaptation experiments.

4.3.3. Noise Masking experiment

A one dimensional dynamic noise is used to mask the gratings that compose the plaid

(Movshon et al 1986). When the noise mask is parallel to the component gratings the coherence thresholds were elevated. When the orientation of the noise mask deviated from that of the component gratings towards orthogonal, the coherence threshold had no effect. This reflects that the initial filtering is oriented and when the noise has the same orientation as the components, it elevates coherence threshold.

4.3.4. Adaptation experiment

The idea that motion processing involves two distinct stages as described in the second model was tested differentially for two stages using adaptation (Movshon et al 1986). The stimuli were a grating and a plaid and there are four possible pairs of adapt and test stimuli. When the test stimulus has the same components as adapt, detection thresholds were considerably elevated. This is shown in the figure below.

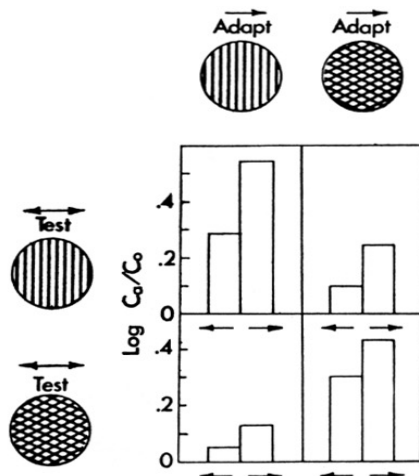


Figure 4.6. Effect of adaptation on the detectability. Contrast threshold elevation is the ratio of adapted to unadapted contrast threshold, expressed in log units (Movshon et al 1986).

The coherence thresholds were measured with the same adapt and test as shown in the figure 4.7. The change in the coherence threshold is shown in the figure 4.7 below for one condition where the adapt is rightward moving grating and the test is a rightward plaid (Movshon et al 1986). For this combination the detection threshold didnot elevate but the coherence thresholds rise for the adapted direction with spatial frequency. The above mentioned adaptation experiments supported the idea of two stage processing of motion. The first stage computing the local motion through spatial analysis of oriented filters since the component motion elevated detection thresholds and the second stage computing the pattern motion using IOC , since pattern motion elevated coherence thresholds.

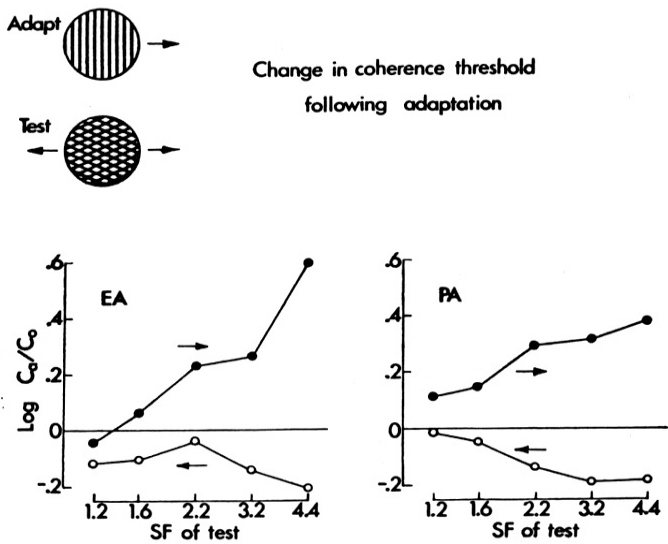


Figure 4.7. Changes in coherence threshold following adaptation for different spatial frequencies (Movshon et al 1986)

4.4. Physiology of plaids

Physiological studies in V1 and MT of the macaque using plaid stimulus has classified cells into component direction selective (CDS) and pattern direction selective (PDS). Responses of CDS and PDS cells to plaid and gratings is shown in the figure 4.8 below. CDS cells respond to the component gratings of the plaid whereas PDS cells respond to the pattern motion. None of the cells in V1 are classified as PDS whereas in MT 25% are classified as PDS and 40% as CDS. This along with the adaptation experiments supported the idea of two stage visual motion processing where the first stage computes the component motion and the second stage combines the component motion signals to compute the pattern motion (Movshon et al 1986;Gizzi et al 1983). Another study investigating direction selectivity in MT found neurons that are functionally distinct (Albright 1984) and in the later study they were classified as pattern direction selective (Rodman & Albright 1989).

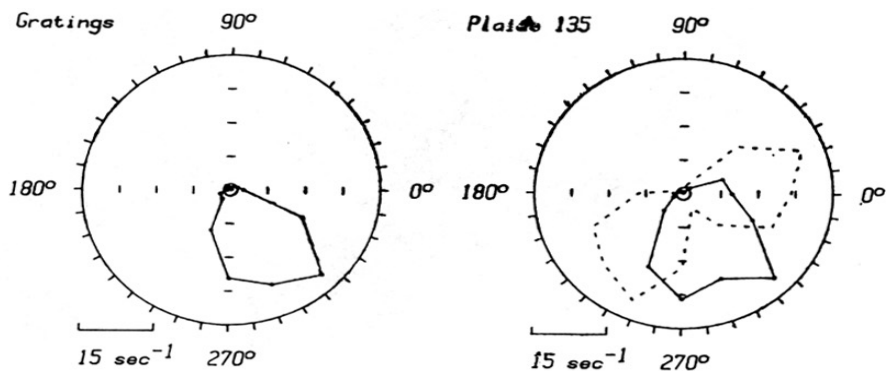


Figure 4.8. Responses of a PDS cell to gratings and plaid stimuli. Dotted lines show expected responses for a CDS cell (Movshon et al 1986; Gizzi et al 1983)

4.5. Alternate computations to IOC

With symmetric plaids (Movshon et al 1986) one can't differentiate, if the pattern velocity is constructed by IOC or VA or the blob features at the intersections of the component gratings. Several other studies used stimuli where IOC solution differs from that of VA and these include type-II plaids(Wilson et al 1992), modified type-II barber pole stimuli (Rubin & Hochstein 1993), multiple line segments each presented in a separate aperture (Mingolla et al 1992) and for a thin rhombus at low contrast (Weiss et al 2002). Results from all of the above studies indicate that the visual motion system doesn't always perform an IOC computation. Some of these studies will be presented in section 4.6.

With Type-II plaids (figure 4.4f) at low contrasts and brief exposure times, the perceived direction is the vector average of the components and after about 150ms it converges towards IOC (same as feature direction). A parallel pathway model is proposed to explain these findings which will be discussed in section 4.9. However, this may not be generalized to all type-II plaids. By increasing the ratio between the speeds of the component gratings, the separation between IOC and VA solutions was increased and for short durations subjects perceived IOC solution (Bowns 1996). Using stimuli for which IOC and VA predict different solutions and adapting one of the solutions through motion adaptation switched perceived direction to the other solution (Bowns & Alais 2006). The effects were symmetrical: shifts from IOC to VA, and from VA to IOC, were observed following adaptation. These large shifts indicated that multiple solutions to global motion processing co-exist and compete to determine perceived motion direction.

4.6. Perceptual account of the dynamic motion integration

4.6.1. Role of terminators in motion integration

From the work of (Wallach 1935), it is known that the perception of barber pole stimuli is dependent on the direction of motion at the edges (Kooi 1993). For example, horizontal apertures result in higher terminators signals at the intersection between oriented lines and the edges of aperture and result in the perception of horizontal moving stimuli. Terminators were classified as intrinsic or extrinsic. Intrinsic terminators belong to the edge of the stimulus and can be coded by disparity information or using an invisible aperture. Extrinsic

terminators are created by occluding edges (Shimojo et al 1989). Extrinsic terminators facilitate integration of motion signals from different apertures whereas intrinsic terminators would not facilitate integration (Lorenceau & Shiffrar 1992). Masking intrinsic terminators using low contrast or blurring facilitate motion integration of 1D motion signals across space. It has also been shown that terminators play a role in integrating motion signals from different image features (Shiffrar et al 1995). Motion integration across space is also constrained by form (Lorenceau & Alais 2001; Lorenceau & Zago 1999).

Effect of terminator signals on perception of non-rigidity is also investigated. Translation of continuous sinusoidal lines with an angle less than 15^0 at zero crossing result in the perception of non-rigidity because of the aperture problem (Nakayama & Silverman 1988a). Similar lines in different form (cumulative gaussian) but broken, results in the perception of rigidity because of the terminators from the broken segments (Nakayama & Silverman 1988b). The spatial positioning of the terminators relative to the inflection point in the cumulative gaussian form governs the perception.

4.6.2. 1D to 2D

As noted in the previous section, with type-II plaids at low contrasts and short durations, the initial perceived direction is the vector average of the components but at later stages after $\sim 150\text{ms}$ the perceived direction is best predicted by IOC (Wilson et al 1992). Perceptual study on uni-kinetic plaids found similar dynamics in perception (Gorea & Lorenceau 1991). This temporal dynamics is investigated by Lorenceau and colleagues using bar field stimulus shown in figure 4.4a (Lorenceau et al 1993). The bars were oriented 20^0 either to the left or to the right of the vertical. The bars oriented 20^0 to the left of the vertical could move 20^0 either up or down to the horizontal in both left or right directions. If the bars move to left or to the right of horizontal in the direction of 20^0 above horizontal, the local motion signals are in the same direction as the terminator motion signals from the bar endings. This is used as a control (figure 4.10).

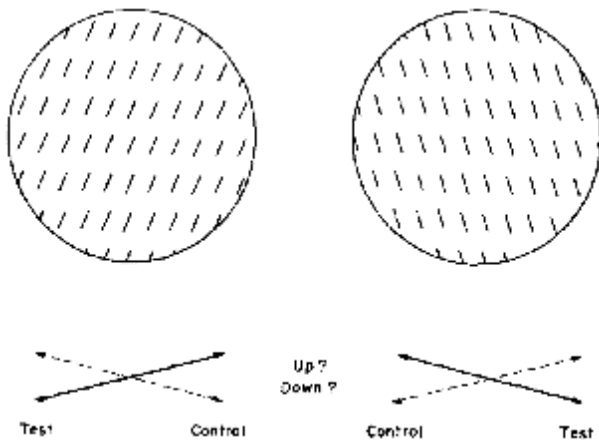


Figure 4.10. Bar field stimulus (Lorenceau et al 1993)

Where as if the bars move to left or to the right of horizontal in the direction of 20° below horizontal, the local motion signals have upward vertical component and the terminator motion signals have a downward vertical component. This is used as test stimulus (figure 4.10). A similar strategy to dissociate local motion signals from terminator motion signals is used if the bars are oriented 20° to the right of the vertical (figure 4.10). Subjects were asked to report if they perceive the bars translating up or down. They varied different parameters including the length of the bars, duration of the stimulus and the contrast. Increasing the length of the bars, short presentation duration and low contrasts made subjects report the perceived direction as indicated by the local motion signals. The overall results of the experiments suggested that different motion sensitive cells were involved in processing motion. The initial processing is driven by 1D motion sensitive cells and in the later stages it is tuned to global motion direction by 2D motion sensitive cells. Similar observations were made with multiple aperture stimuli where initial perceived direction is the vector average of 1D signals and later on 2D motion signals from the intrinsic terminators doesn't facilitate motion linking (Shiffrar & Lorenceau 1996). Another study using moving single bars of varying orientation, lengths, speeds and contrasts suggested there could be two distinct motion sensitive units processing 1D and 2D motion information (Castet et al 1993). This is further supported by the suggested difference between contrast sensitivity functions of 1D motion sensitive units and 2D motion sensitive units (Lorenceau & Shiffrar 1992; Lorenceau et al 1993).

4.7. Physiological account of the dynamics of 1D and 2D motion integration

The psychophysical evidence suggests that the motion integration is dynamic in nature

(Castet et al 1993; Gorea & Lorenceau 1991; Lorenceau et al 1993; Wilson et al 1992). The earlier perception is shaped largely by the 1D motion cues and during the later stages tuned by the 2D motion cues. Here, the physiological studies investigating the dynamic nature of motion integration is presented both for bar field stimulus (Pack & Born 2001) and plaid stimulus (Smith et al 2005).

4.7.1. Bar field stimulus

A field of moving bars was presented in the classical receptive field of an MT neuron. The bars moved at different angles (45° , 90° , 135°) relative to their orientation on each trial. MT neurons start to respond ~ 70 ms after stimulus onset and these early responses are shown in figure 4.11b. The early responses are tuned in the direction orthogonal to the orientation of the bar. The neuron shown in the figure shows strong selectivity for downward or leftward 1D motion. The steady state responses computed ~ 500 ms after stimulus onset are shown in figure 4.11c. The responses irrespective of their orientation select the global motion direction. This change of selectivity of 60 MT neurons from 1D component to 2D component is summarized in the figure 4.11d. The initial preferred direction is orthogonal to the orientation of the bar and over the ~ 60 ms the cells decode the true global motion of the stimulus (Pack & Born 2001).

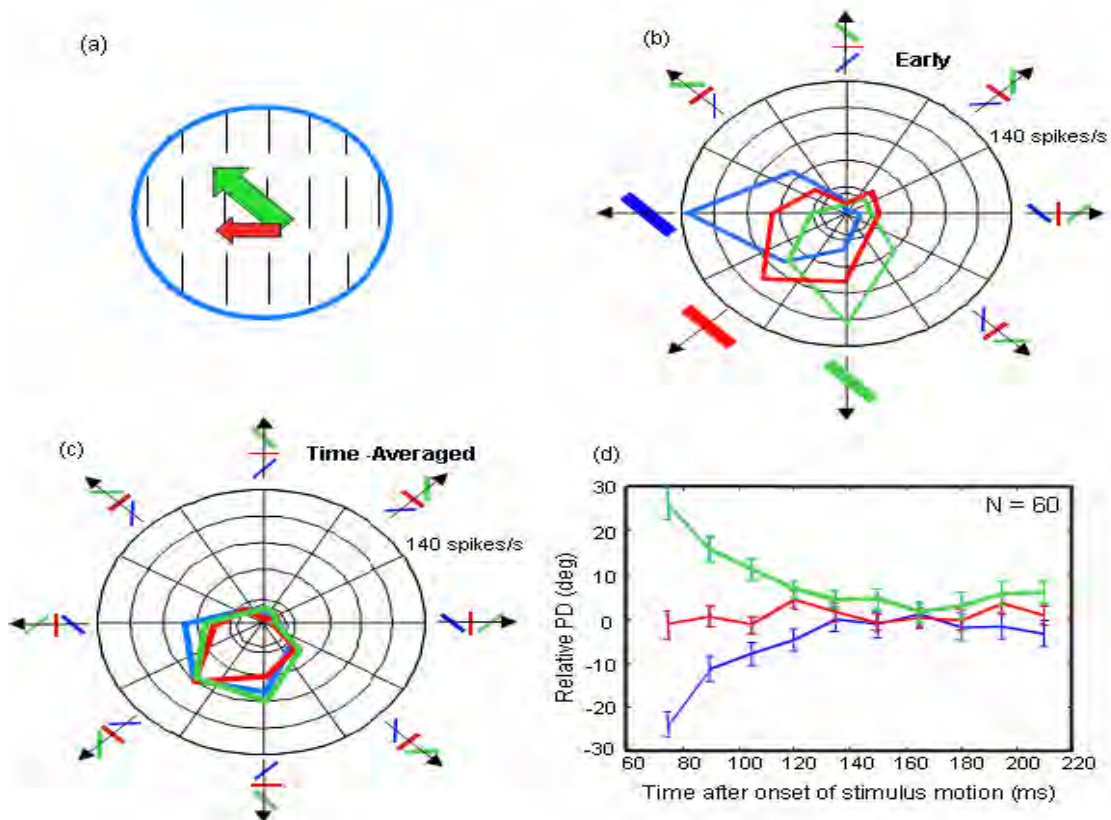


Figure 4.11. Dynamics of motion integration in an MT neuron. (a) bar field stimulus in receptive field (blue circle) of an MT neuron, green arrow indicates the global motion and red arrow indicates local motion direction (b) early responses of an MT neuron (c) later responses of the same neuron (d) dynamic change from orientation dependent responses to purely motion dependent responses for a population of MT neurons ($N=60$) (Pack & Born 2001).

4.7.2. Plaid stimulus

A recent study (Smith et al 2005) investigated the dynamics with which the pattern direction selectivity and component direction selectivity arises in the neurons of MT. A continuous sequence of gratings and plaid stimuli were used. On average PDS cells have a longer latency of ~ 6 ms compared to CDS cells. The dynamics with which the pattern and component direction selectivities arise is shown in the figure 4.12 below. The pattern direction selectivity of the PDS cells didn't reach their significant Z-score (black line in figure 3.12b) which indicates the selective state until 50-75ms after the responses of CDS cells have reached their selective state. These results reflect that initial responses of MT are dominated by component motion signals and only after a substantial time they represent pattern motion.

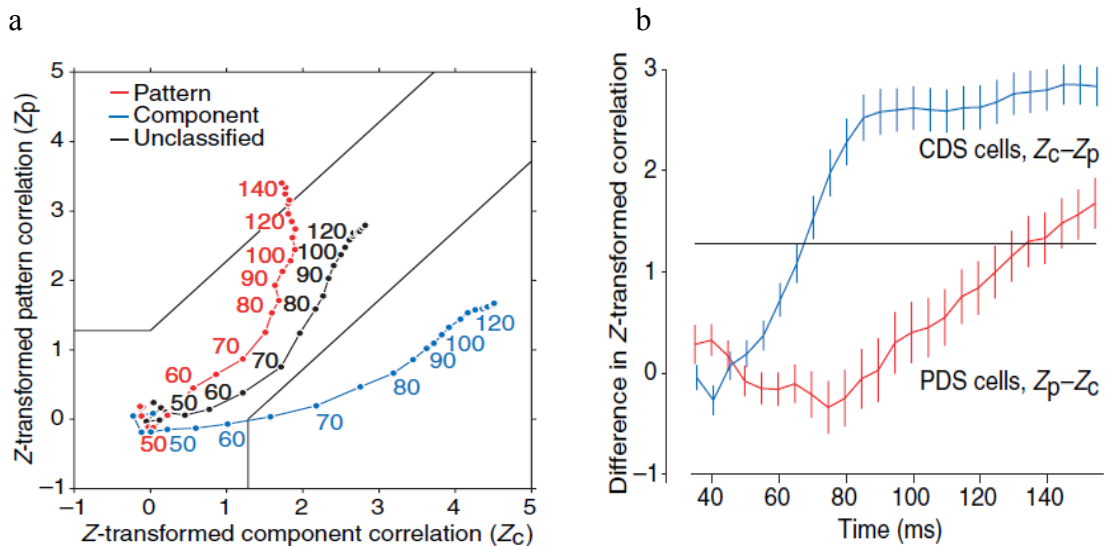


Figure 4.12. Dynamics of component and pattern direction selectivities. (a) time evolution of pattern and component direction selectivities indicated by their respective Z-scores. The numbers along the colored lines indicate time in ms. (b) deviation of PDS and CDS from component direction selectivity and pattern direction selectivity respectively with time as indicated by the difference in their respective Z-scores (Smith et al 2005).

Although both of the above studies suggest that MT encodes the global velocity of the object, recent study (Majaj et al 2007) investigated this by presenting the component gratings as patches in the receptive field of MT neuron. The responses of MT neuron is different when the component gratings are presented in patches to when they are presented overlapped. This suggests MT neuron pools motion information locally but not globally.

4.8. End-stopped V1 cells

The psychophysical studies mentioned in the previous section suggested that there might be two different motion sensitive units (Lorenceau et al 1993), one processing 1D and the other 2D motion information. The physiological studies in MT show that 1D motion selective responses are ~60ms earlier to the 2D motion selective responses (Pack & Born 2001; Smith et al 2005). 90% of the inputs from V1 to MT project from layer 4B (see (Pack & Born 2008) for a review). Majority of these neurons are direction selective (DS) and most of these DS neurons also exhibit strong suppressive surrounds and end-stopping (Pack & Born 2008; Sceniak et al 2001). The properties of end-stopped V1 cells (Hubel & Wiesel 1968) for direction selectivity might reflect that they could contribute to the dynamics of motion integration seen in MT (Pack et al 2003).

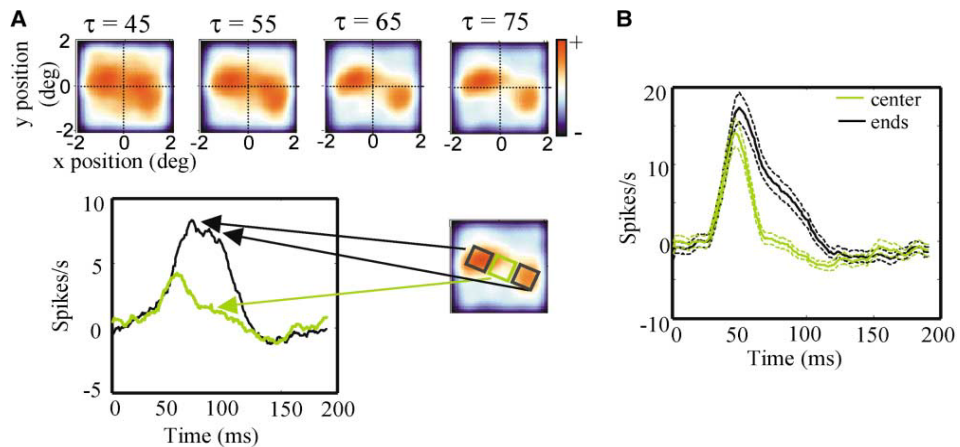


Figure 4.13. End-stopping in V1 neurons. (a) first row shows the successive snapshots of the bar in the receptive field of an end-stopped V1 cell. Second row shows the time course of the response when the bar is in the center of the receptive field (green) and when the endpoints of the bar appeared in the receptive field. (b) responses averaged across population of cells (Pack et al 2003).

The main finding of the study is that the end-stopped cells in V1 whose responses are

suppressed because of the extended contours decode 2D motion information independent of the orientation. End-stopped cell responds to a bar placed anywhere in the receptive field but over 20-30ms only responds to the endpoints of the bar. V1 end-stopped responses like MT cell responses take time to develop (Pack et al 2003).

4.9. Models for motion integration

Psychophysical evidence suggests that there might be two separate motion detection mechanisms for 1D and 2D motion cues (Lorenceau et al 1993). Physiology in MT suggests 1D components lead the way for motion integration whereas 2D components contribute later (Pack & Born 2001). However, Majaj and colleagues (Majaj et al 2002) suggested the analysis of 2D motion cues could be done within the same 1D motion analysis pathways without a need for end-stopped mechanism in the earlier stages analysing 2D motion cues. Such a two stage model is an extended version of S and H model which is presented in this section. In reality, this might not be the case as the contrast sensitivity functions for 1D motion cues and 2D motion cues is found to be different through eye movement responses (Masson & Castet 2002) as suggested by some of the psychophysical studies (Lorenceau & Shiffrar 1992). Here, two models implementing the two parallel pathway framework are discussed. The drawback of the two stage and two parallel pathway models is that they lack spatial structure which is essential to integration as shown by previous psychophysical studies (Lorenceau & Alais 2001; Lorenceau & Zago 1999; Nakayama & Silverman 1988; Weiss & Adelson 2000). A group of models investigating form-motion interactions implement spatial structure unlike the previous class of models and are mentioned in this section.

4.9.1. Two stage model : Extended S and H Model

The final stage of the S and H model described earlier in the chapter (Rust et al 2006; Simoncelli & Heeger 1998) often equated to MT is pattern direction selective which is velocity tuned. It doesn't account for the heterogeneity seen at the stage of MT which has both CDS and PDS cells. The model is updated to account for this heterogeneity. This is done by introducing non-linearities into the model. A schema of the model is shown in the figure 4.14 below (Rust et al 2006). The first stage of the model consists of equally spaced direction selective V1 neurons. The tuning curves of each neuron is shown in the figure 4.14. The output of the V1 neurons is divisively normalized both by the responses of the population (untuned normalization) and the neuron itself (tuned normalization). This is considered

equivalent to the suppression that arises within the receptive field and from the surround of the V1 neuron respectively.

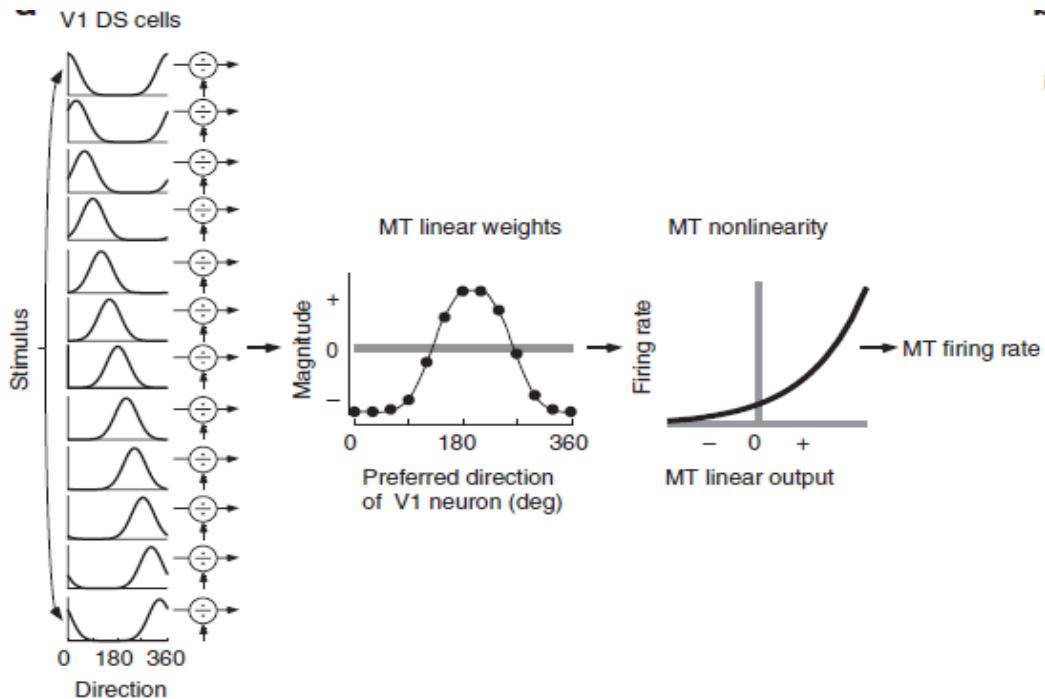


Figure 4.14. A schematic of the extended S and H model (Rust et al 2006)

The MT neuron in the next stage weighs the normalized output of the V1 neurons. The weights can be excitatory (positive) or inhibitory (negative). The result is then transformed into a MT neuron firing rate using a non-linear function. The tuning bandwidth for a PDS cell is larger compared to that for a CDS cell (Albright 1984). The tuned normalization component along with feed-forward inhibition shapes the responses of MT cells to be classified as CDS and PDS cells. However, the model lacks the dynamics of motion integration seen in MT cells for both plaids (Smith et al 2005) and bar field stimuli (Pack & Born 2001) as well as in psychophysical studies (Castet et al 1993; Lorenceau et al 1993).

4.9.2. Parallel Pathway models

To explain the psychophysics of type-II plaid stimuli for lower contrasts and shorter durations, Wilson and colleagues (1992) classified the motion components in the stimuli to Fourier (1D) and non-Fourier (features), and proposed a model with two parallel pathways for Fourier and non-Fourier motion processing. The details of the model is shown in the figure

4.15 below.

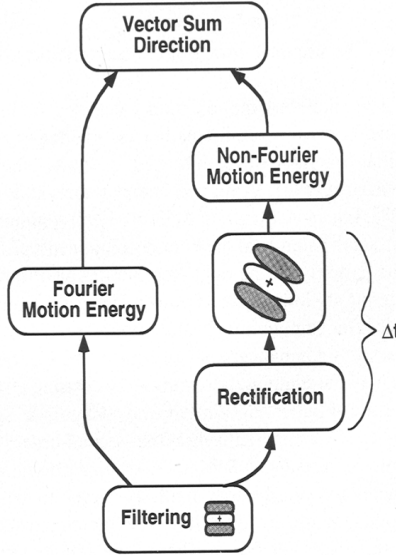


Figure 4.15. Fourier and Non-fourier pathway model

The model consists of two parallel pathways namely the motion energy pathway and the texture boundary motion pathway. With type-II plaids, the intital percept is the VA and slowly the percept approaches IOC. This is explained by a time delay Δt that is necessary for the additional procesing of the non-fourier motion component. The authors related fourier pathway to V1-MT and non-fourier to V1-V2-MT pathways. The weighted sum of the two pathways followed by a competitive feed-back inhibition accurately predicts a variety of perceptual tasks. This model is further extended to explain translating line motion perception (Loffler & Orbach 1999).

The other model which involves selection of reliable components is shown in the figure below (Nowlan & Sejnowski 1995). The model consists of three stages. The first stage is the motion energy computation. The next stage involves two parallel pathways whose input is the normalized motion energy ouputs. The second stage operates following selective integration principle.

This involves evaluating the reliability of the local velocity estimates and selects a coarse, discontinuous representation of the motion of the objects in the visual scene by combining only the most valid subsets of local velocity measurements. The local velocity estimates and the reliability estimates are computed in parallel by a feed-forward network (Nowlan & Sejnowski 1995).

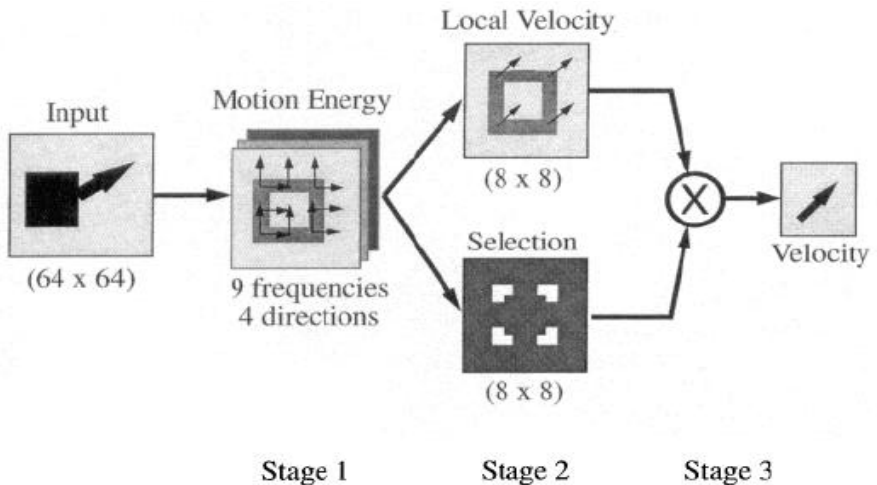


Figure 4.16. Selection model (Nowlan and Sejnowsky, 1995)

4.9.3. Form-Motion Models

Form-motion models use information about form in a direct or indirect way to disambiguate visual motion (Bayerl & Neumann 2007; Berzhanskaya et al 2007; Tlapale et al 2010). One common thing about all the three models is, output of local motion detectors (V1) is integrated at next stage equated to MT which is recurrently connected to V1. What is different is the modulation of this integration by different mechanisms. An example of the schematic is shown in the figure 4.17 for the model by Tlapale and colleagues. Models by Bayerl and Neumann make use of different explicit feature detectors (V2) to modulate the V1-MT integration in disambiguating local motion (Bayerl & Neumann 2004, 2007). Models by Grossberg and Mingolla take a simpler approach by avoiding explicit feature extraction by implementing a modulatory MT-V1 feed-back to disambiguate the ambiguous initial local velocity estimates by local motion detectors because of the aperture problem. However, they implement a form-motion interaction mechanism in their model to modify the erroneous motion signals at T-junctions that are integrated along with the local motion signals from the moving object of interest.

A luminance based gated-diffusion model is proposed by Tlapale and colleagues. Similar to the previous models, the local motion signals in V1 are integrated at MT which is recurrently connected to V1. However, unlike the two previous models which extract explicit features or T-junctions they implement a luminance smoothness based gating on diffusion of motion information. Because of the smoothness constraint, motion information can only be integrated in certain orientations.

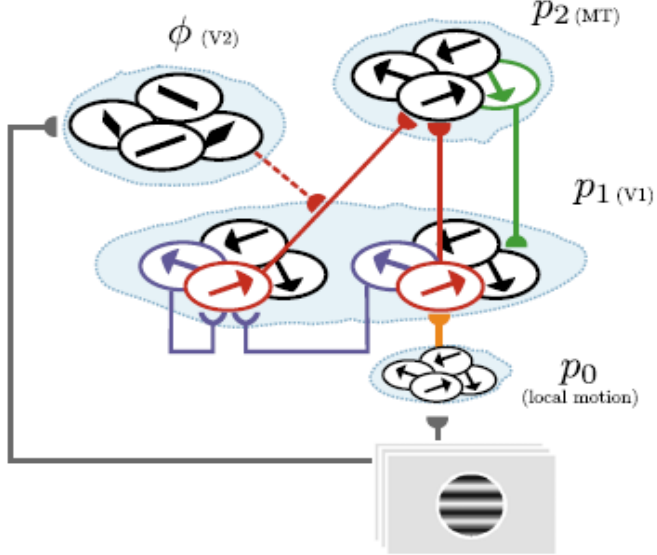


Figure 4.17. Gated-diffusion model. Local motion in V1 is integrated in MT. The recurrent motion diffusion between V1-MT is gated by V2 based on luminance smoothness (Tlapale et al 2010).

4.10. General framework : Bayesian approach

The perceived direction is explained by different rules for different stimuli, for e.g. IOC/FT for type-I plaid and VA for type-II plaid. Similar results are obtained with different stimulus. Figure 4.18 below shows one such example. Thin rhombus at high contrast appears to move horizontally which is consistent with IOC/FT and at low contrast appears to move diagonally which is consistent with VA. Similarly, a fat rhombus at high or low contrast appears to move horizontally which is consistent with IOC/FT.

Clearly, VA and IOC mechanisms doesn't take into account the contrast stimuli in computing the global estimate of the object. A more general framework to compute global object velocity is proposed by weiss and colleagues which can take contrast into account (Weiss & Adelson 1998; Weiss et al 2002). The framework is based on the Bayes rule which combines the measured likelihoods with a prior in velocity space to obtain the posterior. The basic assumption is that measurement of the images is noisy and prior prefers slow speeds. An application of this is shown in the figure 4.19 below.

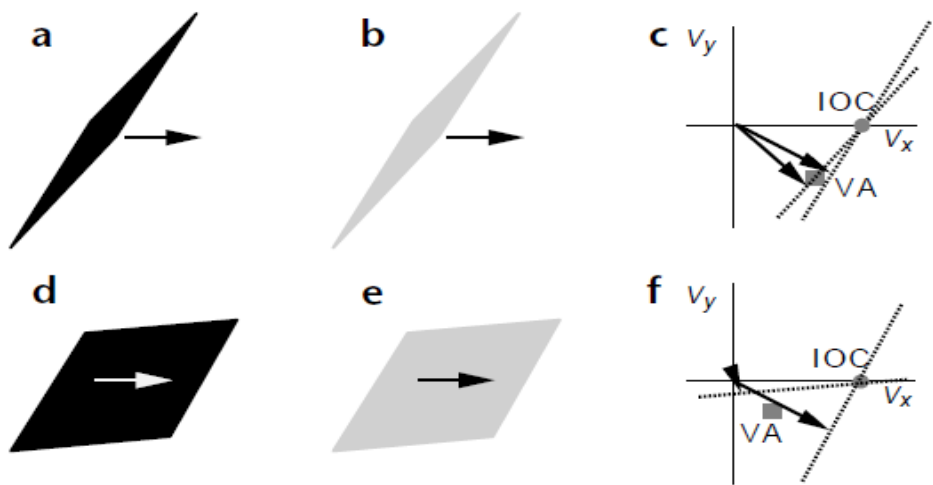


Figure 4.18. IOC and VA computation for rhombus of different sizes and contrasts. Rhombus at high contrast (a,d) and Rhombus at low contrast (b,e). (c,f) indicated IOC and VA solutions respectively for (a,b) and (d,e) (Weiss et al 2002)

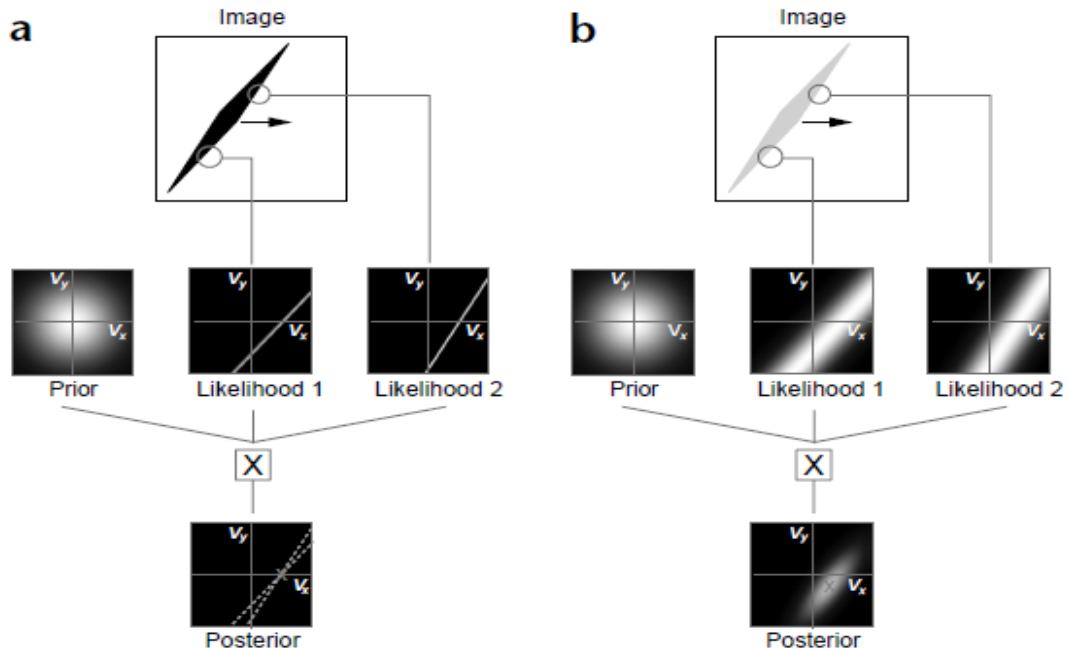


Figure 4.19. Combining likelihoods with the prior in a bayesian framework for thin rhombus at high contrast (a) and low contrast (b) (Weiss et al 2002)

The noise in the image measurement is represented in the uncertainty of the likelihood (Simoncelli et al 1991). When the rhombus is at low contrast, the likelihoods are

broader and when combined with slow prior, the resulting posterior shows a global velocity estimate that is in the diagonal direction (figure 4.19b). When the rhombus is at high contrast, similar computation yields a global velocity estimate in the horizontal direction (figure 4.19a). Over all, the bayesian approach to motion perception provides a more generalized and simple framework which is extended to explain the motion integration for smooth pursuit in chapter6.

4.11. Summary

The local motion signals in visual motion scene are integrated to obtain the object's global velocity. Noise masking and adaptation experiments suggested a two stage mechanism, where the first stage involved oriented filters and local motion analyzers that respond to component direction (Movshon et al 1986). The second stage results in the pattern direction selectivity. Physiological studies with type-I plaids supported the two stage model (Movshon et al 1986). IOC computation is proposed as the likely integration rule. S and H model (Simoncelli & Heeger 1998) implemented IOC, where the the first stage of the model is motion energy stage (Adelson & Bergen 1985) and the second stage of the model has velocity tuned cells which is equated to MT. However, type-II plaid stimuli at low contrasts and brief durations (Wilson et al 1992) suggested mechanisms other than IOC are also implemented.

Experiments with bar field stimuli suggested two different motion sensitive units are involved in motion integration which is dynamic in nature (Lorenceau et al 1993). The dynamic nature of motion integration is also observed in the physiological studies in MT using bar field (Pack & Born 2001) and plaid stimuli (Smith et al 2005). The early part of the dynamics is driven by the 1D component, later by the 2D component for both perception and in MT neurons. Studies on end-stopped cells of V1 show that they encode 2D motion independent of the orientation by supressing extended contours (Pack et al 2003). The responses of the end-stopped cells take time to develop like MT neurons. Although its not clear, end-stopped cells might play a role tuning the component driven initial responses of MT neurons to evolve for encoding the pattern direction. A similar tuned normalization is introduced into a recent version of S and H model to explain the heterogeneity seen in MT neurons with CDS and PDS (Rust et al 2006). However, this model would not explain the dynamics of pattern direction selectivity.

The perceived direction, explained by different rules for different stimuli, for e.g. IOC/FT for type-I plaid and VA for type-II plaid pointed that a more general rule might be at

work. Rightly so, the bayesian framework assuming slow prior provides a more general framework to model perception for different stimuli under different conditions (Weiss et al 2002). The model output is a perceptual response which is essentially static. However, other models for motion perception using explicit features or luminance smoothness could explain the dynamics associated with motion perception (Berzhanskaya et al 2007; Tlapale et al 2010; Bayerl & Neumann 2007).

Eye movements provide a better metric to study the dynamic motion processing (Miles et al 1986) and modelling motion integration for eye movements can provide a better understanding of the dynamic nature of motion processing in the brain. Next chapter provides a much finer perspective of dynamic motion processing observed through smooth eye movements.

Part - 3

Motion Integration for behaviour

Chapter 5

Smooth eye movements and dynamic motion integration

The physiological studies investigating motion integration has shown the dynamic nature associated with it. The perceptual studies can only provide with a discrete judgements of this dynamics. Behavioural studies would provide a continuous read out of the dynamic motion integration. This chapter provides a brief introduction to the smooth eye movements both voluntary (smooth pursuit) and involuntary (ocular following response). It also describes some of the Ocular Following and Smooth Pursuit studies using a variety of stimuli that provide a better metric for understanding motion integration.

5.1. Smooth eye movements

The physiological studies in MT has shown the dynamic nature of motion integration (Pack & Born 2001; Smith et al 2005). The perceptual readout is a static readout of this dynamic process either over an instant or pooled over a period of time. A more continuous read out can be obtained with behavior which evolves continuously over time unlike perceptual read out. An ideal behavioral readout to study dynamic motion integration would be one that requires sensory to motor transformation of the visual motion stimuli and share a common physiological structures with visual motion processing. Smooth eye movements have been tightly linked to neural signals in physiological structures like MT and MST involved in visual motion processing (Groh et al 1997; Ilg 1997; Kawano 1999; Newsome et al 1985; Pack et al 2001). The initial smooth eye movements also provide a window into the early visual motion processing of low-level motion signals (Sheliga et al 2005; Wilmer & Nakayama 2007). For this reason, smooth eye movements provide a unique platform to study the dynamic nature of motion integration.

Here, we focus on studies using two kinds of smooth eye movements, Ocular following and Smooth pursuit. Both eye movements serve to stabilize the moving object onto the retina to facilitate high acuity vision and the physiology driving both the eye movements is largely similar (Ilg 1997). Ocular following is a short latency, reflexive eye

movement driven by large field visual motion stimulus (Ilg 1997; Kawano 1999; Masson 2004; Miles 1998; Miles et al 1986). The stimuli used to study motion integration with short latency ocular following response include barber pole stimuli(Masson et al 2000), plaids (Masson & Castet 2002). Smooth pursuit, on the other hand is voluntary tracking of a single object of interest, usually a dot (Kowler 2011; Krauzlis 2004; Lisberger 2010; Thier & Ilg 2005). To study motion integration for pursuit, different stimuli have been used including simple translating tilted bars (Bogadhi et al 2011; Born et al 2006; Montagnini et al 2006) and more complex complex shapes like rhombus (Masson & Stone 2002; Wallace et al 2005).

5.2. 1D to 2D

Psychophysical (Lorenceau et al 1993; Wilson et al 1992) results indicate to a parallel processing of 1D and 2D motion signals. Physiological results (Pack & Born 2001; Smith et al 2005) suggest that the 1D motion signals drive the initial visual motion processing and the 2D motion signals are integrated at later stages. This section provides a behavioral account of this transformation from 1D to 2D in visual motion processing, using different stimulus and smooth eye movements.

5.2.1. *Barberpole stimulus*

Ocular following responses were recorded for a barbergole stimulus with different aspect ratios. By increasing the aspect ratio, 2D motion signals in the stimulus are increased. 1D motion signals are oriented in the upward direction where as the 2D motion signals have a horizontal component, as shown in figure 5.1a. In the control, the 2D motion signals are in the same direction as 1D signals. Ocular following responses are shown in the figure 5.1b. The vertical component of eye velocity has a latency ~20ms shorter to horizontal component, which is contributed by 2D signals alone. The strength of horizontal component increases with aspect ratio which increases 2D motion signals in the stimulus.

An elongated mask at the center of the stimulus didn't have an effect on the latency difference between 1D and 2D motion signals. When the mask covered 90% of the area, the early component of the eye velocity driven by 1D motion signals is reduced. Similarly, when the 2D motion signals are reduced by lowering contrast or indenting the edges, the later component of the eye velocity is reduced. These results indicate to a parallel visual motion processing of 1D and 2D motion signals, where early integration is primarily driven by 1D motion signals, later by 2D motion signals.

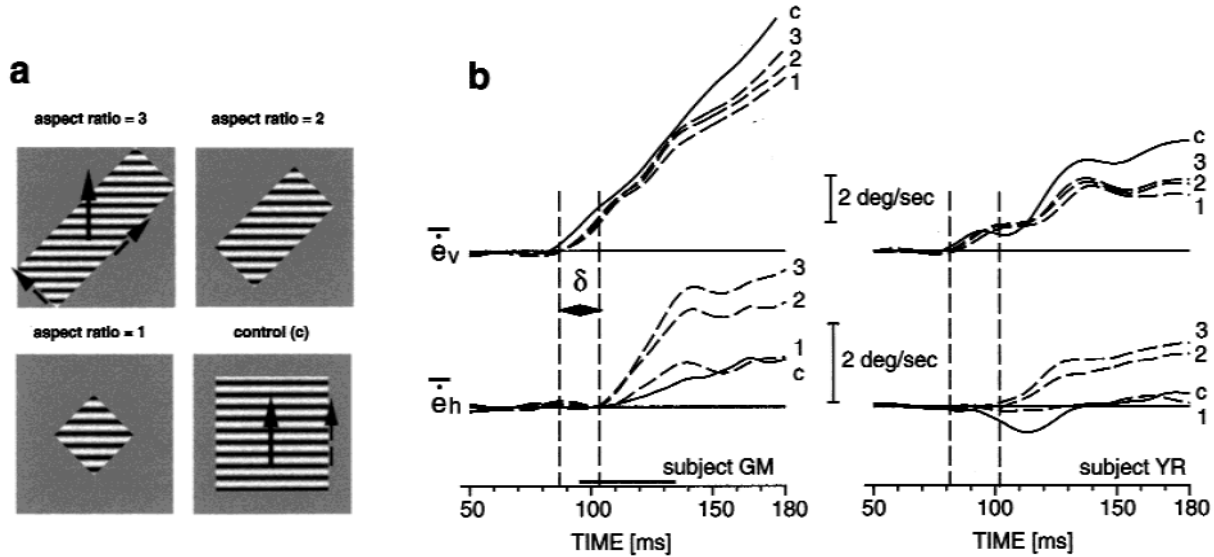


Figure 5.1. Ocular following for barberpole stimuli viewed through apertures of different aspect ratios. (a) barberpole stimuli with different aspect ratios (b) Ocular following responses for different stimuli. δ indicates the latency difference between horizontal eye velocity component (driven by 2D motion signals alone) and vertical eye velocity component (Masson et al 2000).

5.2.2. Uni-kinetic Plaids

Type-I and Type-II plaids have component gratings that are both moving. Uni-kinetic plaids has a static grating over which another grating moves. The advantage it offers is to tease apart the Ocular following responses that are due to 2D motion signals alone from the intersections of the two component gratings, from the 1D motion signals. This is shown in figure 5.2a. The 1D motion component is pure veridical where as the 2D has a horizontal component. The ocular following responses to the uni-kinetic plaids are shown in figure 5.2b.

Similar to the results seen with barber pole stimulus, the ocular following responses to uni-kinetic plaids show an early eye velocity component in the direction of 1D motion signals and the late eye velocity component is in the direction which is signalled by 2D motion signals alone. These results suggest for a parallel processing of 1D and 2D visual motion signals, where 1D motion signals drive the early responses followed by the 2D. Section 5.3 describes a compelling evidence for a parallel processing of 1D and 2D motion signals by evaluating the contrast response functions for 1D and 2D motion signals.

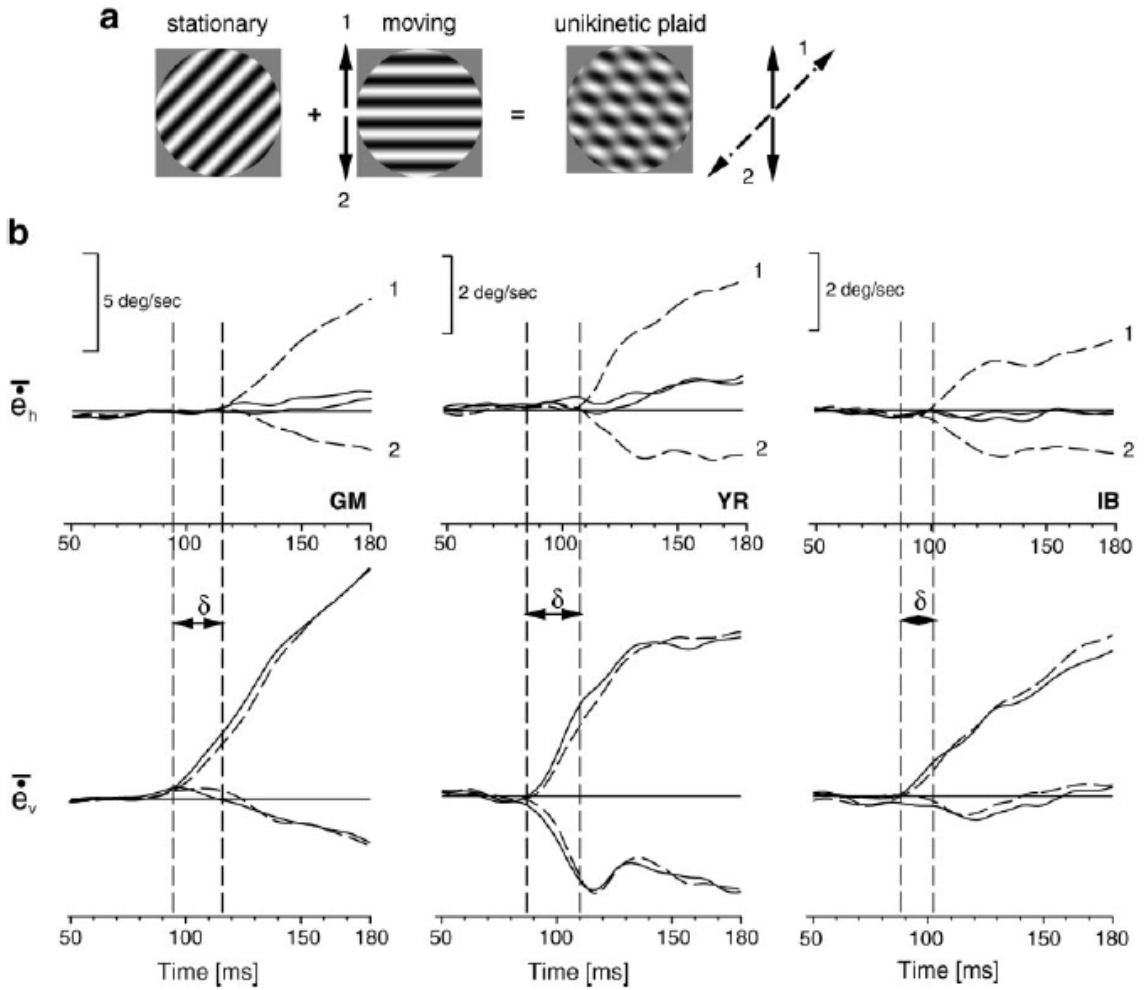


Figure 5.2. Ocular following responses for uni-kinetic plaids. (a) a stationary grating and a moving grating form a uni-kinetic plaid in which 1D motion signals are purely vertical and 2D motion signals has a horizontal component. (b) Ocular following responses to the uni-kinetic plaids. δ shows the latency difference between horizontal and vertical eye velocity components (Masson & Castet 2002).

5.2.3. Type-I and Type-II Diamonds

Perceptual studies using Type-I plaids couldn't distinguish between VA and IOC/FT as VA of the component gratings is same the IOC/FT (Movshon et al 1986). Where as with type-II plaids, initial perceived direction is the VA of the component gratings and in the later stages the perceived direction is IOC/FT (Wilson et al 1992). To study the dynamic version of this transformation from VA to IOC/FT, type-I and type-II diamonds were used. With type-I diamonds (square shown in the figure 5.3), VA=IOC=FT and for type-II diamonds (Counter Clock-wise (CCW) and Clock-wise (CW) tilted diamonds), VA \neq IOC=FT.

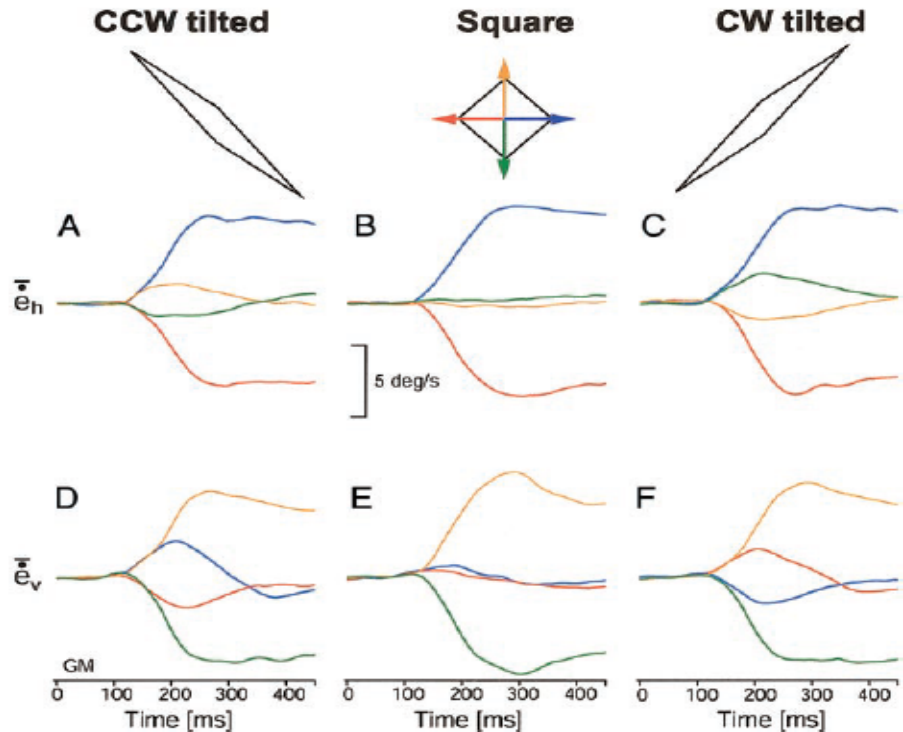


Figure 5.3. Smooth pursuit responses to type-II (CCW and CW) and type-I diamonds shown in the first row. Different colors indicate the direction motion. Second row (A, B, C) shows the horizontal component of eye velocity. Third row (D, E, F) shows the vertical component of eye velocity (Masson & Stone 2002).

Subjects were asked to track the diamonds and the tracking responses are shown in the figure 5.3. For type-II diamonds where $VA \neq IOC = FT$, the tracking is initiated in the VA direction and over the next 300ms, responses converged to IOC/FT (Wallace et al 2005). This dynamics has a time constant of 90ms. For type-I diamonds where $VA = IOC = FT$, there is no bias to be observed. At low contrasts and high speeds, the initial bias is larger and the time constant is longer (Wallace et al 2005). When the 2D information is increased using a texture filled type-II diamond, the directional bias is largely reduced. These results suggest that motion integration is flexible using both 1D and 2D motion information to compute the object's global velocity.

5.2.4. Tilted bar stimuli

Simple stimuli like translating tilted bar also reflects the temporal dynamics of motion integration. Similar to masking of 1D motion information in barberpole stimulus and textured type-II diamond stimulus, the relative amount of 1D and 2D motion information can be manipulated by bar length. This is illustrated in the figure 5.4.

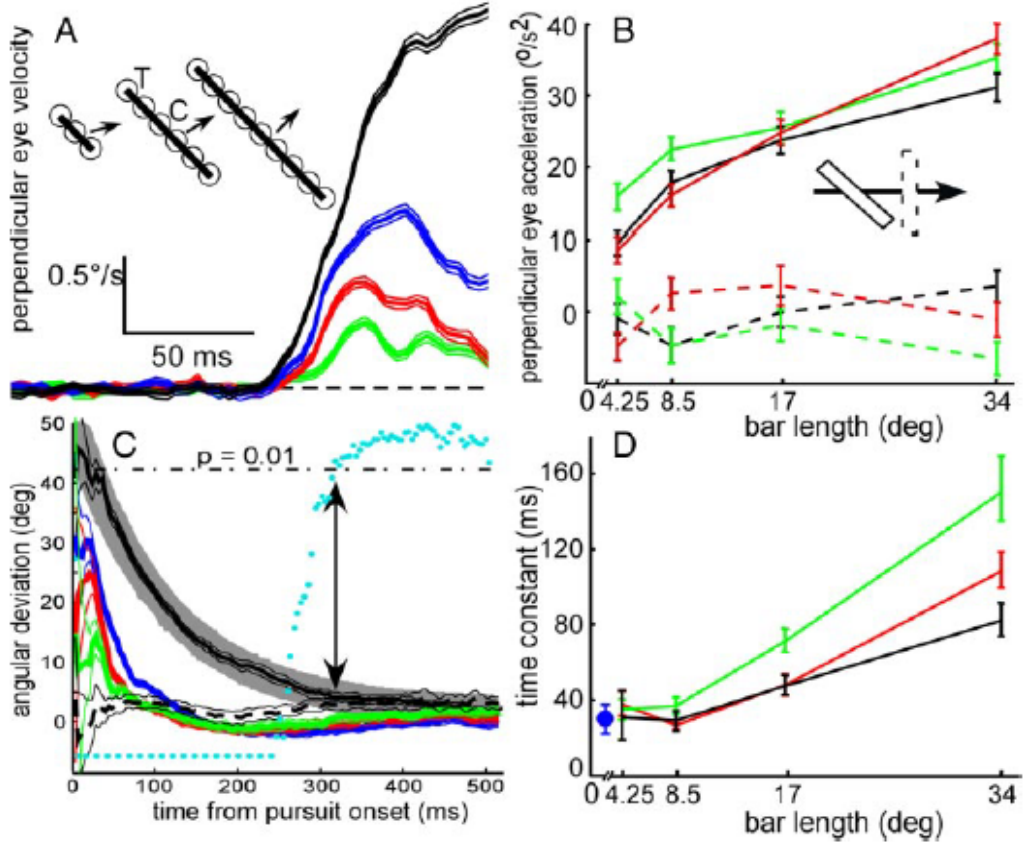


Figure 5.4. Smooth pursuit responses for a tilted bar of different lengths. (A) eye velocity perpendicular to the direction of the target motion for different bar lengths (B) perpendicular eye velocity acceleration for varying bar lengths (C) dynamics of the direction error in the tracking responses with time for different bar lengths (D) time constant of the dynamics shown in C. (Born et al 2006)

Subjects were asked to track the center of the bar. Smooth pursuit responses has two components, one that is in the direction of the translating bar and the other in the direction perpendicular to the translating bar. The perpendicular component shows the effect of 1D motion information that is along the length of the bar. It increases with the length of the bar as shown in figure 5.4a. The acceleration of the perpendicular component also increases with length of the bar (figure 5.4b). The direction of the tracking responses are shown in figure 5.4c over time. Longer the bar, higher is the initial directional bias and longer is the time constant of the dynamics associated with motion integration (figure 5.4d). These results also suggest that early responses are driven by 1D motion signals and later by 2D motion signals. The evolution of 2D signals can be as short as 50ms for shorter bars and as long as 400ms for longer bars depending upon the relative amount of 1D and 2D motion information.

5.3. 1D and 2D

The studies presented in the previous sections have all suggested that the early responses are driven by 1D motion information, later by 2D motion information. Varying the relative strength of the 1D and 2D motion information effect the dynamics of motion integration. The hypothesis that 1D and 2D motion information is processed parallelly cannot be supported or rejected by the observations presented in the previous section alone.

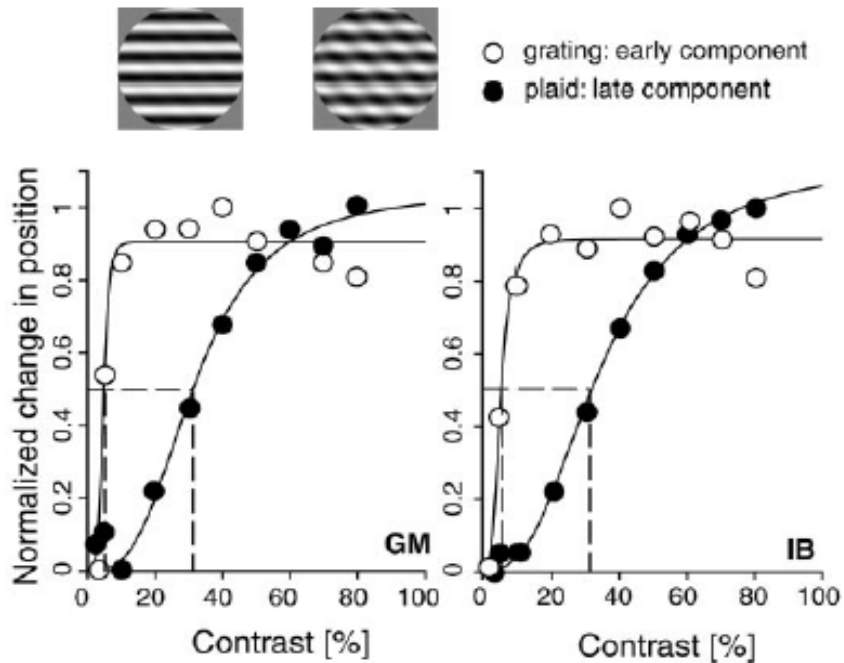


Figure 5.5. Contrast response functions for 1D (early) and 2D (late) motion components (Masson & Castet 2002)

However, the measurement of contrast response functions from the early and later ocular following responses as a function of contrast shows a distinct difference (figure 5.5). The contrast sensitivity of 2D motion pathway is lower as suggested by (Lorenceau & Shiffrar 1992). This provides a strong case in support of the parallel pathway for 1D and 2D motion information processing.

5.4. Summary

The studies briefly described here (Born et al 2006; Masson & Castet 2002; Masson et al 2000; Masson & Stone 2002; Wallace et al 2005) show that both the smooth eye movements, short latency ocular following and smooth pursuit provide an accurate account of the dynamics in motion integration unlike a snap shot readout of the perceptual studies. The

physiological studies in MT (Pack & Born 2001) investigating dynamic nature of motion integration tell a similar story.

A model (Montagnini et al 2007) processing 1D and 2D motion information parallelly in a recurrent bayesian framework has been proposed to understand the dynamic nature of motion integration in MT. The motion information in visual scene is represented as likelihoods (1D and 2D likelihoods) which are combined with a prior preferring slow speeds to obtain a posterior distribution. On every iteration, the posterior is used to update prior. This recurrent update of the prior which is combined with likelihoods solves the aperture problem and the dynamics associated with it is equated to dynamics observed in MT for motion integration. Recurrent bayesian is equivalent to a kalman except that measure likelihoods are combined with the prior unconditionally.

Smooth eye movements have been tightly linked to neural signals in physiological structures like MT and MST involved in visual motion processing (Groh et al 1997; Ilg 1997; Kawano 1999; Newsome et al 1985; Pack et al 2001). This underlines requirement of a model describing the sensori-motor transformation for smooth eye movements. The models for smooth pursuit (Bennett & Barnes 2003; Churchland et al 2003; Krauzlis & Lisberger 1994; Robinson et al 1986) have focussed on modeling the oculomotor dynamics investigated using a simple stimulus like a dot. The next chapter presents an open-loop version of the model (Bogadhi et al 2011) which is an extension of the previously proposed model (Montagnini et al 2007) describing the dynamic motion integration for smooth pursuit.

Chapter 6

Pursuing motion illusions: a realistic oculomotor framework for Bayesian inference

Accuracy in estimating an object's global motion over time is not only affected by the noise in visual motion information but also by the spatial limitation of the local motion analyzers (aperture problem). Perceptual and oculomotor data demonstrate that during the initial stages of the motion information processing, 1D motion cues related to the object's edges have a dominating influence over the estimate of the object's global motion. However, during the later stages, 2D motion cues related to terminators (edge-endings) progressively take over, leading to a final correct estimate of the object's global motion. Here, we propose a recursive extension to the Bayesian framework for motion processing (Weiss, Simoncelli and Adelson 2002) cascaded with a model oculomotor plant to describe the dynamic integration of 1D and 2D motion information in the context of smooth pursuit eye movements. In the recurrent Bayesian framework, the prior defined in the velocity space is combined with the two independent measurement likelihood functions, representing edge-related and terminator-related information, respectively to obtain the posterior. The prior is updated with the posterior at the end of each iteration step. The maximum-a-posteriori (MAP) of the posterior distribution at every time step is fed into the oculomotor plant to produce eye velocity responses that are compared to the human smooth pursuit data. The recurrent model was tuned with the variance of pursuit responses to either "pure" 1D or "pure" 2D motion. The oculomotor plant was tuned with an independent set of oculomotor data, including the effects of line length (i.e. stimulus energy) and directional anisotropies in the smooth pursuit responses. The model not only provides an accurate qualitative account of dynamic motion integration but also a quantitative account that is close to the smooth pursuit response across several conditions (3 contrasts and 3 speeds) for two human subjects.

This study is published in Vision Research - Bogadhi AR, Montagnini A, Mamassian P, Perrinet LU, Masson GS. 2011. Pursuing motion illusions: A realistic oculomotor framework for Bayesian inference. Vision Res 51:867-80

6.1. Introduction

Motion illusions help us to better understand how motion information is processed by the visual system. In particular, they illuminate how the brain processes ambiguous information to infer the most probable source from the external world (Kersten et al., 2004). The aperture problem, and its perceptual consequences, is one of the most investigated cases of motion illusions since it can be investigated at both perceptual, motor and neuronal levels (see Masson & Ilg, 2010 for a collection of reviews). Motion sensitive cells in early visual stages have small receptive fields and, therefore, a limited access to the motion information present in the images. Neurons with receptive fields located at different positions along a simple moving stimulus such as a bar will provide different velocity measurements as illustrated in Figure 6.1a. Consider two frames of a tilted line translating horizontally but seen through three small, circular apertures (locations 1, 2 and 3). The translation vector in the 1st and 3rd apertures is unique as there is only one possible way to recover the translation of the line between the two frames, thanks to the two-dimensional (2D) profile of luminance information. Thus, motion recovered from the translation of these line-endings (also called features, terminators, or local 2D motion) is unambiguous, as illustrated by the small gaussian-like distribution of the most probable velocities in the (V_x, V_y) space, for a high signal-to-noise ratio. On the contrary, analyzing the translation of a one-dimensional luminance profile as seen in the 2nd aperture yields to an infinite number of possible velocity vectors. Such 1D motion is highly ambiguous (Movshon et al., 1986) leading to the aperture problem. One can compute the 1D velocity likelihoods in the same (V_x, V_y) space, which under some assumptions about noise properties, would correspond to an elongated Gaussian distribution crossing an entire quadrant (Simoncelli et al., 1991; Weiss et al., 2001). Understanding how purely horizontal motion of the entire visual pattern is recovered has been the goal of dozens of psychophysical and physiological studies (see Bradley & Goyal, 2005; Masson & Ilg, 2010 for reviews) but several key aspects remain unclear such as the role of feature motion, the rule governing the integration of 1D and 2D local motion (Weiss et al., 2001) or the exact physiological mechanisms used to reconstruct global motion (see Rust et al., 2006; Tlapale et al., 2010; Tsui et al., 2010 for recent computational studies).

A key observation with the aperture problem is that perceived direction of a single tilted bar translating horizontally is biased towards the oblique direction, corresponding to the velocity vector orthogonal to the bar orientation (Wallach, 1935; Castet et al., 1993), at least for short stimulus durations and low contrast. Such observations also hold for motor actions such as voluntary pursuit. Example of smooth pursuit eye movements driven by a

rightward motion of a 45° tilted line is shown in Figure 6.1b. At pursuit onset, there is always a transient vertical component, reflecting the directional bias induced by the aperture problem.

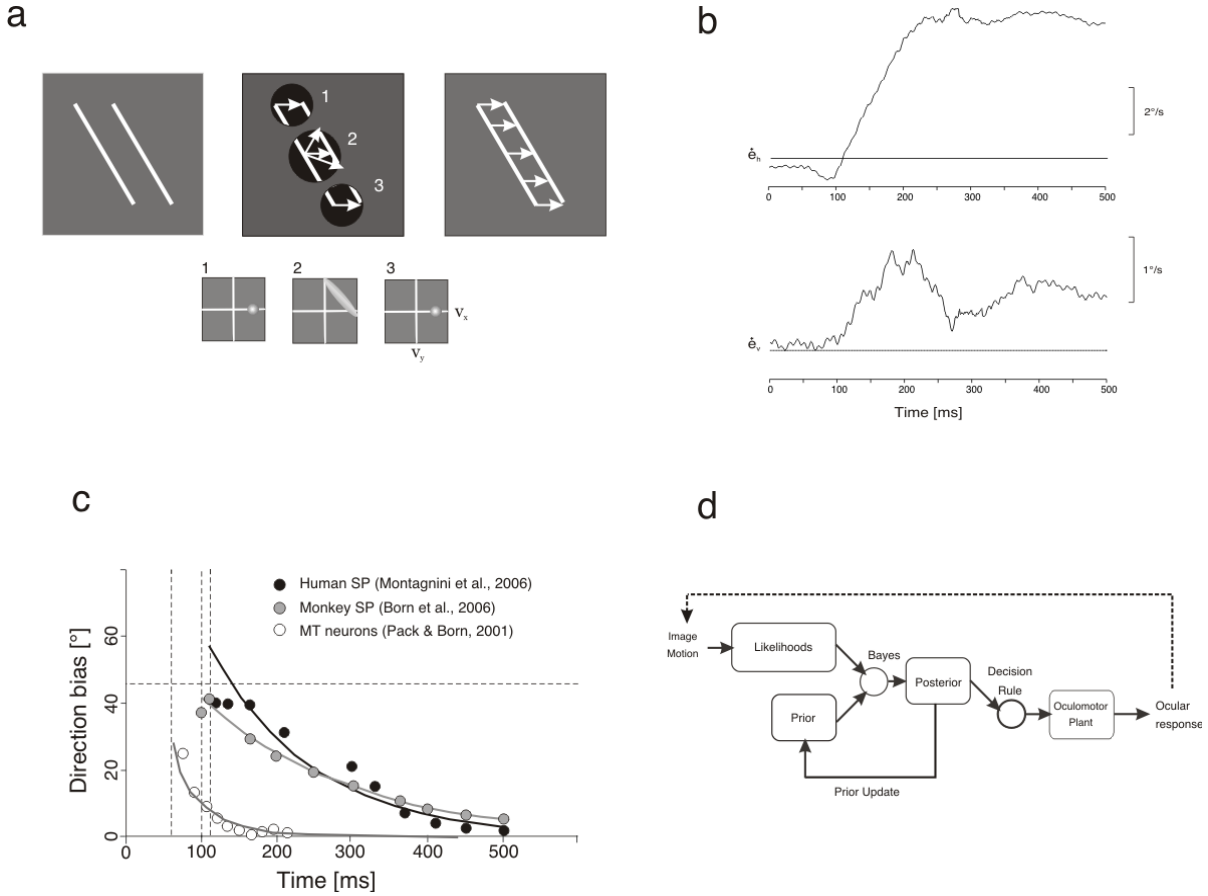


Figure 6.1. Aperture problem and dynamics of motion integration. (a) Upper row illustrate the aperture problem during translation of a single tilted line. From left to right: two successive frames of a pure horizontal translation; velocity vectors extracted through three different apertures; the correct solution of the aperture problem is reached when global motion consistent with translation of a rigid object is obtained. Shown are three different instances during pursuit of a tilted line. Lower row illustrates the velocity likelihoods computed at the three locations (ambiguous (2) and unambiguous (1, 3)). *(b)* Mean smooth pursuit eye velocity traces (horizontal (\dot{e}_h) and vertical (\dot{e}_v)) for a tilted line translating to right at $7^\circ/\text{s}$. *(c)* Pursuit direction error plotted against time for human (black dots) and monkey (grey dots) pursuit of a 45° tilted line. Open circles plot the time course of direction estimate from a population of MT neurons presented with a set of small tilted lines translating in the classical receptive field. *(d)* Block model of the model for motion inference

and pursuit. The front-end infers optimal motion estimation using a Bayesian model. Such estimate is dynamical due to prior updating, implementing a recurrent Bayesian network. The decision rule extracts the optimal image velocity at a given point in time and feeds two independent oculomotor plants, driving horizontal and vertical eye velocity.

Once that 2D motion information begins to be integrated along with 1D motion, there is a slow reduction in the directional bias. Such observation was made both in humans (Masson & Stone, 2002; Wallace et al., 2005; Montagnini et al., 2006) and monkeys (Born et al., 2006). Figure 6.1c plots the time course of the tracking direction error (i.e. the difference between the instantaneous 2D eye movement direction and the 2D translation of the bar) observed in either monkeys (closed symbols) or humans (open symbols). At high contrast, tracking error decays with a time constant ~90ms so that, after 200ms of pursuit both eye and target motions almost perfectly matched. Grey symbols plot the time course of the population vector of direction-selective cells recorded from macaque area MT using a somewhat similar stimulus. MT neurons initially respond primarily to the component of motion perpendicular to a contour's orientation, but over a short period of time (time constant: ~60ms) their responses gradually shift to encode the true stimulus direction 100-150ms after stimulus onset (Pack and Born 2001).

Numerous mechanisms such as vector averaging (VA), Intersection of Constraints (IOC) and 2D features (2DFT) (see Bradley and Goyal 2008 for a review) have been proposed as solutions to the aperture problem. The Bayesian framework, based on the idea that the visual system makes inferences from noisy signals offers a simple explanation for two-dimensional motion illusions observed with a large pool of stimuli (Weiss, Simoncelli and Adelson 2002). Their seminal suggestion was that primate visual system prefers slow and smooth motions. In the Bayesian framework of probabilistic inference, such preference can be instantiated as a Prior distribution centered at $V_x=V_y=0$. When presented with 1D motion of single bars, yielding to elongated likelihood distributions, the posterior distribution that is the product of prior and likelihood distributions is centered along the 45° oblique axis, corresponding to the perceived direction along the orthogonal direction. This model was extended to plaid pattern motion direction (Weiss & Adelson 2002) to demonstrate that it can easily implement the IOC rule by combining different 1D likelihoods. In their model, no specific role was attributed to 2D motion features, thus ignoring some of the information present in the images. However, such framework can be easily extended to combine likelihoods of various local motion cues (1D and 2D) with the slow motion prior into a single

path. To account for the different dynamics that are observed for 1D and 2D motion cues respectively (e.g. Masson et al., 2000; Masson & Castet, 2002), such two pathways model was proposed, taking into account both the different variances in 1D and 2D likelihoods and their different timing (Barthelemy, et al. 2008).

Although the Bayesian framework gives an accurate account of perception and psychophysical data (e.g. Stocker and Simoncelli 2006; Hurlimann et al., 2002), this type of models is essentially static. They cannot explain the time course of 2D motion perception as illustrated in Figure 6.1c. However, there have been a few attempts to use dynamical inference to solve the aperture problem (e.g. Montagnini et al., 2007; Dimova & Denham, 2010). A recurrent Bayesian model, where the prior is iteratively updated using the full posterior distribution was proposed by Montagnini et al. (2007) to model such dynamics, using smooth pursuit responses as a hallmark. The variances of the likelihoods and prior in this model were estimated on the basis of an independent set of eye movement data, unlike the other models where these variances were free parameters. In the Bayesian framework, the model output is a posterior distribution that is interpreted as the information used for an optimal perceptual estimate of motion. Different decoding rules can be used such as taking the mean or the Maximum a Posteriori (MAP) of the distribution, but such value can hardly be compared to the eye movement data. There is thus the need for a realistic oculomotor back-end to the Bayesian framework to explain smooth pursuit eye movement data and in particular to render their exact time course. Moreover, our original article stressed the need for additional data in order to better constraint the recurrent model. The present study was conducted to answer these two limitations of the model.

Here, we propose an open loop two stage model (see Figure 6.1d) to explain the dynamics of motion integration in the context of smooth pursuit eye movements. The first step of the model is a sensory information processing stage where likelihoods of all different motion information (as shown in Figure 6.1a for different locations) are combined with a prior favoring slow speeds (Weiss et al., 2002). We implemented the different latencies of 1D and 2D likelihoods computation as well as the time constant of the recurrent Bayesian network, assuming that such sensory information stage corresponds to motion processing done in area MT for smooth pursuit (see Lisberger, 2010 for a review). The likelihood functions for 1D and 2D and prior are assumed to be Gaussian. The next stage implements the sensorimotor transformation generating the smooth pursuit response as output by taking the maximum a posteriori (MAP) as a decision rule applied to the Bayesian Posterior and using it as input. For simplicity, we model the dynamics of motion integration in an open

loop phase mode, ignoring the oculomotor feed-back (dotted line). A main objective of the study was to determine the model parameters from a set of “pure” 1D and 2D stimuli and test it against a full set of tilted bars, presented at different contrast and speed values. In addition, our implementation of the oculomotor plant attempts to take into account the directional anisotropies affecting smooth pursuit as well as the possible nonlinearities due to the use of extended line drawings instead of the classical moving dots. Our two-stage model could reproduce in considerable detail the individual mean eye velocity traces for subjects tracking tilted lines. In particular, we could mimic the transient directional bias due to the aperture problem and the dynamic motion integration as its solution as well as its sensitivity to different low-level image attributes.

6.2. Methods

6.2.1. Experimental methods:

To estimate both likelihood and prior variances for the recurrent Bayesian model, as well as to tune the parameters of the oculomotor plant, we performed a new set of experiments. Eye movements were recorded from two observers, both authors (AM & GM) and naïve subjects (JD (*experiment2*) & AR (*experiment3 – varying contrast*)) using the ReX software package running on a PC with the QNX Momentics operating system. The ReX PC controlled both stimulus presentation and data acquisition (see details in Masson, Rybarczyk, et al. 2000). Stimuli were generated with an Sgi Octane workstation and back-projected along with the red fixation point onto a large translucent screen (80 X 60°) using a 3 CRT video-projector (1280 X 1024 pixels at 76 Hz). The peak luminance of the stimuli for all experiments was of 45cd/m². We have divided the conditions into (i) a contrast set, with stimuli moving at a steady velocity of 7 °/s for three different contrast conditions (10%, 30% and 90%) against a grey background and (ii) a velocity set, described as stimulus moving at 100% contrast for three different speeds (5 °/s, 10 °/s and 15 °/s) against a dark background.

For all experiments, observers had their head stabilized by chin and forehead rests. Each trial started with the presentation of a fixation point for a random duration of 600±100ms. Observers were required to fixate within a 1°x1° window. The fixation point was then extinguished and the motion stimulus was presented after a 350ms blank. The object moved for 500ms. Observers were instructed to track the object center and trials were aborted if eye position did not remain within a square window of 5° width, located at the object center. All conditions were randomly interleaved to minimize cognitive expectations

and anticipatory pursuit. We collected a minimum of 80 and a maximum of 100 trials per condition for each observer over several days.

Vertical and horizontal position of the right eye was recorded at a sampling rate of 1 KHz by means of the scleral eye coil technique and low-pass filtered (Collewijn, van der Mark and Jansen 1975). Eye-position data were linearized, smoothed with a spline interpolation (Busettini, Miles and Schwarz 1991) and then differentiated to obtain vertical and horizontal eye-velocity profiles. After visual inspection using MATLAB, we used a conjoint velocity and acceleration threshold to detect and remove saccades (Krauzlis and Miles 1996). Latency of each trial was computed for both horizontal and vertical eye-velocity profiles using an objective method (Krauzlis & Miles 1996; Masson & Castet 2002). Oculomotor traces were aligned to the stimulus onset. An offline inspection was done to eliminate outlier trials (less than 5%). The outlier trials are those in which saccades could not be eliminated without excluding the majority of the trial or in which high levels of noise exist during fixation and persist during pursuit.

6.2.2. Experiment 1: Pursuing pure 1D and pure 2D stimuli

In order to estimate the initial prior and likelihood variances of the Bayesian inference from the smooth pursuit responses of pure 1D and pure 2D stimuli, subjects were asked to pursue “pure 1D” (48^0 long line) and “pure 2D” (blob) stimulus. The “pure 2D” stimulus is a central blob with Gaussian luminosity profile (standard deviation $\sim 0.2^0$ of visual angle). The 48^0 long vertical has terminators far in the peripheral visual field and thus their influence was assumed to be limited. Therefore this stimulus can be approximated to a “pure 1D” stimulus. The target was moving horizontally to the right or left, for both contrast and velocity sets of conditions.

6.2.3. Experiment 2: Effect of line length on smooth pursuit

We investigated the effect of line length on different properties of smooth pursuit. Latency and eye velocity during either initial acceleration or steady state time windows provide an account of the oculomotor dynamics in the smooth pursuit response. Keeping the edge motion direction and orientation constant, we varied line length to tune the oculomotor gain parameters in the model. The stimuli were a blob (control condition) and vertical lines of lengths 5^0 , 10^0 , 20^0 and 48^0 moving horizontally rightward or leftward, with three different contrast values.

6.2.4. Experiment 3: Directional anisotropies in initial and steady state velocities

To define horizontal and vertical oculomotor plants of the model, we needed to evaluate any directional anisotropies and consider them while tuning plant parameters. This is particularly important for a model where several parameters are estimated from the variance of the motor responses. To do so, we used a line of length of 17^0 , moving orthogonal to its orientation in four cardinal and four diagonal directions. These 8 motion directions were presented interleaved, at three contrast (10, 30 and 90%, fixed speed: $7^{\circ}/s$) values and three speeds (5, 10 and $15^{\circ}/s$, 100% contrast).

6.2.5. Experiment 4: Pursuing a tilted line

We compared the model eye velocity traces with human smooth pursuit responses obtained with a tilted line for which initial perceived direction is biased towards the orthogonal axis. Subjects were instructed to track a 45^0 tilted line (length: 17^0) translating horizontally, either rightward or leftward. Such 45^0 tilted line was presented at three different speeds (5, 10 and $15^{\circ}/s$) and contrast (10, 30 and 90%). All conditions were presented interleaved.

6.2.6. Mathematical methods: tuning the Bayesian recurrent model

The variances of the likelihood functions were estimated from smooth pursuit data. Assuming that variance in smooth pursuit response almost entirely comes from the sensory source (Osborne, Lisberger and Bialek 2005), the variance of the smooth pursuit responses to a reference stimulus (i.e. either “pure 1D” or “pure 2D”) was considered as the posterior variance and used to estimate respective likelihood variance and prior variance. The prior was assumed to favoring slow speeds. This estimation of likelihood variance was done for different speeds since we know that speed is not homogeneously represented in MT (DeAngelis & Uka 2003) as well as for different contrasts since their parameters are known to influence both perceived direction (Lorenceau et al. 1993) and pursuit initiation (Spering et al. 2005). We used the mean eye velocity measured in a 40ms time interval centered at the peak acceleration time as an approximate estimate of the posterior distribution variance considering that the open loop dynamics might better reflect the initial posterior function (Montagnini et al., 2007).

As noted in the introduction, the visual stimulus has 1D (edge related) and 2D (terminator related) motion information. We assume both of them to be independent and Gaussian distributions. If v_0 is velocity of the stimulus, the likelihood function L_1 for the

edge related information (1D) in velocity space (v_x, v_y) is given by

$$L_1 = \frac{1}{Z} \exp \left(-\frac{((v_x - v_0) \cos \theta + v_y \sin \theta)^2}{2 \sigma_1^2} \right) \quad \dots \dots (1) \quad (\text{See figure 6.6})$$

where Z is the partition function (used in this section, for all distributions), θ is the orientation of the line relative to the vertical, taken as positive in anti-clockwise direction and σ_1 is the standard deviation of the speed in the orthogonal direction to the line. The likelihood function L_2 for the terminator related information in velocity space (v_x, v_y) is given by

$$L_2 = \frac{1}{Z} \exp \left(-\frac{(v_x - v_0)^2 + v_y^2}{2 \sigma_2^2} \right) \quad \dots \dots (2)$$

where σ_2 is the standard deviation of the speed. The overall likelihood function is the product of the two likelihoods 1D and 2D (since, both are assumed to be independent):

$$L(v_x, v_y) = L_1(v_x, v_y) L_2(v_x, v_y) \quad \dots \dots (3)$$

Assuming a prior favoring slow speeds (mean centered at origin) and directionally unbiased (normally distributed with a variance σ_0), the initial prior P_0 can be written in velocity space (v_x, v_y) as

$$P_0 = \frac{1}{Z} \exp \left(-\frac{v_x^2 + v_y^2}{2 \sigma_0^2} \right) \quad \dots \dots (4)$$

The likelihood function (L) is combined with the initial prior (P_0) using bayes rule to obtain the initial posterior distribution (Q_0)

$$Q_0(v_x, v_y) = L(v_x, v_y) P_0(v_x, v_y) \quad \dots \dots (5)$$

To obtain a read out of the distribution that is used for the later stages a decision rule called maximum-a-posteriori (MAP), in this case equivalent to the mean of the distribution is implemented as:

$$\left(\begin{matrix} v'_x \\ v'_y \end{matrix} \right) = \operatorname{argmax}_{(v_x, v_y)} Q_0(v_x, v_y) \quad \dots \dots (6)$$

The posterior distribution at every instant t is used to dynamically update the prior (recurrent Bayesian framework) that is used for the next iteration which is expressed as,

$$P_t(v_x, v_y) = Q_{t-1}(v_x, v_y) \quad \dots \dots (7)$$

This recurrent Bayesian framework can be summarized as,

$$Q_t(v_x, v_y) = L(v_x, v_y) P_t(v_x, v_y) \quad \dots \dots (8)$$

The variance terms σ_0^2 , σ_1^2 and σ_2^2 are estimated applying Bayes rule to pure 1D and pure 2D motion stimuli (experiment 1):

$$Q_{0,i}(v_x, v_y) = L_i(v_x, v_y) P_0(v_x, v_y) \quad \dots (9)$$

with $i=1$ and 2 for 1D and 2D stimulus respectively. Given that both the likelihoods and prior are normal distributions, their product is also a normal distribution. Thus it is possible to write two simple equations relating the means and variances of the three distributions involved in equation 9, yielding:

$$\begin{cases} \mu_{Q_{0,i}} \sigma_{Q_{0,i}}^{-2} = \mu_i \sigma_i^{-2} + \mu_0 \sigma_0^{-2} \\ \sigma_{Q_{0,i}}^{-2} = \sigma_i^{-2} + \sigma_0^{-2} \end{cases} \quad \dots (10)$$

The values $\mu_{Q_{0,i}}$ and $\sigma_{Q_{0,i}}^{-2}$ are estimated from the oculomotor recordings for the 1D and 2D stimulus respectively. The likelihood mean value μ_i assumed to be stimulus speed v_0 and prior mean μ_0 is assumed to be zero, initially. The above set of equations provide us with two values for the variance of prior one each for $i=1$ and $i=2$ conditions. The final prior variance is taken as the average of the two.

The evolution of the posterior across time is evaluated numerically, by means of an iterative algorithm. However, note that analytical derivations are possible given the assumption of normal distribution (see Montagnini et al., 2007).

6.3. RESULTS

6.3.1. Experiment 1: Tuning the recurrent Bayesian model with variances of pursuit responses to a blob or a line of varying contrast

To estimate the prior and likelihood variances of the Bayesian inference from the smooth pursuit responses to pure 1D and pure 2D stimuli, subjects were asked to pursue 1D (48° long vertical line) and 2D (blob) stimulus. In Figure 6.2, mean velocity profiles of pursuit responses to either a “pure” 2D (Figure 6.2a) or a “pure” 1D stimulus (Figure 6.2b) of three different contrasts are shown for subject GM. The shaded area around the smooth pursuit traces represents the standard deviation across all trials for all times during the pursuit. Standard deviation of mean eye velocity computed in the peak acceleration time window (shown in figure 6.2a & 6.2b) is plotted against contrast for the two subjects and each stimulus type in Figure 6.2C. Overall, variance of pursuit responses decreased with higher contrast values.

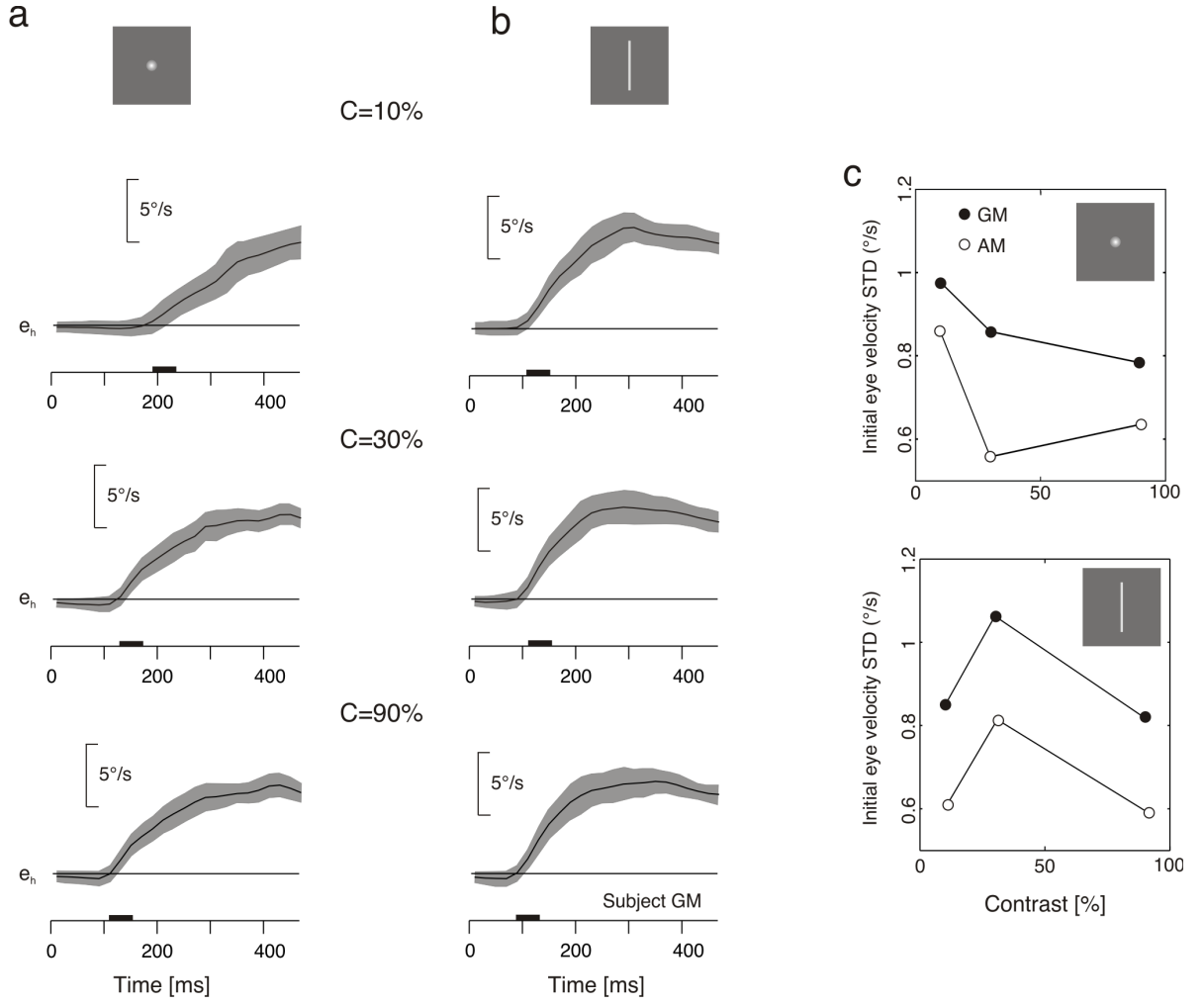


Figure 6.2: Pursuing pure 1D and pure 2D stimulus. Mean eye velocity profiles of pursuit responses to a blob (a) or a 48° long line (b), presented at three different contrasts. Profiles of standard deviation of eye velocity (across trials) is illustrated by the grey shaded area. The bars shown on the time axes indicate the peak acceleration time window(c) Standard deviation in the peak acceleration time window is plotted against contrast, for the two objects and two subjects.

In particular, with the “pure 2D” stimulus standard deviation of responses in the peak acceleration time window regularly decreased with increasing contrast. With upright moving lines, at very low contrast, we found a decrease in eye velocity variance, which could be related to a large reduction in initial eye velocity. A stronger variance was observed at 30 % contrast for both the subjects. The variance of the pursuit response in the peak acceleration time is used to estimate the prior and likelihood variances as described in the mathematical methods. The latency for 1D stimulus for three contrasts spans in the interval 90-110ms,

which is lower compared to the latency for 2D stimulus (110-160ms). For both stimuli, we found a decrease in latency with an increase in the contrast of the stimuli. The mean response to the 2D stimulus is much slower compared to the 1D stimulus, accounting for the difference in the energy of the stimuli.

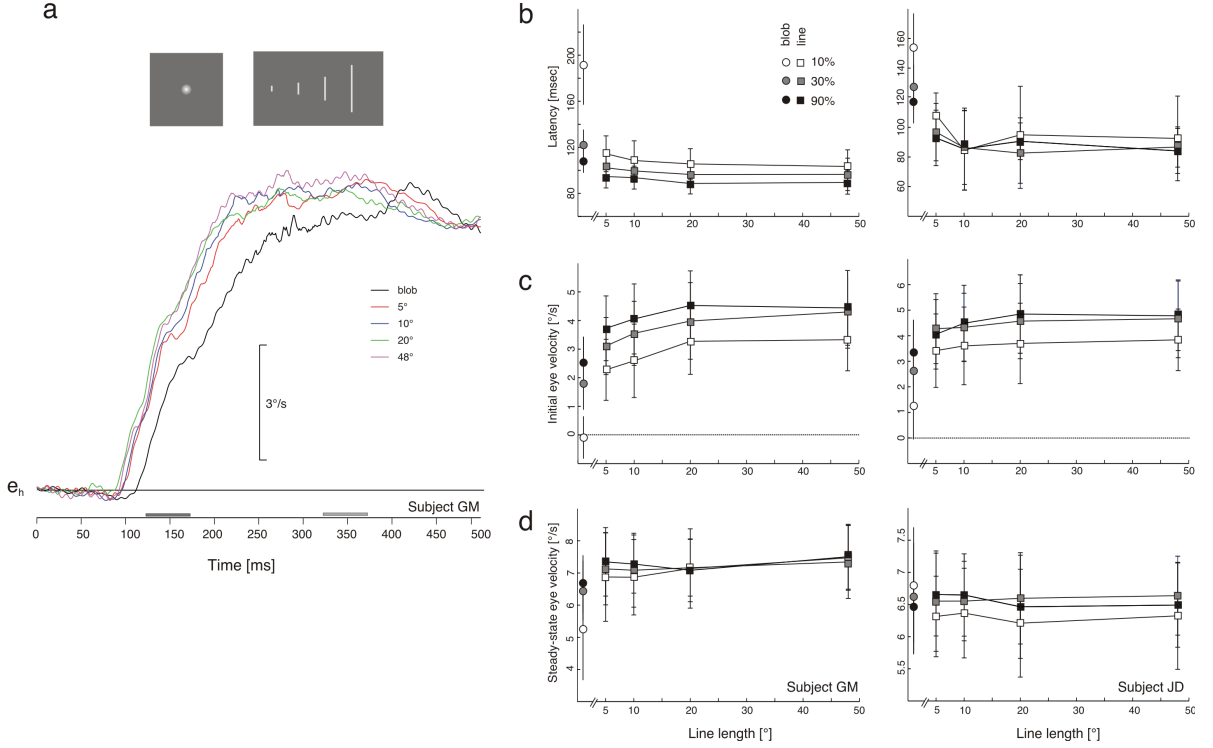


Figure 6.3. Effect of line length. (a) Mean eye velocity profiles of pursuit responses to either blob or lines of different lengths. (b) Mean latency of horizontal pursuit for blobs (circles) and lines (squares), plotted against line length. (c,d) Dependency of initial and steady-state eye velocity upon line-length, for three different contrasts. Subject GM. Similar data were obtained with Subject AM.

6.3.2. Experiment 2: Using effects of line length to tune the 2D oculomotor plant

Next, we considered the effect of line length while tuning the parameters of the oculomotor plant. We recorded smooth pursuit responses to stimuli consisting of blob, and vertical line of varying lengths (5, 10, 20, 48°). The blob is considered to be a limiting case and is excluded from the statistical repeated measures 2-way ANOVA test. Figure 6.3a plots mean eye velocity profiles for blob motion (black curve) and lines of increasing lengths. Figures 6.3b-d illustrates the changes in different parameters. Latency exhibited a consistent dependence upon line-length, in particular at low contrast. The statistical repeated measures

2-way ANOVA test done indicated a significant effect of contrast ($F(2,1015)=154.4$ and $p<0.0001$) and line-length ($F(3,1014)=19.92$ and $p<0.0001$). There is no interaction between the two factors ($F(6,1006)=1.22$ and $p<0.2923$). For any given line length, higher contrast resulted in shorter latency. The mean latency difference between blob and line conditions was of ~ 75 ms for a length of 5° and a contrast of 10% and was reduced to less than 20ms by increasing contrast to 30% and 90%. At high contrast (30% and 90%), line lengths above 20° affected only little pursuit latency. There was a small decay to pursuit latency with line-length in the range $5-20^\circ$. This seems to indicate to a fast decaying type of dependence of latency on the amount of 1D information in the stimulus.

The mean of the initial pursuit velocity in the [120,180ms] time window is plotted for different contrast conditions against line length in Figure 6.3c. The ANOVA test indicated a significant effect of contrast ($F(2,1015)=113.63$; $p<0.0001$) and line length ($F(3,1014)=41.12$; $p<0.0001$) upon initial eye velocity. There is no interaction between the two factors ($F(6,1006)=0.9$; $p<0.4946$). The relationship between initial eye velocity and line length was inverted when compared to the modulation found for latency. Across all line lengths, higher contrast resulted in higher eye acceleration. The difference between mean velocities for blob and 5° long line at 90% contrast was of ~ 1.2 °/s and increased gradually when lowering contrast, from 1.32 °/s at 30% contrast to 2.3 °/s at 10% contrast. Initial eye velocity increased with longer lines in the range $5-20^\circ$ and then saturated with longer bars, irrespective of contrast.

Lastly, we analyzed steady-state tracking by measuring eye velocity in the [320, 380 ms] time window. Steady-state eye velocity (mean \pm SD across trials) is plotted against line length, for the 3 different contrast values in Figure 6.3d. The ANOVA conducted on steady-state eye velocity showed significant effect of line length ($F(3,1014)=7.73$; $p<0.0001$) and an effect of contrast ($F(2,1015)=4.86$; $p<0.0079$) at least for smaller line lengths ($=< 10^\circ$) and a non-significant interaction between the two parameters ($F(6,1006)=1.87$; $p<0.0823$). For line lengths 5° and 10° , higher the contrast, higher is the velocity in the steady state. The difference between the velocities of blob to that of 5° long line at 10% contrast (1.6 °/s) decreases to (0.7 °/s) at 90%. With increasing line length above 10° , the differences in the steady state velocity for different contrasts cease to exist.

These results clearly indicate an effect of line length at least for line lengths less than 20° on latency, velocities in peak acceleration time window for any given contrast. This effect is coherent with the size of spatial integration for human pursuit (Heinen & Watamaniuk, 1998). These results indicate that we need to consider low-level properties of

the moving target such as line length and contrast when tuning parameters of the oculomotor model.

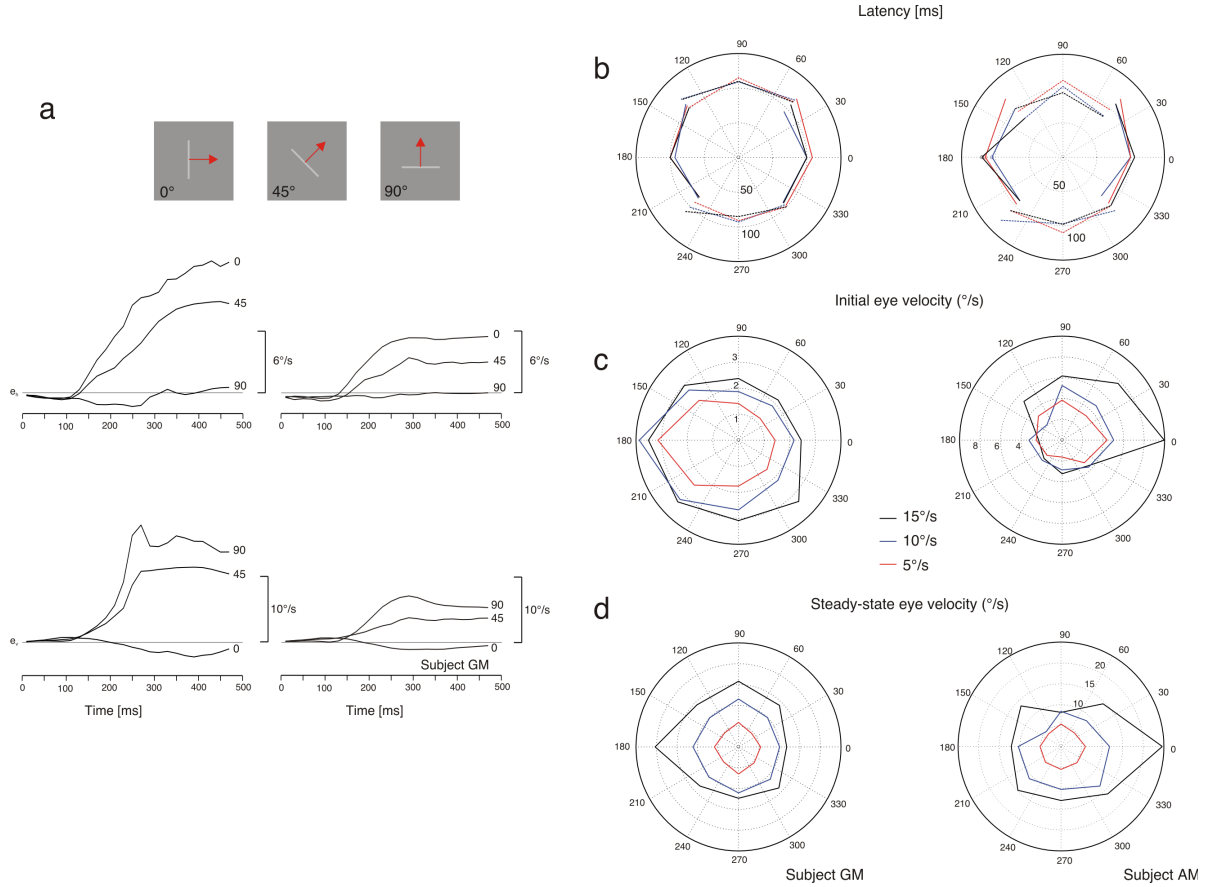


Figure 6.4. Directional anisotropies of speed. (a) Mean velocity profiles of pursuit responses to a 17° long line, moving orthogonally to its orientation along three directions (0° , 45° and 90° shown at the top of the figure with red arrows), for two different speeds (left panel: $15^\circ/\text{s}$, right panel: $5^\circ/\text{s}$ (horizontal component (\dot{e}_h)-top; vertical component (\dot{e}_v)-bottom)). *(b)* Mean horizontal (shown by solid line) and vertical (shown by dotted line) latencies, for all 8 motion directions and 3 speeds. *(c,d)* Directional anisotropies for initial and steady-state eye velocity, respectively. Colors indicate different target velocities. Left and right panels are for subject GM and AM, respectively.

6.3.3. Experiment 3: Using directional anisotropies to tune a 2D oculomotor model

We recorded pursuit responses to a single line of length (17°) moving in different directions in order to probe directional anisotropies to be considered when tuning an oculomotor model for simulating two-dimensional pursuit responses as those obtained with tilted lines (see

Figure 6.1). In the third experiment, we presented a line (length: 17°) moving orthogonal to its orientation along four cardinal and four diagonal directions. We collected data at different speeds (5, 10 and 15°/s, fixed contrast: 100%) and contrasts (10, 30 and 90%, fixed speed: 5°/s).

Horizontal (\dot{e}_h) and vertical (\dot{e}_v) components of smooth pursuit responses to a line moving along the directions in the first quadrant (0, 45 and 90°) at two different speeds are shown in Figure 6.4a. Clearly, responses to motion along different directions exhibited different dynamics, which were scaled with target speed. For each motion direction, we measured latency, initial and steady-state eye velocities of both horizontal and vertical components of two-dimensional pursuit. The horizontal and vertical component latencies of the responses along all eight directions for different speeds are shown in Figure 6.4b. We observed differences between h-latency and v-latency for target motion along diagonal directions that were highly idiosyncratic, as reported by Soechting, Mrotek and Flanders (2005). The mean initial velocity computed in the early time window [120,180ms] is shown in Figure 6.4c. An ANOVA test revealed a significant main effect of motion direction (Subject GM: $F(7,1888)=23.21$, $p<0.0001$; Subject AM: $F(7,1769)=55.88$, $p<0.0001$), indicating that some directions yielded stronger eye accelerations. However, the characteristics of directional anisotropies were again highly idiosyncratic. Main effect of speed indicated that higher speeds resulted in stronger eye accelerations (Subject GM: $F(2,1893)=42.48$, $p<0.0001$; Subject AM: $F(2,1774)=41.61$, $p<0.0001$). We found significant interactions between direction and speed (Subject GM: $F(14,1872)=2.06$, $p<0.01$; Subject AM: $F(14,1753)=8.87$, $p<0.0001$), indicating that anisotropies changed with target speed. The mean steady state eye velocity was measured over the [320,380ms] time window and is plotted in Figure 6.4d. Again, there was a significant effect of target motion direction (Subject GM: $F(7,1888)=32.34$, $p<0.0001$; Subject AM: $F(7,1769)=89.04$, $p<0.0001$), indicating that pursuit had higher gain for some directions. Interestingly, for both subjects, such directional anisotropy disappeared at very low speed. The interactions between direction and speed were significant. (Subject GM: $F(14,1872)=17.31$, $p<0.0001$; Subject AM: $F(14,1753)=39.59$, $p<0.0001$), again indicating that anisotropies in measured eye velocity are speed-dependent.

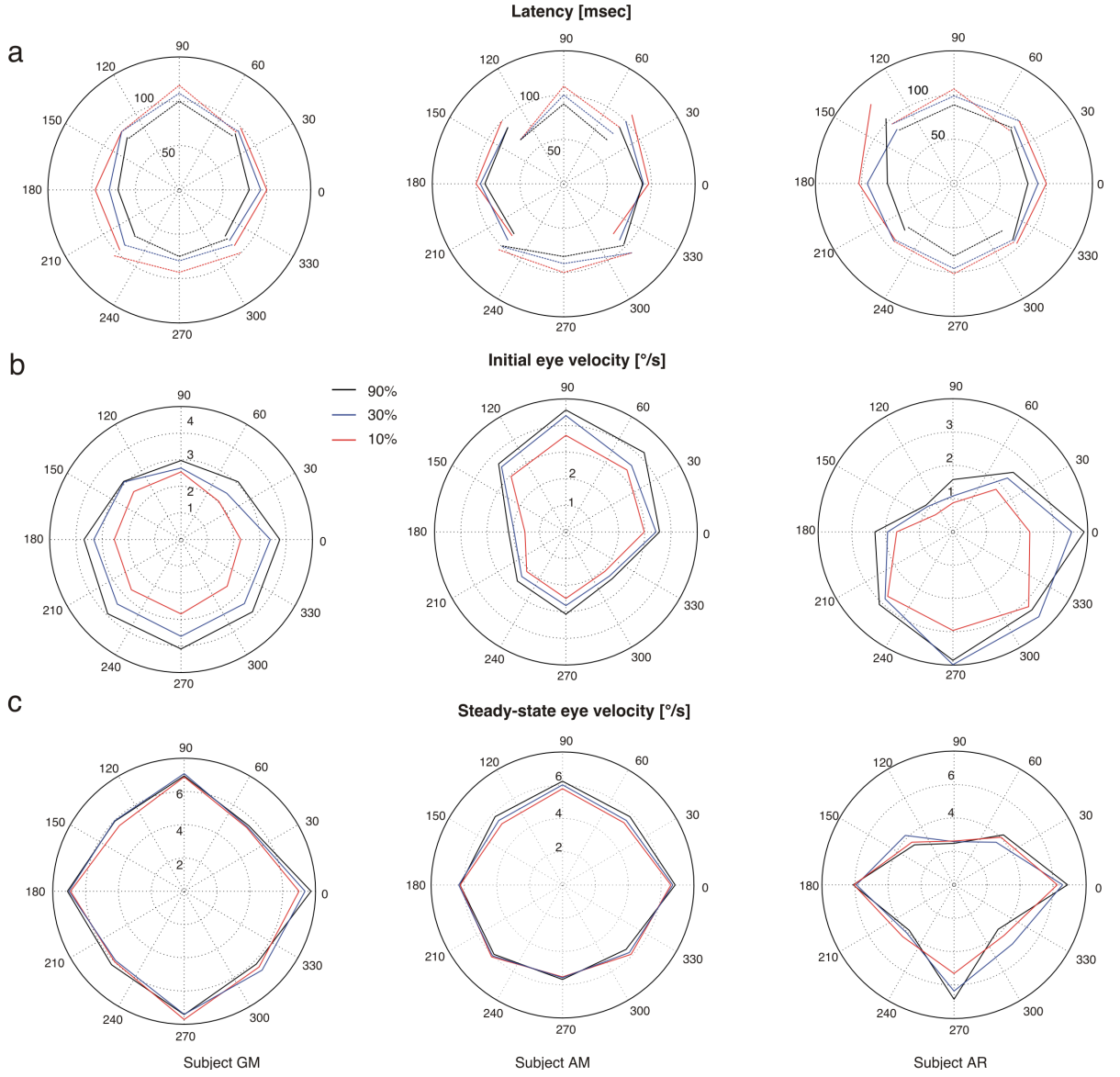


Figure 6.5: Directional anisotropies of contrast. Directional anisotropies for pursuit latencies (a), initial eye velocity (b) and steady-state eye velocity (c), for three different target contrasts. Three columns are for subject GM, AM and AR respectively.

We performed a similar analysis for smooth pursuit responses to different motion directions, presented at 3 different contrasts. Figure 6.5a plots both horizontal (continuous lines) and vertical (broken lines) latency, for 8 motion directions and 3 contrasts, for subjects GM (first column), AM (second column) and AR (third column). Consistent with the previous experiment, both horizontal and vertical latencies were shorter across all directions for higher contrast values. Again, there are subject-specific differences between x-latency and y-latency for some diagonal directions (Soechting et al., 2005).

The mean initial eye velocity in the time window (120, 180ms) is shown in Figure

6.5b. There are clearly some subject-specific anisotropies, indicating stronger eye acceleration for some motion directions than for others. An ANOVA revealed a significant main effect of motion direction (Subject GM: $F(7,1887)=17.38$, $p<0.0001$; Subject AM: $F(7,2137)=177.35$, $p<0.0001$; Subject AR: $F(7,960)=49.05$, $p<0.0001$) and, again, of contrast (Subject GM: $F(2,1892)=88.66$, $p<0.0001$; Subject AM: $F(2,2142)=40.08$, $p<0.0001$; Subject AR: $F(2,965)=16.46$, $p<0.0001$). The main direction effect indicates that initial eye velocity is strongly directionally anisotropic and idiosyncratic. For example, the initial eye velocity (subject: AM) along 180° is $1.6^\circ/\text{s}$ which is significantly lower when compared to the initial eye velocity ($3.63^\circ/\text{s}$) reached at the same point in time when pursuing in the upward direction (90°). On the contrary, the effect of contrast was directionally isotropic: across all motion directions, initial eye velocity increased with contrast. For the three subjects, varying contrast did not change the idiosyncratic directional anisotropies. Similar results were observed with steady-state eye velocity, as computed in the [320-380ms] time window (Figure 6.5c). A main effect of direction was found when performing an ANOVA test (Subject GM: $F(7,1887)=77.06$, $p<0.0001$; Subject AM: $F(7,2137)=56.91$, $p<0.0001$; Subject AR: $F(7,960)=27.2$, $p<0.0001$). Interestingly, the main directions for steady-state eye velocity were different from those observed with initial eye velocity. Again, contrast only marginally modulated steady-state eye velocity (Subject GM: $F(2,1892)=4.68$, $p<0.009$; Subject AM: $F(2,2142)=8.24$, $p<0.0003$) and the interaction between direction and contrast factors was marginally significant (Subject GM: $F(14,1871)=1.99$, $p<0.01$; Subject AM: $F(14,2121)=2.99$, $p<0.0001$). However, one can notice that steady-state eye velocity was almost identical across all 8 motion directions with very low contrast (red curves). These results suggest that subject specific directional anisotropies indeed exist for different conditions (Tanaka and Lisberger 2001) and should be taken into consideration when tuning the parameters of the oculomotor plant.

6.3.4. A recurrent Bayesian model for dynamic motion integration

We propose a recursive extension to the Bayesian framework (Weiss, Simoncelli and Adelson 2002) to describe the dynamic integration of 1D and 2D motion information. In the recurrent Bayesian framework (Montagnini, et al. 2007), the prior defined in the velocity space is combined with the two independent measurement likelihood functions (Likelihood functions representing edge-related (1D) and terminator-related information (2D)) to obtain the posterior, which updates the prior at the end of the iteration.

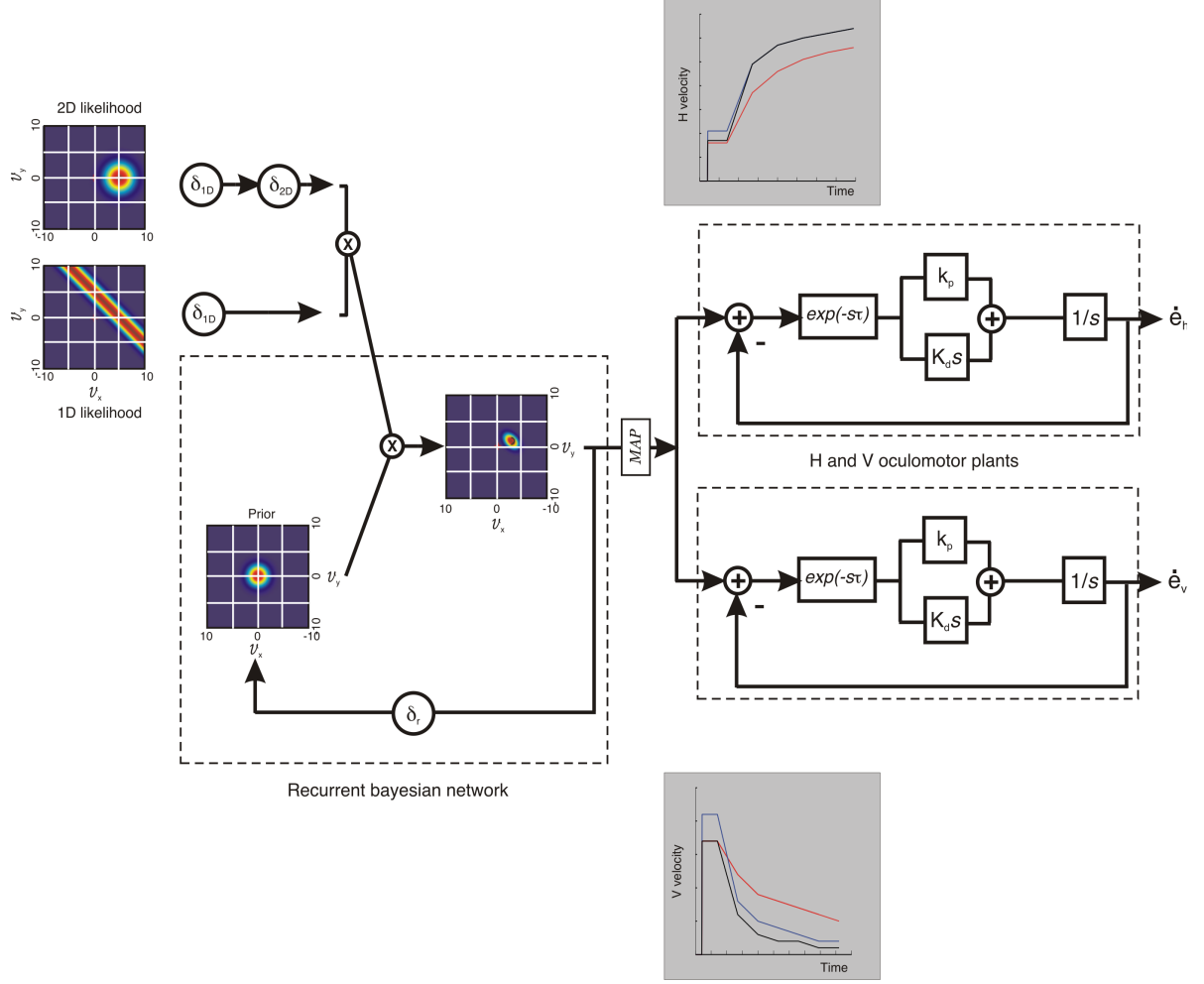


Figure 6.6: Model of recurrent inference for pursuit eye movements. The 1D and 2D motion information likelihoods are delayed by δ_{ID} and $(\delta_{ID} + \delta_{ID})$ respectively, and combined with the prior in a recurrent Bayesian framework. The prior is updated by the posterior for every δ_f ms. The readout of the posterior is obtained using the maximum-a-posteriori (MAP) decision rule. The transient of the horizontal and vertical components of the MAP (shown at the top and bottom in grey plots respectively for three different contrasts 10 %(red), 30 %(blue) and 90 %(black)) are fed as inputs to the horizontal (H) and vertical (V) oculomotor plants to produce pursuit velocity traces \dot{e}_h & \dot{e}_v respectively.

6.3.5. Model description

The block diagram of the model is illustrated in Figure 6.6. The model consists of three blocks, from left to right. The first block describes the sensory information processing as a recurrent Bayesian network and incorporates some fixed delays. The output is read-out using

Maximum-A-Posteriori (MAP) rule to extract desired horizontal and vertical eye velocity. These dynamical signals are then converted into eye velocity by two independent oculomotor plants.

The 1D and 2D motion information likelihoods are delayed by δt_{1d} , a fixed sensory delay of 20ms. In addition to that, the 2D information is delayed (δt_{2d}) by a fixed lag of 50ms. This lag results in (50-70ms) time delay for the initiation of encoding the true global velocity of the stimulus which is in agreement with the dynamics of motion signaling by neurons in MT (Smith, Majaj and Movshon 2005). The consequence of this delay is that 1D information is dominant in the initial stages of motion integration. It was long enough to allow a sufficient response from the filter implementing the oculomotor plant. The prior is updated with the posterior at the end of each iteration step with a delay (δt_{fb}). This delay accounts for the transient in the MAP of the recurrent Bayesian network. The horizontal and vertical MAP transient is also shown in Figure 6.6 as inputs to the respective oculomotor plants. The time constant of the vertical component of the Bayesian MAP is fixed around 65ms with δt_{fb} , in agreement with the time constant of the change in preferred direction as observed with a population of MT neurons (Pack and Born 2001; see Figure 6.1c).

The recurrent Bayesian network is cascaded with a Proportional-Derivative (PD) control model (Goldreich, Krauzlis and Lisberger 1992) to mimic the oculomotor dynamics and produce velocity traces comparable to the smooth pursuit eye velocity traces. The PD control essentially is a first order control system consisting of a delay τ , along with a proportional gain k_p and derivative gain k_d . The proportional gain k_p is directly proportional to the speed error signal whereas the differential gain k_d is proportional to the change in error. The latency of pursuit onset for the model is the sum of the fixed sensory delay δt_{1d} and the variable oculomotor delay τ .

6.3.6. Tuning the model parameters

Since the timing parameters in the recurrent Bayesian model are fixed delays, the parameters that remained to be tuned were k_d , k_p , τ . The delay τ is a free parameter and its value is equal to the latency of pursuit onset as measured in the above mentioned experiments. Knowing both the effects of line length (Figure 6.3) and directional anisotropy (Figures 6.4 and 6.5), we choose to tune the horizontal and vertical oculomotor plant gain parameters across all conditions (different speeds and different contrasts) with the smooth pursuit horizontal and vertical components respectively for a line of same length as the tilted line and moving orthogonal to its orientation along the 45° diagonal since the initial dynamics of the smooth

pursuit response for a 45° tilted line is biased toward the 45° direction because of the aperture problem. The fixed delay values in the recurrent Bayesian block for the two subjects are shown in the Table 1. The parameters of horizontal and vertical oculomotor plants obtained for both the subjects (AM & GM) across the different conditions are shown in Table 2. The parameters are estimated using a least square error fit.

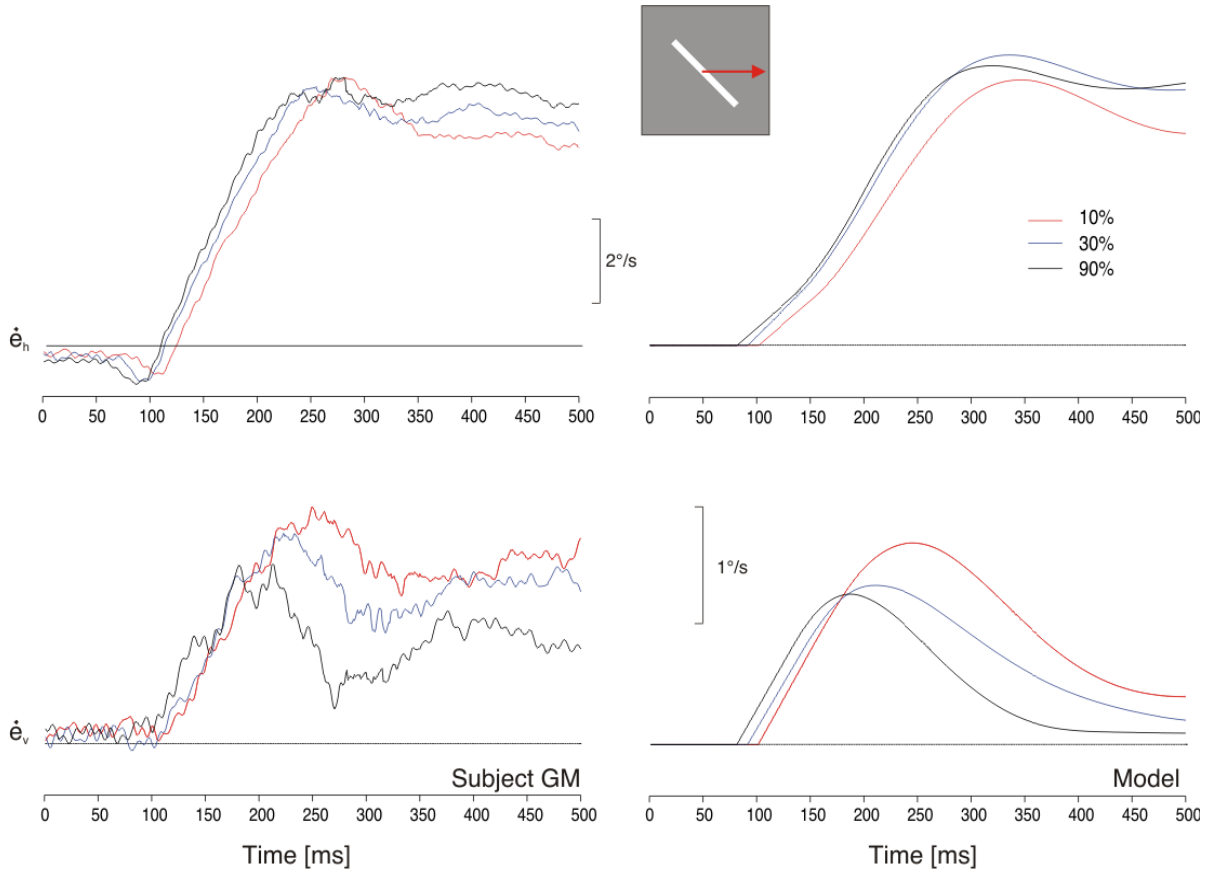


Figure 6.7: Pursuit eye velocity traces for data and the model (varying contrast). Human (right column) and model (left column) responses to a tilted line ($+45^\circ$) moving at $7^\circ/\text{s}$ and presented at three different contrast (10, 30 and 90%: red, blue and black curves, respectively). Curves are mean horizontal (horizontal \dot{e}_h) and vertical (\dot{e}_v) eye velocities.

subject	$\delta t_{1d}(\text{ms})$	$\delta t_{2d}(\text{ms})$	$\delta t_{fb}(\text{ms})$
GM	20	50	65
AM	20	50	92

Table 6.1. Timing parameter values for the recurrent Bayesian model.

Condition (contrast & speed)	Oculomotor plant (X)				Oculomotor plant (Y)				τ
	k_p	K_d	k_p	K_d					
10% & 7 °/s	10.66	13.74	0.22	0.07	6.56	9.88	0.26	0.05	82
30% & 7 °/s	10.43	12.22	0.26	0.12	9.23	7.87	0.1	0.32	72
90% & 7 °/s	9.93	13.22	0.30	0.09	8.35	9.66	0.23	0.07	62
100% & 5 °/s	11.05	8.1	0.26	0.38	8.59	6.54	0.41	0.36	100
100% & 10 °/s	10.12	7.89	0.31	0.42	8.22	6.51	0.40	0.37	100
100% & 15 °/s	12.06	7.32	0.15	0.47	8.27	7.31	0.45	0.35	100

Table 6.2. Best-fit parameters of the oculomotor plant model.

6.3.7. Experiment 4: Model and Smooth pursuit responses to translating tilted lines

We compared human pursuit and model using a different set of stimuli, tilted lines, where the aperture problem results in different initial and steady-state perceived directions, as shown in Figure 6.1. The velocity traces of the model and smooth pursuit responses obtained with such as 45° tilted line are presented for three different contrast values in Figure 6.7. After pursuit onset, there was a transient vertical component observed for both model and the data, reflecting the directional bias in the initial pursuit direction as previously observed (Masson & Stone, 2002; Born et al., 2006; Montagnini et al., 2006). Such bias corresponds to the shift in perceived direction due to the aperture problem. As expected, lower contrast resulted in stronger vertical eye acceleration and thus stronger pursuit bias towards the direction orthogonal to the bar orientation. Once the 2D motion information was integrated into target motion estimation, a rapid reduction in the vertical response component was observed, corresponding to a gradual rotation of pursuit direction towards the true translation direction. In the recording time window, such steady-state bias was remarkably reduced when target contrast increased. The model reproduced all of these observations. In particular, lower contrast resulted in delayed pursuit onset and stronger vertical responses. Interestingly, even for higher contrasts the steady state vertical bias didn't cancel out over the time scale under investigation. The steady state vertical bias for the model completely disappeared at high contrast for much longer pursuit duration (~1000ms). The horizontal component of the model response was slower as compared to that in data, particularly during the initial 50ms (20-70ms of MAP dynamics in figure 6.6) where the model responded to 1D information

alone, delaying the steady-state phase. Lastly, steady state eye velocity (horizontal component) of smooth pursuit responses increased with contrast, in agreement with Spering et al. (2005). Root mean square deviation (RMSD) values for the model and mean smooth pursuit traces for a moving tilted line are shown in table 3. Since the model is for the open loop, we have evaluated RMSD for duration of 250ms, starting from 20ms before pursuit initiation to 230ms after pursuit initiation. The RMSD values indicate that the model provides a quantitative description of the motion integration which is close to what is observed in smooth pursuit data, especially in the open loop.

The horizontal and vertical components of the model responses for different speeds are shown in Figure 6.8, in comparison with human pursuit. At pursuit onset, a transient vertical component was observed for all speeds. Maximum velocity of such transient vertical component increased with target speed, for both human data and model, as found by Wallace et al. (2005). A slow reduction in the vertical component leads to a steady state bias, which again scaled with target velocity. Model output resulted in a gradual increase in both horizontal and vertical eye velocity with increasing target speed, indicating that inference is further biased at high speed. The steady state velocity (horizontal component) of the smooth pursuit response was accurate for lower speeds but overestimated target speed, in particular for higher speed ($15^{\circ}/s$).

	Subject: AM		Subject: GM	
Contrast	Horizontal component (\dot{e}_h)	Vertical component (\dot{e}_v)	Horizontal component (\dot{e}_h)	Vertical component (\dot{e}_v)
10%	0.87	0.27	0.57	0.12
30%	1.09	0.22	0.61	0.18
90%	0.81	0.21	0.60	0.12

Table 6.3. Root mean square deviation (deg/s) for the model output and mean smooth pursuit traces for a moving tilted line.

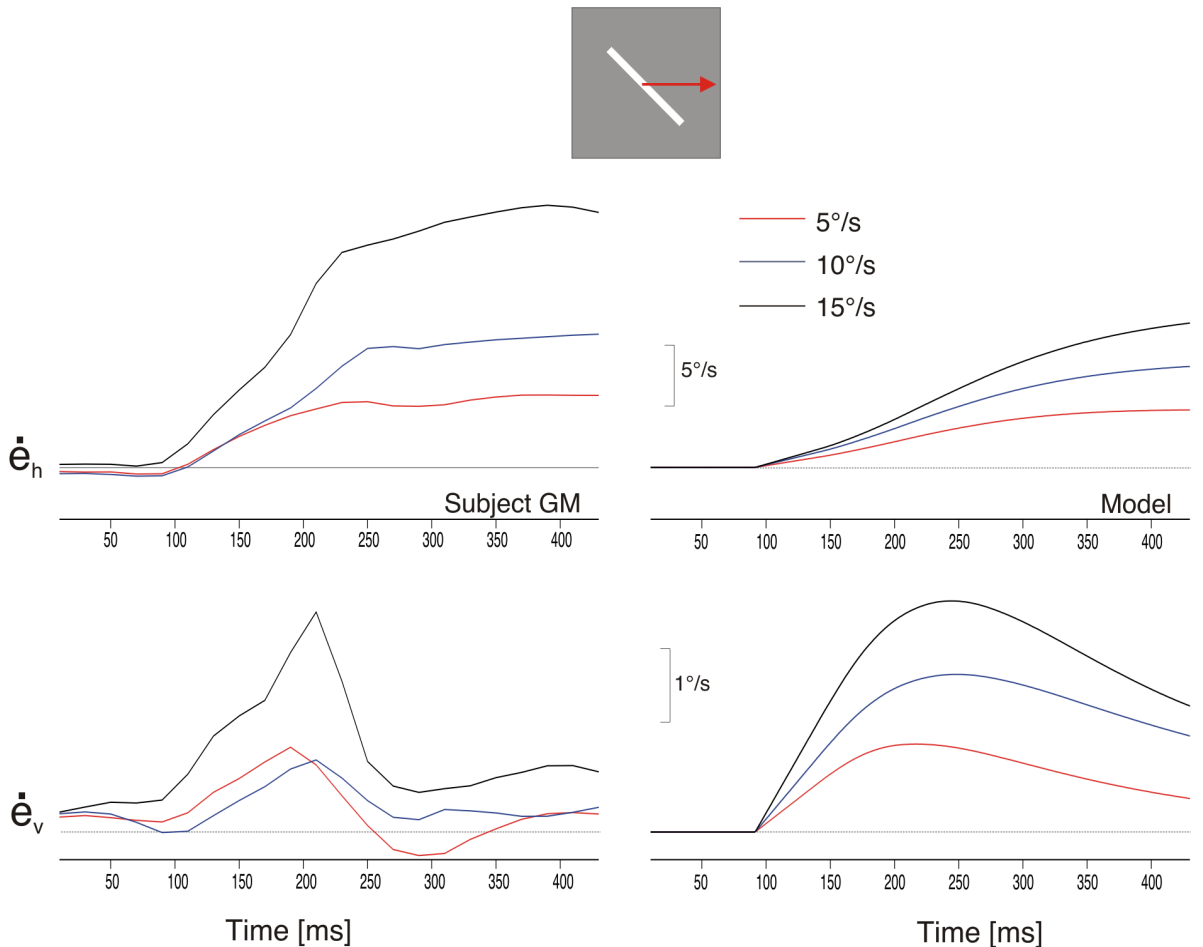


Figure 6.8: Pursuit eye velocity traces for data and the model (varying speed). Human (right column) and model (left column) responses to a tilted line (+45°) moving at 7°/s and presented at three different speeds (5, 10 and 15°/s: red, blue and black curves, respectively). Curves are mean horizontal (horizontal \dot{e}_h) and vertical (\dot{e}_v) eye velocities.

The dynamics of the direction bias is better illustrated when plotting initial tracking error against time (Figure 6.9) for both the smooth pursuit and the model across three contrasts. Notice that direction biases are estimated from time 100ms after pursuit onset for human tracking and time 140ms for model output, to take into account the 40-50ms lag introduced in the horizontal component of the model. The initial direction bias in the smooth pursuit responses was highest for low contrast (10%), reaching the oblique direction (45°, dotted horizontal line). It then decayed over time. Such initial bias was reduced with increasing contrast, as found previously with multiple edges objects (Wallace et al., 2005) (Figure 6.9a & 9b). Model output successfully reproduced these effects about time course and contrast-dependency. However, when the initial directional error for the model was

compared with that of the data obtained with subject AM, the initial directional bias values for the model was slightly higher for 30% and 90% contrast values and low directional bias for low contrast unlike what is observed with the data and the model performance for subject GM. This result was the only difference between observed and predicted values. This could be due to the significant directional anisotropies found for this particular subject (Figure 6.5b) that are used to tune the model as well as the lower variances observed with blob and upright target (Figure 6.2c) that are used as inputs to the model.

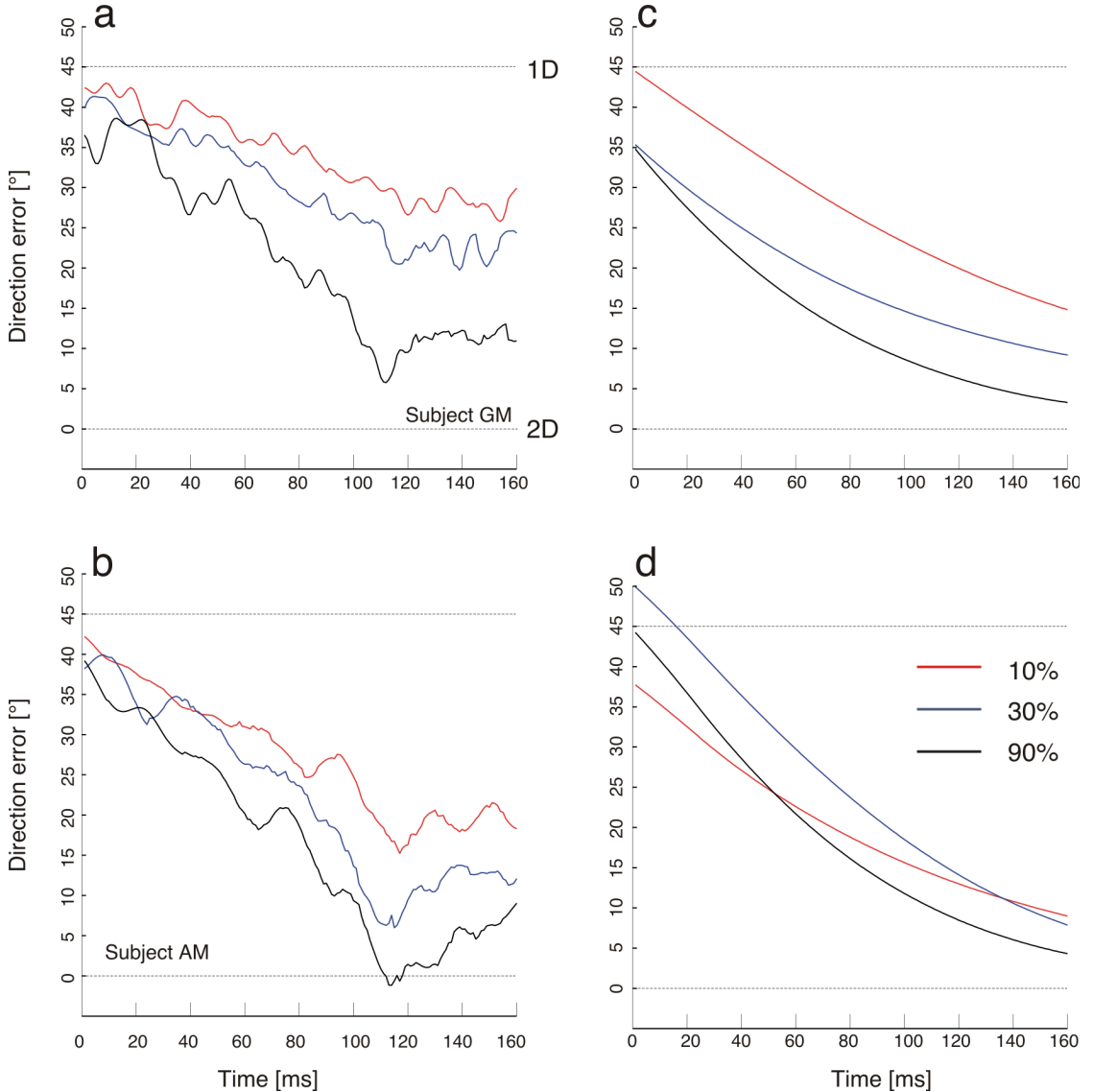


Figure 6.9: direction bias in data and the model (varying contrast). Tracking direction errors for two human subjects (left columns) plotted against time. Model responses obtained with parameters fitted for each subject with the data presented in Figures 2-5 are plotted in the right columns. Model has been run for three different contrast values: 10% (red), 30% (blue) and 90% (black). Data are direction biases (i.e. atan (\dot{e}_v/\dot{e}_h)) measured from 100 and

140ms after pursuit onset for human and model data, respectively, to account for the time lag of 40-50ms introduced in the horizontal component of the model.

6.4. Discussion

In the present study, we attempted to explain the dynamics of motion integration in the context of smooth pursuit responses using a recurrent Bayesian model. Our model has two stages. The first stage is a sensory integration stage, implemented as a recurrent Bayesian loop and the second stage is an oculomotor plant. The model takes the initial independent likelihoods of ambiguous 1D information and unambiguous 2D information as input (for all times) and combines them with an updating prior thereby optimally integrating the motion information to obtain a coherent percept of object's global motion. The dynamic MAP of the first stage is fed into the oculomotor plant to produce the final output of the model.

Such Bayesian framework has been successfully applied to model perceived motion direction and speed perception (Weiss et al. 2002; Stocker and Simoncelli 2006). However, these earlier models depart from ours in three important aspects. First, they did not predict any significant bias at full contrast. Second, they were static models and did not try to account for the temporal dynamics of motion integration. Third, they did not consider all different motion information available from the images and thus ignored the role of 2D feature motions in the actual implementation of the model. Here, we extended this theoretical approach to a dynamic implementation, by recurrently updating the Prior knowledge with the Posterior at the end of each iteration. A model describing the dynamic solution to the aperture problem is needed to explain the characteristic time course of eye movement velocity profiles while tracking, for instance a horizontally moving tilted line. Our first attempt to implement a recurrent Bayesian model of motion integration (Montagnini, et al. 2007) could not provide a complete account of the dynamic motion integration as observed in the oculomotor traces. The previous version of the model was limited to a qualitative description of the tracking direction error with arbitrary time scales, similar to a subsequent study by Dimova and Denham, 2009, reproducing our results. Here, we improved the Recurrent Bayesian model with an extension of oculomotor plant as a back end in order to produce realistic eye velocity profiles reflecting the characteristic dynamics of motion integration. This model not only gives an accurate qualitative account of the motion integration dynamics but also a quantitative account that is closely comparable to the smooth pursuit responses for different speeds and contrasts.

The final output mimics the open loop phase of smooth pursuit response to a horizontally moving tilted line-stimulus. The choice to limit the model to the open-loop phase, allows us to avoid the computational complexity involved in updating the measurement likelihood functions (1D & 2D) during the closed loop phase when the oculomotor feed-back is integrated in the smooth pursuit control. This recurrent Bayesian model is equivalent to a simple Kalman filter with a gain equal to 1 for the initial measurement that is the same for all iterations. Further work is needed to extend the current model to the closed-loop mode. This will need to include the effect of the positive feed-back loop involved in maintaining steady-state pursuit (Miles & Fuller, 1975; Goldreich et al., 1992). One difficulty will then be to estimate the variance of such internal signal, building eye velocity likelihood or combining image motion or pursued target estimates (Freeman, Champion & Warren, 2010) in head-centered coordinates.

A strong point of our approach is that the free parameters of the Bayesian distributions (the Prior, 1D- and 2D-Likelihood's variance) are estimated from an independent set of oculomotor data. We assumed that smooth pursuit variance at the peak acceleration time for pure 1D and pure 2D stimulus was closely related to the 1D and 2D likelihoods. The results obtained with subject AM (Figure 6.9) suggest that this method is not always accurate when rendering the effects of very low contrasts. Further work is needed to compare model outputs when estimating velocity likelihoods at different point in time since contrast is known to affect the intrinsic dynamics of motion processing, including latency and temporal dynamics of early visual neurons (Albrecht et al., 2002). This would improve the model to give a better quantitative account of the dynamic motion integration that is closer to the smooth pursuit responses.

In the sensory integration stage, appropriate internal delays were introduced, independently for the 1D and 2D information processing pathways, and they were chosen in such a way that the dynamics of the recurrent Bayesian MAP is comparable to the dynamics of MT neurons (Pack & Born, 2001). The time for the initiation of encoding the true global velocity of the stimulus (~70ms) for the model is in agreement with the dynamics of motion signaling by neurons in MT (Smith et al., 2005). However, such additional delay introduced in 2D velocity likelihood computation slightly over-estimates the values obtained in human subjects with ocular following responses. Earlier work from our group showed that 2D-driven responses were delayed by about 20-30ms relative to tracking onset driven by the 1D edges (Masson et al., 2000; Masson & Castet, 2002). Such delay increased to 40-50ms with low contrast values. Moreover, the changes in both 1D- and 2D-driven responses observed

with ocular following when lowering contrast is highly non-linear (Barthélemy et al., 2008). Further work will implement such nonlinear effects to make the system dynamics more realistic across a large range of contrast or noise levels. The decay time constant ($\sim 65\text{ms}$) of the vertical component of MAP, for a horizontally-moving tilted line, was set in agreement with the time constant of the change in preferred direction as observed with a population of MT neurons (Pack and Born 2001; see Figure 6.1c) and results obtained at high contrast with tilted lines (Figure 6.9) show that such values are in fact consistent with pursuit dynamics.

Finally, the gain parameters of the oculomotor plant were tuned with an independent set of data to incorporate both anisotropies and non-linearities that can be seen in human smooth pursuit oculomotor recordings. This is unlike previous oculomotor models that adopted a free parameter tuning strategy that would give a best fit of the model to the data, mostly along one direction only. Clearly, we need to better document the properties of smooth pursuit along oblique direction and more complex trajectories (e.g. De'Sperati & Viviani, 1997; Soechting et al., 2005) in order to simulate pursuit to 2D motion trajectories. Another difficulty we encountered is the ability of the oculomotor plant model to respond to transient input such as the vertical component of the MAP estimate with tilted lines. Transient changes in direction often occur in natural scenes. Moreover, as in the aperture problem, sensory estimate can quickly vary over time. MT neurons can follow these dynamics (e.g. Pack & Born, 2001; Osborne et al. 2004) and primate pursuit can cope with these (Osborne et al., 2007). However, we need to better model pursuit responses to these transient changes such as illustrated in MAP signals in Figure 6.6.

To conclude, our two stage model provides a novel approach to bridge the gap between a well-established theoretical framework like the Bayesian theory and the eye movement data, in modeling the transient behavioral dynamics. Importantly, this two stage framework can be extended to implement an independent perceptual mechanism operating on the posterior distribution of the recurrent Bayesian stage. In addition, decision rules other than MAP might be considered, possibly allowing us to take into account the posterior variance, instead of the mere maximum. Lastly, how different decision rules can better describe different data from the posterior distribution need to be investigated.

Part - 4

Prediction for Smooth Pursuit

Chapter 7

Role of prediction for smooth pursuit during transient disappearance of a target

This chapter describes the literature investigating the role of extra-retinal signals for smooth pursuit. A brief introduction to different paradigms namely repetitive patterns, expected target motion and transient blanking is provided. Studies using transient blanking were described in detail. Different oculomotor models employing positive feed-back alone and short term memory as extra-retinal drive for smooth pursuit are also described.

7.1. Role of extra-retinal signals for smooth pursuit - different paradigms

Different paradigms have been used to demonstrate the role of extra-retinal signals (often termed as predictive signals) for ocular tracking (see (Kowler 2011) for a review). Here, an example study for each paradigm is presented. In all the studies, stimulus used is a simple dot stimulus.

7.1.1. Repetitive Patterns

Typical stimulus is a dot whose displacement followed a periodic waveform which reverses direction at the half period. Subjects tracking the dot show responses that are delayed with typical latency for the first two or three cycles of exposure. Later, the subject's responses precede the stimulus indicating that the subject has learnt the timing of the changes in the trajectory (Barnes & Asselman 1991). When the waveform is not periodic and thus unpredictable, the subject employs a weighted averaging of past stimulus timing for the reversal (Collins & Barnes 2009).

This is shown in figure 7.1. For the first three cycles, eye displacement lags behind the stimulus at reversal after which the eye displacement predicts the reversal and precedes the stimulus. These results support the hypothesis for a short term storage of premotor drive which is used as an anticipatory drive in the subsequent stages (Barnes & Schmid 2002).

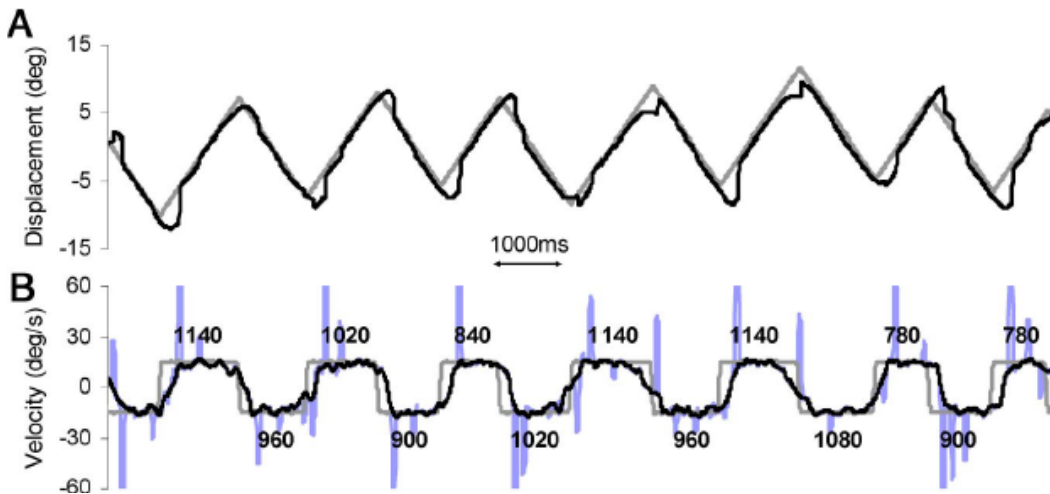


Figure 7.1. Prediction in Pursuit. (A) target displacement (grey) and eye displacement (black) (B) target velocity (grey) and eye velocity (black). (Collins & Barnes 2009)

7.1.2. Expected target motion

Subject's expectation about the future target motion can evoke smooth pursuit responses in the expected direction (Kowler & Steinman 1979a; b; De Hemptinne et al 2006). These effects of expectation cannot be eliminated by making target displacement unpredictable (Kowler & Steinman 1981) and the smooth eye movements depend on the prior target displacement (Kowler et al 1984) similar to what is observed with the repetitive patterns. When the target's motion is predictable, the smooth eye velocity component in the expected direction is higher compared to the smooth eye velocity component when the target's motion is unpredictable. This is shown in the figure 7.2.

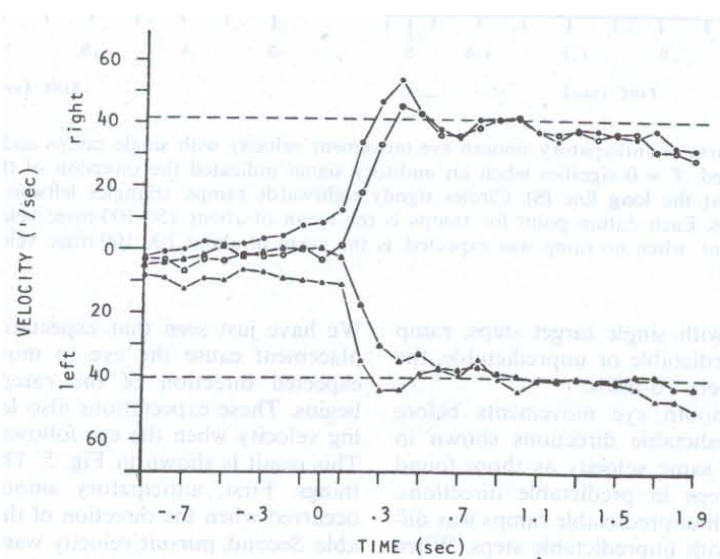


Figure 7.2. Time course of smooth eye velocity before and during ramp, when the target is

predictable (closed symbols) and unpredictable (open symbols) (Kowler & Steinman 1979b).

Not only expectation driven by the prior target motion effect smooth eye velocity, even the presence of static cues or verbal cues effect the anticipatory smooth velocity (Kowler 1989). Even causal knowledge of physical world can elicit anticipatory eye movements (Badler et al 2010). These results suggest that cues, either prior information about stimulus, or static and verbal cues influence expectation of target future motion and further anticipatory pursuit. This could be better understood with a mechanism where expectation drives pursuit using the short term memory of the premotor drive information (Bennett & Barnes 2004). The timing of anticipatory pursuit is related to the probability of the target motion onset (de Hemptinne et al 2007) and in the presence of external cues, a mix of both internally generated prediction and external cues are used to determine timing of anticipatory pursuit (Badler & Heinen 2006).

7.1.3. Transient blanking

In the previously mentioned two paradigms, the short-term memory of the premotor drive that drives anticipatory pursuit operates on a longer time scale i.e. over two or three repetitions of the pattern and several trials respectively. Transient blanking of the target provides with an opportunity to investigate the short term store and its dynamics in the space of a trial, albeit with expectation.

7.1.3.1. Blanking in steady-state

Transient blanking of a target results in the deceleration of the eye velocity for about 280ms after blank (figure 7.3B). The eye velocity stabilizes only if the target is expected to reappear after a short blank (Pola & Wyatt 1997) else eye velocity drops exponentially to zero (Mitrani & Dimitrov 1978). Subjects could maintain pursuit in the absence of the visual target for about 4s. This residual velocity is higher in the presence of a cue like a static occluder (Churchland et al 2003) and can be improved by training (Madelain & Krauzlis 2003).

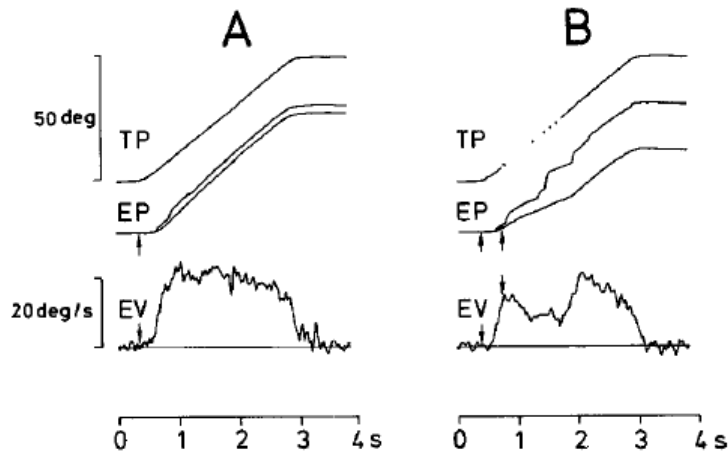


Figure 7.3. Effect of transient blanking during steady-state of pursuit. (A) target position (TP), eye position (EP) and eye velocity in a ramp paradigm. (B) target position (TP), eye position (EP) and eye velocity in a blanking paradigm. (Becker & Fuchs 1985)

This dynamics is often modeled as a reduction in the positive feed-back gain (Churchland et al 2003; Madelain & Krauzlis 2003). These models have a short coming which would be discussed in the section 7.2. They are not equipped to deal with the anticipatory increase during the blank observed in a number of studies.

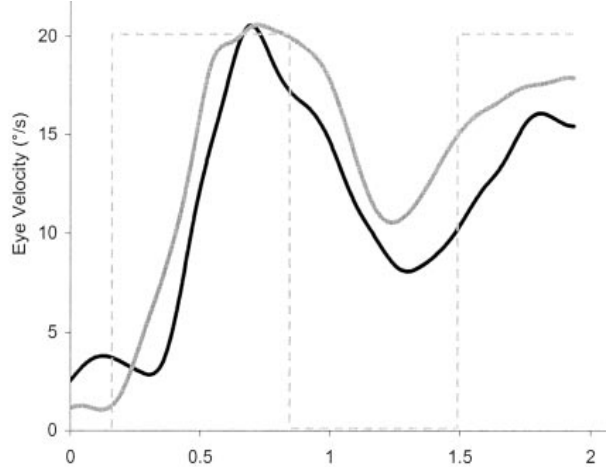


Figure 7.4. Effect of blocked and random presentation on smooth pursuit during a transient blank. Smooth eye velocity traces for a single blank duration are shown. The dotted blocks show the presence of the target on screen. Experiment consisted of blocked (grey) and random (black) presentation of different blank durations (Bennett & Barnes 2003).

When the time and duration of blank is randomized, the eye velocity doesn't show any anticipatory increase during the blank (Becker & Fuchs 1985). However, when the

duration and time of the blank is predictable, eye velocity shows an anticipatory increase before the end of blank as shown in the figure 7.4. Even when the change in the velocity of the target during the blank is predictable, anticipatory pursuit during the blank reflects the anticipated change in the target velocity (Bennett & Barnes 2004). This anticipatory increase is modeled using a short term store of the premotor drive (Bennett & Barnes 2004; 2006).

7.1.3.2. Blanking at initiation

When the target is blanked at initiation of pursuit and subject expects the target to reappear, eye velocity during the blank rises slowly. This is shown in the figure below for various blank times. When the target is blanked later at 200ms the familiar dip in the eye velocity during the blank is clear.

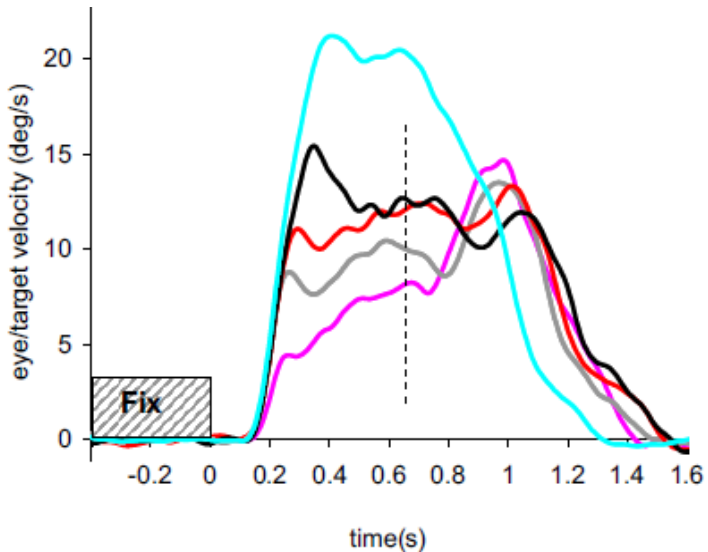


Figure 7.5. Effect of transient blanking during open-loop period of pursuit. Smooth pursuit traces for different blank starting times i.e. 50ms (magenta), 100ms (grey), 150ms (red), 200ms (black) and no blank condition (cyan). Duration of the blank is 600ms. (Barnes & Collins 2008b)

When the target reappears after blank, eye velocity increases to catch up with the target. The velocity at the end of the blank duration scales with the target velocity only when the target is blanked after 150ms. When the target is blanked earlier than 100ms, the target velocity at the end of the blank doesn't scale with the target velocity. These results suggest that a sample of the target velocity is acquired during the first 100ms after target initiation and 50ms later further refinement of the target velocity representation is done (Barnes & Collins 2008b). These results cannot be explained by models employing positive feed-back

gain where there is no extra source in the model that drives the eyes during the blank unlike the models employing a short term store of premotor drive (Bennett & Barnes 2004; 2006). Furthermore, this slow extra-retinal component driving pursuit in the absence of retinal stimulation is linked to anticipatory pursuit at initiation when the target's motion is predictable (Barnes & Collins 2008a). This further supports the idea of a short term sample of premotor drive.

Studies discussed here use target moving at a constant velocity. However, other studies employing an accelerating target or a more complex trajectory suggest for a dynamic representation of target motion for predictive pursuit and that target acceleration could be represented in predictive drive for pursuit (Bennett & Barnes 2006; Bennett et al 2007; Bennett et al 2010; Orban de Xivry et al 2008).

7.2. Models

This section describes two classes of oculomotor models for smooth pursuit, proposed to account for the dynamics observed during the transient blanking of a target. For ease of reference, they are classified as positive feed-back gain models (Churchland et al 2003; Madelain & Krauzlis 2003) and short term memory models (Bennett & Barnes 2004; 2006).

7.2.1. Positive feed-back gain model

The schematic of the model is shown in the figure 7.6. When the image velocity is zero during the steady state, the positive feed-back loop with its gain maintains pursuit. When there is no image motion during a blank, by reducing the gain of the positive feed-back loop momentarily the pursuit velocity is reduced and maintained at a reduced level as observed in the data.

However, anticipatory pursuit at the end of blank which is observed in the blank at initiation (Barnes & Collins 2008b) and other experiments (Bennett & Barnes 2003) cannot be mimicked with the positive feed-back gain. This model can accommodate learning effects during transient blanking by making the dynamics of the positive feed-back loop gain faster. To explain the anticipatory pursuit during transient blank and during predictable motion onset, model would need a short term memory of the ongoing motor drive which is implemented in the next class of model.

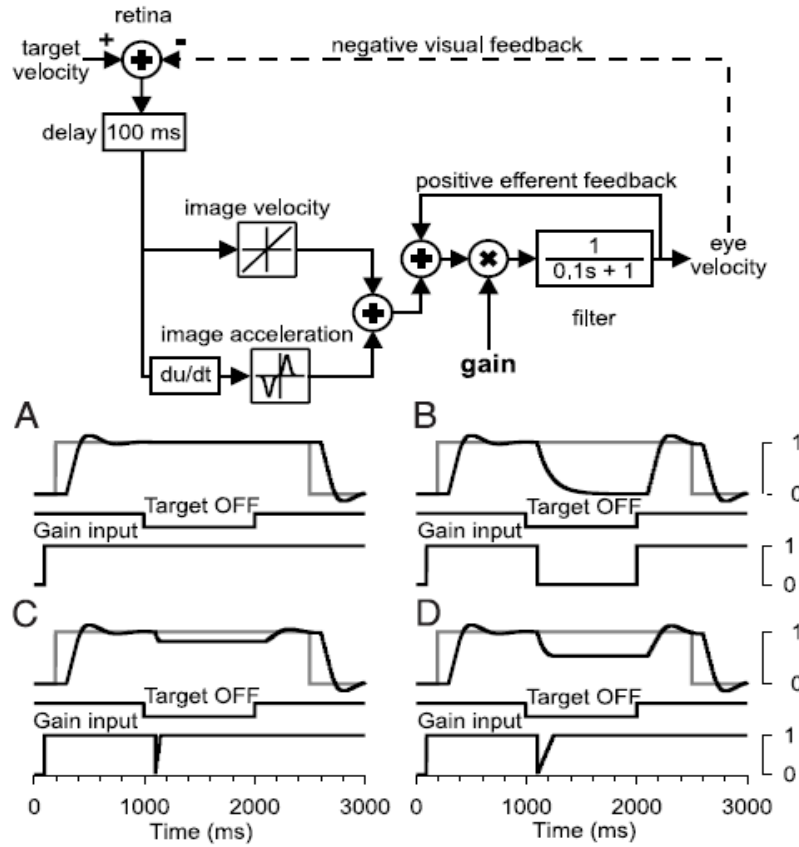


Figure 7.6. Positive feed-back gain model (Churchland et al 2003; Madelain & Krauzlis 2003). (A-D) Different gain functions and corresponding smooth pursuit responses

7.2.2. Short term memory model

The model consists of two loops, one direct loop similar to the positive feed-back loop in the previously described model and an indirect loop which acts as a short term memory of the target velocity (figure 7.7). The decision to switch between the loops depends on the expectation about the timing and velocity of the upcoming target presentation. The value of the memory is held when the gain (β) is less than 1. This enables the model to attain highest level of target velocity in expectation of the target appearance using the target velocity representation in short term memory. This means the model can mimick anticipatory velocity at the end of the blank or at initiation for predictable target motion.

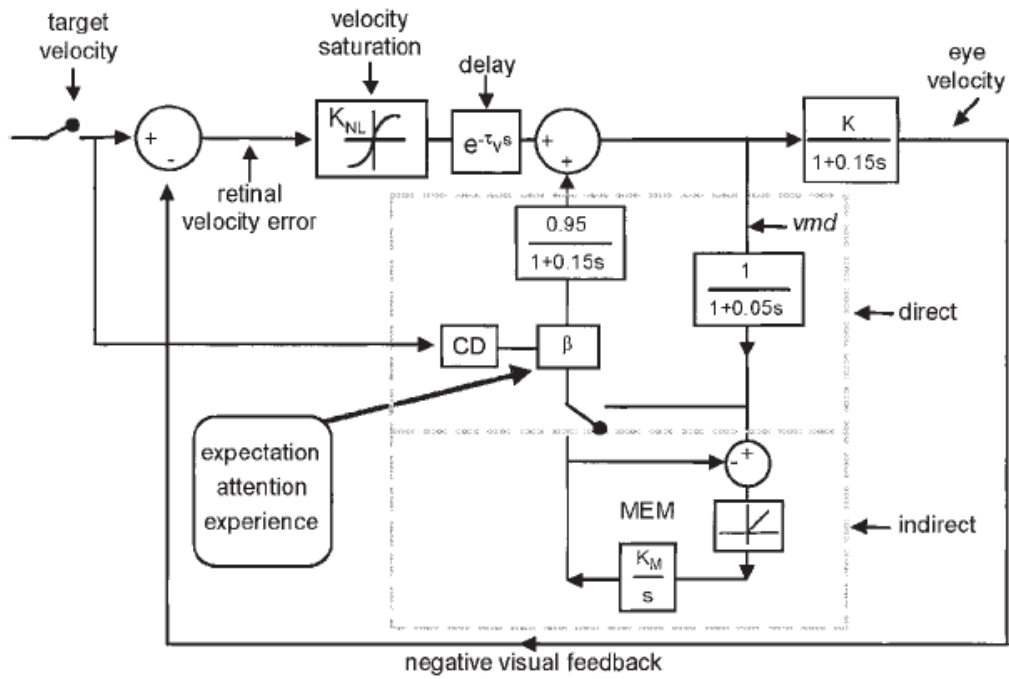


Figure 7.7. Short term memory model (Bennett & Barnes 2004)

The gain (β) is influenced by factors such as expectation, attention and experience. It is set by a conflict detector (CD) when there is a blank.

7.3. Summary

Different paradigms used to investigate the role of extra-retinal signals has been described. Studies using repetitive patterns show that if the pattern is periodic, after two or three cycles eye movements precede the pattern in anticipation (Barnes & Asselman 1991) and if the pattern is not periodic, a running average of the past stimulus timing is used to drive anticipatory pursuit (Collins & Barnes 2009). Studies using the expected target motion paradigm show that anticipatory pursuit is observed (Kowler & Steinman 1979a; b) even when the target is unpredictable (Kowler & Steinman 1981). All the above mentioned studies from different paradigms suggest for a short term storage of premotor drive that could be used in the subsequent stages depending on factors like expectation, attention and prior experience (Barnes & Schmid 2002). In both the paradigms, the learning of the pattern or expectation is on the order of two or three repetitions or trials. Transient blanking paradigm allows to investigate the nature of the short term store of the premotor drive in a single trial. Results from the blanking experiments in steady-state (Bennett & Barnes 2003) and at initiation (Barnes & Collins 2008b) suggest that previous models employing positive feedback gain (Churchland et al 2003; Madelain & Krauzlis 2003) alone cannot account for the

anticipatory pursuit and a short term memory of the ongoing premotor drive is needed. A model following this idea is discussed which could explain observations from several blanking studies (Barnes & Collins 2008b; Bennett & Barnes 2003; 2004). Coming chapters describe studies using one of the above mentioned paradigms to investigate role of extra-retinal signals on motion integration for smooth pursuit.

Chapter 8

Dynamic Interaction between retinal and extra-retinal signals in motion integration for smooth pursuit

Due to the aperture problem, the initial direction of tracking responses to a translating tilted bar is biased towards the direction orthogonal to the orientation of the bar. Previous studies have shown that such initial directional error is largely reduced over the first 200ms of tracking, consistent with the neural solution of the aperture problem and is fully corrected during the steady-state. Such simple paradigm also offers a powerful way to explore interactions between retinal and extra-retinal signals in controlling action. We conducted two experiments to investigate these interactions by transiently blanking the target at different moments during the steady state and initiation of pursuit. In the blanking at steady state experiment, a 45° or 135° tilted bar translating horizontally to right or left was blanked for two different durations (200 and 400 ms) at 600ms. Bar orientation after reappearance changed on half of the trials. We found a marginal but statistically significant directional bias on target reappearance for all subjects in at least one blank condition (200ms or 400ms). In the blanking at initiation experiment, a 45° or 135° tilted bar translating horizontally to right or left was blanked for 200ms at 100, 120, 140, 160 or 180ms after stimulus onset. A no blank condition is included as a control. Majority of the subjects (5 out of 6) show no bias that is statistically significant on target reappearance in at least one blank condition. These results suggest that a dynamical weighting of retinal and extra retina signals is necessary to accurately drive smooth pursuit. Based on our previous theoretical work on motion integration, we propose a new version of our closed-loop two stage recurrent Bayesian model where retinal and extra-retinal signals are dynamically weighted and combined to compute the visuomotor drive. This model reproduces many aspects of smooth pursuit during target blanking and provides a powerful theoretical framework to understand how different signals are dynamically combined to adaptively control our actions.

This study is submitted for publication - Bogadhi AR, Montagnini A, Masson GS. 2012. Dynamic Interaction between retinal and extra-retinal signals in motion integration for smooth pursuit. (Submitted)

8.1. Introduction

Primates use smooth pursuit eye movements to stabilize the image of a moving object on the retina. The visual system processes the retinal slip of the target image to obtain speed and direction estimates of the moving target and the accuracy in tracking is determined by the accuracy in this visual motion estimation since pursuit eye movements are primarily driven by target velocity (Rashbass 1961). Consequently, tracking responses carry the signature of visual motion information processing and the subsequent motor transformation (see Lisberger 2010 for a review). For instance, due to the aperture problem, the initial direction of tracking responses is largely driven by the ambiguous local motion signals of the moving object. The initial smooth pursuit responses to a tilted bar stimulus moving horizontally are biased in the direction orthogonal to the orientation of the bar (Born et al 2006; Masson & Stone 2002; Montagnini et al 2006; Wallace et al 2005). This directional bias is reduced in the subsequent 200ms of pursuit so that when reaching steady state tracking, pursuit is fully aligned with the 2D target motion. This temporal dynamics is consistent with that of neural solution to the aperture problem (Masson et al 2010; Pack & Born 2001).

Pursuit dynamics does not only reflect the visual motion processing stage. In the absence of retinal image motion during steady state tracking, extra-retinal signals can still drive pursuit. Indeed, the role of an internal positive feed-back during steady state tracking is a feature of several oculomotor models (Churchland et al 2003; Krauzlis & Lisberger 1994; Krauzlis & Miles 1996b; Robinson et al 1986). A transient disappearance of a target during pursuit results in an exponential drop in the eye velocity (Mitrani & Dimitrov 1978; Pola & Wyatt 1997) towards zero. However, if the subjects expect the target to reappear, the eye velocity decays for about 280ms (Becker & Fuchs 1985) but then stabilizes at a constant, non-zero value. Subjects can maintain pursuit in the absence of visual target for about 4sec before gradually dropping to zero (Becker & Fuchs 1985). During blanking, eye velocity can be steadily maintained at about 70% of pre-blanking target velocity although higher eye speed can be achieved with training (Madelain & Krauzlis 2003). The nature of the drive for the eye velocity in the absence of a visual target is still debated (see Kowler 2011 for a review). It could either be an efference copy serving as a positive feed-back (Churchland et al 2003; Madelain & Krauzlis 2003) or a sample of it being held in working memory (Bennett & Barnes 2003). Moreover, while the role of extra-retinal signals for smooth pursuit in the absence of a visual target is well investigated, less is known how these extra-retinal signals interact with retinal signals.

The aperture problem has been used to a large extent in investigating how the visual system processes the motion information coming through the retina. It also offers a way to probe the interactions between retinal and extra-retinal signals in motion integration for smooth pursuit (Montagnini et al 2006). A repetitive presentation of the horizontally moving tilted bar stimulus resulted in anticipatory horizontal smooth pursuit as observed in the previous studies with a dot like stimulus indicating an unbiased motion prediction. However, a directional bias was seen at the initiation of visually guided smooth pursuit similar to a randomized presentation. These results suggest that extra-retinal signals don't influence motion integration during pursuit initiation. However, (Masson & Stone 2002) originally reported that during peri-foveal pursuit of tilted diamonds, steady-state pursuit after target blanking and reappearance is not perturbed by ambiguous 1D motion signals but rather maintain the pursuit direction reached once the aperture problem has been solved after pursuit initiation. In a later preliminary study, we showed in monkeys that such behavior could depend upon the predictability of target reappearance (Masson et al 2008). Overall, our previous works indicate that the visual aperture problem can be an excellent tool to probe the dynamics of pursuit under different drive conditions (See Masson et al 2010 for a review).

In the present study, we conduct a more detailed investigation of how extra-retinal signals interact with retinal signals during pursuit using a tilted moving bar as a stimulus and by blanking it at different moments of the pursuit response. As said above, extra-retinal signals drive pursuit in the absence of a visual stimulus albeit with a reduced velocity (Becker & Fuchs 1985; Bennett & Barnes 2003; Churchland et al 2003; Madelain & Krauzlis 2003). The dynamics of the extra- retinal drive for pursuit during a transient blank is different when the stimulus is blanked early during rising phase of pursuit (Barnes & Collins 2008a) or late during its steady state phase (Becker & Fuchs 1985; Bennett & Barnes 2003). Since the dynamics of the extra-retinal drive for pursuit during a transient blank is different in the open loop and steady state stages of pursuit, we conducted two experiments where the tilted bar stimulus is blanked during the open loop stage of pursuit (open loop blanking experiment) and during the steady state stage of pursuit (steady state blanking experiment) to investigate the interactions between retinal and extra-retinal signals on target reappearance.

When the stimulus reappears after blanking, there is a finite retinal slip of the image which could result again in the aperture problem and, consequently a direction bias in the tracking responses. We reasoned that if extra-retinal signals that have been driving pursuit in the absence of the visual target would interact with retinal signals upon the target reappearance then these interactions might be tractable by measuring direction bias in the

tracking responses. We will show that the dynamics of these interactions change with the time at which the stimulus is blanked. Extra-retinal signals dominate retinal signals upon the target reappearance after the blanking during the open-loop phase resulting in a non significant directional bias in the tracking responses. When the stimulus reappears after a short blank in the steady state, the tracking responses show a significant bias suggesting a weaker influence of extra-retinal signals on retinal signals on target reappearance.

All previous ocular smooth pursuit models have focused on understanding the dynamics of smooth pursuit for simple, non ambiguous motion stimuli such as a translating dot. This approach has neglected the impact of visual motion integration in the sensorimotor transformation (e.g. (Bennett & Barnes 2003; Churchland & Lisberger 2001; Goldreich et al 1992; Krauzlis & Lisberger 1989; 1994; Madelain & Krauzlis 2003; Robinson et al 1986; Tavassoli 2009)). By contrast, we have recently proposed that the dynamics of the smooth pursuit responses, as probed with ambiguous inputs, reflects the dynamics of motion integration and can be modeled as a dynamic Bayesian inference of 2D target motion (Bogadhi et al 2011; Montagnini et al 2007). Here, we extend our previous open-loop recurrent Bayesian model to a closed-loop, two stage recurrent Bayesian model in order to understand the interactions between retinal and extra-retinal signals in motion integration for smooth pursuit. The first stage of the model is a retinal recurrent Bayesian block which combines likelihoods of the ambiguous and unambiguous motion information together with a prior distribution in velocity space (Weiss et al 2002). The resultant posterior is used to update the prior after every iteration (Montagnini et al 2007). The second stage of the model is an extra-retinal recurrent Bayesian block whose prior is combined with an internal estimate of eye velocity and recurrently updated with this extra-retinal posterior distribution. The input to extra-retinal recurrent Bayesian block is the premotor drive that is used both as the input to the oculomotor plant driving the eye and the efference copy, internal positive feed-back loop. We will show that such an hierarchical Bayesian model can account for pursuit dynamics under various conditions of sensory and motor evidence as collected at different phases of pursuit behavior.

8.2. Methods

Subjects

A total of six subjects participated in the study (mean age 31.5 yrs; SD 7.06) of which three were completely naive to the present as well as eye movement research. All subjects were

healthy and had normal or corrected to normal vision and had no relevant medical and psychiatric history. The experiments were conducted in accordance with CNRS ethical regulations for behavioral research. All subjects participated with informed consent.

Visual Stimulus and Apparatus

The visual stimulus used in the experiments described below was a 17° long and 0.126° wide tilted bar with different orientations. All stimuli were presented on a 21" CRT monitor at refresh rate of 100Hz against a Grey background. The display was gamma calibrated and the peak luminance of the Grey background was 60 cd/m^2 . The spatial resolution of the screen was set to 1280(H) X 1024(V) pixels.

Experimental Design

We conducted two main experiments to investigate the interactions between retinal and extra-retinal signals in motion integration for smooth pursuit at different stages of pursuit. The stimulus was blanked for different durations at different stages of pursuit i.e., open-loop and steady state of pursuit. The details of the experiments are described below.

Experiment 1: Blanking during the steady-state phase of pursuit

Stimulus was either a 45° or a 135° tilted bar translating horizontally to right or left at a constant velocity of $8.4^{\circ}/\text{s}$. In $4/6^{\text{th}}$ of the trials, the stimulus was blanked for 200ms or 400ms at 600ms after stimulus onset, that is, during the steady state of pursuit. In half of the blanking trials, the target reappeared with a 90° change of orientation after blanking. In half of the no blanking trials, an instantaneous 90° change of orientation occurred at 600ms after stimulus onset. Responses were compared to a control condition, where bar orientation remained constant during the whole stimulus duration. The duration of the trial was always fixed at 1500ms and all conditions were randomly interleaved. At least 50 trials per condition were recorded.

Experiment 2: Blanking during the initial, open-loop phase of pursuit

Stimulus was a 45° or a 135° tilted bar translating horizontally to right or left at a constant velocity of $8.4^{\circ}/\text{s}$. The total duration of the trial was of 900ms. In $5/6^{\text{th}}$ of the trials, the stimulus was blanked for 200ms, starting at either 100, 120, 140, 160 or 180ms after target onset. Thus, all target blanking conditions began during the open-loop phase of pursuit. In

the remaining trials the stimulus was not blanked and this was used as a control condition. All the conditions were randomly presented. At least 50 trials per condition were recorded.

Experimental protocol

Subjects (3 non-naive, 3 naive) were sitting in front of the monitor at a distance of 43cm, with their head stabilized by chin and forehead rests. Each trial started with subjects fixating a dot at the center of the screen for a random duration of 400 to 600ms. The diameter of the fixation dot was 0.33° . Once fixation was achieved, fixation dot was turned off, leaving a completely dark screen for 100ms. This introduces a gap between fixation target offset and moving target onset. The tilted bar was presented at 1° of eccentricity and moved in the opposite direction, similar to the step-ramp paradigm introduced by (Rashbass 1961). Subjects were instructed to track the center of the bar and to maintain pursuit during the blank period since the target would always reappear at the end of it.

Data recording and treatment

Eye movements were recorded using an Eyelink1000 eye tracker. Horizontal and vertical positions of the right eye were recorded at a sampling rate of 1KHz. Eye position time series were low-pass filtered with a cutoff frequency of 50Hz. The resultant eye position data were differentiated to obtain the velocity traces. The velocity traces were low-pass filtered with a cutoff frequency of 50Hz to remove the noise from the computation differentiation. The velocity traces were smoothed using the *csaps* spline function in MATLAB with a spline coefficient of 0.0001. During the visual inspection in MATLAB, we used a conjoint acceleration and velocity threshold to detect and remove catch-up saccades (Krauzlis & Miles 1996a). An objective method was used to compute the smooth pursuit latency in each trial and the method is based on the intersection between the two linear regression lines with a threshold criterion for slope increase (Krauzlis & Miles 1996a; Masson & Castet 2002). Oculomotor traces were aligned to stimulus onset. Outlier trails (less than 5%) were eliminated using an offline inspection. The outlier trials are those in which saccades could not be eliminated without excluding the majority of the trial or in which high levels of noise exist during fixation and persist during pursuit.

Data Analysis

For ease of analysis, smooth pursuit responses for different conditions (e.g. 45° oriented bar translating left or 135° oriented bar translating right) were realigned so as to appear like the

responses for 45° oriented bar translating right. This resulted in a total of at least 200 trials (at least 50 trials for each of the 4 conditions). Mean smooth pursuit responses (over 200 trials) to a brief blank of 200ms at starting at 600ms are shown in Figure 8.s 1a. Horizontal and vertical components of eye velocity will be referred to as \dot{e}_h and \dot{e}_v respectively. Figure 8.s 1a shows the different parameters that were extracted from \dot{e}_h on each trial for quantitative analysis. δt_{drop} corresponds to the duration for which eye velocity dropped before reaching a minimum during the next 300ms or 500ms of the blank (for 200ms or 400ms blank respectively) starting 80ms after blank initiation. The minimum eye velocity reached during the blanking period is denoted V_{min} . V_{80} is the velocity observed 80ms after blank initiation and V_{ext} is the velocity measured 80ms after the reappearance of the target, that is the end of the blanking target (Figure 8. 1c). δV_{drop} is the drop in the eye velocity because of the blank and is computed as the difference between V_{min} and V_{80} i.e. $(V_{min} - V_{80})$. δV_{ant} is the anticipatory rise in the eye velocity before target reappearance and is calculated as the difference between V_{ext} and V_{min} i.e. $(V_{ext} - V_{min})$ as shown in Figure 8.1c.

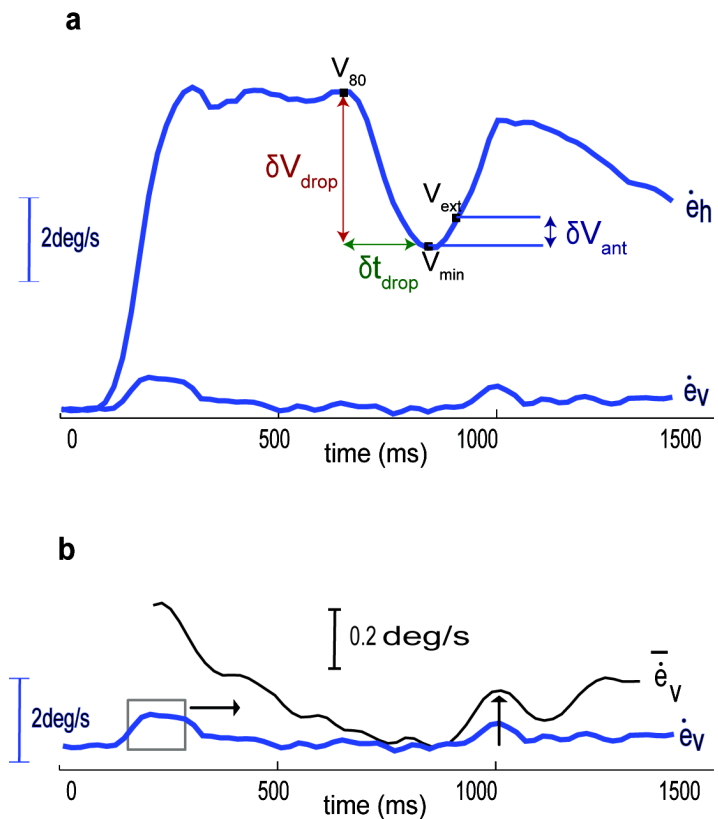


Figure 8.1: Different measures quantifying the dynamics in a pursuit response for 200ms blank duration. a. Schematic of the different measures on the horizontal component of eye velocity (\dot{e}_h). V_{min} is the minimum eye velocity reached during the blanking period. V_{80} is the velocity observed 80ms after blank initiation and V_{ext} is the velocity measured 80ms after the reappearance of the target. δV_{drop} is the drop in the eye velocity during the blank ($V_{min} - V_{80}$) and the corresponding time duration is δt_{drop} . δV_{ant} is the anticipatory rise in the eye velocity before target reappearance ($V_{ext} - V_{min}$). b. slide average vertical eye velocity $\bar{\dot{e}}_v$ (black) computed to highlight change in vertical eye velocity (\dot{e}_v) on target reappearance (shown with black arrow) using a 140ms wide sliding window initially centered at 210ms on vertical eye velocity (\dot{e}_v)(blue).

Although the stimulus was translating to the right, because of the aperture problem the pursuit started in a direction orthogonal to the orientation of the bar. This can be seen from the vertical eye velocity component in Figure 8.1a. This vertical eye velocity peaked at ~210ms and started to decelerate towards zero for the next ~150ms by the end of which the horizontal eye velocity reached target velocity as shown in Figure 8.1a. Throughout the present study, this vertical eye velocity component was used as a measure of the impact of the aperture problem upon the sensorimotor transformation, and its dynamics during pursuit initiation is known to reflect the dynamics of motion integration (see Masson et al 2010). Note that, with our experimental conditions required by the blanking experiments, peak vertical eye velocity was always rather small. In order to be able to measure any small changes in vertical eye velocity on target reappearance this visually-driven vertical has to be highlighted. For this purpose, a sliding window average of the vertical eye velocity component $\bar{\dot{e}}_v$ was computed using a 140ms wide time window sliding at steps of 20ms, initially centered at ~210ms where vertical eye velocity peaks as shown in Figure 8.1b. Figure 8.1b also shows the slide average vertical eye velocity $\bar{\dot{e}}_v$ in black. The black arrow indicates the bias in the vertical component on target reappearance at 800ms.

Statistical Analysis

We conducted an ANOVA on the different quantities (δt_{drop} , δV_{drop} , δV_{ant}) measured from the horizontal eye velocity component with the blank condition as the factor in both open loop and steady state blanking experiments. We conducted paired t-test on the slide average

vertical eye velocity component to measure the significance of the change in the slide average vertical eye velocity component on target reappearance from the baseline during the blank.

8.3. Results

8.3.1. Experiment 1: Target blanking during the steady-state phase of pursuit

The mean horizontal (\dot{e}_h) and vertical (\dot{e}_v) eye velocity traces across different conditions are shown in Figure 8.2 for a naive subject (subject 4) and a non-naive subject (subject 3). The velocity traces in red are responses to a no blank condition. In all blanking conditions, the target disappeared at 600ms (shown by the black dotted line). At ~690 ms the horizontal component of eye velocity began decelerating for ~180ms and ~280 ms for blanking durations of 200 and 400ms, respectively. After the deceleration, horizontal eye velocity reached a stable value (V_{min}) 400ms blank duration as seen in Figure 8.2a. Subjects show a brief acceleration within 80ms of target reappearance (target reappearance indicated by colored vertical line) as seen in Figure 8.2b.

Once the target had reappeared at the end of the blank duration, the horizontal eye velocity accelerated until it matched target velocity, as illustrated in Figure 8.2a,b. There was a marginal change in the vertical eye velocity before it peaks at ~200ms after target reappearance and gradually reduced or stayed constant as shown in the insets *d* and *f* of Figure 8.2. These changes in vertical eye velocity were dependent on the change in line orientation at reappearance as shown in the same insets of Figure 8.2. At target reappearance, if the orientation of the line stayed constant at 45° , the vertical component increased only marginally as shown by the blue and black traces. If the orientation was flipped by 90° at target reappearance, the vertical eye velocity changed direction as illustrated by the magenta and green traces. This change in direction of the vertical component corresponds to the effect of the aperture problem that is now introducing a downward bias in line motion perception. We ran a control condition where the target orientation was suddenly changed during steady-state pursuit at a fixed timing (600ms) relative to target motion onset. About 80ms after line rotation, the horizontal eye velocity was reduced for about 80ms before recovering the actual, horizontal target velocity. At the same time, the vertical eye velocity changed direction before being stabilized at a small, but significant (t-test ; $P<0.05$) downward velocity, as shown by cyan traces in insets *d* and *f* of Figure 8.2.

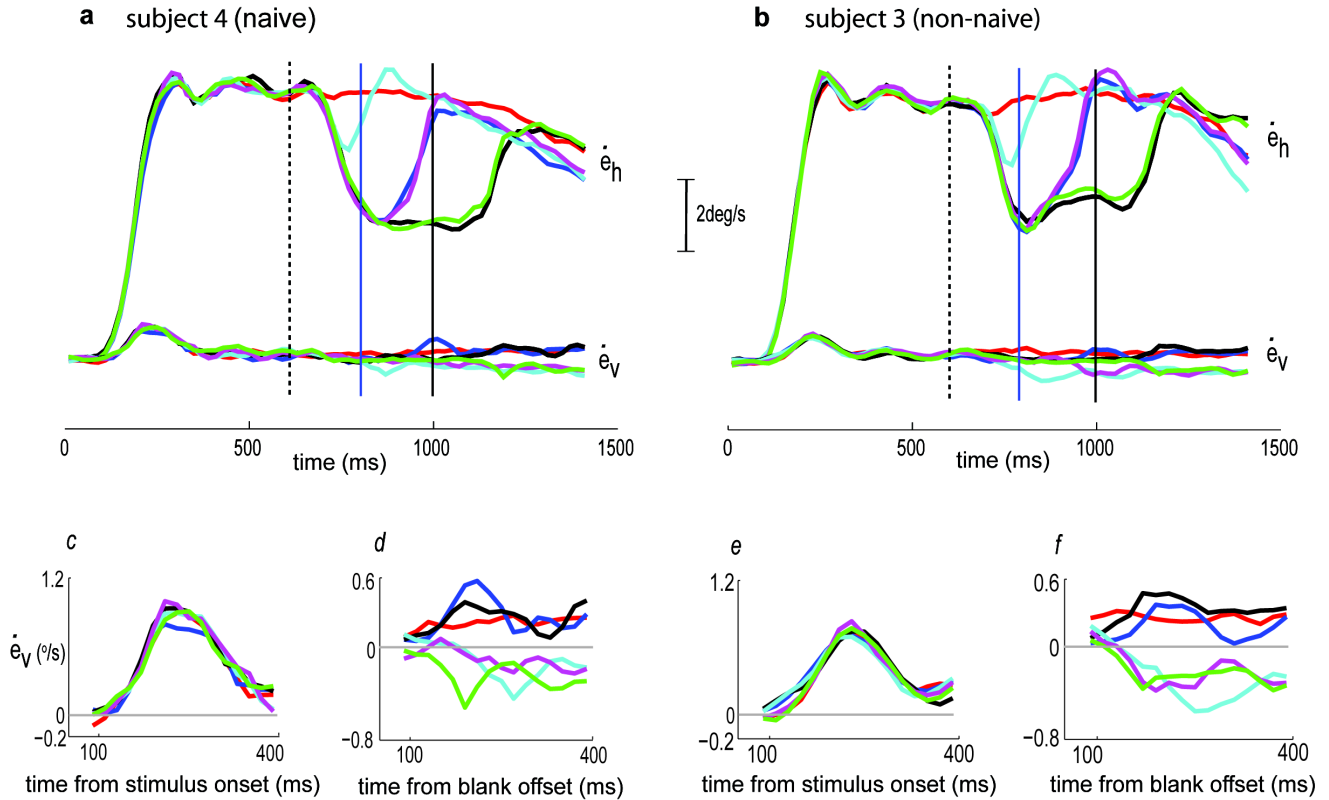
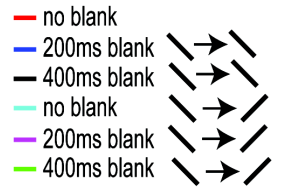


Figure 8.2: Mean smooth pursuit responses for blanking in steady state experiment.

a & b. Mean horizontal (\dot{e}_h) and vertical (\dot{e}_v) eye velocity traces (across 200 trials) for a naïve subject (subject4) shown in **a** and for a non-naive subject (subject3) shown in **b**. Dotted vertical line (black) indicates blank onset at 600ms and the solid colored vertical lines indicate end of blank duration for the corresponding blanking condition shown by the respective color. Insets **c** and **e** below indicate the vertical eye velocity component (\dot{e}_v) across all conditions for 300ms duration starting from 100ms after stimulus onset. Insets **d** and **f** below indicate the vertical eye velocity component (\dot{e}_v) across all conditions for 300ms duration starting from 100ms after blank offset (i.e. on target reappearance) for blanking conditions, and starting from 700ms for the condition in which orientation of the line changes instantaneously at 600ms. For no blank condition (red), vertical eye velocity component is taken for the same duration as the 600-1000ms blanking condition. Stimulus is blanked at 600ms after stimulus onset, for 200ms or 400ms duration.

The horizontal eye velocity component (e_h)

The quantitative changes in the horizontal eye velocity component during the blank are shown in Figure 8.3. In plot a, δt_{drop} is plotted for different blank durations. All the subjects showed a similar increase in δt_{drop} with longer blank durations ($p < 0.001$). In Figure 8.3b, the amplitude of the drop in the horizontal eye velocity (δV_{drop}) is plotted against blank durations. This drop was marginally, but significantly, higher for the longer blank durations ($p < 0.001$). Subjects with larger pursuit experience (red and blue lines) showed a smaller drop.

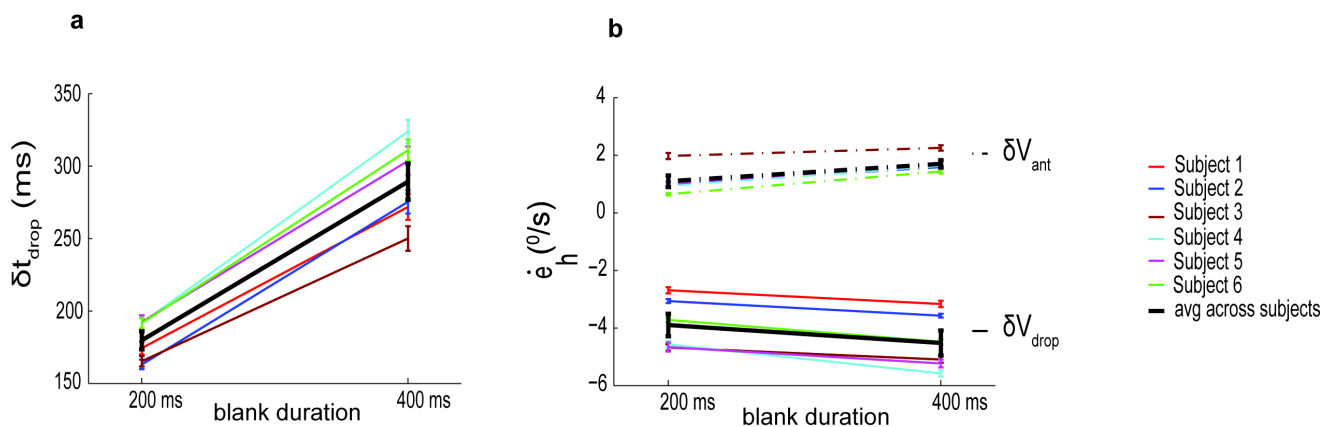


Figure 8.3: Blanking in steady-state :Horizontal component Analysis.

a. δt_{drop} for two blanking durations shown for all subjects (thin and colored lines) and average across subjects (thick black line). b. δV_{drop} and δV_{ant} for two blank durations shown for all subjects (thin and colored lines) and average across subjects (thick black line).

The anticipatory rise in eye velocity was quantified as δV_{ant} which is shown in Figure 8.3b for 200 and 400ms blank durations. The anticipatory pursuit was higher with a 400ms blank duration, as compared to the 200ms condition. This can be explained by the fact that expectation of target reappearance was higher for trials with long blank durations. It shall be noted that all subjects exhibited larger anticipatory pursuit with longer blank duration ($p < 0.001$).

The vertical eye velocity component (e_v)

To quantify the changes elicited in the vertical pursuit component by either target reappearance or a sudden change in target orientation, we evaluated slide average vertical

eye velocity \bar{e}_v using a sliding window as described in Methods. The mean (across subjects) value is plotted in Figure 8.4a for all conditions. This sliding window was initially centered at ~ 210 ms after stimulus onset, corresponding to the peak of vertical bias introduced in pursuit direction by the aperture problem. This gives a higher starting slide average vertical velocity \bar{e}_v as shown in Figure 8.4a for all conditions. As the window slides through the vertical eye velocity component, slide average vertical eye velocity \bar{e}_v decreases due to motion integration and it gradually falls off to a constant during the steady state as shown for the no blank condition (red curve) in Figure 8.4a. For all the blanking conditions, the slide average vertical eye velocity \bar{e}_v starts to decrease at 620 ms towards zero and stabilizes at a negative value near zero. This is followed by an increase on the target reappearance when the orientation of the bar is 45^0 (blue and black curves). The slide average vertical eye velocity \bar{e}_v on target reappearance reaches the peak at 1010 ms (200 ms blank) and 1210 ms (400 ms blank) i.e. ~ 210 ms after target reappearance as with the initial vertical bias due to the aperture problem (pointed by the colored arrows in Figure 8.4a). When the target orientation changes by 90^0 after the blank, the slide average vertical eye velocity \bar{e}_v reduces to negative. Arrows in Figure 8.4a show a clear demarcation in the responses to change in the orientation after blank when compared with the responses to no change in orientation after blank for both 200 ms (blue and magenta) and 400 ms (black and green) durations. The change in the slide average vertical component on target reappearance (indicated by the length of the arrows) is calculated as the difference between slide average vertical component taken at ~ 210 ms after target reappearance (\bar{e}_{vr} , pointed by the respective colored arrows in Figure 8.4a) and the slide average vertical component taken ~ 150 ms after blank initiation (\bar{e}_{vb} , pointed by the grey arrow in Figure 8.4a). This change ($\bar{e}_{vr} - \bar{e}_{vb}$) is used as a measure of vertical bias on target reappearance and is quantified as a percentage of the initial peak slide average vertical component due to the aperture problem. The same is computed for the no blank condition. The mean for all subjects is shown in the panels of Figure 8.4b and the error bars show the standard error.

To test if the slide average vertical component of the eye velocity on target reappearance (\bar{e}_{vr}), (pointed by the respective colored arrows in Figure 8.4a) is statistically different from the slide average vertical eye velocity during the blank \bar{e}_{vb} (pointed by the

grey arrow in Figure 8.4a), we conducted a paired t-test between the two velocities (\bar{e}_{vr} & \bar{e}_{vb}). Slide average vertical eye velocity during the blank \bar{e}_{vb} is taken at 150ms after blank initiation i.e. ~750ms as shown by grey arrow in Figure 8.4a. Slide average vertical eye velocity on target reappearance \bar{e}_{vr} is taken at ~210ms after target reappearance as indicated by respective colored arrows i.e. at 1010ms for 200ms blank, at 1210ms for 400ms blank and at 810ms for sudden orientation change conditions, across all trials. The t-test reveals there is a significant change ($P < 0.05$) in the slide average vertical component on target reappearance for all experimental conditions in at least three subjects (Subjects 2, 3, 4). Subject 6 shows a significant change for all conditions except in the condition where the target reappears with a change in orientation after a 400ms blank. Subject 1 shows no significant change for all conditions except in the condition where the target reappears with no change in orientation after a 400ms blank. Subject 5 shows a significant change in the conditions where target reappears with the same tilt after 400ms blank, where the target undergoes a sudden change in orientation and also when the target reappears with a change in orientation after a 200ms blank. A similar t-test is conducted in a no blank condition. Except subject 1, all the subjects show no significant change. The results suggest that although there is a change in the vertical bias on target reappearance across all conditions, the significance of the change is variable across subjects and conditions, coherent with previously reported results in a preliminary study (Montagnini et al 2006).

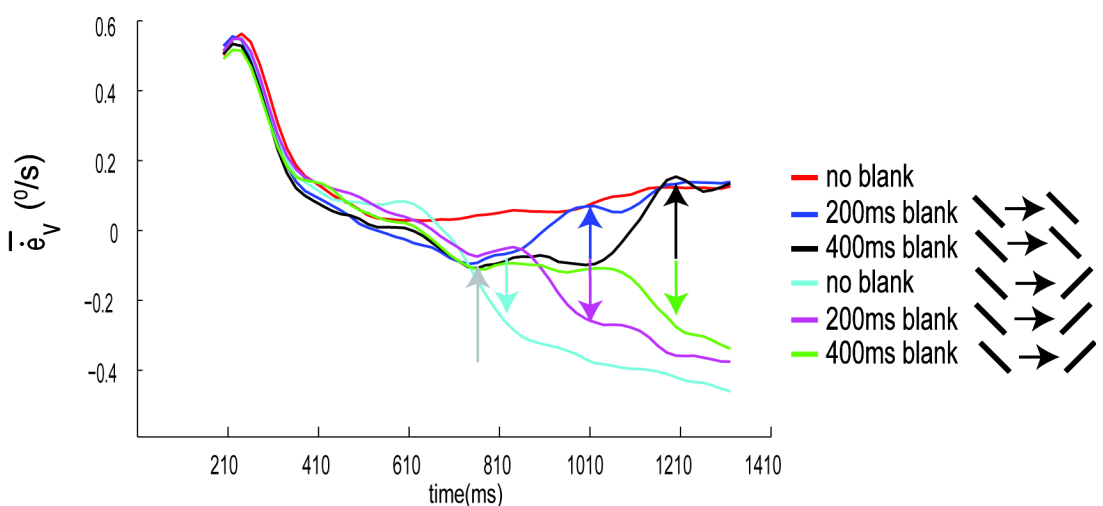
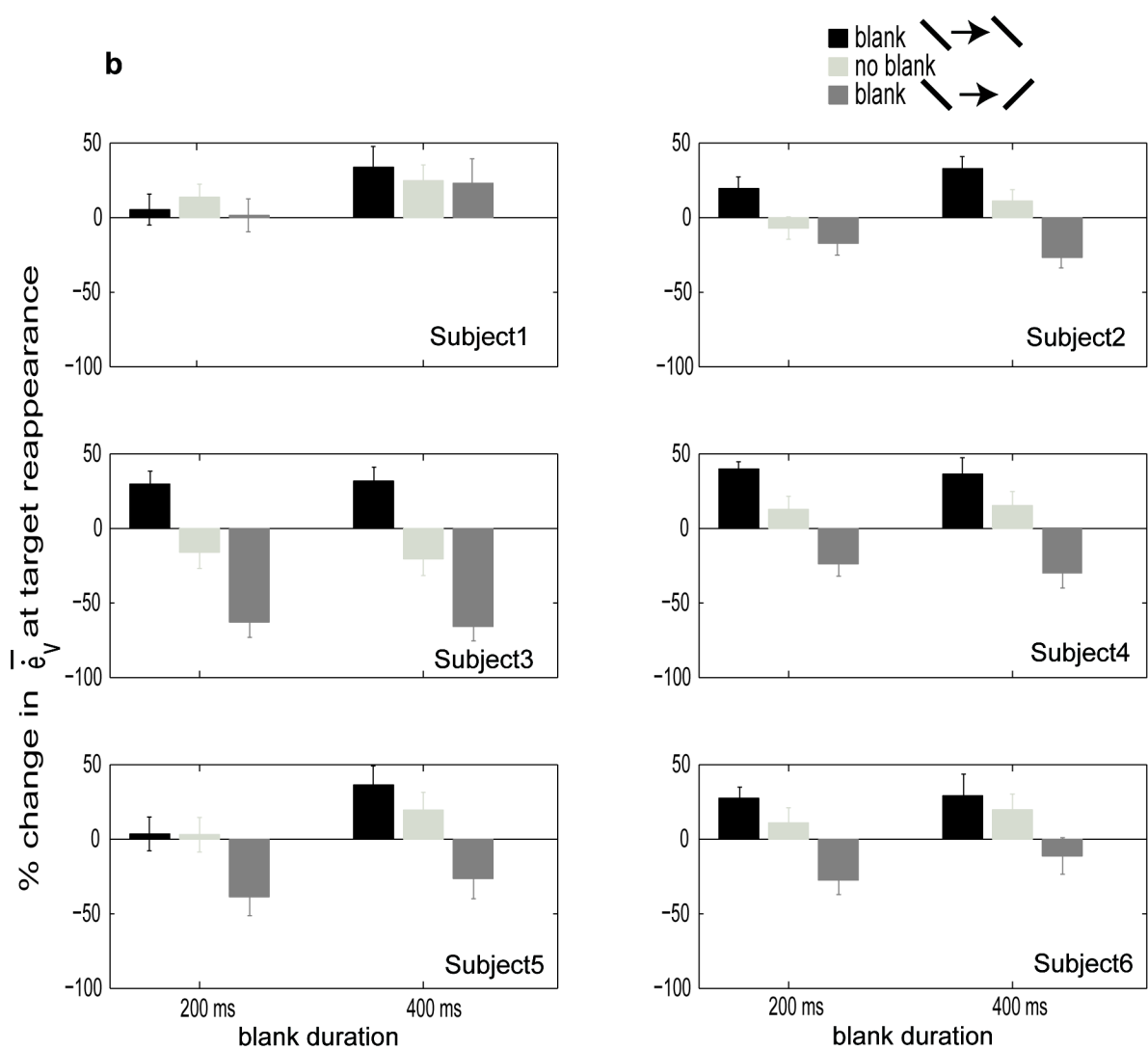
a**b**

Figure 8.4 : Blanking at steady-state : Vertical component Analysis.

a. Mean across subjects of the slide average vertical eye velocity $\bar{\dot{e}}_v$ for all conditions. The colored arrows point to the slide average vertical eye velocity for the respective conditions, at $\sim 210\text{ms}$ after target reappearance ($\bar{\dot{e}}_{vr}$). The grey arrow points to the slide average vertical eye velocity during the blank ($\bar{\dot{e}}_{vb}$). The length of the arrow indicates the change in the slide average vertical eye velocity on target reappearance relative to slide average vertical eye velocity during the blank ($\bar{\dot{e}}_{vr} - \bar{\dot{e}}_{vb}$), which is used as a measure of vertical bias on target reappearance. The two velocities ($\bar{\dot{e}}_{vr}$ & $\bar{\dot{e}}_{vb}$) are used for the paired difference t-test. **b.** The change in slide average vertical eye velocity (indicated by the length of the colored arrows) on target reappearance as a percentage of the initial peak due to the aperture problem for all blanking conditions. Each panel plots for each subject. The same is computed for a no blank condition. Error bars show SE. At least 200 trials were used per condition for each subject.

8.3.2. Experiment 2: Target blanking during the initiation of pursuit

Figure 8.5 plots both mean horizontal (\dot{e}_h) and vertical components (\dot{e}_v) of eye velocity observed when blanking target motion during the open-loop phase of smooth pursuit. Figure 8.5a,b illustrates mean eye velocity profiles obtained with a naive (Subject 4) and a non-naive subject (Subject 3) respectively. The no blank condition is plotted in red. The dotted lines indicate the blank initiation and the solid lines indicate the blank extinction for different conditions shown by the respective colors. The initial increase in the vertical pursuit component was clipped off when the moving stimulus disappeared. This is clearly evident when the moving line was blanked 140ms after target motion onset or earlier. The horizontal component started to decrease down to a plateau and then reaccelerated in during the first 80ms of target reappearance. Given the typical latency of $\sim 80\text{ms}$ for the bar stimulus, this brief acceleration indicates the anticipatory pursuit for target reappearance. Insets *c* and *e* zoom the vertical eye velocity profiles for two 300ms epochs, starting 100ms after stimulus onset. Insets *d* and *f* zoom the vertical eye velocity profiles for two 300ms epochs, starting 100ms after target reappearance.

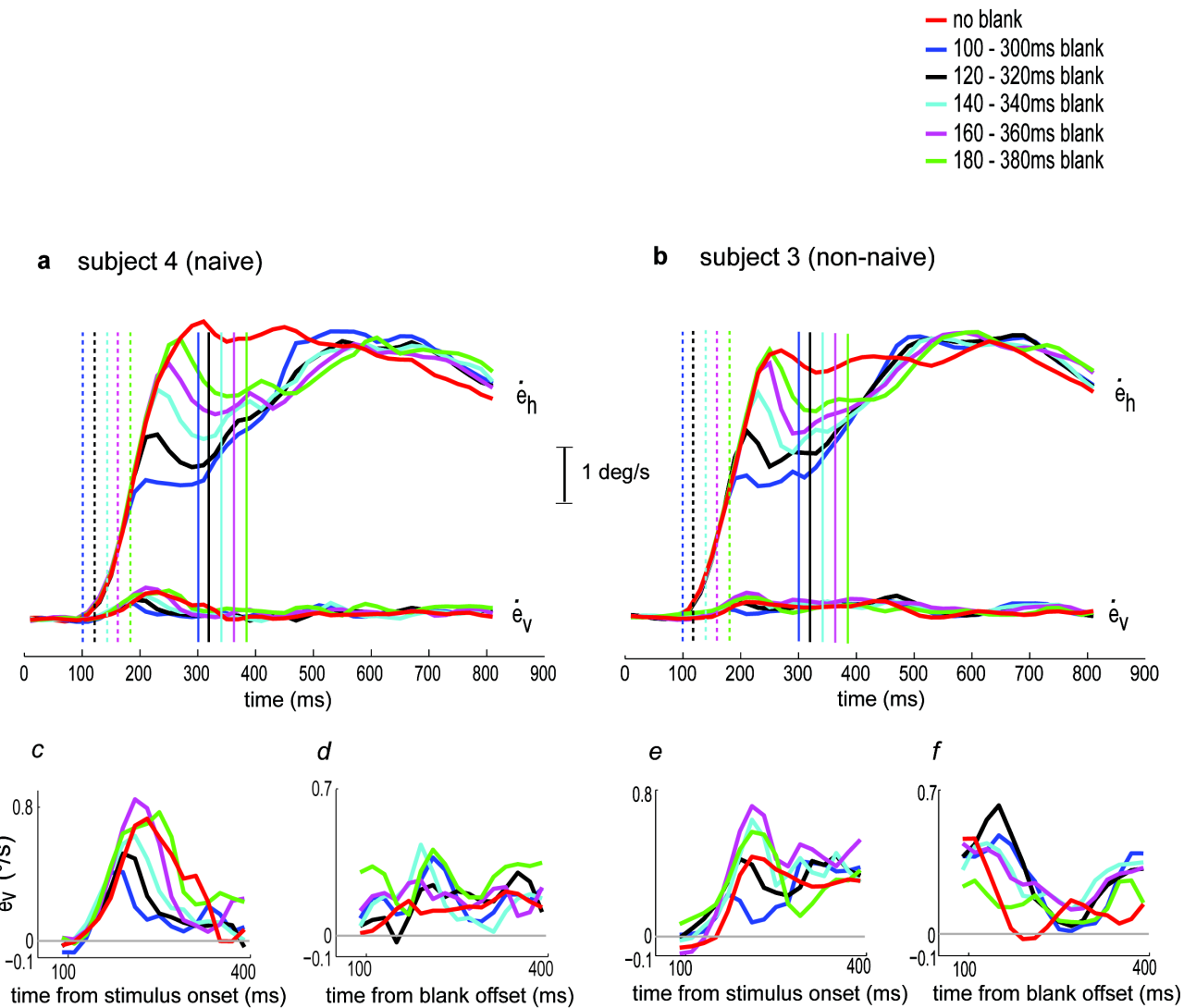


Figure 8.5: Mean smooth pursuit responses for open-loop blanking experiment.

a & b. Mean horizontal (\dot{e}_h) and vertical (\dot{e}_v) eye velocity traces (across 200 trials) for a naïve subject (subject4) shown in **a** and for a non-naive subject (subject3) shown in **b**. Dotted colored vertical line indicates blank onset at 600ms and the solid colored vertical lines indicate end of blank duration for the corresponding blanking condition shown by the respective color. Insets **c** and **e** below indicate the vertical eye velocity component across all conditions for 300ms duration starting from 100ms after stimulus onset. Insets **d** and **f** below indicate the vertical eye velocity component across all conditions for 300ms duration starting from 100ms after blank offset. For no blank condition (red), vertical eye velocity component is taken for the same duration as the blanking at 140ms condition. Stimulus is blanked for 200ms duration at different times during the 100ms after pursuit initiation.

The initial horizontal eye velocity component (e_h)

The decaying time of horizontal eye velocity (δt_{drop}) is shown in Figure 8.6a for different blanking times. It showed a significant dependence upon the timing of stimulus blanking ($p < 0.001$). When blanking the moving target at either 100 or 180ms, mean deceleration phases (across subjects) lasted ~ 90 or ~ 140 ms, respectively. Thus, earlier target blanking resulted in shorter phases of horizontal pursuit deceleration. The drop in the eye velocity during blanking (δV_{drop}) is plotted in Figure 8.6b (solid lines) against timing of target disappearance. An early blanking (100ms) resulted in a small reduction in eye velocity with a mean \pm SE across subjects of $0.55\pm 0.22^\circ/\text{s}$ while a later blanking (180ms after stimulus onset) resulted in a larger drop with a mean (\pm SE) across subjects of $2.3\pm 0.29^\circ/\text{s}$. The drop in eye velocity increased with later blanking, as shown by the significant effect of the timing of target blanking upon δV_{drop} ($p < 0.001$). Similar to the steady-state conditions, pursuit started to re-accelerate in expectation of the target reappearance (Figure 8.6b) and such anticipatory rise in eye velocity was stronger for early blank conditions with a mean \pm SE across subjects equal to $2.9\pm 0.13^\circ/\text{s}$ and $2.76\pm 0.22^\circ/\text{s}$ for blanking onset time of 100 and 120ms, respectively. Except for subject 2 (blue line in Figure 8.6b) all the subjects show a statistically significant ($P < 0.001$) dependence of δV_{ant} on the time at which blank starts.

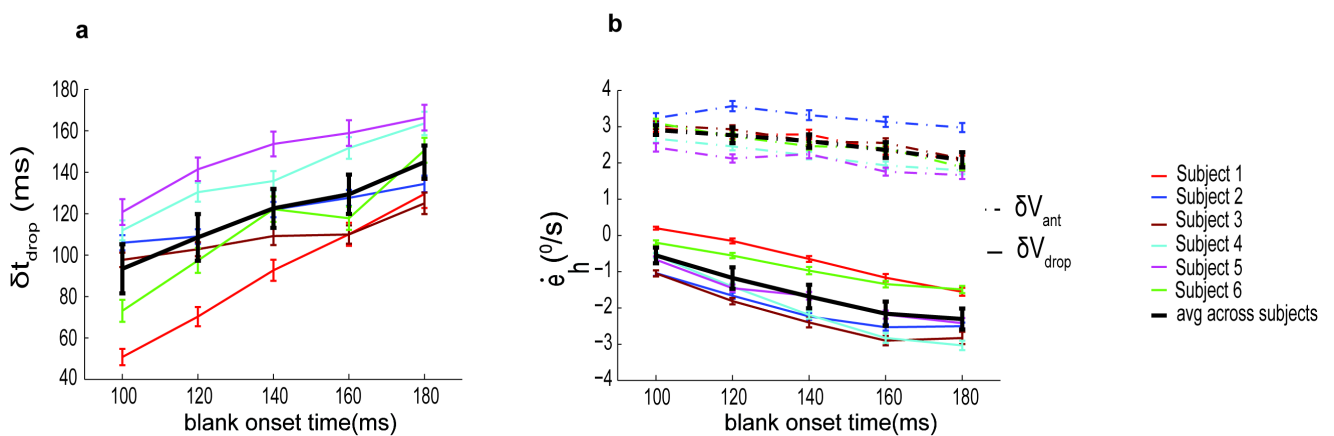


Figure 8.6: Blanking in open-loop : Horizontal component analysis .

a. δt_{drop} for all blanking conditions shown for all subjects (thin and colored lines) and average across subjects (thick black line). b. δV_{drop} and δV_{ant} for all blanking conditions shown for all subjects (thin and colored lines) and average across subjects (thick black line).

The initial vertical eye velocity component (e_v)

The slide average vertical component of the eye velocity is shown in Figure 8.7a. The clipping of the vertical bias for early as well as late blanks can be well differentiated in this plot. For 100-300ms blank condition, when the target reappears after the blank the slide average peaks well before ~ 210 ms (shown by colored arrow for 100-300ms blank condition) after target reappearance. For the rest of the blank conditions, the change in the slide average peaking at ~ 210 ms after target reappearance is not evident as it is after the steady state blanks. The change in the slide average vertical component on target reappearance is calculated as the difference between slide average vertical component taken at ~ 210 ms after target reappearance (\bar{e}_{vr} , pointed by the colored arrow in Figure 8.7a for 100-300ms blank condition) and the slide average vertical component taken ~ 150 ms after blank initiation (\bar{e}_{vb} , pointed by the grey arrow in Figure 8.7a for 100-300ms blank condition). This change ($\bar{e}_{vr} - \bar{e}_{vb}$) is used as a measure of vertical bias on target reappearance and is quantified as a percentage of the initial peak slide average vertical component due to the aperture problem. The mean percentage across subjects is shown in Figure 8.7b and the error bars show the standard error. Majority of the subjects across all conditions show a drop in the slide average vertical eye velocity component on target reappearance.

Paired t-test ($P < 0.05$) is conducted between slide average vertical eye velocity taken 150ms after the blank initiation and slide average vertical eye velocity taken at ~ 210 ms after the target reappearance across all conditions similar to the vertical component analysis for the blanking at steady state experiment. Except subject 1, no other subjects show a significant change in the condition where blank starts at 100ms. In the condition where blank starts at 120ms, except for subject 2, none of the other subjects show any significant change on target reappearance. For the rest of the blanking conditions, subjects 2 and 3 show a significant change.

Although the paired t-test shows there is a significant change in some of the conditions for two subjects, the change is not an increase but a decrease in the slide average vertical component. However, the difference between the percentage change in a blank condition and the percentage change in a no blank condition is always positive. These results suggest that, in the early blank conditions there is no effect of aperture problem bias to be observed in the vertical eye velocity upon target reappearance.

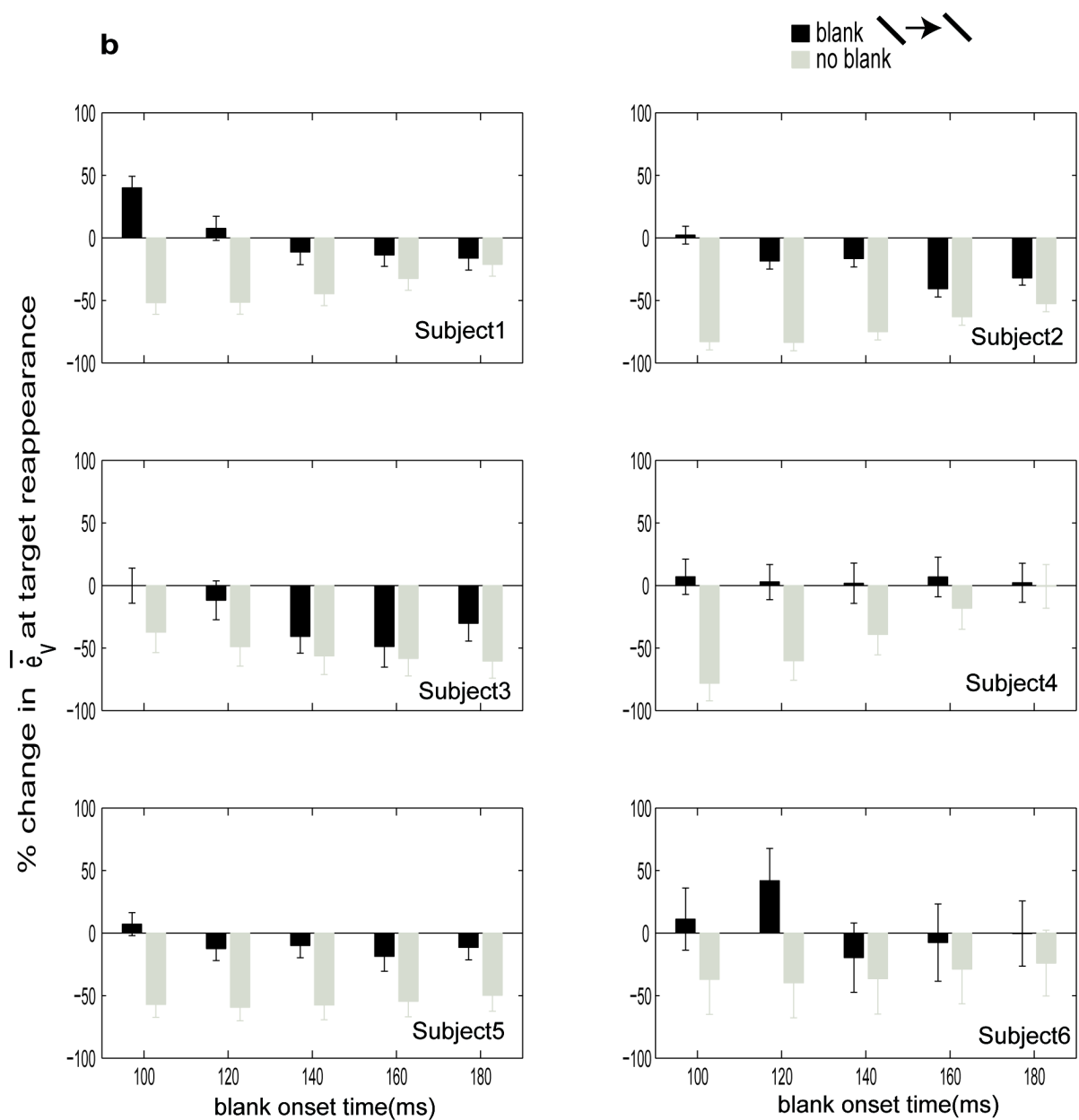
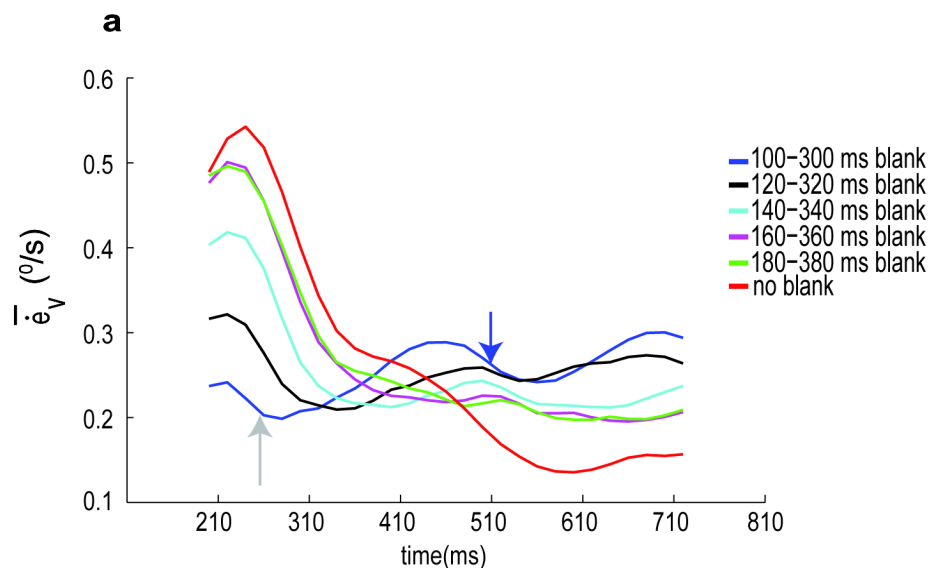


Figure 8.7: Blanking in open-loop : Vertical component analysis .

a. Mean across subjects of the slide average vertical eye velocity $\bar{\dot{e}}_v$ for all conditions. The colored arrow point to the slide average vertical eye velocity for the 100-300ms blanking condition, at ~ 210 ms after target reappearance($\bar{\dot{e}}_{vr}$). The grey arrow points to the slide average vertical eye velocity during the blank($\bar{\dot{e}}_{vb}$) for the 100-300ms blanking condition. The change in the slide average vertical eye velocity on target reappearance relative to slide average vertical eye velocity during the blank ($\bar{\dot{e}}_{vr} - \bar{\dot{e}}_{vb}$) is used as a measure of vertical bias on target reappearance, for all blanking conditions. The two velocities ($\bar{\dot{e}}_{vr}$ & $\bar{\dot{e}}_{vb}$) are used for the paired difference t-test. b. The change in slide average vertical eye velocity $\bar{\dot{e}}_v$ on target reappearance expressed as a percentage of the initial peak due to the aperture problem for all blanking conditions. The same is computed for a no blank condition. Each panel shows data for each subject. Duration of the blank is 200ms. Error bars show SE. At least 200 trials were recorded per condition for each subject.

Contrasting effects of target blanking during initiation and steady-state of pursuit

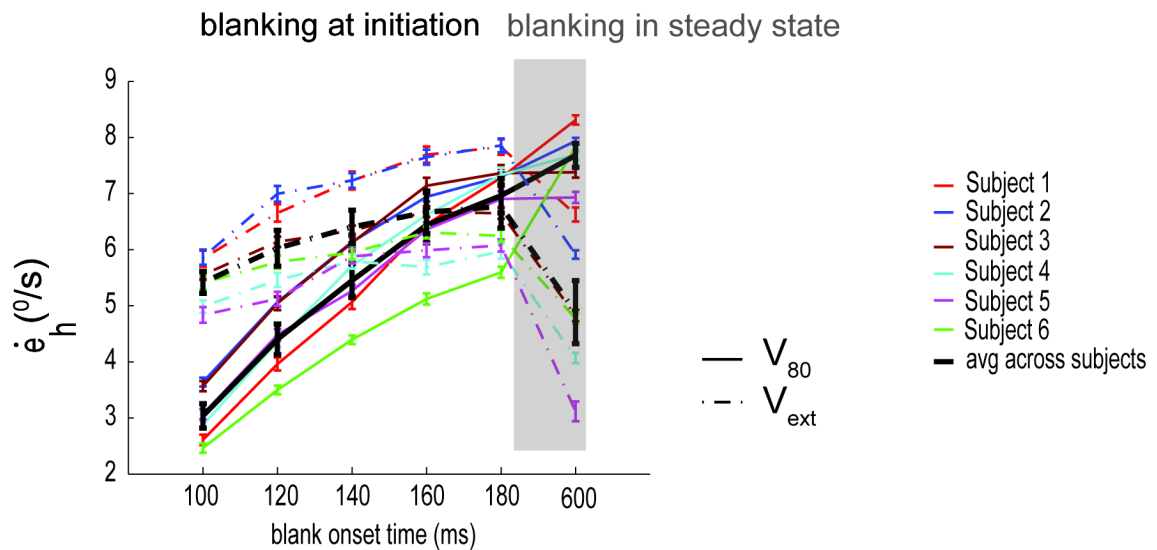


Figure 8.8: Plot summarizing the effect of blank on pursuit

V_{80} and V_{ext} plotted for conditions with 200ms blank duration and blank starting at different times during blanking at initiation and steady state (shaded part) during pursuit. Error bars show SE.

Figure 8.8 summarizes the effect of blank on pursuit, at different times during pursuit from the blanking at initiation experiment and blanking in steady state experiment. Similar to Figure 8.5, the horizontal component of eye velocity 80ms after the blank onset (V_{80}) and horizontal component of eye velocity 80ms after the blank extinction (V_{ext}) for all 200ms blank conditions are plotted. The difference between V_{80} and V_{ext} for different blank conditions shows that the effect of the blank on the eye velocity. As the eye velocity at the time of the blank (V_{80}) increases ($3\pm0.21^\circ/\text{s}$ for blank at 100ms to $6.96\pm0.3^\circ/\text{s}$ for blank at 180ms), the velocity at the end of the blank (V_{ext}) also increases by a smaller amount ($5.41\pm0.19^\circ/\text{s}$ for blank at 100ms to $6.77\pm0.38^\circ/\text{s}$ for blank at 180ms) yet, statistically significant (ANOVA ; $P<0.001$) and the difference between the two narrows down by $\sim 180\text{ms}$. All the subjects show a similar behavior. The earlier the stimulus is blanked, the higher is the difference and the lower is the over all effect of the blank on the eye velocity. However, for the steady state blanking condition the eye velocity drops by considerable amount (difference between V_{80} and V_{ext}) during the blank even though the eye velocity before blank V_{80} is closer to the target velocity. In summary, blanking target motion during steady state of pursuit results in the reduction of eye velocity in contrast to an increase in eye velocity during a blank at pursuit initiation.

8.4. Discussion

In the present study, we investigated the effects of target blanking upon pursuit eye velocity under different conditions. We used ambiguous but yet simple targets resulting in well known biases in horizontal or vertical eye velocities (Masson & Stone 2002) to probe the relative strength of visual and non-visual drives that have been postulated to explain tracking performance during both normal (Yasui & Young 1984; Robinson et al 1986) and target blanking conditions. In particular, our objective was to probe the contribution of predictive signals in the absence of visual inputs (i.e. during blank) as well as in the presence of ambiguous target motion directions (i.e. on target reappearance). Comparing the pursuit biases seen after target first appearance or at reappearance allowed us to titrate the weight of visual inputs and their dynamics. Overall, the present results indicate that when the extra-retinal signals during the blank play a larger role in driving pursuit as summarized in Figure 8.8, the ambiguous motion signals from the retina upon target reappearance after the blank are barely seen from pursuit responses. By blanking the target at different time after motion onset, we have been able to measure the temporal dynamics of these biases and therefore the

relative contribution of visual and non-visual, predictive signals (Masson & Stone, 2002; Montagnini et al., 2006).

A transient disappearance of the target during smooth pursuit results in an exponential decay of eye velocity if there is no expectation of the target reappearance (Mitrani & Dimitrov 1978; Pola & Wyatt 1997). When the target is expected to reappear after a blank lasting more than 400ms, the eye velocity stops decaying after 280ms and stabilizes at a constant level at about 70-80% of target speed (Becker & Fuchs 1985). Interestingly, learning improves the residual level of the velocity during the blank (Madelain & Krauzlis 2003). This dynamics in the eye velocity during the blank is well investigated at steady state (Bennett & Barnes 2003) and open loop stages of pursuit (Barnes & Collins 2008a; Churchland et al 2003). Most of the models use an efference copy positive feed back that is continuously relayed to drive the pursuit in the absence of the visual stimulus to explain this behavior (Krauzlis and Lisberger, 1994; Churchland et al 2003; Madelain & Krauzlis 2003). However this type of model cannot explain the anticipatory rise during the blank in the open loop phase of pursuit that we, and others (Barnes & Collins 2008a) have observed. Note that in the present experiments, we used a single 200ms blank duration with various blanking onset times during the open loop phase of pursuit, unlike the study conducted in monkeys by Churchland et al. (2003). This could have reinforced the role of expectation signals, relative to visual signals and eye velocity memory (Barnes and Collins, 2008a; Montagnini et al., 2006). Still, the fact that several studies have reported a considerable influence of cognitive and voluntary factors argue for the need of an extra-retinal signal carrying more information than the instantaneous eye velocity. Barnes and colleagues have proposed that the anticipatory rise in eye velocity observed before the end of target blanking is explained by the existence of an indirect loop that samples the visuo-motor drive during pursuit (Bennett & Barnes 2004; 2006). They reasoned that if eye velocity at the time of the blank is lower compared to the sample of the visuo-motor drive acquired by the pursuit system during early pursuit then eye velocity after an initial drop due to the blank, increases to match the sample of the visuo-motor drive during blank but with a lower acceleration. This is summarized in Figure 8.5. The difference between V_{80} and V_{ext} reflects the effect of the blank on smooth eye velocity. The effect of blanking on eye velocity is reduced when the blank is initiated later.

8.4.1. Dynamic weighting of retinal and extra-retinal signals

Considering the δt_{drop} , δV_{drop} for the 200ms duration blank at 600ms during steady state from Figure 8.3a,b along with the open-loop blanking conditions from Figure 8.6a,b respectively,

we can infer that the earlier the stimulus is blanked, the shorter are δt_{drop} and δV_{drop} indicating that extra-retinal signals more quickly influence the responses to a transient disappearance of the target. Thus, when a moving target is blanked during steady state pursuit (e.g. at 600ms after target motion onset), the sensory-motor transformation weights extra-retinal signals with a slower dynamics and gives higher weight to retinal inputs. This results in deceleration of eye velocity over a longer time period and therefore in a larger drop in the steady-state eye velocity during blanking. Conversely, when the moving target is blanked during the open-loop phase of pursuit, the sensory-motor transformation changes the weights of extra-retinal signals more rapidly. Consequently, the eye velocity drops for a shorter time period, resulting in a smaller decrease in the eye velocity. During the open-loop phase blanking, even though the sampled visuo-motor drive might not be matching target velocity (Barnes and Collins, 2008a) the extra-retinal signals are given enough weight to maintain high pursuit velocity. This is illustrated by the difference between V_{80} and V_{ext} in Figure 8.8, for open loop blanking conditions.

This dynamic weighting explanation for the effect of blank on horizontal component is further supported by the observations made on the vertical component of the eye velocity after target reappearance. Once the target reappears after blanking, we might expect to see a small pursuit bias driven by the aperture problem when processing the small retinal slip due to the difference between target and pursuit speeds. Since the retinal input is given more weight on target reappearance after steady-state blanking, we indeed find a small but significant increase in the vertical component of the eye velocity when pursuit re-accelerates. On the contrary, we find very little evidence for direction biases at the end of open-loop blanking despite the large retinal slip occurring at target reappearance. This indicates that the extra-retinal signals driving pursuit during the blank in open-loop blanking conditions are given enough weight even in the presence of the retinal signals on target reappearance to overcome the strong directional biases that would be seen in the vertical eye velocity component.

Although some of the previously proposed models (Bennett & Barnes 2004; Barnes and Collins, 2008b) could explain the anticipatory rise in the horizontal component of eye velocity during the blank in an early blank condition, they are not equipped to deal with the motion integration and the effect of blanking on motion integration that is observed in the vertical component of eye velocity. In these models (Bennett & Barnes 2004; Barnes and Collins, 2008b), indirect loop drives the pursuit during the blank and on target reappearance the drive is switched to the direct loop and the gain (β) to its normal value. If this switching

is indeed the case, we should observe vertical bias on target reappearance in the early blanking conditions as in the steady state blanking conditions. But that is not the case. As reasoned in the earlier paragraph, these results from the vertical eye velocity component suggest that the transfer of weights from extra-retinal signals during the blank to retina input on target reappearance is not mere switching but rather is associated with a transient dynamics.

We have previously shown that many aspects of the temporal dynamics of pursuit eye movements driven by ambiguous inputs can be modeled with a recurrent Bayesian model of motion integration (Montagnini et al., 2006; Bogadhi et al., 2011). Inspired by the framework set by Bennet & Barnes (2004, 2006), we propose now an extension of our probabilistic model using the theoretical framework of Hierarchical recurrent Bayesian inference to better understand these interactions between retinal and extra-retinal signals for motion integration in smooth pursuit. Our goal is to achieve a more complete model for smooth pursuit which is fully dynamical and can incorporate the constraints imposed by both types of inputs.

8.4.2. A hierarchical inference model for smooth pursuit

Bayesian models have been successful in explaining the perceptual and psychophysical data in motion integration (Hurlmann et al 2002; Stocker & Simoncelli 2006; Weiss et al 2002). These models are essentially static and could not explain the dynamics of motion integration for pursuit. The first attempt to explain dynamic motion integration was made using a recurrent Bayesian framework where the likelihoods of the 1D and 2D motion information is combined with a prior preferring slow speeds (Montagnini et al 2007). However the model output was not comparable with the behavioral results. This recurrent Bayesian framework was further extended by cascading it with a oculomotor plant there by producing smooth pursuit traces that are comparable with the human smooth pursuit responses to a translating tilted bar (Bogadhi et al 2011). The model was operating in open-loop conditions with no physical feed-back from the retina.

Here we extend the model to a closed loop version by including the physical negative feed-back and the positive efference copy feed-back. The model consists of two stages. The first stage is a retinal recurrent bayesian network which is adapted from Montagnini et al. (2007) along with the oculomotor plants. The second stage is a recurrent bayesian network which is labeled as extra-retinal recurrent bayesian network in the block diagram shown in Figure 8.9. The inputs to the model are 1D and 2D likelihood distributions for target velocity.

The prior and likelihood distributions of the model are assumed to be Gaussian (Weiss et al 2002). The priors in the retinal and extra-retinal blocks are centered on zero in the 2D velocity space. The variance of the likelihood and prior distributions in the retinal block are derived from the oculomotor data (see Bogadhi et al 2011; Montagnini et al 2007). The role of the retinal recurrent Bayesian module is to integrate motion information over time, following a temporal dynamics that is comparable with that of motion integration in macaque area MT (Pack & Born 2001; see Masson et al. 2010 and Tlapale et al., 2011). A transient blank is considered as a Gaussian likelihood centered on zero with an infinitely large variance. When the stimulus disappears, the prior in the retinal recurrent block is set to its initial distribution centered on the zero of the 2D velocity space since the prior in the retinal block is considered as the physiological equivalent of MT and previous physiological studies have shown that MT neurons stop firing during target blanking (Ilg & Thier 2003; Newsome et al 1988). Note that if the prior were not reset to its initial distribution during blanking, the target speed and direction that would be decoded from the posterior distribution would be, and remained, non zero which contradicts these neurophysiological findings (Ilg & Thier 2003; Newsome et al 1988).

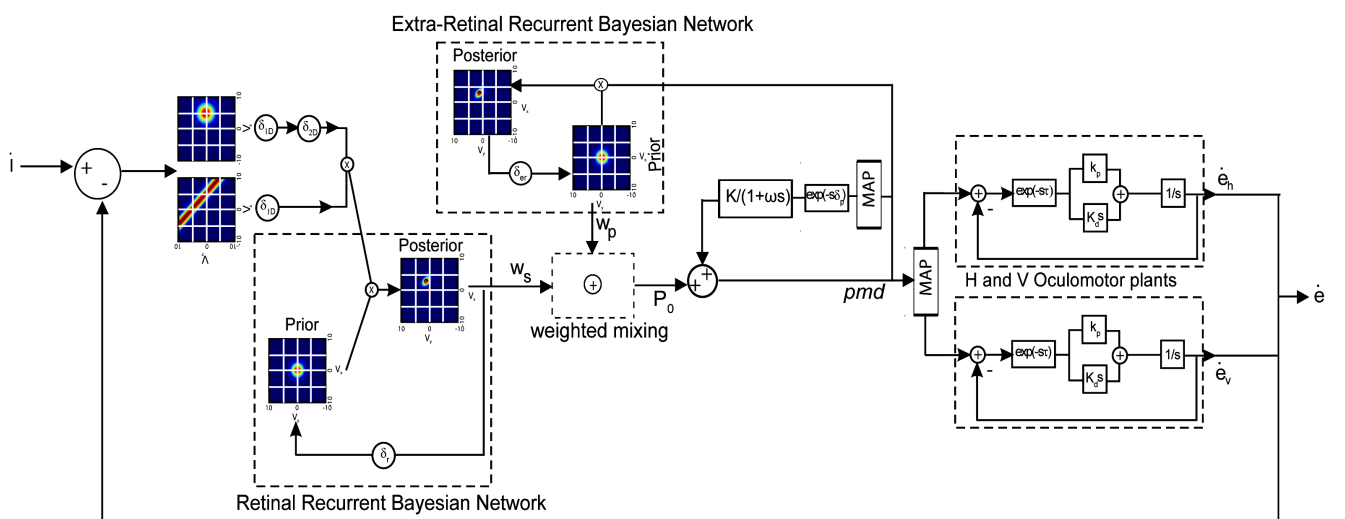


Figure 8.9: A hierarchical recurrent Bayesian model for smooth pursuit

The 1D and 2D motion information are likelihoods are delayed by $\delta 1D$ and $(\delta 1D + \delta 2D)$ respectively and combined with a prior to obtain a posterior as shown in the retinal

*recurrent Bayesian network. The prior is updated every δt_r ms. The logarithms of the posterior from the retinal recurrent bayesian network and prior from the extra-retinal bayesian network are weighted and combined to form the Post-sensory output (P_0). Weights (W_s and W_p) are dynamic and the change in the retinal posterior variance acts as a trigger to the weight fuctions, both on blank initiation and blank extinction. The maximum-a-posteriori of the pre-motor drive serves as an input to both the positive feed back system as well as the oculomotor plants. The output of the oculomotor plant is subtracted from the target velocity to form the image velocity (physical feed-back loop shown as broken line). During the transient blank when there is no target on the retina, the physical feed-back loop is not functional so that the retinal recurrent block doesn't decode any motion. The output of the positive feed-back system (shown in broken line) is added to the Post-sensory output (P_0) only when the physical feed-back loop is functional. The pre-motor drive (*pmd*) is provided as an input to the extra-retinal recurrent bayesian network where it is combined with a prior to obtain a posterior which is used to update the prior every δt_{er} ms. The extra-retinal prior is updated only when the retinal weight (W_s) is 1 indicating the extra-retinal block stores only the visuo-motor drive reflecting the reliable retinal motion information.*

A complete block diagram schema of the model is shown in Figure 8.9. The logarithms of the prior from the extra-retinal block and the posterior from the retinal recurrent block are weighted and combined to form the post-sensory output (P_0 in equation1 and Figure 8.9). The efference copy of the premotor drive (*pmd*) is given as input to the extra-retinal block and combined with a prior preferring slow speeds (Freeman et al. 2010). The resultant posterior is then used to update the prior with a constant delay (δ_{er}). Imposing a conditional update of the extra-retinal (prediction) component, similar to what can be found in a simple Kalman filter is beyond the scope of this study. For the sake of simplicity, we decided here that the extra-retinal prior can be updated only when the retinal weight (W_s) is equal to 1 indicating the extra-retinal block stores a visuomotor drive triggered by reliable retinal motion information. This delayed update of prior with posterior can be viewed as a sample and hold mechanism with the prior being the memory equivalent to the indirect loop of the model described (Bennett & Barnes 2004). The delay (δ_{er}) is set as 1.5 times the update delay in the retinal block (δ_r) to yield a sample velocity that is ~70% of the target velocity during the open-loop. This indicates that the physiological equivalent of the extra-retinal recurrent Bayesian block is higher up in the cortex given the larger time scale

compared to the retinal recurrent Bayesian block. Since the value of (δ_r) is high enough (see Bogadhi et al 2011) and since (δ_{er}) is set as 1.5 times (δ_r), the extra-retinal eye velocity sample remains at 70% of the target velocity through out the open loop after which it starts to update towards the target velocity. The maximum-a-posteriori (MAP) of the premotor drive serves as an input to the oculomotor plants and to the positive feed-back system.

The oculomotor plant produces the smooth pursuit eye velocity that is subtracted from the target velocity to form image velocity. Since during the transient blank there is no target on the retina, the physical feed-back loop is not functional (broken line in Figure 8.9). Having this feed-back being non-functional during the blank keeps the likelihood distribution of the blank centered at zero. Without such disabling, the retinal recurrent Bayesian block would show a preference for a negative velocity because of the physical negative feed-back. Again, this would not be in agreement with the physiological observations (Ilg & Thier 2003; Newsome et al 1988). The output of the positive feed-back system is added to the Post-sensory output (P_0) only when the physical negative feed-back is functional (broken line in Figure 8.9). The horizontal (V_x) and vertical (V_y) components of the MAP is delayed by (δ_p) and passed through respective low pass filters with gain (K) and cutoff frequency (ω) ($K=(K_x, K_y)$; $\omega=(\omega_x, \omega_y)$) as shown in Figure 8.9. For simplicity, the horizontal and vertical components of the positive feed-back system are shown as one single unit in Figure 8.9. The delay (δ_p) and the filter parameters are fixed constant for both V_x and V_y across all conditions ($\delta_p=110ms$; $K_x=3$; $\omega_x=1$; $K_y=2$; $\omega_y=1$). The values of the positive feed-back system are set to compensate for the combined dynamics of the horizontal and vertical oculomotor plants along with the retinal recurrent Bayesian block, before and after the physical negative feed-back respectively.

$$\ln(P_o(v_x, v_y)) = \underbrace{(r_{max} * \frac{c^n}{c^n + t^n}) * \ln(P_{ret}(v_x, v_y))}_{\text{retinal weight function}} + \underbrace{(r_{max} * \frac{r^n}{c^n + t^n}) * \ln(P_{ext}(v_x, v_y))}_{\text{extra-retinal weight function}}; \quad (1)$$

where,

$P_{ret}(v_x, v_y)$ is the posterior from the retinal recurrent Bayesian network

$P_{ext}(v_x, v_y)$ is the prior from the extra-retinal recurrent Bayesian network

Weight function Parameters	Open-loop blanking		Steady state blanking	
	Target disappearance	Target reappearance	Target disappearance	Target reappearance
r_{max}	0.99	0.99	0.99	0.99
co-efficient(c)	600	100	800	20
power(n)	1	1	15	15

Table1: Weight functions parameters for open loop and steady state blanking experiments

Model parameters

The weights are modeled as S-shaped functions of time in order to explain the different dynamics that is observed during and immediately after blank. These weights change as a function of time. A sudden change in the retinal posterior variance would act as a trigger to the weight function (Figure 8.10), both when the target disappears and when it reappears after a short blank. r_{max} sets the steady state value of weights and, thereby the residual velocity observed during the blank. The higher is r_{max} , the lower is the residual velocity during the blank. r_{max} is constant for a subject across all conditions and would decrease with learning (e.g. Madelain & Krauzlis 2003). The coefficient (c) and the power (n) in the weight function determine the dynamics with which the weights change, as shown in Figure 8.10b. This dynamics explains the anticipatory pursuit before the blank ends as well as the suppression of the directional bias when the target reappears (Figure 8.10a), predominantly in the early blank condition. A single set of parameters (Table 1) has been used for all open-loop blanking conditions since the expectation is the same. This is reflected in the similar dynamics of weights for all open-loop blanking conditions (Figure 8.10). Similarly, the parameters involved in the weight functions are same for all steady-state blanking conditions (Table1) and this is evident in the weight functions for steady-state blanking as shown in Figure 8.10. The power (n) in the weight functions shown in Figure 8.10 shows a dependence upon the time at which the stimulus is blanked (see Table1). The value of n is higher if the stimulus is blanked during the steady state phase of pursuit. The parameters of the positive efference copy feed-back are kept constant across all conditions. The parameters of the recurrent visual Bayesian networks as well the oculomotor plant are taken from our previous study (Bogadhi et al 2011).

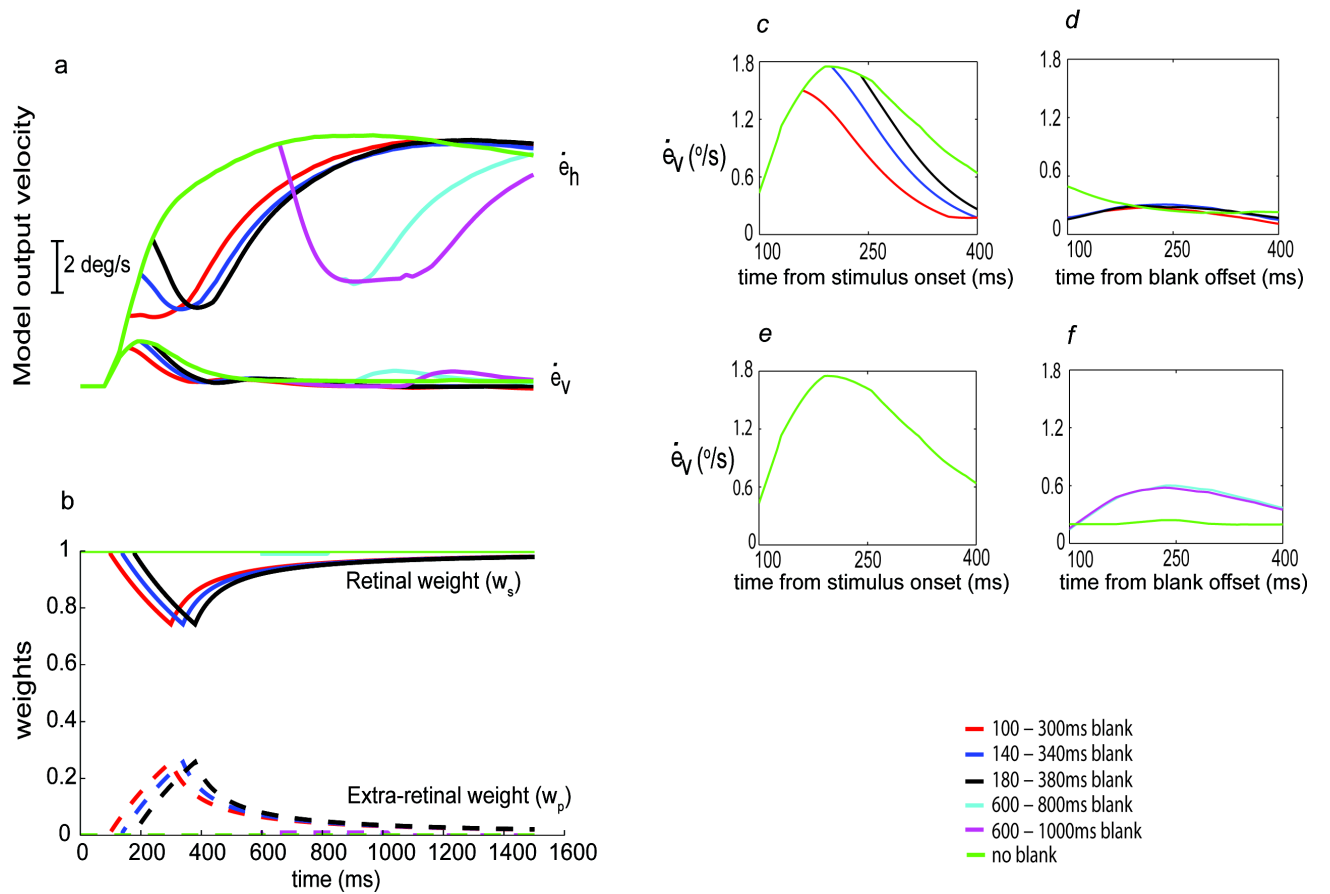


Figure 8.10: Model simulation and temporal dynamics of weights. a. Simulated smooth pursuit responses in different blanking and no blanking conditions. b. Temporal dynamics of the retinal and extra-retinal weights for same experimental condition. Insets c and e below indicate the vertical eye velocity component across all conditions (see the legend) for 300ms duration starting from 100ms after stimulus onset. Inset e, since the initial model responses are the same for the steady state blanking conditions, colors are overlapped and hence one response is seen. Insets d and f below indicate the vertical eye velocity component across all conditions (see the legend) for 300ms duration starting from 100ms after blank offset. For no blank condition (green) in inset d, vertical eye velocity component is taken for the same duration as the blanking at 140ms condition. For no blank condition (green) in inset f, vertical eye velocity component is taken for the same duration as the 600–1000ms blanking condition.

8.4.3. Model Results

Eye movements were simulated for different blank conditions and a control, no blank condition. The resulting smooth pursuit responses (horizontal and vertical) of the model are shown in Figure 8.10a together with the respective dynamics of weights (Figure 8.10b). The model parameters are set to qualitatively reproduce the main aspects of the results presented here. When the stimulus is blanked during the open-loop phase of pursuit, the weights change much faster than observed during steady-state blanking. Moreover, extra-retinal weights increase while retinal weights decrease during the blanking period. The retinal weights are higher in steady state blanking conditions compared to the open-loop blanking conditions. This suggests that the visuomotor system is driven by the blank more in the steady state compared to the open-loop which is reflected as higher drop in the horizontal velocity component during the steady state blank. Although, the dynamics of the weights are same for all the open-loop conditions, in the early blank condition (i.e. blanking onset at 100ms) the horizontal component of pursuit doesn't drop but is held constant before slowly rising in anticipation of target reappearance. With later blanking onsets, the dip in the eye velocity progressively increases with respect to this timing, as observed in the data (see Figure 8.4b). Our model predicts that when using the same parameter setting for all open-loop blanking conditions, the anticipatory responses seen before target reappearance is larger with earlier blanking onset.

At the moment of target reappearance, the weights to the extra-retinal signals is higher in open-loop blanking conditions compared to the steady-state blanking conditions, thereby suppressing the output from the retinal recurrent block which reflects the aperture problem and the dynamics of motion integration. This is shown in the insets *d* and *f* of Figure 8.10. Insets *d* and *f* show dynamics in the vertical eye velocity component on target reappearance for blanking at initiation and steady state respectively. Vertical bias is higher on target reappearance for steady state blanking compared to blanking at initiation. The peak vertical bias on target reappearance is slightly higher to the vertical bias seen in the similar plots of Figure 8.2. This is because of the over all scaling in model responses as the initial peak vertical bias is higher for the model (See Bogadhi et al 2011 for details). Insets *c* and *e* show vertical eye velocity at initiation. As expected, for the steady state blanking conditions the initial vertical eye velocity component is similar to no blank condition as seen in the data (see Figure 8.2). For blanking at initiation conditions, the initial vertical component is clipped off and is comparable to the data (see Figure 8.5). Overall results of the model show that with the same weight functions that explain the dynamics of the horizontal component of

eye velocity because of the blank, the model provides an accurate qualitative account of the dynamics of the vertical component of eye velocity on target reappearance after blank for both open loop and steady state blanking conditions.

8.4.4. Comparison with previous models (Bennett & Barnes 2004; Barnes and Collins, 2008b)

The extra-retinal part of the hierarchical recurrent Bayesian framework proposed here is similar to the previously proposed models (Bennett & Barnes 2004; Barnes and Collins, 2008b). One way to look at the prior in the Recurrent Bayesian network is, as a sample and hold mechanism as put forward by the previous models (Bennett & Barnes 2004; Barnes and Collins, 2008b). With the simulated results by the model proposed by Barnes and Collins (Figure 9 B & C in Barnes and Collins, 2008b) for blanking at 100ms and 150ms, the difference in the drop is not evident. The proposed model here gives an accurate qualitative account of the increasing drop in the horizontal component of the eye velocity with the same weight functions as the blank is initiated later in the open-loop (see Figure 8.10).

The previous models (Barnes & Collins 2008a; Bennett & Barnes 2004) explain the dynamics observed in smooth pursuit during blanking by switching between direct and indirect loops and changing the gain value (β) which depends on expectation. These models (Barnes & Collins 2008a; Bennett & Barnes 2004) would fail to explain different dynamics observed in smooth pursuit during a transient blank applied at different times during open-loop and steady state of pursuit, given the same expectation which is represented by gain value (β).

Probabilistic representation of motion information would allow to represent uncertainty in the velocity information. Sensory noise is the major source of variance in the motor action as motor action is planned so as to minimize motor noise, and hence sensory noise could play a crucial role in the motor transformation of the sensory estimate (Harris & Wolpert 1998; Osborne et al 2005). Following this, it makes sense to suggest that sensory variance could play a role in responding to a change in the motion information on the retina (e.g. a transient blank). Since the evidence about the target motion is lower during the early stages of motion processing (Osborne et al 2007), any changes in the motion information on the retina would be least processed and hence the eye movements show a large extra-retinal influence. Similarly, the evidence collected is higher during the later stages of motion processing, any changes in the motion information on the retina would be processed and hence the eye movements show a large retinal influence.

Although the data presented here doesn't suggest that the extra-retinal efference copy mechanism requires probabilistic representation, such a representation would allow us to represent uncertainties in the velocity information. As expectation alone cannot explain the different dynamics in pursuit during blanking at different times, the variances of retinal prior and extra-retinal prior could be used to design the associated dynamics with their respective weight functions rather than switching between retinal and extra-retinal signals. The advantage of designing weight dynamics as a function of uncertainties in retinal and extra-retinal velocity information is, it gives a much simpler and powerful way of expressing prediction as an adaptive behavior reflecting the dynamic interplay between expectation and measurement as determined by their reliability in contrast to changing the gain value (β) manually as in the previous models which is influenced by expectation and cognitive factors. In effect, this provides an efficient framework for future studies to explore pursuit as an adaptive system mixing retinal and extra-retinal signals like a kalman filter for tracking.

Physiological relevance of the hierarchical inference model

During the blanking of the stimulus, the retinal recurrent Bayesian block doesn't show any sign of decoding target direction or speed as expected from the physiological equivalent of area MT(Ilg & Thier 2003; Newsome et al 1988). The extra-retinal recurrent Bayesian network along with its input can be seen as implementing the contribution of FEF and SEF cortical areas which are known to provide an extra-retinal drive to pursuit (Fukushima et al 2003; Missal & Heinen 2004). Our model suggests that a weighted mixing of the retinal and extra-retinal signals which could be done at the level of the lateral portion of the medio-superior temporal area (MSTl). Several studies have shown that area MSTl receives both retinal and extra-retinal inputs (e.g. Newsome et al 1988). This is supportive of the view that there are two cortical networks, one processing retinal information (V1-MT-MSTl) and the other extra-retinal information (MSTl-FEF-SEF) and both are combined at the level of area MSTl (See (Thier & Ilg 2005)). We have proposed that these two loops implement a hierarchical recurrent model that can infer the most optimal integration for sensorimotor integration in ambiguous conditions (Masson et al., 2010).

8.5. Conclusion

In the present study, we used a tilted bar stimulus as a pursuit target in a blanking paradigm to probe the interactions between retinal and extra-retinal signals on target reappearance after the extinction of the blank. The target was blanked at different times during pursuit both in

the open loop and steady state phases. The results show a similar dynamics in the horizontal component of the eye velocity during to the blank as found in the previous studies (Barnes & Collins 2008a; Becker & Fuchs 1985; Bennett & Barnes 2003; Churchland et al 2003; Madelain & Krauzlis 2003). However, the dynamics in vertical component of eye velocity on target reappearance indicates to a highly dynamic and larger role of extra-retinal signals when the stimulus reappears after the blanking, early in the open loop phase of pursuit compared to a steady state blank. These findings from the vertical component suggest that a simple switching from extra-retinal to retinal signals on target reappearance alone as proposed by previous models (Barnes & Collins 2008b) is insufficient and suggest for transient weight dynamics between retinal and extra-retinal signals. We propose a physiologically relevant dynamic hierarchical recurrent Bayesian model with retinal and extra-retinal recurrent Bayesian blocks where the retinal and extra-retinal signals are dynamically weighted and combined to form the visuomotor drive. With the same weight dynamics that explain the dynamics of the horizontal component of eye velocity because of the blank, the model provides an accurate qualitative account of the dynamics of the vertical component of eye velocity on target reappearance after blank for both open loop and steady state blanking conditions. The simulation results suggest that the interaction between retinal and extra-retinal signals are dynamical in nature and that such dynamics changes between open loop and steady state of pursuit.

Chapter 9

Role of prediction on motion integration for smooth pursuit

This chapter describes the study using expected target motion paradigm to investigate the role of prediction on motion integration at initiation for smooth pursuit. It also describes the simulated responses of the hierarchical model described in the previous chapter. The results from both the data and model indicate that although prediction drives pursuit before target onset, target motion transfers the weight from the extra-retinal signals to retinal signals and induces the initial direction bias in tracking responses.

9.1. Experimental Evidence (Montagnini et al 2006)

Expected target motion paradigm is used by repeating the tilted bar stimulus in the same direction and/or orientation (Montagnini et al 2006) on every trial. In the first experiment, both the orientation of the line ($\pm 45^\circ$) and direction of motion (left or right) were randomized. This resulted in the initial direction bias in the smooth pursuit responses, typically observed in a randomized presentation (see figure 6.1). In the Second experiment, orientation is kept constant and the stimulus could move to either left or right. This is referred to as 50% probability condition. In the third experiment, the stimulus orientation and direction of motion are kept constant for all the trials in any given block. This is referred to as 100% probability condition. The results to the two probability conditions are shown in the figure 9.1.

When the subjects expected the target to move in one direction on every trial (100% probability condition), this resulted in an anticipatory pursuit in the global direction of the object. Target motion onset resulted in the initial direction bias orthogonal to the orientation of the bar and the subsequent dynamics in motion integration that is observed in the smooth pursuit responses similar to a randomized presentation. For 50% probability condition, one of the subjects showed anticipatory response but lower in magnitude compared to the 100% probability condition but the initial direction bias on target motion onset and the corresponding dynamics in motion integration is similar. These results suggested that

predicting global direction of the target doesn't abolish the initial direction bias and the subsequent dynamics of motion integration.

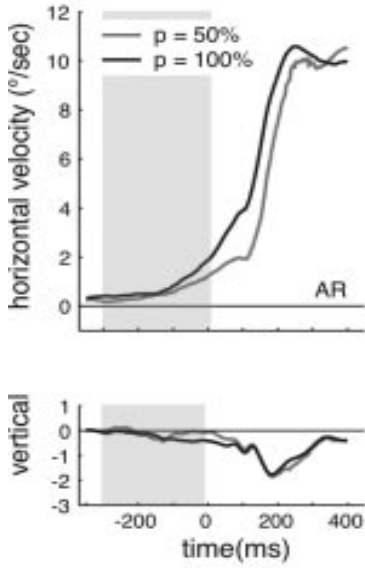


Figure 9.1. Effect of expectation on anticipatory pursuit. Shown are the smooth pursuit responses for a subject to a tilted bar stimulus oriented 45° to the vertical (clock-wise) moving right for different probabilities of expected target motion

9.2. Model Simulation

The hierarchical model described in the previous chapter (see figure 8.9) is simulated qualitatively for the experiment described above. All the parameters in the model are kept constant as a no blank condition simulated in figure 8.10. The extra-retinal prior is a uni-modal or bi-modal Gaussian centered at 5°/s, which is a default speed of the pursuit system when the subjects expect target motion as shown by Becker and Fuchs (1985). Individual direction biases are also taken into account in representing the extra-retinal prior distribution. The smooth pursuit responses and the corresponding weights are shown in figure 9.2. When the subjects expect the target to move in one direction with 100% probability, the extra-retinal weights dominate retinal weights which results in higher anticipatory pursuit. Target motion onset transforms the weights with faster dynamics such that the retinal weight is maximum. This allows the ambiguous 1D motion information driving the pursuit resulting in the initial direction bias. The subsequent dynamics involving 1D and 2D motion integration follows (see chapter 5). When the probability of expected target motion is lower (50%), the weights for the extra-retinal signals is lower, which results in a lower anticipatory pursuit. Given the same faster dynamics of weights on target motion onset the vertical component shows a similar dynamic response. The model results suggest that although extra-retinal

signals drive anticipatory pursuit before target motion onset, on target motion onset the weight of the retinal signal is set to unity such that motion information is processed. This results in a dynamic vertical component of smooth pursuit.

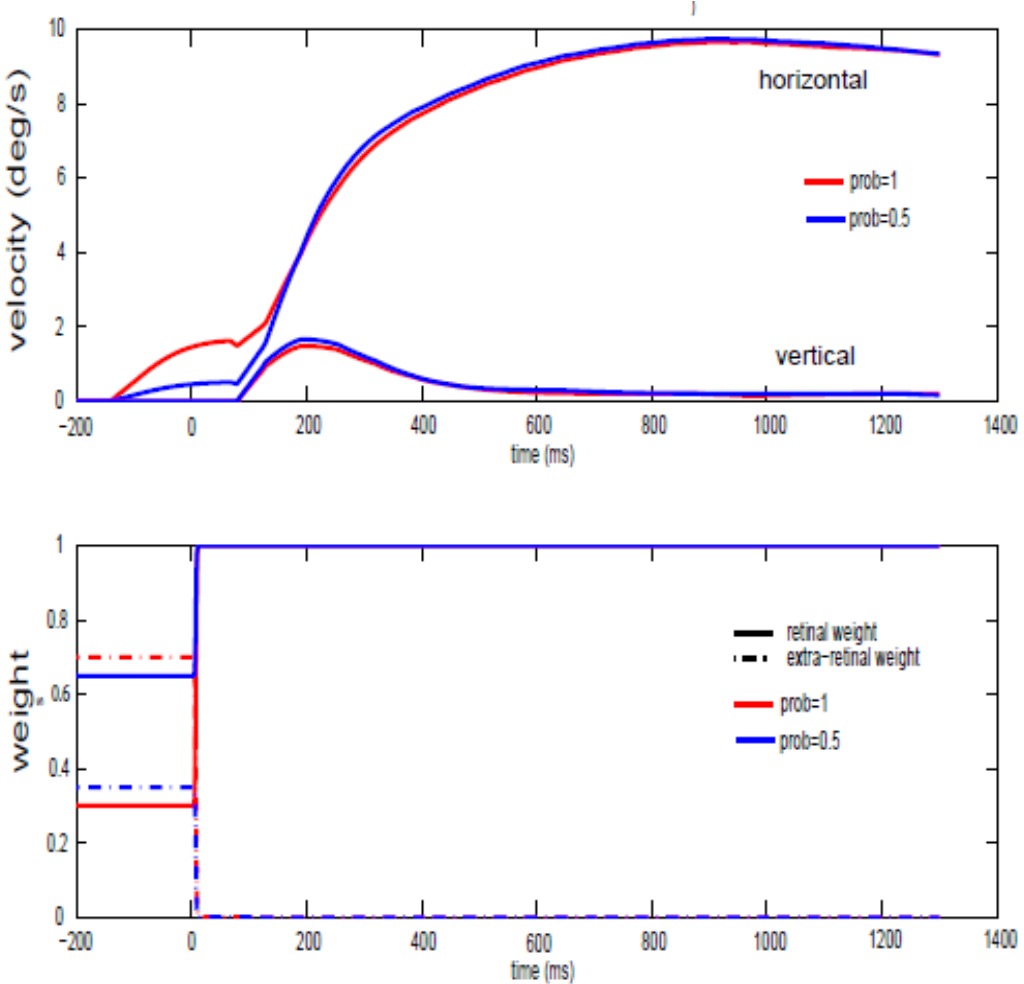


Figure 9.2. Effects of expectation as simulated by the model. Model responses are shown in the top panel and the corresponding retinal (solid colored lines) and extra-retinal (dotted colored lines) weight functions shown in bottom panel for 50% (blue) and 100% (red) probability conditions. Time zero is target motion onset.

9.3. Summary

Expectation of target motion drives anticipatory pursuit in the expected global direction of the target. However this doesn't eliminate the need to integrate local motion signals and results in the initial direction bias on target motion onset. A hierarchical model proposed in the earlier chapter is simulated qualitatively for the same experiment. Higher the probability of the expected target motion higher is the weight for extra-retinal signals which drives anticipatory pursuit. However on target motion onset retinal signals are given all the weight

irrespective of the expectation before target motion. This is evident in the similar vertical eye velocity component for both the probability conditions. The model largely reflects the observations made in the smooth pursuit data. A future model would need to take the advantage of the probabilistic representation and implement the weights as a function of the variances in the retinal and extra-retinal priors that expresses different levels of expectation.

Discussion

Summary

Aperture problem and Motion integration : Background

Local motion measurement (aperture problem (Wallach 1935; Wuerger et al 1996) is ambiguous and hence the responses of the local motion detectors in the early visual system has to be integrated to estimate the global velocity of the moving target. Psychophysical studies show the motion integration is dynamic and suggest that two different motion sensitive units could be involved in motion integration (Castet et al 1993; Lorenceau et al 1993; Wilson et al 1992). The early perception is driven by the ambiguous motion signals (1D), later by unambiguous motion signals (2D). Physiological studies in MT show that MT neurons initially respond to 1D motion signals and later to 2D motion signals (Pack & Born 2001; Smith et al 2005).

Tracking a moving target requires a sensory estimation of the velocity of the target and a subsequent motor transformation of the velocity estimate. Since visual motion processing and tracking share a common physiology at the level of MT and MST (Dursteler & Wurtz 1988; Dursteler et al 1987; Newsome et al 1985; Newsome et al 1988), visuo-motor transformation for tracking provides a better account of temporal dynamics involved in visual motion processing. Behavioral studies (Born et al 2006; Masson & Castet 2002; Masson et al 2000; Masson & Stone 2002; Wallace et al 2005) show that smooth eye movements (ocular following and smooth pursuit) provide an accurate account of the dynamics in motion integration unlike a static readout in the perceptual studies. This dynamics is similar to the dynamics observed in MT (Pack & Born 2001).

Psychophysical results of motion perception were successfully modeled in a Bayesian framework where the local motion measurements from visual motion stimuli were combined with a prior preferring slow speeds (Weiss et al 2002). But this model is essentially static and cannot account for the dynamics observed both in MT and in smooth eye movements. A model (Montagnini et al 2007) processing 1D and 2D motion information in a recurrent bayesian framework has been proposed to understand the dynamic nature of motion integration in MT. The motion information in visual scene is represented as likelihoods (1D and 2D likelihoods) which are combined with a prior preferring slow speeds to obtain a

posterior distribution. On every iteration, the posterior updates the prior. This recurrent update of the prior which is combined with likelihoods solves the aperture problem and the dynamics associated with it is compared to dynamics observed in MT for motion integration.

Recurrent Bayesian model of dynamic motion integration for smooth pursuit

Since tracking responses carry dynamics of motion integration in a greater detail than perceptual accounts, modeling motion integration for eye movements can provide a better understanding of the dynamic nature of motion processing and the subsequent motor transformation for smooth eye movements. The models for smooth pursuit (Bennett & Barnes 2003; Churchland et al 2003; Krauzlis & Lisberger 1994; Robinson et al 1986) have largely focused on the oculomotor dynamics investigated using a simple stimulus like a dot. In this thesis, we extended the previous model (Montagnini et al 2007) by cascading it with an oculomotor plant (Goldreich et al 1992) to an open loop version of the recurrent bayesian model explaining the dynamic motion integration for smooth pursuit (Bogadhi et al 2011).

The model is simulated for different contrasts and speeds using a tilted bar stimuli. Results show that higher speeds and lower contrasts result in higher initial direction bias and subsequent dynamics of motion integration is slower for lower contrasts, similar to the experimental observations. The model responses qualitatively account for the different dynamics observed in smooth pursuit responses to tilted bar stimulus at different speeds and contrasts.

Dynamic Interaction between retinal and extra-retinal signals in motion integration for smooth pursuit

An extension of such a simple paradigm also offers a powerful way to explore interactions between retinal and extra-retinal signals in controlling action. We investigated the dynamic interactions between retinal and extra-retinal signals in motion integration for smooth pursuit by transiently blanking the target at different moments during open-loop and steady-state phases of pursuit. Results show that extra-retinal signals contribute to anticipatory pursuit at the end of the blank in open-loop blanking conditions and are given enough weight even in the presence of the retinal signals on target reappearance to overcome the strong directional biases due to retinal ambiguous motion signals. On the other hand, retinal signals driving pursuit during the blank in steady-state blanking conditions are given enough weight on target reappearance which results in a directional bias due to retinal ambiguous motion signals. This suggests that weights to retinal and extra-retinal signals are dynamic in nature

and the dynamics is dependent on the time at which target is blanked during pursuit.

The previous models (Barnes & Collins 2008a; Bennett & Barnes 2004) explain the dynamics observed in smooth pursuit during blanking by switching between direct and indirect loops and changing the gain value (β) which depends on expectation. Different dynamics is observed in eye movements during blank and on target reappearance at different times during open-loop and steady-state stages of pursuit even though expectation is the same. These models (Barnes & Collins 2008a; Bennett & Barnes 2004) would fail to explain different dynamics observed in smooth pursuit during a transient blank applied at different times during open-loop and steady state of pursuit, given the same expectation which is represented by gain value (β). These findings argue that a simple switching from extra-retinal to retinal signals on target reappearance alone as proposed by previous models (Barnes & Collins 2008b; Bennett & Barnes 2004) is not the case and suggest for transient weight dynamics between retinal and extra-retinal signals.

Hierarchical recurrent Bayesian framework

We extended the open-loop version of the model to a closed-loop dynamic hierarchical recurrent Bayesian model with retinal and extra-retinal recurrent Bayesian blocks where the retinal and extra-retinal signals are dynamically weighted and combined to form the visuo-motor drive. The model results suggest that blanking in steady-state has a little effect on retinal weight resulting in a larger drop and a directional bias on target reappearance after blank. Conversely, blanking in open-loop changes the weights considerably and the extra-retinal signals are given enough weight such that horizontal eye velocity increases in anticipation at the end of blank suppressing the directional bias from the retinal image motion signals on target reappearance after blank. Model parameters suggest that sensory uncertainty could play a role in determining the weight dynamics. With the same weight dynamics that explain the dynamics of the horizontal component of eye velocity because of the blank, the model provides an accurate qualitative account of the dynamics of the vertical component of eye velocity on target reappearance after blank for both open-loop and steady-state blanking conditions.

The model is also simulated for the effect of prediction on motion integration at initiation. The results suggest that extra-retinal signals drive anticipatory pursuit in expectation of target motion and when the target moves, the weight to retinal signals increases with faster dynamics resulting in the initial directional bias in pursuit responses (Montagnini et al 2006).

Perspectives

Role of sensory variance in motion integration for smooth pursuit

Tracking an object involves estimation of sensory parameters and a subsequent motor transformation of the estimates. The noise in sensory estimation and the subsequent motor transformation are equally likely to contribute to variance in pursuit responses. Neuronal and the subsequent pursuit responses vary from trial to trial even though the stimulus characteristics are maintained constant (Lisberger 2010). One of the dominant views is that majority of the variance in pursuit can be explained by the variance in sensory estimation (Osborne et al 2005). This suggests that pursuit can provide a window into the uncertainty involved in sensory estimation.

One way of varying the uncertainty involved in sensory estimation is changing the contrast as it is known to affect the intrinsic dynamics of motion processing, including latency and temporal dynamics of early visual neurons (Albrecht et al., 2002). Lower contrast results in lower signal-to-noise ratio which is associated with high uncertainty and vice-versa. This is also observed as higher directional bias at pursuit initiation for lower contrasts (chapter 6). The data presented in chapter 6 could be taken as an indirect evidence for the role of uncertainty associated with sensory estimation in motion integration for smooth pursuit.

This is successfully used in the Bayesian approach to motion perception where uncertainty of the measurement likelihoods is higher for lower contrasts (Weiss et al 2002). However, pursuit variance which is thought to reflect sensory variance doesn't show any clear distinction between different contrasts. We attempted to extract sensory variance from pursuit for different contrasts assuming that variance at peak acceleration reflects the initial sensory variance that could be used to model the initial likelihoods. Such a method proved to be inaccurate and suggests for a more detailed study of extracting sensory variance from pursuit that could distinguish different contrasts and speeds (Osborne et al 2007).

A possible role of sensory variance in prediction for smooth pursuit

Studies investigating prediction for smooth pursuit have employed transient blanking paradigm at different moments during open-loop or steady-state phases of pursuit (Barnes & Collins 2008; Becker & Fuchs 1985; Bennett & Barnes 2003). Since the blanking in open-loop and steady-state is carried out in different studies, it is difficult to draw a direct

comparison. Nevertheless, theoretically the expectation is essentially the same in both the experiments. However, the observed dynamics in pursuit is different in open-loop and steady-state blanking conditions. Data from one of the recent studies where target is blanked at different times (50ms, 100ms, 150ms and 200ms) after target motion onset show that early blanks doesn't result in the familiar dip in the eye velocity during the blank where as blanking at 200ms results in a significant dip in the eye velocity comparable to what has been observed with blanking in steady-state conditions (Barnes & Collins 2008). The expectation is the same for early blank as well as late blank conditions but the dynamics is clearly different. This doesn't support the claim the expectation alone could shape the predictive component of pursuit. The data presented in chapter 8 suggest for dynamic interaction between retinal and extra-retinal signals investigated using a more ambiguous stimulus like a tilted bar. We are of the view that this dynamics is shaped at least partly by the variance associated with sensory estimation. That leaves with one possible explanation that expectation is necessary to switch on the predictive drive for pursuit but the dynamics associated with it could be determined by variance in sensory estimation as well as predictive component at the time of the blank. There is evidence from the studies in motor control that such an explanation advocating the role of variance in dynamics of prediction is not entirely new.

Sensory noise is the major source of variance in the motor action as motor action is planned so as to minimize motor noise, and hence sensory noise could play a crucial role in the motor transformation of the sensory estimate (Harris & Wolpert 1998; Osborne et al 2005). Furthermore, motor transformation has to minimize the detrimental effects of noise by mixing sensory estimate as well as internal estimate indicative of prediction (See, van Beers et al 2002a for a review). This supports the idea that sensory variance might have a role to play in responding to a change in the motion information on the retina (e.g. a transient blank). Since the evidence about the target motion is lower during the early stages of motion processing (Osborne et al 2007), any changes in the motion information on the retina would be least processed and hence the eye movements show a large extra-retinal influence. Similarly, the evidence collected is higher during the later stages of motion processing, any changes in the motion information on the retina would be processed and hence the eye movements show a large retinal influence.

Overall, blanking at different times can be viewed as an indirect way of probing the effect of sensory variance on prediction for pursuit as the time course of pursuit variance reflects the time course of uncertainty in sensory estimation (Osborne et al 2007). Future

work should focus on investigating a more direct evidence linking variance in sensory estimation to predictive drive for pursuit.

A generic approach to smooth pursuit

Oculomotor models for smooth pursuit has taken a control systems approach to explain the dynamics and stability associated with smooth pursuit (Goldreich et al 1992; Krauzlis & Lisberger 1989; 1994; Robinson et al 1986; Tavassoli & Ringach 2009). However, there are limitations to the approach (Steinman 1986). It has constrained our understanding of sensory processing underlying pursuit as well as effect of cognition on pursuit. Sensory processing is responsible to extract speed and direction of the moving object which cannot be understood in this approach alone.

Numerous studies employing different paradigms have shown the effect of cognition on pursuit (chapter 7). Few of the above mentioned models could explain some of the cognitive properties of pursuit, for e.g. effects of learning on pursuit during transient disappearance of a target (Churchland et al 2003; Madelain & Krauzlis 2003). More recent models have incorporated cognition into smooth pursuit models based on the evidence that a short-term memory of visuo-motor drive could be linked to predictive component of pursuit (Barnes & Collins 2008; Bennett & Barnes 2004). These models have provided a general schema for pursuit. A major short coming of these models is they are not equipped to deal with uncertainty in sensory information that could possibly have a role in the dynamics of prediction as noted earlier. Currently, these models account for the observed dynamics by manually fitting gain parameters and manually switching between retinal and extra-retinal signals. Also, recent work shows that anticipatory pursuit could reflect the statistics of the task (unpublished observations by Montagnini). Since anticipatory pursuit is linked to extra-retinal mechanisms for pursuit, this would suggest for a probabilistic nature of extra-retinal mechanisms for smooth pursuit (Barnes & Collins 2008). Furthermore, all the above models neglect the sensory processing for smooth pursuit.

This thesis proposed a model that overcomes the two shortcomings of the previous models and provides a more general framework for smooth pursuit. The first version of the model could explain the motion integration for pursuit. An extended hierarchical version of the model was proposed following the schema put forward by Barnes & Collins 2008; Bennett & Barnes 2004. With the same weight dynamics that explain the dynamics of the horizontal component of eye velocity because of the blank, the model provides an accurate qualitative account of the dynamics of the vertical component of eye velocity on target

reappearance after blank for both open-loop and steady-state blanking conditions. The model parameters suggest that sensory variance could play a role in determining the dynamics of weights as noted earlier. Since the retinal and extra-retinal processing in the model is probabilistic, it provides a general framework to explore the role of variance in retinal motion integration and also the probabilistic nature of extra-retinal mechanisms.

Probabilistic framework for smooth pursuit

Probabilistic representation of motion information would allow to represent uncertainty in the velocity information. As noted earlier, uncertainty in sensory estimate affects motion integration for smooth pursuit. The probabilistic model proposed in this thesis could explain the motion integration for smooth pursuit at different speeds and contrasts. The uncertainty represented in the likelihoods for different contrasts and speeds determine the initial direction bias and the subsequent dynamics. Altering the prior through training can lead to different percepts (Sotiroopoulos et al 2011).

Such a framework could also incorporate the variance in determining the dynamics between retinal and extra-retinal signals. As expectation alone cannot explain the different dynamics in pursuit during blanking at different times, the variances of retinal prior and extra-retinal prior could be used to design the associated dynamics with their respective weight functions rather than switching between retinal and extra-retinal signals as proposed by previous models (Barnes & Collins 2008; Bennett & Barnes 2004). The advantage of designing weight dynamics as a function of uncertainties in retinal and extra-retinal velocity information is, it gives a much simpler and powerful way of expressing prediction as an adaptive behavior reflecting the dynamic interplay between expectation and measurement as determined by their respective reliabilities (Van Beers et al 2002). Reliability of expectation is determined by the variance in extra-retinal prior and reliability in the measurement is determined by the variance in the retinal posterior. Thus, hierarchical Bayesian framework (Lee & Mumford 2003) allows for a mix of retinal and extra-retinal signals based on their reliability measured from their respective variances. The combined estimate is used to drive the pursuit response. Over all, this provides an efficient framework for future experimental and theoretical studies to explore pursuit as an adaptive system mixing retinal and extra-retinal signals similar to a kalman filter for tracking.

Physiological Perspective

There is evidence that area MT is involved in motion processing of retinal information for smooth pursuit (Dursteler & Wurtz 1988; Komatsu & Wurtz 1988; Newsome et al 1985) and MT shows no activity in the absence of retinal motion information (Ilg & Thier 2003; Newsome et al 1988). Evidence suggests that FEF plays a role in gain control for pursuit (Tanaka & Lisberger 2001; 2002a) and may contribute to predictive component of pursuit (Keating 1991a; MacAvoy et al 1991; Fukushima et al 2003). Individual Neurons in FEFsem are highly correlated with the behavior at specific times during a trial suggesting that FEFsem might regulate pursuit in a temporally selective fashion (Schoppik et al 2008). Stimulation of SEF when the target motion is predictable enhances anticipatory pursuit (Missal & Heinen 2004). SEF might also be involved in encoding decision rule and interpreting sensory signals in the context of the decision rule for smooth pursuit (Kim et al 2005; Yang et al 2010). Studies have shown that area MSTl receives both retinal and extra-retinal inputs as it has projections from MT and FEF-SEF (Newsome et al 1988).

One could put the above physiological evidence into a perspective that is relevant to the idea put forward in this thesis, that retinal and extra-retinal signals could be mixed following a rule that might be indicative of adaptive nature of pursuit. MT processes pure retinal motion information, FEF is involved in regulating pursuit which showcases itself as gain control and to some extent anticipatory pursuit. SEF could be largely responsible for predictive pursuit and most importantly encoding decision rule and interpreting sensory signals in the context of the decision rule for smooth pursuit. MSTl is the most likely candidate to allow for a mix of retinal and extra-retinal signals forming pre-motor drive following the interpretation of sensory signals based on the decision rule for pursuit. This is supportive of the view that there are two cortical networks, one processing retinal information (V1-MT-MSTl) and the other extra-retinal information (MSTl-FEF-SEF) and both are combined at the level of area MSTl (See (Thier & Ilg 2005)). This thesis proposed that these two loops could implement a hierarchical recurrent model that can infer the most optimal integration for sensorimotor integration in ambiguous conditions (Masson et al., 2010).

Pursuit as an adaptive system

Pursuit has been used as a probe to study visual motion processing of retinal motion signals and the subsequent sensory-motor transformation (See, Lisberger 2010, for a review). It has also been used to understand the nature of extra-retinal signals that contribute to motor action

in various paradigms. This thesis made the first attempt to understand the interactions between the retinal and extra-retinal signals and the model results suggest that the sensory variance could determine the dynamics of these interactions. Previous studies investigated the role of uncertainty in target motion estimates on visuo-motor drive for pursuit (Osborne & Lisberger 2009). Future work should address the role of uncertainty in target motion estimates on extra-retinal signals driving pursuit. Expectation of change in target motion estimates drives anticipatory pursuit reflecting the expected change in target motion estimates (Bennett & Barnes 2004). However, it needs to be investigated how the uncertainty in the expected target motion estimates modulate anticipatory pursuit. Adaptive behavior not only takes into account, the reliability of the information acquired but also the reliability of expected changes in information so as to minimize a cost function and maximize an utility function. Future work along these lines can provide an understanding about the adaptive nature of pursuit. That would further lead to investigate the cost and utility functions (Kording & Wolpert 2004) involved with pursuit, thus unveiling a mathematical description of the very purpose smooth pursuit serves.

Abbreviations

1D	Ambiguous motion signals from line endings
2D	Unambiguous motion signals from terminator endings
CCW	Counter Clock-wise
CDS	Component Direction Selective
CW	Clock-wise
FEF	Frontal Eye Fields
FEFsem	Smooth eye movement region of the frontal eye fields
FPA	Frontal Pursuit Area
FT	Feature Tracking
IOC	Intersection of Constraints
LGN	Lateral Geniculate Nucleus
M	Magnocellular
MAP	Maximum a Posteriori
MT	Middle temporal
MST	Medial Superior Temporal
OFR	Ocular following response
OKN	Optokinetic nystagmus
P	Parvocellular
PDS	Pattern Direction Selective
PON	Pontine Nuclei
RMSD	Root Mean Square Deviation
SEF	Supplementary Eye Fields
STS	Superior Temporal Sulcus
V1	Primary Visual Cortex
VA	Vector Average
VERM	Vermis
VN	Vestibular Nucleus
VOR	Vestibular Ocular Reflex
VPF	Ventral ParaFlocculus

List of Figures

- Figure 1.1. Smooth pursuit response to a target moving with a constant velocity preceeded by a step displacement in the target position
- Figure 1.2. Eye velocity traces for a target moving at 30°/s starting at different positions
- Figure 1.3. Effect of feed-back delay on oscillations
- Figure 1.4. Negative feed-back model for pursuit
- Figure 1.5. Internal positive feed-back model for pursuit
- Figure 1.6. Image motion model with multiple pathways
- Figure 1.7. Physiology of Pursuit
- Figure 2.1. Basic Visual Pathway from retina to cortex
- Figure 2.2. Motion processing pathways from the retina to different cortical areas.
- Figure 2.3. Speed tuning in MT neurons
- Figure 3.1. Aperture problem
- Figure 3.2. Reichardt detector
- Figure 3.3. Aperture problem with Reichardt detector
- Figure 3.4. Space-time representation of motion
- Figure 3.5. Extracting motion with space-time oriented filters.
- Figure 3.6. Spatio-temporal filter
- Figure 3.7. Motion energy model
- Figure 4.1. Vector Average for objects of different shapes
- Figure 4.2. Constructing IOC solution from local velocity samples
- Figure 4.3. CDS and PDS cells in frequency space
- Figure 4.4. Different stimuli for motion integration
- Figure 4.5. Conditions for Coherence
- Figure 4.6. Effect of adaptation on the detectability
- Figure 4.7. Changes in coherence threshold following adaptation for different spatial frequencies
- Figure 4.8. Responses of a PDS cell to gratings and plaid stimuli

- Figure 4.10. Bar field stimulus
- Figure 4.11. Dynamics of motion integration in an MT neuron.
- Figure 4.12. Dynamics of component and pattern direction selectivity
- Figure 4.13. End-stopping in V1 neurons
- Figure 4.14. A schematic of the extended S and H model
- Figure 4.15. Fourier and Non-fourier pathway model
- Figure 4.16. Selection model
- Figure 4.17. Gated-diffusion model
- Figure 4.18. IOC and VA computation for rhombus of different sizes and contrasts.
- Figure 4.19. Combining likelihoods with the prior in a bayesian framework for a thin rhombus
-
- Figure 5.1. Ocular following for barberpole stimuli viewed through apertures of different aspect ratios.
- Figure 5.2. Ocular following responses for uni-kinetic plaids.
- Figure 5.3. Smooth pursuit responses to type-II (CCW and CW) and type-I diamonds
- Figure 5.4. Smooth pursuit responses for a tilted bar of different lengths.
- Figure 5.5. Contrast response functions for 1D (early) and 2D (late) motion components
-
- Figure 6.1. Aperture problem and dynamics of motion integration
- Figure 6.2. Pursuing pure 1D and pure 2D stimulus.
- Figure 6.3. Effect of line length.
- Figure 6.4. Directional anisotropies of speed
- Figure 6.5. Directional anisotropies of contrast
- Figure 6.6. Model of recurrent inference for pursuit eye movements
- Figure 6.7. Pursuit eye velocity traces for data and the model (varying contrast)
- Figure 6.8. Pursuit eye velocity traces for data and the model (varying speed)
- Figure 6.9. Direction bias in data and the model (varying contrast)
-
- Figure 7.1. Prediction in Pursuit
- Figure 7.2. Time course of smooth eye velocity before and during ramp, when the target is predictable and unpredictable
- Figure 7.3. Effect of transient blanking during steady-state of pursuit.

- Figure 7.4. Effect of blocked and random presentation on smooth pursuit during a transient blank.
- Figure 7.5. Effect of transient blanking during open-loop period of pursuit.
- Figure 7.6. Positive feed-back gain model
- Figure 7.7. Short term memory model
- Figure 8.1. Different measures quantifying the dynamics in a pursuit response for 200ms blank duration.
- Figure 8.2. Mean smooth pursuit responses for blanking in steady state experiment.
- Figure 8.3. Blanking in steady-state :Horizontal component Analysis.
- Figure 8.4. Blanking at steady-state :Vertical component Analysis.
- Figure 8.5. Mean smooth pursuit responses for open-loop blanking experiment.
- Figure 8.6. Blanking in open-loop : Horizontal component analysis
- Figure 8.7. Blanking in open-loop : Vertical component analysis
- Figure 8.8. Plot summarizing the effect of blank on pursuit
- Figure 8.9. A hierarchical recurrent Bayesian model for smooth pursuit
- Figure 8.10. Model simulation and temporal dynamics of weights
- Figure 9.1. Effect of expectation on anticipatory pursuit.
- Figure 9.2. Effects of expectation as simulated by the model

References

- Adelson EH, Bergen JR. 1985. Spatiotemporal energy models for the perception of motion. *J. Opt. Soc. Am* 2:284-99
- Adelson EH, Movshon JA. 1982. Phenomenal coherence of moving visual patterns. *Nature* 300:523-5
- Albrecht DG, Geisler WS, Frazor RA, Crane AM. 2002. Visual cortex neurons of monkeys and cats: Temporal dynamics of the contrast response function. *J Neurophysiol* 88:888-913
- Albright TD. 1984. Direction and orientation selectivity of neurons in visual area MT of the macaque. *J Neurophysiol* 52:1106-30
- Albright TD, Desimone R, Gross CG. 1984. Columnar organization of directionally selective cells in visual area MT of the macaque. *J Neurophysiol* 51:16-31
- Allman JM, Kaas JH, Lane RH. 1973. The middle temporal visual area(MT)in the bushbaby, Galago senegalensis. *Brain Res* 57:197-202
- Atkeson CG, Hollerbach JM. 1985. Kinematic features of unrestrained vertical arm movements. *J Neurosci* 5:2318-30
- Badler J, Heinen SJ. 2006. Anticipatory Movement Timing Using Prediction and External Cues. *J Neurosci* 26:4519-25
- Badler J, Lefevre P, Missal M. 2010. Causality attribution biases oculomotor responses. *J Neurosci* 30:10517-25
- Baker J, Gibson A, Glickstein M, Stein J. 1976. Visual cells in the pontine nuclei of the cat. *J Physiol* 255:415–33
- Barnes GR, Asselman PT. 1991. THE MECHANISM OF PREDICTION IN HUMAN SMOOTH PURSUIT EYE MOVEMENTS. *J Physiol* 439:439-61
- Barnes GR, Collins CJS. 2008. Evidence for a link between the extra-retinal component of random-onset pursuit and the anticipatory pursuit of predictable object motion. *J Neurophysiol* 100:1135-46
- Barnes GR, Collins CJS. 2008. The influence of briefly presented randomized target motion on the extraretinal component of ocular pursuit. *J Neurophysiol* 99:831-42
- Barnes GR, Schmid AM. 2002. Sequence learning in human ocular smooth pursuit. *Exp Brain Res* 144:322-35
- Barthelemy FV, Perrinet LU, Castet E, Masson GS. 2008. Dynamics of distributed 1D and

- 2D motion representations for short-latency ocular following. *Vision Res* 48:501-22
- Bayerl P, Neumann H. 2004. Disambiguating Visual Motion Through Contextual feed-back Modulation. *Neural Comp* 16:2041-66
- Bayerl P, Neumann H. 2007. Disambiguating visual motion by form-motion interaction - a computational model. *International journal of computer vision* 72:27-45
- Bays PM, Wolpert DM. 2007. Computational principles of sensorimotor control that minimize uncertainty and variability. *J Physiol* 578:387-96
- Becker W, Fuchs AF. 1985. Prediction in the oculomotor system: smooth pursuit during transient disappearance of a visual target. *Exp Brain Res* 57:562-75
- Bennett SJ, Barnes GR. 2003. Human ocular pursuit during the transient disappearance of a visual target. *J Neurophysiol* 90:2504-20
- Bennett SJ, Barnes GR. 2004. Predictive smooth ocular pursuit during the transient disappearance of a visual target. *J Neurophysiol* 92:578-90
- Bennett SJ, Barnes GR. 2006. Smooth ocular pursuit during the transient disappearance of an accelerating visual target: the role of reflexive and voluntary control. *Exp Brain Res* 175:1-10
- Bennett SJ, Orban de Xivry JJ, Barnes GR, Lefevre P. 2007. Target acceleration can be extracted and represented within the predictive drive to ocular pursuit. *J Neurophysiol* 98:1405-14
- Bennett SJ, Orban de Xivry JJ, Lefevre P, Barnes GR. 2010. Oculomotor prediction of accelerative target motion during occlusion: long-term and short-term effects. *Exp Brain Res* 204:493-504
- Berzhanskaya J, Grossberg S, Mingolla E. 2007. Laminar cortical dynamics of visual form and motion interactions during coherent object motion perception. *Spatial Vision* 20:337-95
- Blohm G, Missal M, Lefevre P. 2006. Direct Evidence for a Position Input to the Smooth Pursuit System. *J Neurophysiol* 94:712-21
- Bogadhi AR, Montagnini A, Mamassian P, Perrinet LU, Masson GS. 2011. Pursuing motion illusions: A realistic oculomotor framework for Bayesian inference. *Vision Res* 51:867-80
- Bogadhi AR, Montagnini A, Masson GS. 2012. Dynamic Interaction between retinal and extra-retinal signals in motion integration for smooth pursuit. (Submitted)
- Born RT. 2001. Visual processing: Parallel-er and Parallel-er. *Curr Biol* 11:R566-R8
- Born RT. 2004. Taking strategies to task. *Neuron*
- Born RT, Bradley DC. 2005. Structure and function of visua area MT. *Ann. Rev. Neurosci.* 28:157-89

- Born RT, Pack CC, Ponce CR, Yi S. 2006. Temporal evolution of 2-dimensional direction signals used to guide eye movements. *J Neurophysiol* 95:284-300
- Born RT, Pack CC, Zhao R. 2002. Integration of motion cues for the initiation of smooth pursuit eye movements. *Prog Brain Res* 140:225-37
- Born RT, Tsui JMG, Pack CC. 2010. Temporal dynamics of motion integration. In *Dynamics of visual motion processing*, ed. GS Masson, UJ Ilg. newyork: springer
- Bowns L. 1996. Evidence for a feature tracking explanation of why Type II plaids move in the vector sum direction at short durations. *Vision Res* 36:3685-94
- Bowns L, Alais D. 2006. Large shifts in perceived motion direction reveal multiple global motion solutions. *Vision Res* 46:1170-7
- Bradley DC. 2001. MT signals better with time. *Nature* 4:346-8
- Bradley DC, Goyal MS. 2008. Velocity computation in the primate visual system. *Nat Rev Neurosci* 9:686-95
- Burr D, Thompson P. 2011. Motion Psychophysics. *Vision Res* 51:1431-56
- Busettini C, Miles FA, Schwarz U. 1991. Ocular responses to translation and their dependence on viewing distance. II. Motion of the scene. *J Neurophysiol* 66:865-78
- Carandini M, Demb JB, Mante V, Tolhurst DJ, Dan Y, et al. 2005. Do we know what the early visual system does? *J Neurosci* 25:10577-97
- Carey MR, Medina JF, Lisberger SG. 2005. Instructive signals for motor learning from visual cortical area MT. *Nat Neurosci* 8:813-9
- Carl JR, Gellman RS. 1987. Human smooth pursuit: stimulus-dependent responses. *J Neurophysiol* 57:1446-63
- Castet E, Charton V, Dufour A. 1999. The extrinsic/intrinsic classification of two-dimensional motion signals with barber-pole stimuli. *Vision Res* 39:915-32
- Castet E, Lorenceau J, Shiffra M, Bonnet C. 1993. Perceived speed of moving lines depends on orientation, length, speed and luminance. *Vision Res* 33:1921-36
- Churchland MM, Chou IH, Lisberger SG. 2003. Evidence for object permanence in the smooth-pursuit eye movements of monkeys. *J Neurophysiol* 90:2205-18
- Churchland MM, Lisberger SG. 2001. Experimental and computational analysis of monkey smooth pursuit eye movements. *J Neurophysiol* 86:741-59
- Churchland MM, Lisberger SG. 2001. Shifts in the Population Response in the Middle Temporal Visual Area Parallel Perceptual and Motor Illusions Produced by Apparent Motion. *J Neurosci* 21:9387-402
- Cohen JL. 1981. Corticopontine projections of the lateral suprasylvian cortex: de-emphasis

- of the central visual field. *Brain Res* 219:239-48
- Collewijn H, van der Mark F, Jansen TC. 1975. Precise recording of human eye movements. *Vision Res* 15:447-50
- Collins CJS, Barnes GR. 2009. Predicting the Unpredictable: Weighted Averaging of Past Stimulus Timing Facilitates Ocular Pursuit of Randomly Timed Stimuli. *J Neurosci* 29:13302-14
- De Hemptinne C, Lefevre P, Missal M. 2006. Influence of cognitive expectation on the initiation of anticipatory and visual pursuit eye movements in the rhesus monkey. *J Neurophysiol* 95:3770-82
- de Hemptinne C, Nozaradan S, Duvivier Q, Lefevre P, Missal M. 2007. How Do Primates Anticipate Uncertain Future Events? *J Neurosci* 27:4334-41
- DeAngelis GC, Uka T. 2003. Coding of horizontal disparity and velocity by MT neurons in the alert macaque. *J Neurophysiol* 89:1094-111
- DeSperati C, Viviani P. 1997. The relationship between curvature and velocity in two-dimensional smooth pursuit eye movements. *J Neurosci* 17:3932-45
- Dimova KD, Denham MJ. 2009. A neurally plausible model of the dynamics of motion integration in smooth eye pursuit based on recursive Bayesian estimation. *Biol Cybern* 100:185-201
- Dimova KD, Denham MJ. 2010. A model of plaid motion perception based on recursive Bayesian integration of the 1-D and 2-D motions of plaid features. *Vision Res* 50:585-97
- Dodge R. 1903. Five types of eye movement in the horizontal meridian plane of the field of regard. *Amer. J. Physiol* 8:307-29
- Dodge R, Travis RC, Fox JC. 1930. Optic nystagmus III. Characteristics of the slow phase. *Archives of Neurology & Psychiatry* 24:21-34
- Dubner R, Zeki SM. 1971. Response properties and receptive fields of cells in an anatomically defined region of the superior temporal sulcus in the monkey. *Brain Res* 35:528-32
- Dursteler MR, Wurtz RH. 1988. Pursuit and optokinetic deficits following chemical lesions of cortical areas MT and MST. *J Neurophysiol* 60:940-65
- Dursteler MR, Wurtz RH, Newsome WT. 1987. Directional pursuit deficits following lesions of the foveal representation within the superior temporal sulcus of the macaque monkey. *J Neurophysiol* 57:1262-87
- Felleman DJ, Van Essen DC. 1991. Distributed hierarchical processing in the primate cerebral cortex. *Cereb Cortex* 1:1-47

- Fennema C, Thompson W. 1979. Velocity determination in scenes containing several moving objects. *Computer Graphics and Image Processing* 9:301-15
- Ferrera VP, Nealey TA, Maunsell JHR. 1994. Responses in macaque visual area V4 following inactivation of the parvocellular and magnocellular LGN pathways. *J Neurosci* 14:2080-8
- Freeman TCA, Champion RA, Warren PA. 2010. A Bayesian Model of Perceived Head-Centered Velocity during Smooth Pursuit Eye Movement. *Curr Biol* 20:757-62
- Freyberg S, Ilg UJ. 2008. Anticipatory smooth-pursuit eye movements in man and monkey. *Exp Brain Res* 186:203-14
- Friend SM, Baker CLJ. 1993. Spatio-temporal frequency separability in area 18 neurons of the cat. *Vision Res* 33:1765-71
- Fukushima K, yamanobe T, Shinmei Y, Fukushima J. 2003. Predictive responses of periarcuate pursuit neurons to visual target motion. *Exp Brain Res* 145:104-20
- Gizzi MS, Newsome WT, Movshon JA. 1983. Direction selectivity of neurons in macaque MT. *Invest Ophthalmol Vision Sci Suppl.* 24:107
- Goldreich D, Krauzlis RJ, Lisberger SG. 1992. Effect of changing feed-back delay on spontaneous oscillations in smooth pursuit eye movements of monkeys. *J Neurophysiol* 67:625-38
- Gorea A, Lorenceau J. 1991. Directional performances with moving plaids: component-related and plaid-related processing modes coexist. *Spatial Vision* 5:231-52
- Gottlieb JP, Bruce CJ, MacAvoy MG. 1993. Smooth eye movements elicited by microstimulation in the primate frontal eye field. *J Neurophysiol* 69:786-99
- Groh JM. 2001. Converting neural signals from place codes to rate codes. *Biol Cybern* 85:159-65
- Groh JM, Born RT, Newsome WT. 1997. How Is a Sensory Map Read Out? Effects of Microstimulation in Visual Area MT on Saccades and Smooth Pursuit Eye Movements. *J Neurosci* 17:4312-30
- Grossberg S, Mingolla E. 1985. Neural dynamics of form perception: Boundary completion, illusory figures, and neon color spreading. *Psychological Review* 92:173-211
- Grossberg S, Mingolla E, Viswanathan L. 2001. Neural dynamics of motion integration and segmentation within and across apertures. *Vision Res* 41:2521-53
- Harris CM, Wolpert DM. 1998. Signal-dependent noise determines motor planning. *Nature* 394:780-4
- Hassenstein B, Reichardt W. 1956. Systemtheoretische Analyse der Zeit-,Reihenfolgen und

- Vorzeichenauswertung bei der Bewegungsperzeption des Russelkäfers *Chlorophanus*. Z. Naturforsch 11B:513-24
- Haung X, Lisberger SG. 2009. Noise Correlations in Cortical Area MT and Their Potential Impact on Trial-by-Trial Variation in the Direction and Speed of Smooth-Pursuit Eye Movements. J Neurophysiol 101:3012–30
- Heinen SJ. 1995. Single neuron activity in the dorsomedial frontal cortex during smooth pursuit eye movements. Exp Brain Res 104:357-61
- Heinen SJ, Liu M. 1997. Single-neuron correlates of predictive eye movements in the dorsomedial frontal cortex. Vis Neurosci 14:853-65
- Heinen SJ, Watamaniuk SNJ. 1998. Spatial integration in human smooth pursuit. Vision Res 38:3785-94
- Hildreth EC, Koch C. 1987. "THE ANALYSIS OF VISUAL MOTION" From Computational Theory to Neuronal Mechanisms. Ann. Rev. Neurosci. 10:477-533
- Holub RA, Morton-Gibson M. 1981. Response of Visual Cortical Neurons of the cat to moving sinusoidal gratings: response-contrast functions and spatiotemporal interactions. J Neurophysiol 46:1244-59
- Hubel DH. Eye, Brain and Vision
- Hubel DH. 1963. The visual cortex of the brain. Scientific American 209:54-63
- Hubel DH, Wiesel TN. 1968 Receptive fields and functional architecture of monkey striate cortex. J Physiol 195:215–43
- Hurlimann F, Kiper DC, Carandini M. 2002. Testing the Bayesian model of perceived speed. Vision Res 42:2253-7
- Ilg UJ. 1997. Slow eye movements. Progress in Neurobiology 53:293-329
- Ilg UJ, Churan J. 2010. Second-Order Motion Stimuli : A New Handle to Visual Motion Processing. In Dynamics of Visual Motion Processing Neuronal Behavioral and Computational Approaches, ed. GS Masson, UJ Ilg. Newyork: Springer
- Ilg UJ, Thier P. 2003. Visual tracking neurons in primate area MST are activated by smooth-pursuit eye movements of an "imaginary" target. J Neurophysiol 90:1489-502
- Kalman RE. 1960. A New Approach to Linear Filtering and Prediction Problems. Trans. ASME Ser. D. J. Basic Eng 82:35-45
- Kawano K. 1999. Ocular tracking: behavior and neurophysiology. Curr Opin Neurobiol 9:467-73
- Keating EG. 1991. Frontal eye field lesions impair predictive and visually-guided pursuit eye movements. Exp Brain Res 86:311-23

- Keating EG. 1991. Lesions of the frontal eye field impair pursuit eye movements, but preserve the predictions driving them. *Behav Brain Res* 53:91-104
- Kersten D, Mamassian P, Yuille A. 2004. Object perception as Bayesian inference. *Annual review of psychology* 55:271-304
- Kim YG, Badler J, Heinen SJ. 2005. Trajectory interpretation by supplementary eye field neurons during ocular baseball. *J Neurophysiol* 94:1385-91
- Kodaka Y, Kawano K. 2003. Preparatory modulation of the gain of visuo-motor transmission for smooth pursuit in monkeys. *Exp Brain Res* 149:391-4
- Komatsu H, Wurtz RH. 1988. Relation of cortical areas MT and MST to pursuit eye movements, I. Localization and visual properties of neurons. *J Neurophysiol* 60:580-603
- Komatsu H, Wurtz RH. 1989. Modulation of pursuit eye movements by stimulation of cortical areas MT and MST. *J Neurophysiol* 62:32-47
- Kooi FL. 1993. Local direction of edge motion causes and abolishes the barberpole illusion. *Vision Res* 33:2347-51
- Kording KP, Wolpert DM. 2004. The loss function of sensorimotor learning. *PNAS* 101:9839-42
- Kording KP, Wolpert DM. 2004. Probabilistic inference in human sensorimotor processing. In *Advances in Neural Information Processing Systems* ed. B Schölkopf: MIT Press
- Kowler E. 1989. Cognitive expectations, not habits, control anticipatory smooth oculomotor pursuit. *Vision Res* 29:1049-57
- Kowler E. 2011. Eye movements: The past 25 years. *Vision Res* 51:1457-83
- Kowler E, Martins AJ, Pavel M. 1984. The effect of expectations on slow oculomotor control--IV. Anticipatory smooth eye movements depend on prior target motions. *Vision Res* 24:197-210
- Kowler E, Steinman RM. 1979. The effect of expectations on slow oculomotor control. I. Periodic target steps. *Vision Res* 19:619-32
- Kowler E, Steinman RM. 1979. The effect of expectations on slow oculomotor control. II. Single target displacements. *Vision Res* 19:633-46
- Kowler E, Steinman RM. 1981. The effect of expectations on slow oculomotor control-III: Guessing unpredictable target displacements. *Vision Res* 21:191-203
- Krauzlis RJ. 2004. Recasting the smooth pursuit eye movement system. *J Neurophysiol* 91:591-603
- Krauzlis RJ. 2005. The control of voluntary eye movements : New perspectives. *The Neuroscientist* 11:124-37

- Krauzlis RJ, Lisberger SG. 1987. Smooth pursuit eye movements are not driven simply by target velocity. *Neurosci. Abstr.* 13:170
- Krauzlis RJ, Lisberger SG. 1989. A control systems model of smooth pursuit eye movements with realistic emergent properties. *Neural Comp* 1:116-22
- Krauzlis RJ, Lisberger SG. 1994. A model of visually-guided smooth pursuit eye movements based on behavioral observations. *J comp Neurosci* 1:265-83
- Krauzlis RJ, Lisberger SG. 1994. Temporal properties of visual motion signals for the initiation of smooth pursuit eye movements in monkeys. *J Neurophysiol* 72:150-62
- Krauzlis RJ, Miles FA. 1996. Initiation of saccades during fixation or pursuit: Evidence in humans for a single mechanism. *J Neurophysiol* 76:4175-9
- Krauzlis RJ, Miles FA. 1996. Transitions between pursuit eye movements and fixation in the monkey: dependence on context. *J Neurophysiol* 76:1622-38
- Krekelberg B. 2008. Motion Detection Mechanisms. In *The Senses: A Comprehensive Reference.*, pp. 133-55. oxford: Elsevier Inc
- Krekelberg B, van Wezel RJA, Albright TD. 2006. Interactions between speed and contrast tuning in the middle temporal area: implications for the neural code for speed. *J Neurosci* 26:8988-98
- Kuffler SW. 1953. Discharge patterns and functional organization of mammalian retina. *J Neurophysiol* 16:37-68
- Lagae L, Raiquel S, Orban GA. 1993. Speed and direction selectivity of macaque middle temporal neurons. *J Neurophysiol* 69:19-39
- Lee TS, Mumford D. 2003. Hierarchical Bayesian inference in the visual cortex. *J Opt Soc Am A* 20:1434-48
- Lisberger SG. 2010. Visual Guidance of Smooth-Pursuit Eye Movements: Sensation, Action, and What Happens in Between. *Neuron* 66:477-91
- Lisberger SG, Evinger C, Johanson GW, Fuchs AF. 1981. Relationship between eye acceleration and retinal image velocity during foveal smooth pursuit in man and monkey. *J Neurophysiol* 46:229-49
- Lisberger SG, Morris EJ, Tychsen L. 1987. Visual Motion Processing and Sensory-Motor Integration for Smooth Pursuit Eye Movements. *Ann. Rev. Neurosci.* 10:97-129
- Lisberger SG, Movshon JA. 1999. Visual motion analysis for pursuit eye movements in area MT of macaque monkeys. *J Neurosci* 19:2224-46
- Lisberger SG, Westbrook LE. 1985. Properties of visual inputs that initiate horizontal smooth pursuit eye movements in monkeys. *J Neurosci* 5:1662-73

- Liu J, Newsome WT. 2002. Functional Organization of Speed Tuned Neurons in Visual Area MT. *J Neurophysiol* 89:246-56
- Liu J, Newsome WT. 2006. Correlation between Speed Perception and Neural Activity in the Middle Temporal Visual Area. *J Neurosci* 25:711-22
- Loffler G, Orbach HS. 1999. Computing feature motion without feature detectors: a model for terminator motion without end-stopped cells. *Vision Res* 39:859-71
- Lorenceau J, Alais D. 2001. Form constraints in motion binding. *Nat Neurosci* 4:745-51
- Lorenceau J, Shiffrar M. 1992. The influence of terminators on motion integration across space. *Vision Res* 32:263-73
- Lorenceau J, Shiffrar M, Wells N, Castet E. 1993. Different motion sensitive units are involved in recovering the direction of moving lines. *Vision Res* 33:1207-17
- Lorenceau J, Zago L. 1999. Cooperative and competitive spatial interactions in motion integration. *Vis Neurosci* 16:755-70
- Luebke AE, Robinson DA. 1988. Transition dynamics between pursuit and fixation suggest different systems. *Vision Res* 28:941-6
- Lynch JC. 1987. Frontal eye field lesions in monkeys disrupt visual pursuit. *Exp Brain Res* 68:437-41
- MacAvoy MG, Gottlieb JP, Bruce CJ. 1991. Smooth-Pursuit Eye Movement Representation in the Primate Frontal Eye Field. *Cereb Cortex* 1:95-102
- Madelain L, Krauzlis RJ. 2003. Effects of Learning on Smooth Pursuit During Transient Disappearance of a Visual Target. *J Neurophysiol* 90:972-82
- Majaj NJ, Carandini M, Movshon JA. 2007. Motion Integration by Neurons in Macaque MT Is Local, Not Global. *J Neurosci* 27:366-70
- Majaj NJ, Smith MA, Kohn A, Bair W, Movshon JA. 2002. A role for terminators in motion processing by macaque MT neurons? *J Vision* 2:415,a
- Marr D, Ullman S. 1981. Directional Selectivity and its Use in Early Visual Processing. *Proc. R. Soc. Lond. B* 211:151-80
- Masson G, Fleuriet J, Montagnini A, Mamassian P. 2008. Predicting and computing 2D target motion for smooth-pursuit eye movements in macaque monkeys. *J Vision* 8
- Masson GS. 2004. From 1D to 2D via 3D: dynamics of surface motion segmentation for ocular tracking in primates. *J Physiol Paris* 98:35-52
- Masson GS, Castet E. 2002. Parallel motion processing for the initiation of short-latency ocular following in humans. *J Neurosci* 22:5149-63
- Masson GS, Ilg UJ. 2010. Dynamics of Visual Motion Processing: Neuronal, Behavioral,

- and Computational Approaches. Newyork: Springer
- Masson GS, Montagnini A, Ilg UJ. 2010. When the Brain Meets the Eye: Tracking Object Motion. In Dynamics of Visual Motion Processing: Neuronal, Behavioral, and Computational Approaches, ed. GS Masson, UJ Ilg, pp. 161-88. Newyork: Springer
- Masson GS, Rybarczyk Y, Castet E, Mestre D. 2000. Temporal dynamics of motion integration for the initiation of tracking eye movements at ultra-short latencies. *Vis Neurosci* 17:753-67
- Masson GS, Stone LS. 2002. From following edges to pursuing objects. *J Neurophysiol* 88:2869-73
- Maunsell JHR, Nealey TA, Depriest DD. 1990. Magnocellular and parvocellular contributions to responses in the middle temporal visual area (MT) of the macaque monkey. *J Neurosci* 10:3323-34
- Maunsell JHR, Newsome WT. 1987. Visual Processing in Monkey Extrastriate Cortex. *Ann. Rev. Neurosci.* 10:363-401
- Maunsell JHR, Van Essen DC. 1983. Functional properties of neurons in middle temporal visual area of the macaque monkey. I. Selectivity for stimulus direction, speed, and orientation. *J Neurophysiol* 49:1127-47
- Merigan WH, Maunsell JHR. 1993. How parallel are the primate visual pathways? *Ann. Rev. Neurosci.* 16:369-402
- Miles FA. 1998. The neural processing of 3-D visual information: evidence from eye movements. *Eur J Neurosci* 10:811-22
- Miles FA, Fuller JH. 1975. Visual tracking and the primate flocculus. *Science* 189:1000-3
- Miles FA, Kawano K, Optican LM. 1986. Short-latency ocular following responses of monkey. I. Dependence on temporospatial properties of visual input. *J Neurophysiol* 56:1321-54
- Mingolla E, Todd JT, Norman JF. 1992. The perception of globally coherent motion. *Vision Res* 32:1015-31
- Missal M, Heinen SJ. 2001. Facilitation of Smooth Pursuit Initiation by Electrical Stimulation in the Supplementary Eye Fields. *J Neurophysiol* 86:2413-25
- Missal M, Heinen SJ. 2004. Supplementary eye fields stimulation facilitates anticipatory pursuit. *J Neurophysiol* 92:1257-62
- Mitrani L, Dimitrov G. 1978. Pursuit eye movements of a disappearing moving target. *Vision Res* 18:537-9
- Montagnini A, Mamassian P, Perrinet LU, Castet E, Masson GS. 2007. Bayesian modeling of

- dynamic motion integration. *J Physiol Paris* 101:64-77
- Montagnini A, Spering M, Masson GS. 2006. Combining 1D visual motion and 2D predictive signals to control smooth pursuit eye movements. *J Vision* 6:1a-1106a
- Montagnini A, Spering M, Masson GS. 2006. Predicting 2D target velocity cannot help 2D motion integration for smooth pursuit initiation. *J Neurophysiol* 96:3545-50
- Morris EJ, Lisberger SG. 1985. A computer model that predicts monkey smooth pursuit eye movements on a millisecond timescale. *Soc. Neurosci. Abstr.* 11:79
- Morris EJ, Lisberger SG. 1987. Different responses to small visual errors during initiation and maintenance of smooth-pursuit eye movements in monkeys. *J Neurophysiol* 58:1351-69
- Movshon JA. 1975. The velocity tuning of single units in cat striate cortex. *J Physiol* 249:445-68
- Movshon JA, Adelson EH, Gizzi MS, Newsome WT. 1986. The analysis of moving visual patterns. *Exp Brain Res* 11:117-52
- Movshon JA, Newsome WT. 1996. Visual Response Properties of Striate Cortical Neurons Projecting to Area MT in Macaque Monkeys. *J Neurosci* 16:7733-41
- Nakayama K. 1985. Biological image motion processing : A Review. *Vision Res* 25:625-60
- Nakayama K, Silverman GH. 1988. The aperture problem--I. Perception of non-rigidity and motion detection in translating sinusoidal lines. *Vision Res* 28:739-46
- Nakayama K, Silverman GH. 1988. The aperture problem--II. Spatial integration of velocity information along contours. *Vision Res* 28: 747-53
- Nassi JJ, Callaway EM. 2009. Parallel Processing Strategies of the Primate Visual System. *Nat Rev Neurosci.* 10:360-72
- Nealey TA, Maunsell JHR. 1994. Magnocellular and parvocellular contributions to the responses of neurons in macaque striate cortex. *Journal of Neuroscience. J Neurosci* 14:2069-79
- Newsome WT, Pare EB. 1988. A selective impairment of motion perception following lesions of the middle temporal visual area (MT). *J Neurosci* 8:2201-11
- Newsome WT, Wurtz RH, Dursteler MR, Mikami A. 1985. Deficits in Visual Motion Processing Following Ibotenic Acid Lesions of the Middle Temporal Visual Area of the Macaque Monkey' *J Neurosci* 5
- Newsome WT, Wurtz RH, Komatsu H. 1988. Relation of cortical areas MT and MST to pursuit eye movements. II. Differentiation of retinal from extraretinal inputs. *J Neurophysiol* 60: 604-20
- Nishidha S. 2011. Advancement of motion psychophysics: Review 2001–2010. *J Vision*

- Nowlan SJ, Sejnowski TJ. 1995. A Selection Model for Motion Processing in Area MT of Primates J Neurosci 15:1195-214
- Optican LM, Zee DS, Chu FC. 1985. Adaptive response to ocular muscle weakness in human pursuit and saccadic eye movements. J Neurophysiol 54:110-22
- Orban de Xivry JJ, Missal M, Lefevre P. 2008. A dynamic representation of target motion drives predictive smooth pursuit during target blanking. J Vision
- Osborne LC, Bialek W, Lisberger SG. 2004. Time course of information about motion direction in visual area MT of macaque monkeys. J Neurosci 24:3210-22
- Osborne LC, Hohl SS, Bialek W, Lisberger SG. 2007. Time course of precision in smooth-pursuit eye movements of monkeys. J Neurosci 27:2987-98
- Osborne LC, Lisberger SG. 2009. Spatial and temporal integration of visual motion signals for smooth pursuit eye movements in monkeys. J Neurophysiol 102:2013-25
- Osborne LC, Lisberger SG, Bialek W. 2005. A sensory source for motor variation. Nature 437:412-6
- Pack CC, Berezovskii VK, Born RT. 2001. Dynamic properties of neurons in cortical area MT in alert and anaesthetized macaque monkeys. Nature 414:905-8
- Pack CC, Born RT. 2001. Temporal dynamics of a neural solution to the aperture problem in visual area MT of macaque brain. Nature 409:1040-2
- Pack CC, Born RT. 2008. Cortical mechanisms for integration of visual motion. The Senses - A comprehensive reference 2:189-218
- Pack CC, Gartland AJ, Born RT. 2004. Integration of contour and terminator signals in visual area MT of alert macaque. J Neurosci 24:3268-80
- Pack CC, Hunter JN, Born RT. 2005. Contrast dependence of suppressive influences in cortical area MT of alert macaque. J Neurophysiol 93:1809-15
- Pack CC, Livingstone MS, Duffy KR, Born RT. 2003. End-Stopping and the Aperture Problem: Two-Dimensional Motion Signals in Macaque V1. Neuron 39:671-80
- Perrone JA. 2006. A single mechanism can explain the speed tuning properties of MT and V1 complex neurons. J Neurosci 26:11987-91
- Perrone JA, Thiele A. 2001. Speed skills: measuring the visual speed analyzing properties of primate MT neurons. Nat Neurosci 4:526-32
- Pola J, Wyatt HJ. 1980. Target position and velocity: The stimuli for smooth pursuit eye movements. Vision Res 20:523-34
- Pola J, Wyatt HJ. 1997. Offset dynamics of human smooth pursuit eye movements: Effects

- of target presence and subject attention. *Vision Res* 37:2579-95
- Pouget A, Zhang K, Deneve S, Latham PE. 1999. Statistically efficient estimation using population coding. *Neural Comp* 10
- Price NSC, Born RT. 2009. Representation of movement. *Encyclopedia of neuroscience* 8:107-14
- Priebe NJ, Cassanello CR, Lisberger SG. 2003. The neural representation of speed in macaque area MT/V5. *J Neurosci* 23:5650-61
- Priebe NJ, Lisberger SG. 2004. Estimating Target Speed from the Population Response in Visual Area MT. *J Neurosci* 24:4233-03
- Priebe NJ, Lisberger SG, Movshon JA. 2006. Tuning for Spatiotemporal Frequency and Speed in Directionally Selective Neurons of Macaque Striate Cortex. *J Neurosci* 26:2941-50
- Rashbass C. 1961. The relationship between saccadic and smooth tracking eye movements. *J Physiol* 159 326-38
- Reichardt W. 1961. Autocorrelation, a Principle for the Evaluation of Sensory Information by the Central Nervous System. In *Sensory Communication.*, ed. WA ROSENBLITH. Cambridge, MA: MIT Press.
- Ringach DL. 1995. A 'tachometer' feed-back model of smooth pursuit eye movements. *Biol Cybern* 73:561-8
- Robinson DA. 1964. The mechanics of human saccadic eye movement. *J Physiol* 174:245-64
- Robinson DA. 1965. The mechanics of human smooth pursuit eye movement. *J Physiol* 180:569-91
- Robinson DA. 1971. Models of oculomotor neural organization. In *The Control of Eye Movements*, ed. P Bach-y-rita, CC Collins, pp. 519-38. Newyork
- Robinson DA. 1972. Eye movements evoked by collicular stimulation in the alert monkey. *Vision Res* 12:1795-808
- Robinson DA, Gordon JL, Gordon SE. 1986. A Model of the Smooth Pursuit Eye Movement System *Biol Cybern* 55:43-57
- Rodman HR, Albright TD. 1987. Coding of visual stimulus velocity in area MT of the macaque. *Vision Res* 27:2035-48
- Rodman HR, Albright TD. 1989. Single-unit analysis of pattern-motion selective properties in the middle temporal visual area (MT). *Exp Brain Res* 75:53-64
- Rubin N, Hochstein S. 1993. Isolating the effect of 1D motion signals on the perceived direction of moving 2D objects. *Vision Res* 33:1385-96
- Rudolph K, Pasternek T. 1999. Transient and permanent deficits in motion perception after

- lesions of cortical areas MT and MST in the macaque monkey. *Cereb Cortex* 9:90-100
- Rust NC, Mante V, Simoncelli EP, Movshon JA. 2006. How MT cells analyze the motion of visual patterns. *Nat Neurosci* 9:1421-31
- Salinas E, Abbott LF. 1994. Vector reconstruction from firing rates. *J comp Neurosci* 1:89-107
- Salzman CD, Murasugi CM, Britten KH, Newsome WT. 1992. Microstimulation in visual area MT: effects on direction discrimination performance. *J Neurosci* 12:2331-55
- Sceniak MP, Hawken MJ, Shapley R. 2001. Visual Spatial Characterization of Macaque V1 Neurons. *J Neurophysiol* 85:1873-87
- Schoppik D, Nagel KI, Lisberger SG. 2008. Cortical mechanisms of smooth eye movements revealed by dynamic covariations of neural and behavioral responses. *Neuron* 58:248-60
- Schwartz JD, Lisberger SG. 1994. Initial tracking conditions modulate the gain of visuo-motor transmission for smooth pursuit eye movements in monkeys. *J Neurophysiol* 11:411-24
- Segraves MA, Goldberg ME. 1994. Effect of stimulus position and velocity upon the maintenance of smooth pursuit eye velocity. *Vision Res* 34:2477-82
- Segraves MA, Goldberg ME, Deng SY, Bruce CJ, Ungerleider LG, Mishkin M. 1987. The role of striate cortex in the guidance of eye movements in the monkey. *J Neurosci* 7:3040-58
- Sheliga BM, Chen KJ, FitzGibbon EJ, Miles FA. 2005. Initial ocular following in humans: A response to first-order motion energy. *Vision Res* 45:3307-21
- Shi D, Friedman HR, Bruce CJ. 1998. Deficits in smooth-pursuit eye movements after muscimol inactivation within the primate's frontal eye field. *J Neurophysiol* 80:458-64
- Shiffrar M, Li X, Lorenceau J. 1995. Motion integration across differing image features. *Vision Res* 35:2137-46
- Shiffrar M, Lorenceau J. 1996. Increased motion linking across edges with decreased luminance contrast, edge width and duration. *Vision Res* 36:2061-7
- Shimojo S, Silverman GH, Nakayama K. 1989. Occlusion and the solution to the aperture problem for motion. *Vision Res* 29:619-26
- Simoncelli EP, Adelson EH, Heeger DJ. 1991. Probability distribution of optical flow. IEEE Conference on Computer Vision and Pattern Recognition, pp. 310-5. Hawaii
- Simoncelli EP, Heeger DJ. 1998. A model of neural responses in visual area MT. *Vision Res* 38:743-61
- Smith MA, Majaj NJ, Movshon JA. 2005. Dynamics of motion signaling by neurons in macaque area MT. *Nat Neurosci* 8:220-8

- Soechting JF, Mrotek LA, Flanders M. 2005. Smooth pursuit tracking of an abrupt change in target direction: vector superposition of discrete responses. *Exp Brain Res* 180:245-58
- Sotiropoulos G, Seitz A, Seriès P. 2011. Changing expectations about speed alters perceived motion direction. *Curr Biol* 21:R 883-4
- Spering M, Kerzel D, Braun DI, Hawken MJ, Gegenfurtner KR. 2005. Effects of contrast on smooth pursuit eye movements. *J Vision* 5:455-65
- Steinbach MJ. 1969. Eye tracking of self-moved targets: The role of efference. *J Exp. Psych.* 82:366-76
- Steinman RM. 1986. The need for an eclectic, rather than systems, approach to the study of the primate oculomotor system. *Vision Res* 26:101-12
- Stocker AA, Simoncelli EP. 2006. Noise characteristics and prior expectations in human visual speed perception. *Nat Neurosci* 9:578-85
- Tabata H, Miura K, Kawano K. 2005. Anticipatory Gain Modulation in Preparation for Smooth Pursuit Eye Movements. *J Cogn Neurosci* 17
- Tanaka M, Fukushima K. 1997. Slow eye movement evoked by sudden appearance of a stationary visual stimulus observed in a step-ramp smooth pursuit task in monkey. *Neurosci Res* 29:93-8
- Tanaka M, Lisberger SG. 2000. Context-dependent smooth eye movements evoked by stationary visual stimuli in trained monkeys. *J Neurophysiol* 84:1748-62
- Tanaka M, Lisberger SG. 2001. Regulation of the gain of visually guided smooth-pursuit eye movements by frontal cortex. *Nature* 409:191-4
- Tanaka M, Lisberger SG. 2002. Enhancement of multiple components of pursuit eye movement by microstimulation in the arcuate frontal pursuit area in monkeys. *J Neurophysiol* 87:802-18
- Tanaka M, Lisberger SG. 2002. Role of arcuate frontal cortex of monkeys in smooth pursuit eye movements. I. Basic response properties to retinal image motion and position. *J Neurophysiol* 87:2684-99
- Tavassoli A, Ringach DL. 2009. Dynamics of Smooth Pursuit Maintenance. *J Neurophysiol* 102:110-8
- Thier P, Ilg UJ. 2005. The neural basis of smooth-pursuit eye movements. *Curr Opin Neurobiol* 15:645-52
- Tian JR, Lynch JC. 1995. Slow and saccadic eye movements evoked by microstimulation in the supplementary eye field of the cebus monkey. *J Neurophysiol* 74:2204-10
- Tlapale E, Masson GS, Kornprobst P. 2010. Modelling the dynamics of motion integration

- with a new luminance-gated diffusion mechanism. *Vision Res* 50:1676-92
- Tolhurst DJ, Movshon JA. 1975. Spatial and temporal contrast sensitivity of striate cortical neurones. *Nature* 257:674-5
- Tsui JMG, Hunter JN, Born RT, Pack CC. 2010. The Role of V1 Surround Suppression in MT Motion Integration. *J Neurophysiol* 103:3123-38
- Tychsen L, Lisberger SG. 1985. Visual motion processing for the initiation of smooth-pursuit eye movements in humans. *J Neurophysiol* 56:953-68
- van Beers RJ, Baraduc P, Wolpert DM. 2002. Role of uncertainty in sensorimotor control *Transactions of the Royal Society* 357:1137-45
- Van Beers RJ, Wolpert DM, Haggard P. 2002. When feeling is more important than seeing in sensorimotor adaption. *Curr Biol* 12:834-7
- van Santen, Sperling. 1985. Elaborated Reichardt detectors. *J. Opt. Soc. Am* 2:300-21
- van Wezel RJA, van der Smagt MJ. 2003. Motion processing : how long can you go? *Curr Biol* 13:R840-R2
- Wallace JM, Stone LS, Masson GS. 2005. Object motion computation for the initiation of smooth pursuit eye movements in humans. *J Neurophysiol* 93:2279-93
- Wallach H. 1935. Visual truth movement directions. *Psychologie Forshung* 20:325-80
- Watamaniuk SNJ, Heinen SJ. 2003. Perceptual and oculomotor evidence of limitations on processing accelerating motion. *J Vision* 3:698-709
- Watson AB, Ahumada AJ. 1985. Model of human visual-motion sensing. *J. Opt. Soc. Am* 2:322-42
- Weiss Y, Adelson EH. 1998. Slow and smooth: a Bayesian theory for the combination of local motion signals in human vision. MIT technical report, A.I. Memo 1624
- Weiss Y, Adelson EH. 2000. Adventures with gelatinous ellipses -- constraints on models of human motion analysis. *Perception* 29:543 - 66
- Weiss Y, Simoncelli EP, Adelson EH. 2002. Motion illusions as optimal percepts. *Nat Neurosci* 5:598-604
- Westheimer. 1954. EYE MOVEMENT RESPONSES TO A HORIZONTALLY MOVING VISUAL STIMULUS. *A.M.A. Arch. Ophthal.* 52:932-43
- Wilmer JB, Nakayama K. 2007. Two Distinct Visual Motion Mechanisms for Smooth Pursuit: Evidence from Individual Differences. *Neuron* 54:987-1000
- Wilson HR, Ferrera VP, Yo C. 1992. A psychophysically motivated model for two-dimensional motion perception. *Vis Neurosci* 9:79-97
- Wolfe JM. 2006. *Sensation and Perception*

- Wolpert DM. 2007. Probabilistic models in human sensorimotor control. *Human Movement Science* 26:511-24
- Wolpert DM, Ghahramani Z, Jordan MI. 1995. An internal model for sensorimotor integration. *Science* 269:1880-2
- Wuerger S, Shapley R, Rubin N. 1996. On the visually perceived direction of motion by Hans Wallach: 60 years later. *Perception* 25:1317-67
- Wyatt HJ, Pola J. 1981. Slow eye movements to eccentric targets. *Invest Ophthalmol Vis Sci.* 21:477-83
- Yang S, Hwang H, Ford JS, Heinen SJ. 2010. Supplementary eye field activity reflects a decision rule governing smooth pursuit but not the decision. *J Neurophysiol* 103:2458-69
- Yasui S, Young LR. 1984. On the predictive control of foveal eye tracking and slow phases of optokinetic and vestibular nystagmus. *J. Physiol.* 347:17-33
- Young LR, Forester JD, van Houtte N. 1968. A revised stochastic sampled data model for eye tracking movements. 4th Ann. NASA-Univ. Conf Manual Control., Univ. Michigan
- Young LR, Stark L. 1963. Variable feed-back Experiments Testing a Sampled Data Model for Eye Tracking Movements. Institute of Electrical and Electronics Engineers, Transactions on Human Factors in Electronics. HF E-4:38-51
- Zohary E, Shadlen MN, Newsome WT. 1994. Correlated neuronal discharge rate and its implications for psychophysical performance. *Nature* 370:140 - 3